REC-ERC-79-3

ELECTRONIC FILTER LEVEL OFFSET (EL-FLO) PLUS RESET EQUIPMENT FOR AUTOMATIC CONTROL OF CANALS

Engineering and Research Center
Bureau of Reclamation

June 1979

MS-230 (1-76)
Bureau of Reclamation

TECHNICAL REPORT STANDARD TITLE PAGE

1. REPORT NO.	2. GOVERNMENT ACCESSION NO.	3. RECIPIENT'S CATALOG NO.
REC-ERC-79-3		

4. TITLE AND SUBTITLE

Electronic Filter Level Offset (EL-FLO)
Plus RESET Equipment for Automatic Downstream
Control of Canals

5. REPORT DATE
June 1979

6. PERFORMING ORGANIZATION CODE

7. AUTHOR(S)

Clark P. Buyalski and Edward A. Serfozo

8. PERFORMING ORGANIZATION REPORT NO.
REC-ERC-79-3

9. PERFORMING ORGANIZATION NAME AND ADDRESS

Bureau of Reclamation
Engineering and Research Center
Denver, Colorado 80225

10. WORK UNIT NO.

11. CONTRACT OR GRANT NO.

12. SPONSORING AGENCY NAME AND ADDRESS

Same

13. TYPE OF REPORT AND PERIOD COVERED

14. SPONSORING AGENCY CODE

15. SUPPLEMENTARY NOTES

16. ABSTRACT

A prototype Electronic Filter Level Offset (EL-FLO) plus RESET analog computer-controller for automatic downstream control of canal check gates was designed, constructed, and laboratory-tested at the Engineering and Research Center's Hydraulic Laboratory, Denver, Colo. The EL-FLO plus RESET control system is designed to accommodate complex irrigation water delivery schedules with a high degree of self-regulation and maintains near constant water levels in a canal system. The sustained water level oscillations inherent in automatic flow regulation schemes are eliminated through the use of an electronic time delay circuit developed in this study. Laboratory tests of equipment performance under simulated canal bank environmental conditions were performed to ensure satisfactory operation at high temperatures, 65 °C (150 °F) and high humidity, 100 percent at 18 °C (64 °F). Laboratory simulation tests were performed to confirm that the prototype EL-FLO plus RESET analog computer-controller was designed and constructed as mathematically modeled. Upon completion of the laboratory development and testing, the prototype equipment was installed on the South Gila Canal near Yuma, Ariz., to confirm equipment performance and reliability on an actual operating canal system. From the results of laboratory and field tests, specifications were written and 21 EL-FLO plus RESET controls units were procured for permanent installation on the Corning and Coalinga Canals in California. Initial installation of the procured units was made on the first four reaches of the Corning Canal near Red Bluff, Calif., and field operation was continued to establish equipment performance and reliability. Field test data of the prototype and permanent installations are included in this report to demonstrate that the mathematical model does simulate the "real" operating canal system with reasonable accuracy.

17. KEY WORDS AND DOCUMENT ANALYSIS

a. *DESCRIPTORS--* / downstream/ *control/ automation/ *automatic control/ irrigation canals/ *canals/ hydraulics/ damping/ timing circuits/ control systems/ water levels/ water level fluctuations/ offsets/ analog computers/ laboratory tests/ test results/ simulation/ mathematical models

b. *IDENTIFIERS--* / schematic diagrams/ *equipment design/ South Gila Canal, Ariz./ Corning Canal, Calif.

c. *COSATI Field/Group* 13G *COWRR:* 1307

18. DISTRIBUTION STATEMENT	19. SECURITY CLASS (THIS REPORT)	21. NO. OF PAGES
Available from the National Technical Information Service, Operations Division, Springfield, Virginia 22151.	UNCLASSIFIED	145
	20. SECURITY CLASS (THIS PAGE) UNCLASSIFIED	22. PRICE

REC-ERC-79-3

ELECTRONIC FILTER LEVEL OFFSET (EL-FLO) PLUS RESET EQUIPMENT FOR AUTOMATIC DOWNSTREAM CONTROL OF CANALS

by
Clark P. Buyalski
Edward A. Serfozo

June 1979

Division of Research
Division of Design
Engineering and Research Center
Denver, Colorado

SI METRIC

UNITED STATES DEPARTMENT OF THE INTERIOR * BUREAU OF RECLAMATION

PREFACE

This report covers work accomplished prior to December 1975. No attempt has been made to incorporate succeeding research and analysis.

Funds for the laboratory development and testing of equipment were supplied principally by the Water Systems Automation Program as part of ongoing research at the E&R Center.

ACKNOWLEDGMENT

The construction of the EL-FLO plus RESET prototype control equipment was performed by R. H. Kuemmich. W. B. Gish, Electrical Power Branch, provided assistance wherever required in the design of the control circuits. The Electrical Power Branch furnished electronic components from their supply when needed. R. A. Paul, Hydraulic Structures Branch, assisted in the many mathematical model simulation studies made to select control parameters. The field testing of the prototype electronic filters and the prototype EL-FLO plus RESET controller on actual operating canal systems resulted from the cooperative efforts of operating and maintenance personnel of the Red Bluff O&M Office, Red Bluff, Calif., the Yuma Projects Office, and the Yuma Irrigation District, Yuma, Ariz.

CONTENTS

Page

Preface
Acknowledgment
Purpose 1
Conclusions 1
Applications 1
Background 1

General theory of EL-FLO plus RESET 7

Laboratory verification test 13

General 13
Laboratory simulation 13
Laboratory verification test results 13
Summary of analysis of laboratory verification test 13

Field verification tests 14

General 14
South Gila Canal prototype field test 14
Summary of the South Gila prototype field test 16
Corning Canal prototype field test 16
Summary—May 1974 field test 23

Bibliography 27

Appendix I. Electronic filter and EL-FLO plus RESET control chassis environmental tests 59

Summary 59
High humidity tests 59
High heat tests 61

Appendix II. Electronic filter time constant calibration 71

General 71
Electronic filter calibration 71

Appendix III. Technical description of each EL-FLO plus RESET feedback control system element 77

General 77
System Description 77
Circuit descriptions 79
Packaging design 90
Calibration, testing, and maintenance 91
Maintenance strategy 92
Summary 93
Detailed circuit analysis 97

Appendix IV. Report on the condition of the EL-FLO controller receiver unit, South Gila Canal automation 117

CONTENTS – Continued

Page

Appendix V. Conversion of selected control parameters to electronic equivalences 127

General 127
South Gila Canal 127
Corning Canal 131

Appendix VI. Detailed analysis of laboratory vertification test 143

TABLES

Table

1 Summary of the laboratory verification studies of the mathematical model versus the prototype EL-FLO plus RESET outputs at time 120 minutes 15
2 Input data for the South Gila Canal mathematical model verification studies 17
3 Corning Canal section properties 19
4 Corning Canal - Summary of properties at each check gate 20
5 Summary of estimated total canalside demand - Corning Canal prototype field tests, May 14-16, 1974 21
6 Corning Canal prototype field verification tests - Pumping plant and floating control system properties, May 14-16, 1974 22
7 Input data for the Corning Canal mathematical model verification studies - First control parameter data set 24
8 Input data for the Corning Canal mathematical model verification studies - Second control parameter data set 25
I-1 Electronic filter humidity test data summary 60
I-2 Summary of temperature drift characteristics of electronic filter units 1 through 4 with MOSFET drain current set at I_{DSS} 62
II-1 Electronic fifter unit 4 time constant calibration, tests No. 64 and 65 72
II-2 Final calibration data for the prototype electronic filter units 1 through 4 73
V-1 South Gila Canal EL-FLO controller prototype field data - Electronic filter unit 4 calibration 129
V-2 Electrical measurements, EL-FLO plus RESET controller - South Gila Canal 129
V-3 Calculation of arc distance versus vertical distance of gate travel for the South Gila Canal headgate 130
V-4 Corning Canal EL-FLO plus RESET control parameters, first set, units of meters (feet) 132
V-5 Corning Canal EL-FLO plus RESET control parameters, first set, electronic equivalences 132
V-6 Corning Canal EL-FLO plus RESET control parameters, second set, units of meters (feet) 134
V-7 Corning Canal EL-FLO plus RESET control parameters, second set, electronic equivalences 134
V-8 Corning Canal alarm probe elevations 135

FIGURES

Figure		Page
1	HyFLO feedback control system	28
2	Schematic of canal and hydraulic filter	28
3	New hydraulic filter and water level sensor assembled components	29
4	Hydraulic filter well plastic bag for clean water supply	30
5	View of the original modified HyFLO control chassis which was used in prototype tests, 1969-72.	30
6	Single line diagram of original electronic filter circuit design	30
7	Model "A" electronic filter field tested in November 1971	31
8	Electronic filter printed circuit boards.	32
9	Laboratory environmental test chamber used to simulate canal bank conditions	33
10	Electronic components of the prototype EL-FLO plus RESET analog computer controller mounted on printed circuit boards	34
11	Laboratory test facilities used for the EL-FLO plus RESET controller laboratory test program	34
12	Prototype EL-FLO plus RESET control chassis mounted inside a wall mount weatherproof cabinet	35
13	Prototype EL-FLO plus RESET control cabinet installed inside one of the South Gila Canal stilling well instrument shelters	36
14	Prototype installation of the EL-FLO plus RESET and the Colvin controllers housed inside the stilling well above the South Gila Canal check gate No. 1	36
15	Final prototype EL-FLO plus RESET controller and installation on the Corning Canal.	37
16	EL-FLO plus RESET feedback control system	39
17	Block diagram of automatic downstream control by the EL-FLO plus RESET prototype equipment	40
18	Canal reach characteristic response by the EL-FLO method of automatic downstream control.	41
19	Canal reach characteristic response by the EL-FLO plus RESET method of automatic downstream control - Proportional mode plus proportional RESET mode of control	42
20	Canal reach characteristic response by the EL-FLO plus RESET versus the EL-FLO method of automatic downstream control	43
21	Parameter δ/ω of a component response versus the ratio $\mathcal{A}$ of two successive amplitudes	44
22	Laboratory verification test mathematical model versus prototype EL-FLO plus RESET control equipment	45
23	Schematic of South Gila Canal configuration at steady-state flow conditions at time zero	46
24	Electronic chart recordings of the South Gila Canal prototype field test	47
25	South Gila Canal field verification test methematical model versus prototype EL-FLO plus RESET control equipment	48
26	Bottom grade profile of Corning Canal	49
27	Corning Canal prototype test - EL-FLO control field verification	51
I-1	Chart recordings for humidity tests of model "A" electronic filter and final prototype electronic filter unit 1	63
I-2	Temperature drift characteristics of the electronic filter units 1 through 4 for various temperatures and at various field effect transistor drain currents	64

FIGURES – Continued

Figure		Page
I-3	Final temperature drift characteristics of the electronic filter output for units 1 through 4 at I_{DSS} drain current versus temperature	65
I-4	An example of a high-temperature test run conducted on electronic filter unit 4	66
I-5	Temperature drift of the EL-FLO plus RESET control chassis	67
I-6	Example heat test run No. 35T for temperature drift characteristics on the final prototype EL-FLO plus RESET control	68
II-1	Recorder charts of electronic filter unit 4	74
II-2	Example of electronic filter time constant calibration using test Nos. 64 and 65 on unit 4	75
II-3	Summary of electronic filter units 1 through 4 time constant calibration of calibration test Nos. 25 through 65	76
III-1	EL-FLO controller system functional block diagram	95
III-2	EL-FLO controller system control panel	96
III-3	EL-FLO controller prototype upstream chassis equipment layout and schematic diagram (801-D-149)	104
III-4	EL-FLO controller prototype downstream chassis equipment layout and schematic diagram (801-D-150)	105
III-5	EL-FLO controller prototype upstream cabinet wiring diagram (801-D-151)	107
III-6	EL-FLO controller prototype downstream cabinet wiring diagram (801-D-152)	109
III-7	EL-FLO controller wall mount cabinet general layout (801-D-166)	111
III-8	EL-FLO controller wall mount cabinet swing rack assembly drawing (801-D-167)	113
III-9	EL-FLO controller schematic wiring diagram (801-D-175)	115
V-1	Sketch of water level sensor-potentiometer operating depth and voltage scale	136
V-2	South Gila Canal EL-FLO plus RESET controller electronic filter unit 4 time constant calibration	136
V-3	Schematic of radial gate properties	136
V-4	South Gila Canal radial headgate calibration	137
V-5	South Gila Canal EL-FLO plus RESET controller RESET integrator calibration	138
V-6	Time constant of electronic filter in seconds with 50- and 100-megohm resistance	139
V-7	RESET integrator motor speed calibration curve No.1	140
V-8	RESET integrator motor speed calibration curve No. 2	141

PURPOSE

This study was conducted to design and develop a reliable prototype electronic filter level offset (EL-FLO) plus RESET analog computer-controller for automatic downstream control of canal check gates. Data collected during field tests conducted on the South Gila Canal near Yuma, Ariz., and on the Corning Canal near Red Bluff, Calif., are compared with mathematical model simulation to verify that the mathematical model does predict hydraulic transients in the canal system with reasonable accuracy as the resultant prototype EL-FLO plus RESET controller responds to changes in downstream canalside demands.

CONCLUSIONS

The results of the laboratory studies and field tests are:

- A reliable electronic time delay circuit was developed to supersede the more cumbersome hydraulic filter.

- A reliable EL-FLO proportional controller using integrated circuits was developed.

- A RESET controller was developed and added to the EL-FLO proportional controller feedback path to eliminate the residual water level offset associated with proportional control.

- Laboratory simulation tests confirmed that the prototype EL-FLO plus RESET feedback control system was designed and constructed as mathematically modeled.

- Data collected during field tests of the prototype EL-FLO plus RESET feedback control system on the South Gila Canal and the production model on Corning Canal verified that the mathematical model predicted with reasonable accuracy the response characteristics of an operating canal system as the controller responds to changes in canalside demands.

- The Corning Canal EL-FLO plus RESET control system has performed satisfactorily as intended in the control of a series of radial gates. There are indications that the control system will have a high degree of reliability in adjusting the canal flow to meet turnout demand. Developing a high degree of reliability combined with a high degree of self-regulation will accomplish the main objectives of the development and testing program; that is, the EL-FLO plus RESET controller will have application and be economically justifiable for many existing and proposed canal systems.

- Further research and development investigations are needed to establish better methods or procedures to arrive at optimum control parameters for the various methods of automatic downstream control of canal check gates.

APPLICATIONS

The proportional plus reset mode of control, such as the EL-FLO plus RESET feedback control system, offers a great deal of versatility and flexibility of operation to automatic flow regulation in canal systems. The large and rapid, as well as the small and slow, changes of canalside demands can be regulated smoothly by the proportional mode of control. Operational stability is maintained by the electronic time delay circuit element between the water level sensor and "real time" analog computer. The reset mode of control eliminates the residual water level offset of the proportional mode and maintains a nearly constant water level as flow demands change. The EL-FLO plus RESET method of downstream control provides an automatic responsive system between the demand and the source of supply. The controller has the capability to meet the demands of modern irrigation practice without supervisory intervention. If the EL-FLO plus RESET controller continues to demonstrate a high degree of reliability, it will have application to and be economically justified for automatic flow regulation of many existing or proposed canal systems serving many distribution laterals having complex irrigation water delivery schedules.

BACKGROUND

Automatic downstream control of canal check gates is one approach to upgrading the conventional mode of operation and achieving optimum efficiency of a canal system. Control of canal check gates from downstream water levels automatically ensures sensible coupling of canalside turnout diversions and canal inlet flow. The application of control theory has made it possible to select suitable control parameters to eliminate instability inherent in automatic feedback control systems and to give a high degree of self-regulation, i.e., the fastest response to canalside turnout demands and the recovery of the canal system to a new steady state without excessive over-shooting of the water levels. [1, 2, 3] [1]

[1] Numbers in brackets refer to references in the Bibliography.

Recognizing the potential of the downstream control concept, the Bureau of Reclamation began an extensive research and development program in 1967 with a research contract with the University of California at Berkeley. The initial investigation developed a mathematical model for canal system simulation and an analytical study for the selection of control parameters. [4, 5] From the results of the 1967 program, four prototype analog proportional controllers known as the hydraulic filter level offset (HyFLO) method were designed, constructed, and field-tested on the Corning Canal near Red Bluff, Calif., in March 1969. The field test data confirmed the analytical studies. [1] A typical HyFLO feedback control system is shown in figure 1. (All main text figures follow the Bibliography.)

The first element of the feedback system, (fig. 1) is a hydraulic filter that develops the necessary large time constant (on the order of 2000 seconds). The hydraulic filter governs the stability of the control system by filtering out the critical frequencies of the disturbances which tend to be amplified by the controller. The hydraulic filter consists of a capillary tube connected between the canal (or a normal stilling well) and a secondary or filter well; see figure 2. The linear resistance of the laminar flow produced by the capillary tube represents the resistance (R) and the surface area of the filter well represents the capacitance (C) of the analogous electronic RC circuit.

A pressure transducer was used during the March 1969 tests as the sensor element to measure the water level inside the filter well. The pressure transducer arrangement proved to be too delicate for field installation and problems with maintaining calibration and proper operation were experienced during the test period. Difficulties were also experienced in the control equipment electronic circuitry. The overall equipment performance during the March 1969 field test was not satisfactory.

With the assistance of the Engineering and Research Center, a new hydraulic filter (fig. 3) using a float-operated potentiometer as the sensor element was designed, constructed, and tested in the hydraulic laboratory. [6] The problems of the analog controller electronic circuitry that were experienced during the March 1969 tests were also resolved. In anticipation that sediment and biological microorganisms present in the canal water might plug the 2.4-mm (3/32-in) inside-diameter capillary tube, a plastic bag containing clean water was added to assist in keeping the capillary tube clean and the hydraulic time delay operating (fig. 4).[2] The delay time constant was not appreciably changed by the addition of the plastic bag and connecting tube.

In March 1970, the new hydraulic filter and a modified original HyFLO control chassis (fig. 5) was installed on the Corning Canal for automatic regulation of check No. 1. The new hydraulic filter was installed in the stilling well immediately upstream of check No. 2. The equipment was put into continuous operation. For a period of 6 months, the performance of the new hydraulic filter and the modified HyFLO controller was excellent. However, after 6 months, the capillary tube became plugged as a result of airborne debris such as dust and insects entering the filter well through the air vent and settling down inside the well and becoming suspended in the water. Dead fly carcasses were the primary cause of plugging the capillary tube, their size was greater than the inside diameter of the capillary tube before they decomposed. Proper screening and filtering of the air vent may have eliminated further problems of this kind.

The canal check No. 1 gate was operated manually until the filter well could be removed and cleaned. During the period of manual operation, high water levels occurred in the canal. The filter well had only a 150-mm (6-in) free board and during high water levels, the 125-mm (5-in) diameter float stopped against the filter well top lid and became submerged. Water then drained into the inside of the float through its top vent hole causing the float to sink. The filter well was then removed and cleaned. However, the water inside the float could not be entirely drained even by the use of a hypodermic needle. In the process of disassembling the filter well, the float tape which was made from brass shim stock became wrinkled and it had stretched to a point where the holes in the tape would not mesh with pins on the specially constructed 50-mm (2-in) float pulley. Because of the problems experienced with the capillary tube plugging, the float sinking, and the float tape becoming easily damaged, it was decided that an improved design would be required to obtain better hydraulic filter well longevity. The hydraulic filter well was not put back into operation. The prototype operation had demonstrated sufficiently that the present design of the hydraulic filter was cumbersome, would require frequent maintenance, and the special design (not *off-the-shelf components*) of the float-tape-pulley would be costly to construct.

[2] Dimensions and other measures in this report were recorded in the inch-pound (U.S. customary) system of units. The reporting of these measures in the SI metric system is per USBR policy. The English equivalents given in parentheses are the more exact values.

As a result of these conclusions, a decision was made to develop a reliable electronic time delay circuit to replace the more cumbersome and costly hydraulic filter well. A float-tape-pulley arrangement would still be required to sense the water level as input to an electronic filter but standard off-the-shelf equipment could be used.

The development of the electronic filter began with a suggested circuit design (fig. 6) furnished by Professor James A. Harder, Professor of Hydraulic Engineering, Department of Civil Engineering, University of California at Berkeley. Professor Harder was the principal investigator for the University on the research contracts for investigating automatic downstream control of canal check gates sponsored by the Bureau of Reclamation, Mid-Pacific Region, which began in 1967 and ended in 1969.

The time delay circuit requires large time constants (R multiplied by C) and typically range from 100 to 4000 seconds. Time constants of this magnitude can be obtained using electrical elements consisting of a low-leakage capacitor, a good-quality resistor, a field effect transistor (FET), and an operational amplifier with a variable feedback resistor. The electrical circuit within the dashed area of figure 6 must be packaged in a hermetically sealed enclosure to shield the electrical high impedance characteristics from the influence of environmental humidity.

An electronic time delay circuit was constructed at the E&R Center with some minor changes to that suggested by Professor Harder. The first unit was labeled the "Model A" (fig. 7) and included an "initialize" feature that would automatically reset the output of the electronic filter to the prevailing canal water level after a power failure in the event that a power failure occurred. Laboratory testing confirmed that the electronic time delay circuit output reproduced the hydraulic filter output using the same input water level variation. [6] The high impedance portion of the electronic filter was coated with a layer of silastic resin. However, laboratory tests were not conducted at this time to determine if the silastic coating was an adequate protection against humidity. The Model A was sent to the Corning Canal for field tests replacing the hydraulic filter.

Field tests of the Model A electronic filter were conducted in November 1971 for a period of 3 days and its performance was satisfactory. To continue the tests for a longer period on an actual operating canal was too risky because the process used to hermetically seal and protect the high impedance properties of the electronic time delay circuit from humidity had not been verified. Therefore, the electronic filter was returned to the laboratory for further tests. However, the test period using actual operating conditions was long enough to demonstrate that the electronic filter could replace the hydraulic filter. The electronic filter would have to operate continuously for very long periods without failure in order to achieve a high degree of reliability and a low maintenance cost.

Shortly after the return of the Model A electronic filter, an extensive program was initiated for testing the filter in simulated canal bank environmental conditions. These tests proved to be very beneficial and showed the Model A filter was not adequately protected against high humidity. Rearrangeing the electronic components and redesign of the "initialize" circuit were necessary to isolate the high-impedance circuit into one area that could be hermetically sealed.

The next step toward the development of a reliable electronic filter was to construct four electronic filters using the same electronic circuit design of the Model A. The electronic components for each filter were mounted on two 80– by 140–mm (3.16– by 5.5–in) printed circuit boards (fig. 8). The high–impedance RC network was placed on one card and encapsulated with Sylgard[3] 184 encapsulating resin. The operational amplifier network was placed on the other card. These four electronic filter units underwent extensive "burn-in" and environmental tests. Each unit was placed in an environmental chamber (fig. 9) and tested at 65 °C (150 ° F) with low humidity and at 18 °C (65 °F) with 100 percent humidity. The results of these studies are detailed in appendixes I and II.

A comparison can be made between the sizes of the electronic filter (fig. 9) and the hydraulic filter (fig. 3). The electronic filter is small and compatible with the electronic circuits of the analog-control chassis.

The first three units of the electronic filter, after the laboratory tests were completed, were sent to the Corning Canal in May 1972 for installation on controllers at the first three check structures. The control chassis used at check No. 1 was the same chassis (with modifications already completed) that was used for the hydraulic filter tests of 1970 and the electronic filter Model A tests of November 1971. Two additional chassis of the March 1969 test program were modified to correct the defects of the original equipment and were installed at checks No. 2 and 3.

After June 1972, the analog computer-controller became known as the electronic filter level offset (EL-FLO) method rather than the hydraulic filter level offset (HyFLO) method because the electronic filter had

[3] Trademark Dow Corning

replaced the hydraulic filter element of the feedback system.

The EL-FLO controllers were operated continuously from June to November of the 1972 irrigation season. From the beginning of operation, problems with "cold" solder connections on the old control chassis began to cause intermittent operations. Although many of the solder connections were corrected during the initial startup, the control chassis at check No. 3 had numerous poor solder connections and it was possible to operate the "Raise" relay of the gate hoist without proper input voltage signal. False operation had occurred at night and was contributed to "cold" solder connections breaking electrical contact when the ambient temperature dropped. In attempts to repair the control chassis at check No. 3, the electronic filter, unit 2, located at check No. 3 was damaged. Because of the failure of the electronic filter and the erratic operation of the check No. 3 controller, the controller was removed and replaced with the equipment at check No. 4. The replacement allowed check No. 2 to be put back into automatic operation with an adjusted time constant in the electronic filter unit 3. The check No. 3 controller and unit 2 filter were returned to the E&R Center laboratory for repair.

Laboratory analysis of the electronic filter unit 2 revealed that poor solder connections on the *RC* network field effect transistor (FET) was the apparent cause of abnormal operation during the initial startup period. The control chassis for check No. 3 was completely reconditioned in the laboratory to correct the solder connections. The control chassis for check No. 3 and the electronic filter unit 2 were returned to the Corning Canal and put into operation by the end of June 1972.

For a period of 3 months, the three EL-FLO controllers performed satisfactorily. However, problems with poor solder connections began to appear again and as time went on, they appeared with greater frequency. Other difficulties began to occur such as an open circuit in an overhead communication wire caused by the birdshot of a dove hunter and short circuits within the control chassis. The frequent intermittent operation of the modified control chassis began to have an effect on the operation of the Corning Canal system. Since the irrigation season was nearly over in November 1972, the EL-FLO control system was turned off for safety reasons. During the 5 months of operation, the electronic filters performed satisfactorily except for one instance. An electrical storm one night in September apparently caused a voltage surge on the power supply and/or the communication channel causing damage to electrical components in the unit 1 electronic filter. Protection against voltage surges which are very destructive to most solid state devices had not been included in the modification of the original control chassis. The unit 1 electronic filter was returned to the E&R Center laboratory for repair because spare equipment was not available at the Corning Canal for quick replacement. The laboratory discovered that the chopper stabilized operational amplifier (233J) and the matching impedance operational amplifier (μ741) on the electronic filter operational amplifier card had been damaged. These electrical components were replaced and the unit 1 filter was returned to the Corning Canal and put into operation after about 1 week.

The primary intent of the 1972 prototype tests on the Corning Canal was to obtain field experience on the electronic filters. The original controllers, although modified, were not satisfactory for field operations. The test program did provide sufficient data to determine that the electronic filters were suitably designed for long and continuous field operation. However, it was evident from the start of the 1972 operations that the 1969 control chassis had become obsolete and that a new design incorporating the latest technology in solid-state circuits and construction on printed circuit boards was necessary to achieve better equipment reliability.

A program to develop a new prototype EL-FLO controller using the electronic filter unit 4 had begun before the 1972 field test program ended. A decision was made to develop a RESET controller and incorporate it into the new prototype EL-FLO controller. The RESET feature would eliminate the residual water level offset characteristic of the proportional control mode of the EL-FLO method. The results of the prototype development program of the EL-FLO plus RESET controller including laboratory and field testing served as a basis for designing and writing specifications for control units to be procured and installed on a permanent basis. Details of the development and testing program for the EL-FLO plus RESET controller are decribed in subsequent paragraphs of this report.

The electrical components necessary for a prototype EL-FLO plus RESET feedback control system were mounted on 11 printed circuit boards; see figure 10. The basic control system of the old modified control chassis for the EL-FLO controller was used with circuit design improvements and medium scale integrated (MSI) circuits were used extensively in the design. Experiences gained from the Corning Canal field tests were used to improve the reliability of the controller.

Lightning protection and power line voltage surge protection were also incorporated into the design of the new prototype controller. The final prototype electrical circuit design is as shown on figures III-3 through III-6.

The electronic filter cards are those which were developed as unit 4 during the electronic filter development and testing program. The RESET control circuit was designed to provide the extremely long integration period required (RESET) on the proportional control signal. The extremely long integration time was acquired by using a slow speed timing d-c motor and varying the motor speed proportional to the control signal level. The d-c motor shaft turns a multiturn potentiometer to provide the necessary d-c reset control signal. A chassis complete with indicating lamps and test panel was constructed for the plug-in circuit boards.

The completed EL-FLO plus RESET control chassis was exposed to high temperatures, 65 °C (150 °F), and 100 percent humidity at 18 °C (65 °F) inside the environmental test chamber. The most significant discovery made during the environmental tests was the abnormal operation of wirewound trimpots in high temeperature use, near 65 °C. It was concluded that thermal expansion caused the wiper of the trimpots to expand resulting in a sudden change in output. The wirewound trimpots were replaced with the cermet metal film type that have infinite resolution and are unaffected by thermal expansion. All trimpots and potentiometers were of the humidity-proof construction. The prototype control chassis performance was excellent when subjected to similar environmental conditions encountered on the canal bank.

Laboratory tests (fig. 11) were conducted to verify that the prototype EL-FLO plus RESET controller was designed and constructed as mathematically modeled. To accomplish this verification, the water level sensor of the downstream control chassis was made to follow the water surface level of a mathematical model output simulating a sudden change of downstream canalside demand. The outputs of the prototype EL-FLO plus RESET controller were then compared to equivalent outputs of the mathematical model. Figure 22 illustrates that close agreement achieved between the EL-FLO plus RESET prototype controller and the simulated controller in the mathematical model. Therefore, the EL-FLO plus RESET method of control was verified on-the-bench.

Upon completion of the laboratory development and testing program for the prototype EL-FLO plus RESET controller, the control chassis were mounted on a swing out rack of a standard weatherproof wall mount cabinet, figure 12. To provide automatic downstream control of one canal reach (between canal check structures), two control cabinets are required, one at the downstream end and one at the upstream end of the canal reach being controlled. The downstream cabinet houses the chassis for the electronic filter, the electronic filter output signal transmitting equipment, and the water level sensor assembly. Figure 12b shows how the water level sensor assembly (using commercially available water level float-tape-pulley hardware) is installed. The upstream cabinet houses the chassis for the EL-FLO plus RESET controller and the electronic filter output receiving equipment.

The EL-FLO controller (fig. 11 and 12) was shipped to the Yuma Projects Office, Yuma, Ariz., and was installed on the first reach of the South Gila Canal in January 1973. The downstream cabinet was installed inside the canal stilling well instrument shelter located immediately upstream of check No. 2, figure 13a. The upstream cabinet was installed at the stilling well located immediately upstream of check No. 1, figures 13b and 14. The control parameters for the EL-FLO plus RESET controller were established to control the check No. 1 from the water level upstream of check No. 2, a distance of 2768 m (9080 ft). A Colvin controller (fig. 12c) which is of the set-operate-variable-rest method of control was installed inside the upstream control cabinet, figure 14. The Colvin controller parameters were established to control the South Gila Canal headgate from the water level upstream of check No. 1, a distance of 168 m (550 ft).

The South Gila Canal prototype control equipment was put into continuous operation on January 29, 1973. Initial tests of the EL-FLO plus RESET controller revealed that the control gains were set too high causing excessive overshot. The gains were adjusted downward to provide a more satisfactory control response to changes of downstream canal demands.

The control system for check No. 1 and the headgate performed satisfactorily for 2 months. At this time, the Colvin controller, an electromechanical device, began to wear out from continuous operations. In March 1973, the Colvin controller was taken out of service, reconditioned for better reliability, and then put back into operation after 3 days elapse time by the Yuma Projects Office. During an additional 2 months time, the Colvin controller developed excessive malfunctions and was thereafter taken out of service permanently because of the high rate of mechanical failure. The control parameters of the EL-FLO plus RESET controller were modified to control the South Gila Canal headgate instead of the Colvin controller, eliminating the use of check No. 1.

The EL-FLO plus RESET controller equipment performed without failure during the first 4 months of field operation and the solid-state electrical circuits showed excellent stability. The South Gila Canal prototype test was terminated in May 1973 until the EL-FLO controller parameters could be changed to control the headgate.

New control parameters were established for the EL-FLO plus RESET controller and the necessary modifications required to control the headgate were completed in the field in August 1973. The EL-FLO plus RESET controller was put back into continuous operation controlling the South Gila Canal headgate from the water level upstream of check No. 2, a distance of 2940 m (9630 ft). The gate at check No. 1 was fully opened and not used to regulate canal flows.

During the initial operation in August 1973, the control parameters for the EL-FLO plus RESET controller had to be decreased in order to reduce the excessive overshot of the downstream canalside demands. After the adjustments were made, the control system provided satisfactory control of the headgate with an acceptable overshot of about 15 percent and flow disturbances were attenuated to a steady state without excessive cycling of the inlet flows.

Shortly after the control system was put into continuous operation, the water level sensor potentiometer developed what appeared to be a "bad spot" on the winding causing a momentary loss of water level signal output. The potentiometer was replaced within 20 minutes elapsed time to prevent possible abnormal operation of the headgate by the controller.

The potentiometer malfunction was the first significant equipment problem that developed during the prototype testing that could be related to circuit design and/or equipment selection.

An intermittent operation "wiper drop out" occurred again in September 1973 with the RESET potentiometer. The potentiometer was replaced after 50 minutes elapse time; however, before replacement, the malfunctioning had caused abnormal operation of the headgate on an intermittent basis.

The two potentiometers were operated with an applied voltage in the laboratory. Only in one brief instance could the intermittent operation that had occurred in the field be duplicated. From all appearances, the potentiometers were functioning normally. The two potentiometers were returned to the manufacturer with a request to examine the potentiometer internally and to furnish the E&R Center with the results of the analysis. The manufacturer reported the following:

> No spurious wiper outputs or loss of wiper continuity could be observed on either unit. Various attempts were made by changing speed of rotation application of radial and axial shaft loads, etc., without an indication of malfunction.
>
> Both units were disassembled and an internal inspection indicated no abnormalities. All contact points had proper pressure. Elements were clean and showed little signs of wear.

The testing of the two potentiometers did not lead to a conclusion as to the exact cause of the apparent wiper drop-out. It is possible the instrumentation connected to monitor and record the activity of the canal system may had affected the operation of the controller. Test points being monitored were located in critical portions of the electronic circuits and spurious electrical outputs from the recorders could have caused the erratic operation of the control system. In addition, improper grounding of the instrumentation, when connected to the EL-FLO controller circuit ground, can produce an effect similar to that experienced.

On September 23, 1973, a serious malfunction of the control system occurred. The receiver unit in the upstream control cabinet (fig. 13b) failed internally causing the input to the EL-FLO plus RESET controller chassis to suddenly change from a normal control signal input representing 1.3 m (4.2 ft) of water depth upstream of check No. 2 to a complete loss of signal representing zero feet. The controller, functioning normally, proceeded to open the headgate to supply additional water based on the false input signal and continued to open the headgate until it reached its maximum opening. The headgate remained in this position until manually closed by the ditchrider. With the headgate opened to maximum position, the flow into the South Gila Canal increased from about 1 to 3 m^3/s (40 to about 110 ft^3/s). The increased flow was sustained long enough to cause flooding and extensive damage at the end of the canal 11.4 km (7.1 mi) downstream. A detailed analysis of the defective receiver unit was made in the laboratory. The results of this study are included as appendix IV of this report.

The September 23, 1973 malfunction of the EL-FLO plus RESET receiver unit ended the prototype test program on the South Gila Canal. The prototype equipment did not include an alarm system to notify operating personnel in the event of equipment failure. Further testing of the prototype equipment, if continued, would have required hiring additional ditchriders

just to patrol the canal to avoid a recurrence of canal damage resulting from equipment failures.

The program was sufficient to enable the Yuma Irrigation District (the agency responsible for the operation and maintenance of the South Gila Canal) to understand clearly the benefits they would receive with controllers installed at all of the canal check structures on a permanent basis. However, the 5-month duration of the 1973 prototype test program, together with interruptions, required modification of equipment and the September malfunction which caused damage to the canal during this period failed to demonstrate sufficient equipment reliability to the District. They foresaw the possibility of having considerable maintenance cost associated with the installation which could easily negate associated benefits. After discussion, a recommendation was made to defer a permanent installation of the EL-FLO plus RESET controllers at all the South Gila Canal check structures until high equipment reliability could be achieved.

Plans were underway at the time of the recommendation to install the EL-FLO plus RESET controllers and an alarm system (the same design as proposed for the South Gila Canal) on the Corning Canal, Central Valley Project, near Red Bluff, Calif. at 12 check structures. The results of the 1973 test program served as the basis for writing specifications (solicitation No. (D)J-33, 451-A) to procure EL-FLO plus RESET control units (fig. 15) to be installed on the Corning Canal and the Coalinga Canal on a permanent basis.

The initial installation of the procured control units was made on the first four check structures of the Corning Canal and put into continuous operation in May 1974. The initial installation was limited to the first four check structures because the alarm system (being procured under separate contract) was not available. The alarm system could be installed at a later date when the remaining nine control units would be installed and put into operation.

During the first month of operation, a number of problems were experienced on the Corning Canal installation and long-time water outages were being created because of malfunctions in previously installed equipment. All the problems experienced were caused by the combination of faulty check gate control relays and improperly connected control circuits and short circuits in control wiring of the existing electrical control equipment. No failure was found to be directly attributable to the EL-FLO plus RESET control system equipment. Modifications and rehabilitation of existing equipment prevented the further occurrence of these problems. The period of equipment malfunctions did emphasize the need to correct deficiencies in existing equipment before automatic equipment can be expected to operate properly.

Lightning struck the communication channel between checks No. 1 and 2. Lightning arresters (to be included with the alarm system) had not yet been installed. Failure of the control equipment was very similar to the failure during the 1972 prototype test program when an electrical storm occurred in the same locality. Equipment repairs were easily made in a short time by simply replacing damaged printed circuit boards with replacements furnished with the control equipment. The damaged boards were sent to the E&R Center and defective components were replaced. The printed circuit boards were then returned to the Corning Canal to serve as replacements.

GENERAL THEORY OF EL-FLO PLUS RESET

The feedback system of the EL-FLO plus RESET controller has been applied to automatic downstream control of canal check gates. The downstream control concept is basically that of a negative feedback relationship between the water level in the canal reach, usually measured at the downstream end, and the discharge into the canal reach through a motor-operated check gate at the upstream end. "Downstream control" in this context means that the control of the changes in canalside demands downstream will progress toward the head of the canal or to the source of supply. This control, although contrived through electronic sensors, real-time analog computer-comparators, and electromechanical gate controls, is like natural control in subcritical flow observed in backwater curves, namely, the control is from downstream to upstream.[1]

The signal generated by a change in canalside demand is transmitted nearly instantaneously from the downstream sensor to the upstream check gate. However, the speed at which the canal reach can respond to the signal, to satisfy the change of the downstream canalside demand, is very slow. The flow response time is relative to the time required for the change of discharge into the upstream end to traverse the canal reach and arrive at the downstream end through transient hydraulic wave action.

Rapid canal response times are necessary to ensure sensible coupling of the canalside turnout diversions and canal inlet flow. Rapid response times are limited by canal flow stability considerations and practical

water level recovery characteristics. The design problem is how to achieve the best canal flow response and meet selected stability criteria. [1]

The elements of the EL-FLO plus RESET feedback system are shown in figure 16. A technical description of each element is included in appendix III.

Figure 17 illustrates the location of each element relative to the canal reach and adjacent canal reaches. The first element is the sensor that measures the water level in the canal reach at the downstream end. The water level sensor converts the vertical change of the water level to rotation of a potentiometer to produce a voltage signal output, *YC*. The output signal of the water level sensor is delayed by the electronic filter to produce a phase lag between the point of sensing and filter output. The delay limits the response of the total flow change within the period of potential oscillation of the transient hydraulic traveling wave between check structures, figures 18c and 19c.

The output signal, *YF*, of the electronic filter is transmitted to and received at the upstream check gate. The received *YF* is the input to the EL-FLO proportional controller and is used in solving the equation:

$$GP = K1\,[YT - YF] \qquad (1)$$

where *GP* is the desired gate opening of the proportional mode of the feedback system, *K1* is the proportionality factor of the gain constant of the EL-FLO proportional controller, *YT* is the target value or the referenced input. The target value is the desired water level to be maintained for all steady state flows.

The output signal, *GP*, of the EL-FLO proportional controller provides the input signal to the RESET controller and electronically performs the following integration:

$$GR = K2 \int_0^t GP\,dt \qquad (2)$$

where *GR* is the desired gate opening of the reset mode of the feedback system, *K2* is the proportionality factor or the gain constant of the RESET controller, and *t* is time.

The total desired gate position, *GD*, is represented mathematically by the following equation:

$$GD = K1\,[YT - YF] + K2 \int_0^t K1\,[YT - YF]\,dt \qquad (3)$$

or

$$GD = GP + GR \qquad (4)$$

The output signals of the EL-FLO and RESET controllers, *GP* and *GR*, are the inputs to the comparator unit. The comparator unit sums the two inputs to obtain the desired gate position, *GD* (equation 4), and compares *GD* to the actual gate position, *GA*, to obtain the error signal, $\pm\Delta G$, as follows:

$$\pm\Delta G = GP + GR - GA = GD - GA \qquad (5)$$

where *GA* has an opposite polarity to *GP* and *GR*. The value of *GA* is measured by a potentiometer driven by the check gate hoist shaft. If the error signal $\pm\Delta G$ is greater than the referenced input or gate movement dead band, *DB*, (typically 0.03 m (0.10 ft) of gate opening), the comparator unit will energize the raise or lower relay of the actuator which in turn energizes the gate motor to raise or lower the gate depending on the polarity of the comparator unit output signal. The gate will then raise or lower until the comparator unit difference or error signal output is zero, at which time the gate motion stops. The referenced input, *DB*, of the comparator unit is necessary because of the very fast rate of gate movement relative to the computed desired gate position. [2]

All measured and computed values of the feedback control system must be correctly scaled and calibrated if each element in the feedback path is to perform in accordance with equations 3 through 5.

The selection of proper control parameters is essential to the stable operation of the EL-FLO plus RESET feedback control system and achieving desirable water level response characteristics. Control parameters are selected to eliminate instability inherent in automatic feedback control systems and to give a high degree of self-regulation, namely, the fastest response to the change of downstream canalside demands with recovery of the canal reach to a new steady state without excessive overshooting of the inlet flows or fluctuation of the water levels. The system must function over a wide range of canalside demand changes from a rapid change of 50 percent of designed capacity of a canal reach to a small change of less than 1 percent. The response characteristics of the EL-FLO controller without RESET will be described first, then with the RESET control action added, and then a comparison of control with and without the RESET action will be made.

Three control parameters used by the El-FLO controller provide primary control action during the unsteady-state flow conditions that occur immediately after a flow change downstream. These three control parameters are (1) the electronic filter time constant, *TF*,

(2) the water level offset ($YT - YF$) of equation 1, and (3) the proportionality factor or gain, $K1$ of equation 1.

The time constant of the electronic filter provides the stability of the control system by attenuating the critical frequencies of water level disturbances that tend to be amplified by the controller. The selection of the proper time constant is based on considerations of the hydraulic transient behavior of the open channel under study, the desired response of control action for the system or the amount of damping desired within a period of potential oscillation, as well as the desired magnitude of the "offset" from the target value. The offset ($YT - YF$), when multiplied by the proportionality factor $K1$, results in a positioning of the upstream gate to the proper opening to control the flow into the canal reach, equation 1. For stability, a decrease in the sensed depth (modified by the electronic filter) must produce an increase in flow into the canal reach to satisfy the requirements of a negative feedback system.

Figure 18 shows the characteristic response of a canal reach using the EL-FLO method of automatic downstream control (proportional mode of control) without the RESET controller (when $K2$ of equation 3 is zero). The response to a turnout of 0.3 m^3/s (11 ft^3/s) was plotted from the output of a mathematical model which simulated the canal reach and the EL-FLO method of proportional control. Figure 18a shows the schematic of the canal reach and the water surface profile at time zero. At time 10 minutes, a downstream canalside turnout flow was suddenly increased to 0.3 m^3/s, figure 18e. Figure 18c shows how the change in the downstream water level, YC, decreased and the lag or phase shift by the electronic filter, YF.

Figure 18b shows the required gate opening, GD, of the upstream check gate as computed by the EL-FLO controller using equation 1. The actual gate opening, GA, is the result of the comparator unit action using equation 5 (where reset control action, GR, is zero in this illustration). A narrow referenced input, DB, 0.009 m (0.03 ft) to the comparator unit was used for this example to increase the resolution of the computed and actual gate positions at steady-state flow conditions.

Figure 18d is a graph of the discharge through the upstream gate controlling the flow into the canal reach. This plot is primarily used to measure the success of the proper selection of the control parameters mentioned above. The ratio of two successive amplitudes, $\mathcal{K}$, shown on the discharge plot can be used to determine the degree of damping or attenuation of the initial disturbance. At time 80 minutes, figure 18d, the first amplitude, $A1$, measured from the base flow of 0.3 m^3/s is 0.054 m^3/s (1.9 ft^3/s). The second successive amplitude, $A2$, is measured at time 200 minutes and is 0.0057 m^3/s (0.2 ft^3/s). Therefore, the ratio, $\mathcal{K}$, of the two successive amplitudes of this example is:

$$\mathcal{K} = \frac{A2}{A1} = \frac{0.0057\ m^3/s}{0.054\ m^3/s} = \frac{0.2\ ft^3/s}{1.9\ ft^3/s} = 0.11 \qquad (6)$$

Using figure 21 [5], the damping ratio, δ/ω, is 0.70 for this example. A damping ratio of 0.6 or a successive amplitude ratio of 0.15 is considered ideal. Thus, in this example, the canal reach appears slightly overdamped. The report will show later that the EL-FLO proportional mode needs to be overdamped because the RESET control action, when added, reduces the damping or attenuation of the overall feedback control system. The percent overshoot can be determined by using the first amplitude, $A1$, and dividing it by the baseflow at the new steady state. The percent overshoot, from figure 18d, is:

$$\text{PERCENT OVERSHOOT} = \frac{0.05\ m^3/s}{0.3\ m^3/s} \times 100 = 18\ \text{percent} \qquad (7)$$

A smaller percent overshoot can be achieved if the gain, $K1$, is reduced; the offset, $YT - YF$, is increased; and the time constant, TF, is increased. However, the water level, YC, drawdown at time 60 minutes, figure 18c, will be greater and the recovery time to a new steady state will take a longer period of time. If a larger percent overshoot can be tolerated upstream at the source of supply, then the water level recovery, figure 18c, can be faster with less deviation or drawdown by increasing the gain and decreasing the offset and time constant.

The performance of the EL-FLO proportional mode of control can be demonstrated at 275 minutes by using equation 1 and figure 18. In this illustration, the gain was set at 3.0. Therefore, the upstream gate opening, GP, can be computed as follows:

$$\begin{aligned} GP &= K1\,(YT - YF) \\ &= 3.0\ [1.28\ m - 1.25\ m] = 0.09\ m \\ &= 3.0\ [4.20\ ft - 4.103\ ft] = 0.29\ ft \end{aligned} \qquad (8)$$

The upstream gate opening can be computed in this manner at any selected time and the EL-FLO proportional controller is continuously doing this computation.

The coupling of the downstream canalside demand to the flow into the canal reach upstream through the upstream check gate has been satisfactorily accomplished.

The downstream demand of 0.3 m^3/s (11 ft^3/s) is proportional to the downstream water level offset *(YT - YF)* of 0.03 m (0.097 ft) and to the upstream gate opening through the proportional gain. The resultant gate opening at the new steady state will produce a flow of 0.3 m^3/s into the canal reach to balance the quantity being taken out of the canal reach as a downstream demand.

The water surface profile of the canal reach at the new steady-state flow is shown in figure 18f at time 400 minutes. However, the steady-state flow has essentially been reached at time 120 minutes after the change in the canalside demand downstream had taken place. The recovery time is typical of the response characteristic of the EL-FLO proportional mode of control.

The offset at the new steady-state flow is 0.03 m. Another way of expressing the offset is in terms of the steady-state discharge per length of offset or $(m^3/s)/m$ or $(ft^3/s)/ft$. Per this illustration, the discharge per unit length of offset is:

$$\frac{0.3\ m^3/s}{0.03\ m} = 10\ (m^3/s)\ /m \quad \text{or}$$

$$\frac{11\ ft^3/s}{0.097\ ft} = 113.4\ (ft^3/s)\ /ft \qquad (9)$$

The purpose of the calculation of equation 9 is to eliminate the maximum offset in the water level at maximum designed discharge of the canal reach which in this example is 3.1 m^3/s (110 ft^3/s). The maximum offset in this example would be about 0.3 m (1 ft). It is emphasized that the change of discharge is not linear over the offset distance because the gain of the feedback system is held constant. The example illustrates two restrictions the proportional mode of control imposes on operating the canal: (1) the maximum discharge of the reach cannot be achieved at the 0.3-meter (1-ft) offset because the reach was designed for maximum flow at a target depth, *YT*, of 1.28 m (4.20 ft), and (2) the 0.3-meter (1-ft) offset may interfere with proper delivery to gravity-type turnouts if the loss of head (equal to the offset) on the turnout gate was not taken into account in the design of the reach.

One way to eliminate the two problems above is to set the referenced input to the EL-FLO proportional controller or the target depth, *YT*, to 1.59 m (5.20 ft) instead of 1.28 m (4.20 ft). However, most canal reaches are not designed or constructed with sufficient canal freeboard to permit a higher operating depth. Another way to eliminate these restrictions is to have a canal operator periodically manually adjust the target value to fit the flow conditions of the canal system during the irrigation season. The two solutions, increased canal freeboard or manual adjustment by an operator, to eliminate the potential reduction of canal capacity and turnout flow capability previously described would probably be too costly. Greater canal freeboard and larger-size turnouts would have to be constructed and would add to the cost of construction. A canal system that has pump-type turnouts would probably not be affected by the offset or reduced water level at the pump intake but the reduced flow capacity of the canal system caused by the offset would still remain a problem.

Therefore, the EL-FLO proportional control method of automatic downstream control introduces an offset resulting in reduced canal flow and turnout capacities unless costly adjustments are made to the normal design of the canal reach.

The least expensive method for eliminating the limitations of the EL-FLO proportional control method is to add RESET capability to the feedback control system. The primary function of a RESET controller is to eliminate the residual water level offset of the EL-FLO proportional controller and thereby restore the canal capability for maximum flow and designed turnout capacities. The referenced input target value, for the EL-FLO plus RESET feedback control system is selected for the depth at the maximum designed discharge.

In the example, the target value is 1.28 m (4.20 ft) for a maximum designed flow of 3.1 m^3/s (110 ft^3/s).

Figure 19 shows the response of the example canal reach using the EL-FLO plus RESET method of automatic downstream control (proportional mode plus proportional RESET action mode of control). A turnout of 0.3 m^3/s (11 ft^3/s) was made at the downstream canalside at time 10 minutes starting from zero flow conditions in the canal reach, figures 19a and e.

The most significant change noted with RESET action is the recovery of the downstrean water level, *YC*, (fig. 19c) to within 0.003 m (0.01 ft) of the target value, *YT*, of 1.28 m (4.20 ft) at time 140 minutes. Figure 19b shows the desired gate opening, *GD*, of the upstream check gate as computed by the EL-FLO plus RESET controller using equations 3 and 4. The actual gate position, *GA*, is the result of the comparator unit action using equation 5 (in this illustration, the gain (*K2*) of the RESET controller is **not** zero). Figure 19b also shows a plot of EL-FLO proportional and the RESET action control outputs separately. If the separate outputs were added (*GR* + *GP*), the sum

would be the desired gate opening. Observe that the EL-FLO proportional controller output (*GP*), provides the primary control response immediately after the flow change downstream has taken place. As a new steady-state flow condition develops at target water depth, the EL-FLO proportional mode control influence approaches zero and the RESET controller provides the primary control response.

Figure 19d is the discharge through the upstream gate. The success of control parameter selection with RESET action can be measured again. The ratio, $\mathcal{K}$, of two successive discharge amplitudes is:

$$\mathcal{K} = \frac{A2}{A1} = \frac{0.023\ m^3/s}{0.153\ m^3/s} = \frac{0.8\ ft^3/s}{5.4\ ft^3/s} = 0.148 \qquad (10)$$

From figure 21, the damping ratio (δ/ω) is 0.60. This value is the desired damping or attenuation of the disturbance that will give the fastest recovery to a new steady state without excessive cycling of the inlet flows or deviation of the canal water levels. The overdamped feedback system of the EL-FLO controller without RESET (fig. 18d) has been reduced from a damping ratio of 0.70 to 0.60 by adding the RESET controller. This example demonstrates that the RESET control has the tendency of reducing the damping or attenuation when added and, if precautions are not taken, it could cause underdamping and result in a stable feedback control system becoming unstable.

The percent overshoot of the inlet discharge, figure 19d, is:

$$\text{PERCENT OVERSHOOT} = \frac{0.153\ m^3/s}{0.3\ m^3/s} \times 100 = 51 \text{ percent} \qquad (11)$$

In this illustration, the percent overshoot appears too high and can be reduced by decreasing the proportional reset gain (*K2*) of equation 3. However, the recovery time to eliminate 90 percent of the residual offset and to achieve a new steady state will be longer. The percent overshoot has increased from 18 percent (equation 7) without RESET control action to 51 percent (equation 10) with the RESET control action. The additional inlet flow to eliminate the residual offset is accumulative for each successive canal reach upstream. The excess flow can become very large if elimination of the residual offset is to be accomplished within 2 hours after the initial disturbance has taken place as shown in figure 19c. To permit an accumulation of inlet flow at the head of the canal to eliminate the residual water level offsets in the canal downstream, the source of supply must have the flexibility to accommodate the larger overshoot of canal flow demand. If the canal system inlet is a pumping plant, then the accumulation of canal flows in response to a change in canalside demands may require additional units to be turned on during the period that the canal water levels are recovering to their target valves. The additional units needed may exceed the capacity of the pumping plant when the accumulation of inlet flows occur at higher baseflow conditions. As a result, the recovery will take longer if required additional pump capacity is not available.

The selection of the RESET gain (*K2*) is somewhat arbitrary. Previous discussion of a fast elimination of the residual offset inherent to the EL-FLO proportional mode or a large RESET proportional gain showed undesirable effects can occur at the headworks of a canal system. However, the gain cannot be too small because a too long period of adjustment may be required to eliminate the residual offset. The long period would allow the canal level to decrease and reduce the capacity of gravity-type canal turnouts. The reduction of canal flow capacity could still be eliminated, but only after a long period of time. Therefore, the selection of the RESET gain is based primarily on how fast the system should recover. A practical recovery characteristic for the EL-FLO plus RESET feedback control system is a 90 percent recovery rate of the residual offset after about 4 hours from the time of the initial disturbance and a damping ratio, δ/ω, of 0.6 with only one major initial cycle of the inlet flow (fig. 19d).

The performance of the EL-FLO plus RESET feedback control system can be demonstrated at 140 minutes by using equation 3 and figure 19. In this illustration, the proportional mode gain (*K1*) remains the same as the previous example at 3.0. The RESET gain (*K2*) is 0.010 per minute.

The RESET controller provides integration of the EL-FLO proportional mode output *(GP)* with respect to time, figure 19b. In this illustration, the area of 2.57 m·min (8.42 ft·min) under the graph of the electronic filter output (*YF*) was measured by planimeter. The area under the output of the EL-FLO proportional mode output (*GP*) is larger by a factor equal to the proportional gain, or 7.71 m·min (25.26 ft·min). Therefore, the total upstream desired gate opening can be computed as follows:

$$GD = GP + GR$$

$$GD = K1\,(YT - YF) + K2 \int_0^t K1\,(YT - YF)\,dt$$

$$= 3.0\,(1.280\ m - 1.273\ m) + (0.010\ min^{-1})\,(7.71\ m \cdot min)$$

$$= 0.022\ m + 0.077\ m = 0.099\ m \quad \text{or} \qquad (12)$$

$= 3.0\ (4.20\ \text{ft} - 4.176\ \text{ft}) + 0.010\ \text{min}^{-1}\ (25.26\ \text{ft}\cdot\text{min})$

$= 0.072\ \text{ft} + 0.253\ \text{ft} = 0.325\ \text{ft}$

The upstream desired gate opening can be computed in this manner at any selected time. The EL-FLO plus RESET feedback control system does this computation continuously. Note that although the RESET controller is physically eliminating the residual offset of the canal water level (*YC*), the RESET controller is essentially storing this information as the EL-FLO controller output (*GP*) approaches zero. The stored offset (*YT* - *YF*) can be calculated by taking the integration of the RESET controller, 7.71 m·min (25.26 ft·min), and multiplying by the ratio of the two controller gains (*K2* divided by *K1*) at time 140 minutes from figure 19 as follows:

$$\text{Stored offset} = \frac{K2}{K1} \int_0^t K1\ (YT - YF)\ dt \qquad (13)$$

$$= \frac{0.010}{3.0}(7.71\ \text{m}\cdot\text{min.}) = 0.026\ \text{m} \qquad (14)$$

$$= \frac{0.010}{3.0}(25.26\ \text{ft}\cdot\text{min}) = 0.084\ \text{ft}$$

This calculation and the previous gate position calculation, equations 12 and 13, are presented to demonstrate that the EL-FLO plus RESET feedback control system functions with a negative feedback characteristic. A relationship coupling the downstream demands to the inlet flow exists at all times and provides a high degree of self-regulation requiring virtually no manual intervention.

The water surface profile of the canal reach at the new steady-state flow at time 400 minutes is shown in figure 19f. The steady-state flow, however, had essentially been reached in about 140 minutes after the downstream change in canalside demand. A comparison of water surface profiles between figures 18f without RESET action and 19f with RESET action shows that the head differential across the upstream check gate would be slightly smaller when the downstream water level recovers to the target value. The decrease in head differential accounts for a slightly larger gate opening requirement, 0.099 m (0.32 ft) (fig. 19b), to that shown in figure 18b, 0.09 m (0.29 ft), to produce the same discharge at steady-state flow.

Figure 20 (a composite of figs. 18 and 19) compares the characteristic canal reach response between the EL-FLO proportional plus RESET action versus the EL-FLO proportional method (without RESET) of automatic downstream control for the 31.4 m^3/s (111 ft^3/s) downstream turnout. The graphs allow direct comparison of the differences with and without RESET control action.

The elimination of the residual offset with RESET action can be observed in figure 20c. Note that the initial drawdown of the canal reach downstream water level (*YC*) is essentially the same for both methods of control. The upstream gate opening is much larger with RESET action in order to supply additional inlet flow to recover the downstream water level back to the target value, *YT*. The upstream gate with RESET action remains open slightly more than without RESET action to accommodate the smaller head differential across the gate, figure 20f.

The discharge through the upstream check gate with and without the RESET controller is compared in figure 20d. The main difference illustrated is the larger overshoot that occurs with RESET control action. Figure 20d also demonstrates the desirable attenuation of the inlet flow and steady-state recovery after only 1.5 cycles. The 1.5 cycles is an important recovery characteristic if the canal is supplied from a pumping plant. More cycling would probably require additional on and off cycles of the pump units, increasing the pumping plant maintenance cost.

Control parameters must be selected carefully to achieve a stable control system and obtain the desired recovery characteristics if all the canal reaches are equipped with the EL-FLO plus RESET feedback control system. The selection must consider the delivery capability of canal system inlet facilities.

Information on selection of control parameters for the proportional mode of control without RESET action can be found in references 4 and 5. However, the procedure described in these references is being improved and the improvement will include a method to select the gain factor (*K2*) for the RESET controller. The method of selection under study requires mathematical model simulation of the system being controlled and the imposed controller. The mathematical simulation involves the use of a large digital computer system such as the E&R Center's CYBER 70 computer. It is not known at this time if the proper control parameter selection for the EL-FLO plus RESET feedback control system can be presented in nomograph form which would be advantageous to designers who do not have the mathematical model simulation capability.

Appendix V specifically describes the procedure used to convert the control parameters (once they have been selected) into electrical equivalent values that are used within the EL-FLO plus RESET feedback control system equipment.

LABORATORY VERIFICATION TEST

General

The purpose of the laboratory test was to verify that the final prototype EL-FLO plus RESET controller operated identically to the mathematical model simulated controller. The control parameters used in the mathematical model were converted into equivalent electronic values and adjusted into final prototype EL-FLO plus RESET control equipment.

Laboratory Simulation

The laboratory test facilities used for the prototype EL-FLO plus RESET control equipment verification tests are shown in figure 11. The downstream chassis which includes the water level sensor, electronic filter, and the transmitting equipment was placed over a water tank. The water level inside the tank was changed manually by manipulating water pressure inlet and drain valves to follow, as closely as possible, the change in canal water level (*YC*) predicted by the mathematical model. The upstream control chassis which includes the analog computer-comparator circuits and the receiver unit was placed on an adjacent table. A simulated canal gate hoist motor drive with a potentiometer was used to complete the comparator unit feedback circuit of the actual gate opening, *GA*.

Testing of the EL-FLO plus RESET controller in an open-loop feedback system was necessary in order to analyze the performance of the control equipment as compared to the mathematical model simulated control system.

The laboratory verification test program included the elements of the feedback path as shown in figure 16 with the exception of the canal reach between sensor and upstream gate. The feedback system was, therefore, an open loop. The input was the water level sensor response to the change in the tank water level. The tank water level was adjusted according to the mathematical model prediction of the canal response to a change in a downstream canalside demand. Deviations of the equipment response could then be examined and defined with greater accuracy. In the closed-loop system with the downstream canal reach present, errors that may be in the control equipment would be self-compensating and, therefore, would be greatly reduced or appear not to occur when examining the total feedback control system.

Laboratory Verification Test Results

The summary of the final prototype EL-FLO plus RESET control equipment versus the mathematical model laboratory verification test results is shown in figure 22. The equipment output voltages were converted to feet for plotting in figure 22 with the same scaling factors (volts per foot) used to develop the control parameters in electronic equivalences.

The input to the laboratory test system corresponded to the mathematical model computed canal water depth, *YC*, figure 22a. The dashed lines in figure 22 are the mathematical model outputs and the solid lines with circled data points are the data of the prototype equipment output collected during the laboratory test run lasting for a period of 400 minutes. The upper graph includes the electronic filter output, *YF*. At time 260 minutes as the water level was rising, the float counterweight came to rest on top of the 0.3-m (12-in) float. The stoppage caused a deviation of the water level sensor and the electronic filter output until the counterweight was released at time 324 minutes. The sensor output immediately returned to the prevailing water level in the tank and the electronic filter to its proper output 25 minutes later. Figure 22b is a plot of the EL-FLO plus RESET control equipment actual gate opening and the computed gate openings corresponding to equations 1 through 5.

Figure 22a illustrates the close agreement between the water level sensor and electronic filter output of the controller and the mathematical model output for most of the test run. During the time period, 10 to about 25 minutes, the water level sensor output deviated from the mathematical model primarily because of the difficulty of manually changing the water level in the tank. During this period, the water level fall indicated by the mathematical model was at the fastest rate. As mentioned previously, there was a deviation in the equipment output during the period of time 260 to 324 minutes when the float counterweight was resting on top of the 0.30-m (12-in) float.

Figure 22b close agreement of the EL-FLO and RESET controller to the mathematical model during the first 60 minutes of the test run. After 60 minutes, the prototype equipment of the upstream chassis deviated from the mathematical model indicating that the equipment design was in error or the calibration of the control parameters was incorrect. However, at the end of the test run (time 400 minutes), all equipment outputs were in very close agreement with the mathematical model. The greatest deviation between the prototype equipment and the mathematical model appears at time 120 minutes.

Summary of Analysis of Laboratory Verification Test

An analysis of the prototype equipment output conditions was made at time 120 minutes of the test run to

define the differences and possible cause of error as compared to the mathematical model output at the same period of time. It was concluded that the prototype equipment was designed and constructed as represented by the algorithms in the mathematical model. A difference of 26.5 mm (0.087 ft) occurred at time 120 minutes (fig. 22b) between the mathematical model computed gate position, *GD* and the prototype EL-FLO plus RESET controller computed output. The detailed analysis, provided in appendix VI, determined that 10.4 mm (0.034 ft), 39 percent, of the 26.5-mm difference was caused by electronic drift and nonlinearity of the filter and EL-FLO plus RESET equipment components. Calibration errors contributed to 14.0 mm (0.046 ft), 53 percent, of the difference. The remaining 2.1 mm (0.007 ft), 8 percent, of the difference is attributed to accumulated errors in measurements by test voltmeters of the various equipment test points. Therefore, all of the difference between the mathematical model and the prototype equipment was identified as errors in drift, calibration, and measurement and not to incorrect design or construction.

Table 1 summarizes the outputs of the mathematical model and the EL-FLO plus RESET prototype equipment of time 120 minutes. The errors caused by calibration and drift are tabulated for each element of the feedback path and are accumulated from the water level input to the EL-FLO plus RESET controller output, *GD*.

The prototype equipment operated with reasonable accuracy. The accumulated errors from the actual water level to the computed gate position, identified as drift and nonlinearity of the electronic circuitry, amounted to −6.1 percent. This magnitude of error is considered to be within the range of typical analog control equipment. The −6.1 percent error would not cause system instability and in a closed-loop negative feedback system, by definition, would be self-compensating and would be negligible. The errors of calibration can be easily eliminated by either adjusting the control parameters of the mathematical model to correspond to the actual calibration values of the prototype equipment or recalibrate the prototype equipment. Better agreement between the mathematical model and the prototype EL-FLO plus RESET controller in figure 22 would have been achieved by eliminating the calibration errors.

Figure 22b also shows the actual gate opening, *GA*, and the performance of the comparator unit, ΔG (equation 5). The mathematical model output shows a very precise operation of the comparator unit with a $\pm\Delta G$ equal to ±16.8 mm (0.055 ft). The prototype comparator unit averaged about ±18.3 mm (0.06 ft). A simulated gate hoist mechanism was used in the laboratory verification tests. However, the results of the prototype equipment actual gate openings in the laboratory provided a good representation of an actual canal check gate hoist mechanism. It should be noted (referring to fig. 22) that the operation of the comparator unit, $\pm\Delta G$, of the prototype equipment is not as precise as the mathematical model, particularly the "off" point when ΔG is zero. Usually, the prototype gate hoist mechanism will overrun after the gate hoist motor drive is shut off, particularly when the gate is in a lowering cycle such as occurred at time 120 minutes.

FIELD VERIFICATION TESTS

General

The purpose of the field tests was to verify that the mathematical model predicts with reasonable accuracy the performance of the prototype EL-FLO plus RESET controller and the hydraulic transients in a canal system. Field tests were conducted on the first reach of the South Gila Canal on September 19, 1973, and on the first five reaches of the Corning Canal on May 14 to 16, 1974. The collection of field data was not extensive and consisted primarily of recorded data of water levels immediately upstream of the check structures and the actual gate opening using electronic and mechanical chart recorders. Periodically, staff gage readings were recorded by operating personnel.

Because the data collection was minimal (not sufficient in quantity to identify precisely all the necessary input data to the mathematical model), a detailed analysis of the difference between the mathematical model output and the field scale prototype tests will not be made as was done in the laboratory verification tests. However, a general discussion on the overall performance of the prototype equipment compared to the mathematical model is presented.

South Gila Canal Prototype Field Test

Figure 23 is a schematic of the first reach of the South Gila Canal and includes the basic physical design properties used in the mathematical model. Reference is also made to appendix V that includes the control parameters and their electronic equivalences used in the prototype EL-FLO plus RESET controller.

Figure 24 is the electronic chart recordings of the South Gila Canal prototype field test conducted on

Table 1. — *Summary of the laboratory verification studies of the mathematical model versus the prototype EL-FLO plus RESET outputs at time 120 minutes (Refer to fig. 22)*

Feedback path	Mathematical model output mm (ft)	Prototype equpiment output mm (ft)	Difference between outputs mm (ft)	Error Identification			Equip. error per-cent	Accumulative equipment error	
				Accum. error mm (ft)	Calib. error [c] mm (ft)	Equip. error mm (ft)		mm (ft)	percent
Water level, *YC*	1262.8 (4.143)	1262.5 (4.142)	−0.3 (−0.001)	−0.0 (−0.000)	−0.3 (−0.001)	0.0 (0.000)			
Water level sensor, *YC*	1262.8 (4.143)	1262.5 (4.142)	−0.3 (−0.001)	−0.3 (−0.001)	0.0 (0.000)	0.0 (0.000)	0.0	0.0 (0.000)	0.0
Electronic Filter, *YF*	1243.6 (4.080)	1245.4 (4.086)	+1.8 (+0.006)	−0.3 (−0.001)	0.0 (0.000)	+2.1 (+0.007)	+0.2	+2.1 (+0.007)	+0.2
EL-FLO controller, *GP* [a]	109.1 (0.358)	96.9 (0.318)	−12.2 (−0.040)	−6.1 (−0.020)	−3.4 (−0.011)	−2.7 (−0.009)	−2.8	−8.8 (−0.029)	−9.1
RESET controller, *GR*	87.2 (0.286)	72.8 (0.239)	−14.3 (−0.047)	−3.0 (−0.010) [b]	−8.5 (−0.028)	−2.1 (−0.007)	−2.9	−4.3 (−0.014)	−5.9
EL-FLO plus RESET, *GD*	196.3 (0.644)	169.8 (0.557)	−26.5 (−0.087)	−26.5 (−0.087)	0.0 (0.000)	0.0 (0.000)	0.0	−10.4 (−0.034)	−6.1

[a] Includes the transmitter and receiver elements of the feedback path.

[b] 1.8 mm (0.006 ft) of the accumulated error is attributed to the calibration error of the EL-FLO controller, *GP*.

[c] The accumulated calibration error of the filter and EL-FLO plus RESET controller is 14.0 mm (0.046 ft) and includes the 1.8 mm (0.006 ft) identified in footnote b.

September 19, 1973. The upper chart (fig. 24a) was recorded at the downstream end of the first canal reach of mile post (M. P.) 1.9 and measured the canal water level, *YC*, and the electronic filter output, *YF*. The lower chart (fig. 24b) was recorded near the headworks of the canal (at M. P. 0.14) and measured the actual headgate opening, *GA*, and the RESET controller output, *GR*. Periodically, the water level and gate opening staff gages were read and recorded on the chart paper including the test points electronic values of the EL-FLO plus RESET controller. The electronic values of the downstream water level (M. P. 1.9) and the headgate opening (M. P. 0.0) from figure 24 chart recordings were converted to linear measure and plotted on figure 25. The graph was made to better define the prototype test canal response characteristics and to better compare the mathematical model output.

The test period is 780 minutes or 13 hours and began and ended with steady-state flow conditions. The chronological order of events that occurred during the test period are listed and described as follows:

Time of the event (minutes)	Description of the Event
0	Beginning of test period (steady-state flow conditions). Headgate (M. P. 0.0) opening at 0.213 m (0.70 ft) discharging 1.16 m^3/s (41 ft^3/s). Turnout lateral M. P. 0.5 flow was zero. Turnout lateral M. P. 1.9 flow was 0.15 m^3/s (5.2 ft^3/s) and remained constant throughout the test period. The M. P. 1.9 gate opening was 0.317 m (1.04 ft) discharging 1.03 m^3/s (35.8 ft^3/s).
16	The check M. P. 1.9 gate opening increased from 0.317 m (1.04 ft) to 0.378 m (1.24 ft).
226	The check M. P. 1.9 gate opening decreased from 0.378 m (1.24 ft) to 0.344 m (1.13 ft).
262	The canalside turnout lateral M. P. 0.5 was turned on to increase the flow from 0 to 0.35 m^3/s (12.8 ft^3/s).
557	The check M. P. 1.9 gate opening decreased from 0.344 m (1.13 ft) to 0.256 m (0.84 ft).
780	End of test period (steady-state flow conditions). Headgate (M. P. 0.0) opening at 0.229 m (0.75 ft). Turnout lateral M. P. 0.5 flow was 0.36 m^3/s (12.8 ft^3/s). Turnout lateral M. P. 1.9 flow was 0.15 m^3/s (5.2 ft^3/s). The check M. P. 1.9 gate opening was 0.256 m (0.84 ft).

Summary of the South Gila Prototype Field Test

Figure 25 compares the mathematical model output to the collected field data for the prototype EL-FLO plus RESET controller. The comparison illustrates the mathematical model simulated the prototype EL-FLO plus RESET automatic downstream canal system with reasonable accuracy.

The first major difference between the mathematical model and the actual field data occurred at time 262 minutes (fig. 25). A canalside demand was increased from 0 to 0.36 m^3/s (12.8 ft^3/s) at the turnout to lateral M. P. 0.5 at 262 minutes. The mathematical model, however, simulated the canalside turnout flow increase at the downstream end of the canal reach at M. P. 1.9. Therefore, the mathematical model did not show a delay of about 13 minutes for the flow change effect on the canal water level to arrive (time 275 minutes) at the downstream end of the canal reach and the water level sensor as it occurred in the actual canal system. The assumed location of the outflow in the mathematical model, being different from the location of lateral 0.5, may also partially account for the differences between the mathematical model output and the collected field data during the remainder of the test period.

Better agreement of the mathematical model output to the field data could have been shown if the water levels upstream of the canal headgate and downstream of check gate M. P. 1.9 had been recorded on a continuous basis. These water levels changed during the test period but were not recorded; estimations of these changes were used in the mathematical model. Also, the values of canalside diversions used in the mathematical model were average discharges and continuous recording may have shown variations of flow during the test period. Table 2 is the input data listing used in the South Gila Canal mathematical model verification studies and the listing is included for record purposes. The identification of the input data in table 2 may be found in reference 5.

Corning Canal Prototype Field Test

The Corning Canal prototype field test conducted May 14 to 16, 1974, provided data to verify the mathematical model of a canal and the EL-FLO plus

Table 2.—*Input data for the South Gila Canal mathematical model verification studies.*

```
      1          0          0
      2                                900
   .021    500.              40.     50000.
  -572.
-10239.
  6.0         .0          .00023
  5.0        1.5          .00023
  5.0        1.5          .00023
  4.75      41.0
  4.18      41.0
  2.40      35.8
     2         3       30
  .710    .666    .644    .636    .626    .619    .613    .606    .599    .591    .585
  0.70       1.04
  6.0        5.0
  1.81       0.09
 .00005     .000041
  0.05       0.0
  1.0        100.        2.0     1120.0       1.39         4.18
   .0080
  0.02       0.0         0.8        4.0        0.00033
       0.         0.          0.         0.          0.         0.          0.         0.
       0.         0.          0.         0.          0.         0.          0.         0.
       0.         0.          0          0.          0.         0.          0.         0.
       0.         0.          0.         0.          0.         0.          0.         0.
       0.         0.          0.         0.          0.         0.          0.         0.
       0.         0.          0.         0.          0.         5.2     15720.        18.
    00.   4.75 0.0  0.
          0.   0.   0.
          0.   0.00 0.
          0.   0.   0.
          0.   0.   0.
    16.   4.75 0.0  0.
          0.   2.60 0.
          0.   1.24 0.
    45.   5.55 0.0  0.
          0.   2.60 0.
          0.   1.24 0.
   102.   4.75 0.0  0.
          0.   2.60 0.
          0.   1.24 0.
   170.   5.15 0.0  0.
          0.   2.60 0.
          0.   1.24 0.
   226.   5.15 0.0  0.
          0.   2.76 0.
          0.   1.13 0.
   450.   5.75 0.0  0.
          0.   2.76 0.
          0.   1.13 0.
   557.   5.55 0.0  0.
          0.   2.86 0.
          0.   0.84 0.
   900.   0.   0.   0.
          0.   0.   0.
          0.   0.   0.
```

RESET method of control to an operating system much longer than the South Gila Canal. The Corning Canal test section included five canal reaches of various lengths for a total length of 21 km (13.03 mi.), four canal check gate structures, and the automatic Corning Canal pumping plant at the headworks. The final prototype EL-FLO plus RESET controllers (figs. 15a and b) were installed at the first four canal check gate structures. However, the water level sensor for the controller at check No. 4 (M. P. 10.65) was located immediately upstream of check No. 5 (M. P. 13.03). Figure 15c illustrates a typical installation of an EL-FLO plus RESET controller inside the stilling well shelter immediately upstream from a canal check gate structure on the Corning Canal.

The test section used for the May 1974 prototype test program discussed in this report is the same section of the Corning Canal used for the field verification tests conducted in March 1969. The March 1969 test program involved a concentrated effort (requiring 20 field personnel for each test run) to collect all the necessary field data to confirm the theoretical analyses and to observe the performance of a field scale application HyFLO method of control developed through the research and development contracts with the University of California. [7] The HyFLO method is a proportional mode of control and did not include the RESET mode of control. The March 1969 test runs and the mathematical model simulation of actual field contitions provided complete verification of the mathematical model. [1]

A concentrated effort to collect field data of the first order (as outlined in reference 7) was not made in May 1974 because of the cost involved and because complete verification of the mathematical model was accomplished in March 1969. It was reasoned that agreement could be shown between the mathematical model and an actual operating canal system from minimal field data. Fortunately, however, the May 1974 test period lasted 2700 minutes (45 hours), more than six times longer than the March 1969 test period of 6.7 hours. The May 1974 test period involved two steady-state flow conditions and three significant flow changes. The March 1969 test period did not include steady-state flows and involved only two major flow changes for each test run. Therefore, the May 1974 test program provided sufficient data to show the mathematical model simulated the final prototype EL-FLO plus RESET control system,.

Figure 26 is the profile of the Corning Canal system showing the canal check structure locations and the test section used for the May 1974 field test program. Table 3 lists the Corning Canal section properties and canal dimensions that were used in the mathematical model simulation studies. Table 4 summarizes the Corning Canal invert elevation, maximum design depth, and the water surface elevation upstream of each canal check gate structure. Table 5 is a summary of the estimated total canalside demand during the test period. The flow diversions at canalside turnouts for pools No. 1 through 5 were estimated based on the steady-state flow conditions established at the beginning of the test period. Canalside diversions were thought to remain constant throughout the test period. However, close examination of records of the water levels revealed that minor canalside flow changes had occurred and these changes were estimated for mathematical model input data. A better estimate of canalside diversion could have been made by obtaining a copy of the flow recorder charts of each turnout flow measuring device but this action was not considered necessary.

Table 6 lists the Corning Canal pumping plant and floating control system properties. The first three pump units, each having a discharge capacity of 1.5 m^3/s (53 ft^3/s), are automatically controlled from the water surface level immediately upstream of check No. 1 (M. P. 4.55). Pump units Nos. 1, 2, and 3, each has a water level dead band to start and stop pumping. When the water level goes below the low limit of a dead band, the assigned pump unit starts and remains on until the water level rises above the upper limit of the dead band, at which time the pump unit shuts off. The water surface elevation and depth for each dead band for each of the first three pump units are listed in table 6. The larger units (Nos. 4, 5, and 6,), each with a capacity of 3.5 m^3/s (125 ft^3/s), are operated manually. Unit No. 4 was started and stopped manually during the May 1974 test period at the times footnoted in table 6 corresponding to the significant flow changes at the Thomes Creek wasteway gate. A small adjustment had to be made to the target level of the floating control system dead bands of the mathematic model at time 800 minutes of the test period to correspond to the recorded field data. It was not determined if the calibration of the A35 chart recorder or the pump controller water level transmitter (both located immediately upstream of check No. 1) changed at this time. The time at which each automatic pumping unit (Nos. 1, 2, and 3) started and stopped (fig. 27a) was determined from the water level recording upstream from check No. 1 using the dead bands listed in table 6.

A continuous record of the water levels upstream and the gate openings of checks No. 1 through 5 were obtained from A35 type strip chart recorders installed at each location by field personnel. Periodically, the water level and gate opening staff gages (located nearby) were read by field personnel and the time and

Table 3.—*Corning Canal section properties.*

Earth Sect. No.	Length Mi. to Mi.		b Bottom Width	d Water Depth	H Lining Height	L Top Earth Lining Width	Minimum Earth Frbd.	Minimum D Canal Depth	Minimum Width W Lt. Bk.	Minimum Width W Rt. Bk.
			TABLE OF CANAL SECTION PROPERTIES CANAL DIMENSIONS							
1	.01	1.14	22'	7.2'	—	—	3.0'	10.20'	16'	16'
2	1.14	8.11	22'	7.2'	8.70'	56.80'	3.0'	10.20'	12'	10'
3	8.22	13.03	20'	6.39'	7.89'	51.56'	3.0'	9.39'	12'	9'
4	13.30	17.29	16'	4.92'	5.92'	39.68'	2.58'	7.50'	12'	8'
4 A	17.29	17.79	16'	3.55'	4.55'	33.08'	1.85'	5.40'	12'	5'
5	17.35	21.06	10'	3.55'	4.55'	28.20'	1.85'	5.40'	12'	5'

Sect. No.	A	V	h_v	Q	r	n	s
	HYDRAULIC PROPERTIES						
1	262.08	1.91	.057	500	4.84	.0225	.000098
2	261.1	1.91	.057	500	4.84	.0225	.000098
3	209.5	1.78	.049	372	4.31	.0225	.0001
4	127.1	2.09	.068	266	3.35	.0225	.0002
4 A	82.0	1.58	.039	129	2.57	.025	.0002
5	60.7	1.45	.033	88	2.35	.025	.0002

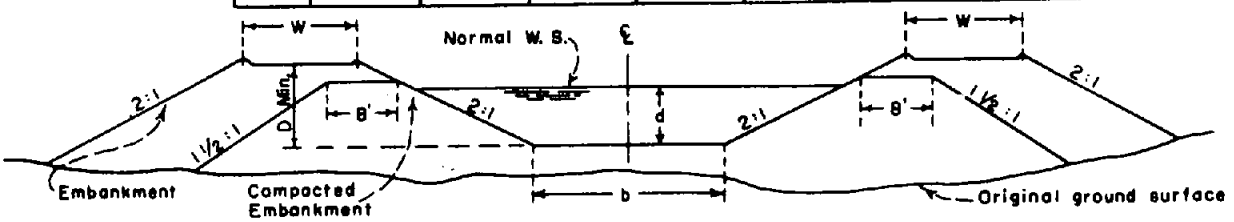

EARTH SECTION NO. 1

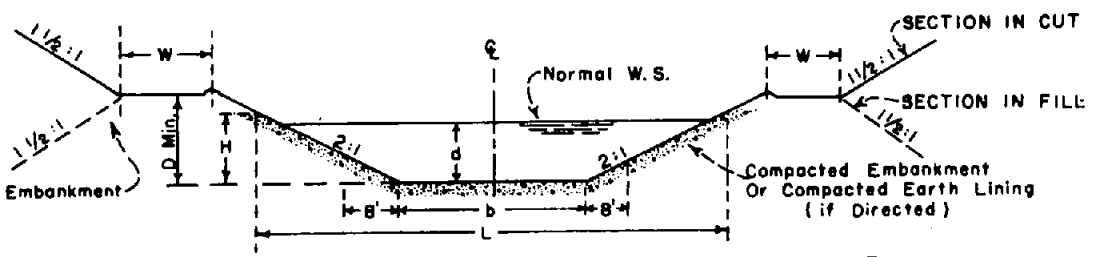

TYPICAL EARTH SECTIONS NO. 2 THRU NO. 5

Table 4.—*Corning Canal - Summary of properties at each check gate*

Check gate No.	Mile post	Upstream invert elevation meters (ft)	Upstream maximum design depth meters (ft)	Upstream water surface elevation meters (ft)
1	4.55	90.32 (296.33)	2.19 (7.20)	92.52 (303.53)
2	6.02	89.92 (295.00)	2.19 (7.20)	92.11 (302.20)
3	8.08	89.50 (293.64)	2.19 (7.20)	91.70 (300.84)
4	10.65	89.04 (292.11)	1.95 (6.39)	90.98 (298.50)
5	13.03	88.46 (290.23)	1.95 (6.39)	90.41 (296.62)
6	15.09	87.86 (288.26)	1.50 (4.92)	89.36 (293.18)
7	16.19	87.44 (286.89)	1.50 (4.92)	88.94 (291.81)
8	17.29	86.96 (285.30)	1.50 (4.92)	88.46 (290.22)
9	17.79	87.02 (285.49)	1.08 (3.55)	88.10 (289.04)
10	18.29	86.72 (284.52)	1.08 (3.55)	87.80 (288.07)
11	18.96	86.22 (282.89)	1.08 (3.55)	87.31 (286.44)
12	19.35	85.94 (281.97)	1.08 (3.55)	87.03 (285.52)
End of canal	20.73	85.22 (279.61)	1.08 (3.55)	86.31 (283.16)

readings were noted on the recorder charts during the test period. The Thomes Creek wasteway gate and check gate No. 5 were operated manually during the test. The water level downstream of check No. 5 was not recorded but should have been because of fluctuations during the test. The downstream water level fluctuation had a minor effect on the flow through check No. 5 gate. An estimate was made of the flow change and entered as a canalside demand in pool No. 5 for input data to the mathematical model. The gate opening recorder measured the arc travel distance of the radial gates, requiring conversion to a vertical distance opening of the gate. The conversion was accomplished by a graph of arc versus vertical distance. The recorded gate opening staff gage readings which are read directly to vertical gate opening, in feet, were used for the vertical distance. The water levels and gate openings (after being converted to vertical distance) were plotted to an expanded scale of depth gate opening, and time to better show the correspondence of the mathematical model simulated flow conditions to the test flow conditions, figures 27b through k.

The Corning Canal, May 1974, prototype field test period (time zero) began at 2000 hours on May 14 and ended at 1700 hours on May 16, 1974. The duration of the test period was 2700 minutes (45 h). However, for 12 hours prior to time zero, Thomes Creek check (M. P. 13.03) gate opening was held at a fixed position of 0.12 m (0.4 ft) discharging 0.96 m^3/s (34 ft^3/s) downstream. Thus, a steady-state flow condition was well established at time zero of the test period with a total canal demand of 2.8 m^3/s (98 ft^3/s) (refer to table 5).

The first major flow change occurred at time 610 minutes into the test when the steady flow was 2.6 m^3/s (93 ft^3/s). At this time, the Thomes Creek wasteway gate (M. P. 13.03, adjacent to the Thomes Creek check No. 5) was opened from zero to 0.21 m (0.68 ft) to discharge 1.7 m^3/s (61 ft^3/s) into Thomes Creek river channel for a total canalside demand of 4.4 m^3/s (154 ft^3/s). Discharging water into Thomes Creek was necessary to create a significant canalside demand for the field test. Usually, the changes of demand for irrigation water during the month of May are small and would not provide suitable test flow conditions. The discharge through the Thomes Creek wasteway was estimated by using an orifice equation with the measured head differential (1.22 m (4.0 ft)) across the gate, the gate width of 2.44 m (8 ft), and a coefficient of discharge of 0.7. A more accurate estimate of the canal flow could have been achieved with a current meter traverse taken immediately upstream of check No. 5. However, velocity measurements were not taken during the May 1974 test.

The second major flow change occurred at time 1080 minutes into the test period when the Thomes Creek wasteway gate was closed to the zero position. At

Table 5.—*Summary of estimated total canalside demand - Corning Canal prototype field tests, May 14-16, 1974*

Time of change, minutes	Canalside demands					Thomes Creek Wasteway flow	Thomes Creek check No. 5 flow	Total* demand
	Pool No.							
	1	2	3	4	5			
	m^3/s (ft^3/s)	m^3/s (ft^3/s)	m^3/s (ft^3/s)	m^3/s (ft^3/s)	m^3/s (ft^3/s)	m^3/s (ft^3/s)	m^3/s (ft^3/s)	m^3/s (ft^3/s)
0	0 (0)	0.42 (15)	0.37 (13)	0.74 (26)	0.28 (10.0)	0 (0)	0.96 (34)	2.77 (98.0)
10	0 (0)	0.42 (15)	0.37 (13)	0.48 (17)	0.28 (10.0)	0 (0)	0.96 (34)	2.52 (89.0)
75	0 (0)	0.42 (15)	0.37 (13)	0.48 (17)	0.40 (14.0)	0 (0)	0.96 (34)	2.63 (93.0)
110	0 (0)	0.42 (15)	0.37 (13)	0.48 (17)	0.48 (16.8)	0 (0)	0.96 (34)	2.71 (95.8)
400	0 (0)	0.42 (15)	0.37 (13)	0.48 (17)	0.42 (14.7)	0 (0)	0.96 (34)	2.65 (93.7)
610	0 (0)	0.42 (15)	0.37 (13)	0.48 (17)	0.40 (14.0)	1.73 (61)	0.96 (34)	4.36 (154.0)
1080	0 (0)	0.42 (15)	0.37 (13)	0.48 (17)	0 (0)	0 (0)	0.96 (34)	2.24 (79.0)
1105	0 (0)	0.42 (15)	0.37 (13)	0.48 (17)	0.56 (19.7)	0 (0)	0.96 (34)	2.79 (98.7)
1525	0 (0)	0.42 (15)	0.37 (13)	0.23 (8)	0.56 (19.7)	0 (0)	0.96 (34)	2.54 (89.7)
1690	0 (0)	0.42 (15)	0.37 (13)	0.48 (17)	0.56 (19.7)	0 (0)	0.96 (34)	2.79 (98.7)
2048	0 (0)	0.42 (15)	0.37 (13)	0.48 (17)	0.56 (19.7)	1.19 (42)	0.65 (23)	3.67 (129.7)
2600	0 (0)	0.42 (15)	0.37 (13)	0.48 (17)	0.56 (19.7)	0 (0)	0.65 (23)	2.48 (87.7)

*Date plotted on figure 27a.

Table 6. — *Corning Canal prototype field verification tests - Pumping plant and floating control system properties, May 14-16, 1974*

Unit No.	Unit capacity m^3/s (ft^3/s)	Status	Existing floating control				Mathematical Model	
			Elevation m (ft)	Depth[a] m (ft)	Adj. depth[b] 0-800 min m (ft)	Adj. depth[b] After 800 min m (ft)	Depth[c] 0-800 min m (ft)	Depth[c] After 800 min m (ft)
3	1.50 (53)	OFF	92.58 (303.75)	2.26 (7.42)	2.22 (7.27)	2.23 (7.32)	2.20 (7.22)	2.22 (7.27)
2	1.50 (53)	OFF	95.55 (303.65)	2.23 (7.32)	2.18 (7.17)	2.20 (7.22)	2.17 (7.12)	2.18 (7.17)
1	1.50 (53)	OFF	92.52 (303.55)	2.20 (7.22)	2.15 (7.07)	2.17 (7.12)	2.15 (7.07)	2.17 (7.12)
2	1.50 (53)	ON	92.49 (303.45)	2.17 (7.12)	2.13 (6.99)	2.15 (7.04)	2.14 (7.02)	2.15 (7.07)
1	1.50 (53)	ON	92.46 (303.35)	2.14 (7.02)	2.09 (6.87)	2.11 (6.92)	2.09 (6.87)	2.11 (6.92)
3	1.50 (53)	ON	92.43 (303.25)	2.11 (6.92)	2.07 (6.79)	2.08 (6.84)	2.08 (6.82)	2.09 (6.87)
4	3.54 (125)	Manual[d]	—	—	—	—	—	—

[a] Depths based on the designed target depth of 2.19 m (7.20 ft) at elevation 92.52 m (303.53 ft)

[b] Depths adjusted to a target depth of 2.15 m (7.05 ft) for the first 800 minutes and then to 2.16 m (7.10 ft) after 800 minutes to correspond to the recorded field data for the upstream water level of check No. 1, figure 27b.

[c] Depths used in the mathematical model studies for verification of mathematical model versus field data using same target depths as in footnote b.

[d] Unit No. 4 started and stopped manually. Started at 720 minutes, stopped at 1075 minutes, and then started at 2165 minutes.

about time 1250, the second steady-state flow condition started and continued until the third major flow change was made at time 2048 minutes into the test. At 2048 minutes, the Thomes Creek wasteway gate was opened 0.10 m (0.33 ft) and the Thomes Creek check gate No. 5 was closed from 0.12 m (0.4 ft) to 0.08 m (0.25 ft) for a net increase of canalside demand of 0.88 m^3/s (31 ft^3/s). The Thomes Creek wasteway gate was then closed to zero position at time 2600 minutes. The test period ended at time 2700 minutes and, thus, there was insufficient time to observe the effect of the flow change on the entire test section. The manual operation of the Thomes Creek wasteway gate and check No. 5 gate is plotted in figure 27k. The total estimated canalside demand is plotted in figure 27a.

Summary – May 1974 Field Test

The comparison of the collected field data of the Corning Canal May 1974 prototype field test and the output of the mathematical model simulating the canal test reach, with the same flow conditions, is shown in figure 27. The black lines are the plotted field data as discussed in previous paragraphs. The red and green lines are the plotted outputs from the mathematical model simulation, representing two different sets of control parameters for the EL-FLO plus RESET controllers at checks No. 1 through 4. The plotted red lines represent the simulated canal response characteristics using the control parameters (appendix V, table V-4) that existed in the EL-FLO plus RESET controllers during the May 1974 test. The green lines represent a second set of control parameters (table V-6) that were adjusted into the EL-FLO plus RESET controllers for checks No. 1 through 4 after controllers were put into operation on the remaining Corning Canal checks No. 5 through 12 downstream. The second set of control parameters will be discussed in detail in subsequent paragraphs.

Of primary interest, however, is the agreement achieved between the "real" and the "simulated" operating canal system (black and red lines, respectively). A cursory examination of figures 27a through k indicates the agreement between the real and the simulated operating canal system is not close. The magnitude of water level and gate opening amplitudes and frequency do not always agree point to point throughout the test period. However, if the comparison is examined over an extended period of time, there is a distinct similarity of the overall response characteristics between the field data and the simulated canal system. For example, the two steady-state flow conditions (time 0 to 610 and 1250 to 2050 minutes) have the same cyclic operation, namely, the amplitude and frequency of the water level fluctuation and gate operation are the same between the real and the simulated canal, figures 27a and b. The response characteristics between the real and the simulated canal during the unsteady-state flow conditions after the three major flow changes (starting at 610, 1080, and 2048 minutes, respectively) also have similar amplitudes and frequencies. Of major importance is the comparison of (1) the first amplitude of the unsteady state which indicates the percent overshoot, (2) the successive amplitudes which measure the attenuation of the disturbance, and (3) the recovery of the water levels to the new steady state (refer to the section on General Theory in this report), all of which are response characteristics to be examined to determine the success of the EL-FLO plus RESET performance. The same response characteristics (the overshoot, attenuation, and recovery) exist between the real and the simulated canal operation during the unsteady-state flow conditions. The cyclic operation of the Corning Canal pumping plant responding to the control characteristics also demonstrates the major effects the pumping units have on the water level and gate operation in the upper reaches of the Corning Canal.

There were short periods of time when there were significant deviations between the field data and the mathematical model output. This summary discussion will not resolve the causes of all deviations between the real and the simulated canal as was accomplished in the laboratory verification test analysis. The summary will illustrate the accuracy of mathematical model simulation of an operating canal system over an extended period of time using minimal field data for input. Table 7 is the input data used in the Corning Canal mathematical model verification studies of the May 1974 prototype field test with the first set of EL-FLO plus RESET control parameters (red line plotted output, fig. 27k). The identification of table 7 may be found in reference 5. The collection of additional field data at shorter intervals of time would have provided better input data to the mathematical model and better agreement could have been obtained on a point by point basis in figure 27k. The additional field data should have included a continuous timed record of (1) the Corning Canal pumping plant operation, (2) all canalside turnout diversions in the test section, (3) the water level downstream from the Thomes Creek check No. 5, and (4) current meter traverses for canal flow measurements at selected points (especially at the end of the test section).

Although lacking complete field information, analysis shows the Corning Canal May 1974 prototype test demonstrated that the mathematical model predicted

Table 7.—*Input data for the Corning Canal mathematical model verification studies - First control parameter data set.*

```
        1          0          0
        5
   .026  1000.              40.    168000. 3000
-23889.
-31056.
-41806.
-55716.
-68633.
22.0         2.0          .000098
22.0         2.0          .000098
22.0         2.0          .000098
20.0         2.0          .0001
20.0         2.0          .0001
16.0         2.0          .0002
 7.10      133.0
 7.17       81.0
 7.05       63.0
 6.24       46.0
 6.51       34.0
 2.77       34.0
      6       25        25        33        44        59        73
  .715    .728    .758    .791    .828    .869    .918    .980   1.052   1.140   1.248
  1.22       0.89       0.39       0.34       0.37
 10.0       10.0       13.0       13.0       8.25
  0.63       0.31       0.26       0.66       0.0
.000000844.000000300.000005087.000002457.0
  0.16       0.0
  1.0      100.          2.0      800.          9.55       7.13
  1.0      100.          2.0     1000.          7.70       6.98
  1.0      100.          2.0     1300.          4.50       6.18
  1.0      100.          2.0     1700.          4.30       6.41
    .00330     .00240     .00420     .00470
  0.02       0.0        0.8        3.0          .00033
       0.         0.           0.         0.          0.         0.          0.         0.
       0.         0.           0.         0.          0.         0.          0.         0.
       0.         0.           0.         0.          0.         0.          0.         0.
       0.         0.           0.         0.          0.         0.          0.         0.
       0.         0.           0.         0.          0.         0.          0.         0.
       0.         0.           0.         0.          0.         0.        000.        15.
       0.         0.           0.         0.          0.         0.          0.         0.
       0.         0.           0.         0.          0.         0.        000.        13.
       0.         0.           0.         0.          0.         0.          0.         0.
       0.        26.         600.        17.       91500.       08.      101400.        17.
       0.0       10.        4500.        14.0       6600.       16.8      24000.        14.7
   36600.        75.       64800.         0.0      69000.       19.7     122880.        61.7
    00.    0.0  0.   0.    0.   0.   0.
                0.   0.    0.   0.   2.77 0.
                0.   0.    0.   0.   0.37 0.
                0.   0.    0.   0.22 0.   0.
                0.   0.    0.   0.   0.   0.
   2045.    0.0  0.   0.    0.   0.   0.
                0.   0.    0.   0.   2.77 0.
                0.   0.    0.   0.   0.25 0.
   3000.        0.   0.    0.   0.   0.   0.
                0.   0.    0.   0.   0.   0.
                0.   0.    0.   0.   0.   0.
                0.   0.    0.   0.   0.   0.
                0.   0.    0.   0.   0.   0.
```

Table 8.—*Input data for the Corning Canal mathematical model verification studies - Second control parameter data set.*

```
         1         0         1
         5
   .026   1000.            40.  168000. 3000
-23889.
-31056.
-41806.
-55716.
-68633.
22.0         2.0         .000098
22.0         2.0         .000098
22.0         2.0         .000098
20.0         2.0         .0001
20.0         2.0         .0001
16.0         2.0         .0002
 7.10      133.0
 7.17       81.0
 7.05       63.0
 6.24       46.0
 6.51       34.0
 2.77       34.0
      6       25       25       33       44       59       73
  .715   .728   .758   .791   .828   .869   .918   .980  1.052  1.140  1.248
  1.22      0.89      0.39      0.34      0.37
 10.0       10.0      13.0      13.0      8.25
  0.63      0.31      0.26      0.66      0.0
.000000844.000000300.000005087.000002457.0
  0.16      0.0
  1.0      100.         2.0     480.         6.50      7.13
  1.0      100.         2.0     730.         5.40      6.98
  1.0      100.         2.0    1030.         3.50      6.18
  1.0      100.         2.0     950.         4.00      6.41
   .00154    .00185    .00286    .00250
  0.02      0.0       0.8       3.0         .00033
      0.       0.          0.       0.          0.       0.          0.       0.
      0.       0.          0.       0.          0.       0.          0.       0.
      0.       0.          0.       0.          0.       0.          0.       0.
      0.       0.          0.       0.          0.       0.          0.       0.
      0.       0.          0.       0.          0.       0.          0.       0.
      0.       0.          0.       0.          0.       0.        000.      15.
      0.       0.          0.       0.          0.       0.          0.       0.
      0.       0.          0.       0.          0.       0.        000.      13.
      0.       0.          0.       0.          0.       0.          0.       0.
      0.      26.        600.      17.       91500.     08.     101400.      17.
      0.0     10.       4500.      14.0       6600.     16.8     24000.      14.7
  36600.      75.      64800.       0.0      69000.     19.7    122880.      61.7
   00.   0.0  0.   0.   0.   0.   0.
             0.   0.   0.   0.   2.77 0.
             0.   0.   0.   0.   0.37 0.
             0.   0.   0.   0.22 0.   0.
             0.   0.   0.   0.   0.   0.
  2045.  0.0  0.   0.   0.   0.   0.
             0.   0.   0.   0.   2.77 0.
             0.   0.   0.   0.   0.25 0.
  3000.      0.   0.   0.   0.   0.   0.
             0.   0.   0.   0.   0.   0.
             0.   0.   0.   0.   0.   0.
             0.   0.   0.   0.   0.   0.
             0.   0.   0.   0.   0.   0.
```

the overall response characteristics of a "real" operating canal system with reasonable precision. The mathematical model investigation of the response characteristics of a canal system for various other types of control methods and/or control parameters and different flow conditions can, therefore, be made with a high degree of confidence.

The confidence achieved was immediately put to use. Additional mathematical model investigations were made on the entire canal system to develop control parameters for the remaining EL-FLO plus RESET control units to be installed at checks No. 5 through 12. The mathematical model studies revealed the first set of control parameters, as used in the controllers for the first four check gates (and used during the May 1974 prototype field test), when applied to controllers on checks No. 5 through 12, caused excessive amplification of the changes of canalside demands made in the lower canal reaches (downstream from check No. 5) into the upper reaches. The excessive amplification of flow change would cause additional pump units to cycle which is not desirable from an efficient operation and maintenance standpoint. The mathematical model studies showed that the attenuation of the amplified flow change and the recovery of the canal to a new steady state would not be altered by the excessive amplification characteristics. However, the control parameters of the first four check structures were reduced to achieve a reduction in the amplification of the disturbance into the upper reaches and to prevent unnecessary additional pump unit cycling during the peak overshoot demand, Table V-6 lists the second set of control parameters established for the EL-FLO plus RESET controllers for the entire canal system (including checks No. 1 through 4) which are currently being used on the Corning Canal.

To demonstrate the effects of the reduced control parameters for the controllers at checks No. 1 through 4, the second set of control parameters (table 8 is the input data used in the mathematical model and the data may be identified using the input format found in reference 5) were inserted into the mathematical model that simulated the same May 1974 prototype field test. The output, plotted on figure 27 as the green lines, compares the canal response characteristics to the output of the first set of control parameters (red lines). The reduction of the amplification (which is the primary objective of the second set of control parameters) of the test flow disturbances at the upper end of the test reach can best be shown soon after each of the three major flow changes at times 725, 1200, and 2150 minutes into the test period, figures 27b through g. The recovery to the new steady state also has different response characteristics, namely, the water levels upstream from each check gate recover to the target levels less rapidly and with smaller transient wave amplitude. There is an overall reduction in the amplitude and frequency of water level fluctuation and gate operation cycling throughout the test period using the second set of control parameters compared to the first set (green and red lines, respectively).

The Corning Canal pumping plant operation, figure 27a, remained about the same in this analysis. The response characteristics at check No.1, figures 27b and c, did not change significantly with the reduced control parameters (table V-6). Thus, the investigation confirmed the pumping plant operation at the headworks of the canal system has a major influence on the canal response characteristics immediately downstream and the selection of the associated control parameters does not.

It was not necessary to conduct additional field tests to verify the improvement of the amplification characteristics in the upper canal reaches for the second set of control parameters. The May 1974 prototype field test verification studies demonstrated that mathematical model simulation of an operating canal system has reasonable precision of predicting the overall canal response characteristics. Therefore, an improvement of the EL-FLO plus RESET control system performance shown by the mathematical model can also be anticipated with a high degree of confidence for "real" canal systems.

BIBLIOGRAPHY

[1.] Harder, J. A., M. J. Shand, and C. P. Buyalski, "Automatic Downstream Control of Canal Check Gates by the Hydraulic Filter Level Offset (HyFLO) Method," a paper presented at Fifth Technical Conference, U. S. Committee on Irrigation, Drainage, and Flood Control, Denver, Colorado, October 8-9, 1971, and to the International Commission on Irrigation and Drainage, Eighth Congress, Varna, Bulgaria, May 1972.

[2.] Buyalski, C. P., "Basic Equipment in Automatic Delivery Systems," a paper presented at the National Irrigation Symposium, Irrigation Today and Tomorrow, Lincoln, Nebraska, November 10-13, 1970.

[3.] Sullivan. E. F., and C. P. Buyalski, "Operation of Central Valley Project Canals," a paper presented at the ASCE Irrigation and Drainage Conference on Automation of Irrigation and Drainage Systems, Phoenix, Arizona, November 13-16, 1968.

[4.] Shand, M. J., "Final Report – Automatic Downstream Control Systems for Irrigation Canals," Technical Report No. HEL-8-4 for Selection of Control Parameters for the Hydraulic Filter Level Offset (HyFLO) Method, University of California, Hydraulic Engineering Laboratory, Berkeley, California, August 1971.

[5.] Shand, M. J., "Final Report – The Hydraulic Filter Level Offset Method for the Feedback Control of Canal Checks," Technical Report No. HEL-8-3, Computer Program for System Simulating, University of California, Hydraulic Engineering Laboratory, Berkeley, California, June 1968.

[6.] Schuster, J. C., and E. A. Serfozo, "Study of Hydraulic Filter Level Offset (HyFLO) Equipment for Automatic Downstream Control of Canals," Report No. REC-ERC-72-3, Engineering and Research Center. Bureau of Reclamation, Denver, Colorado, January 1972.

[7.] Buyalski, C. P., and D. M. Fults, "Corning Canal Automatic Downstream Control Field Scale Application of the 'Feedback Method' Prototype Test Program for Test Schedules No. 1, 2, and 3," Central Valley Project, Sacramento, California, February 1969.

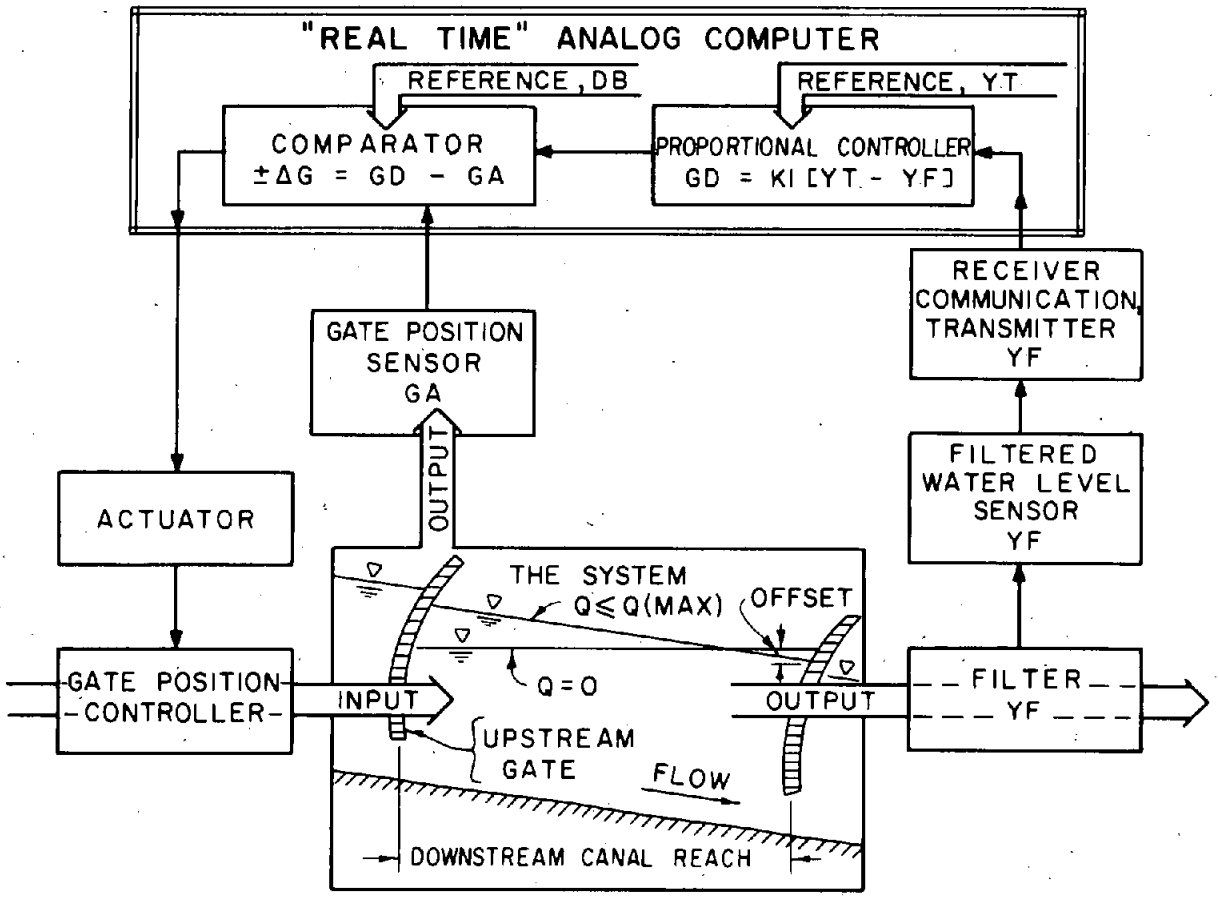

Figure 1.— HyFLO feedback control system.

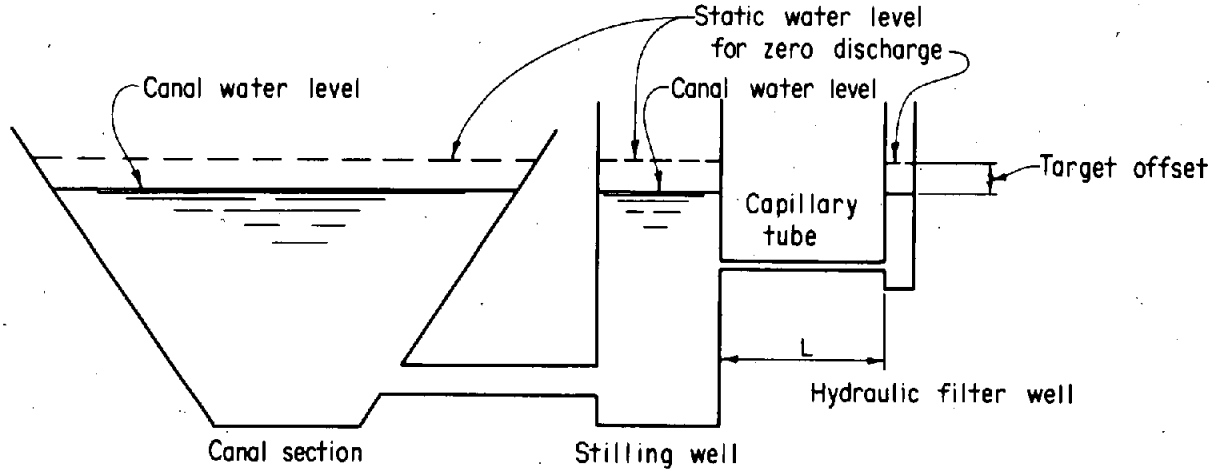

Figure 2.— Schematic of canal and hydraulic filter.

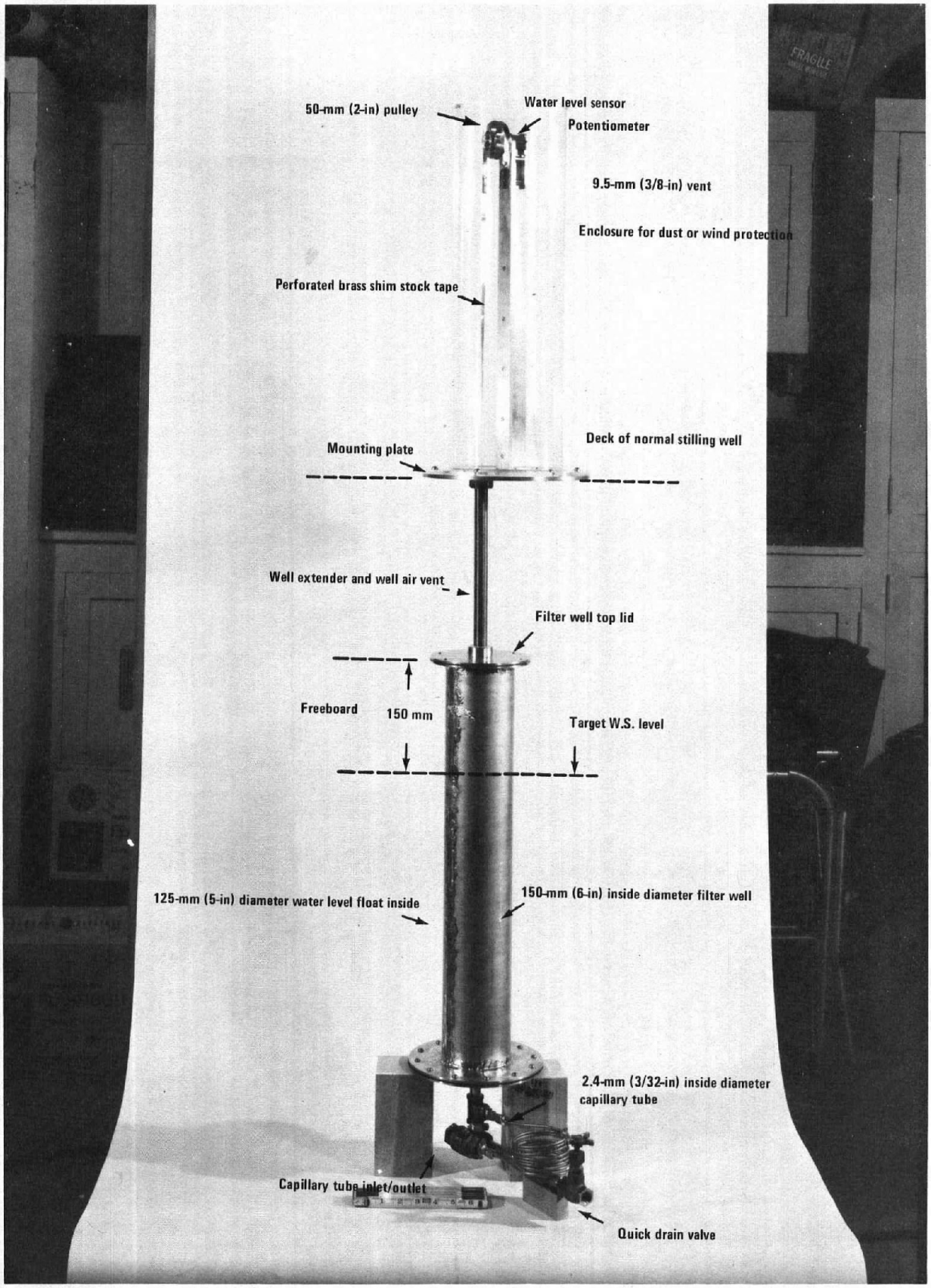

Figure 3.— New hydraulic filter and water level sensor assembled components. Photo P801-D-79048

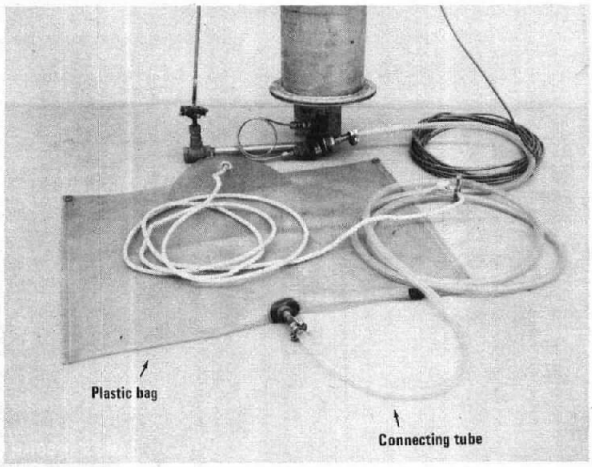

Figure 4.— Hydraulic filter well plastic bag for clean water supply. Photo P801-D-79050

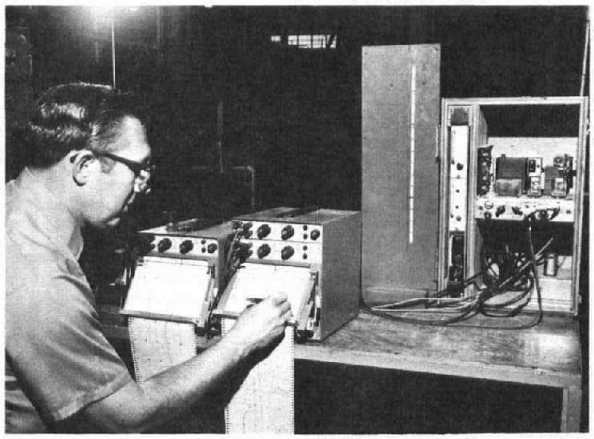

Figure 5.— View of the original modified HyFLO control chassis which was used in prototype tests, 1969-72. Photo P801-D-79049

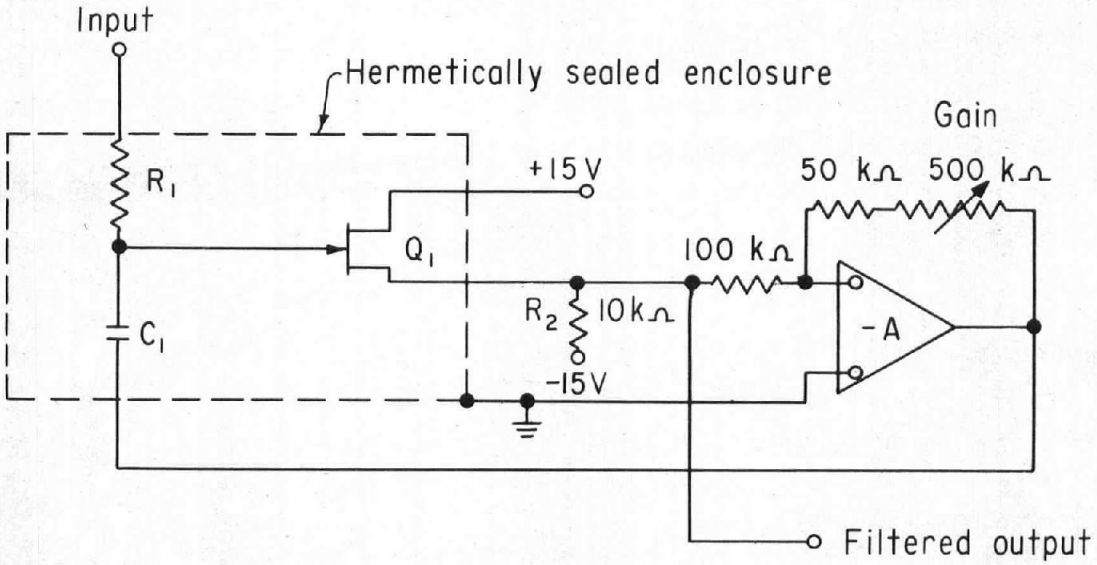

R_1 = 500 megohm
C_1 = 1 microfarad polystyrene
R_2 = 10 kΩ (or more - depends on FET type)
Q_1 = low leakage insulated gate, field effect transistor (FET)
A = operational amplifier

Time constant range: 1.5 to 5.5 times R_1 (R_1 in megohms)
Input range: 0 - 2.0 volts

Figure 6.— Single line diagram of original electronic filter circuit design.

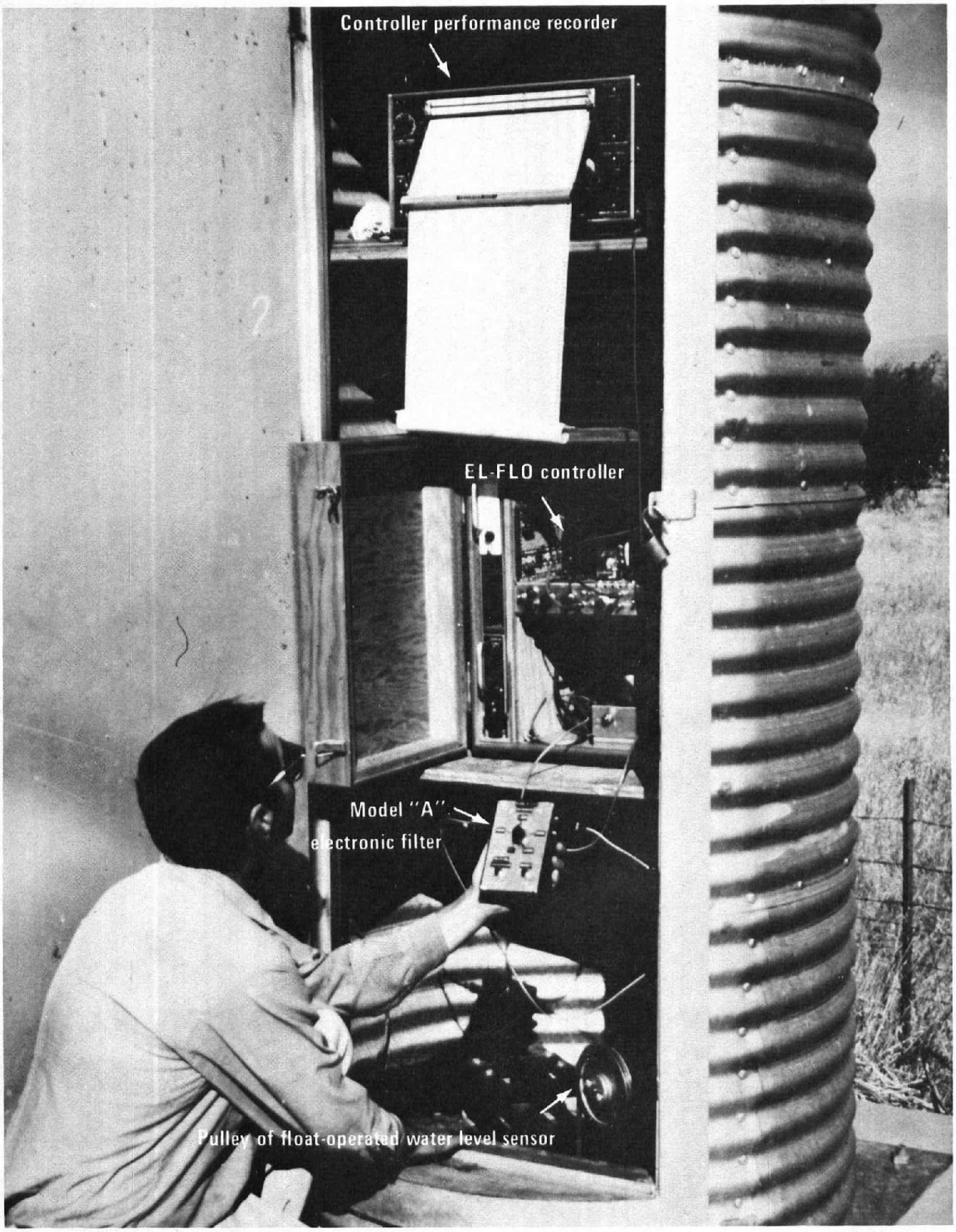

Figure 7.— Model "A" electronic filter field tested in November 1971. Photo P801-D-79051

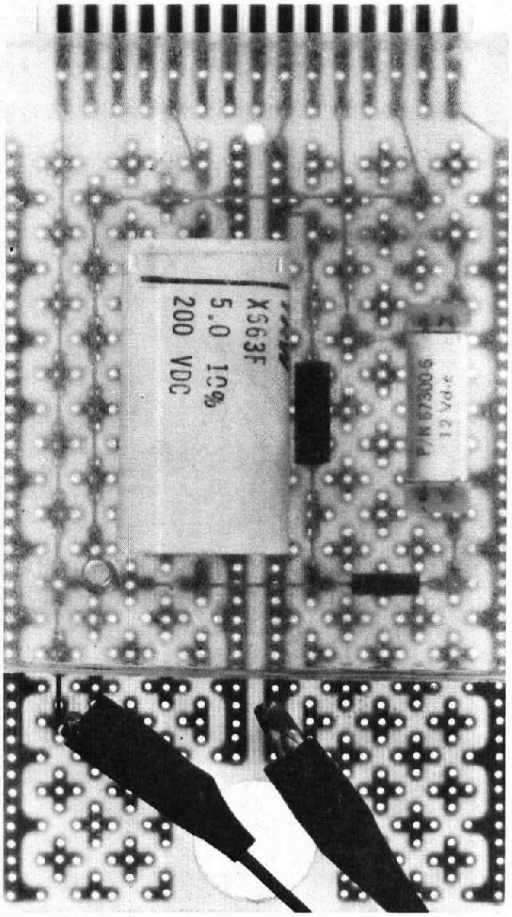

a. Top view of RC network

Photo P801-D-73152

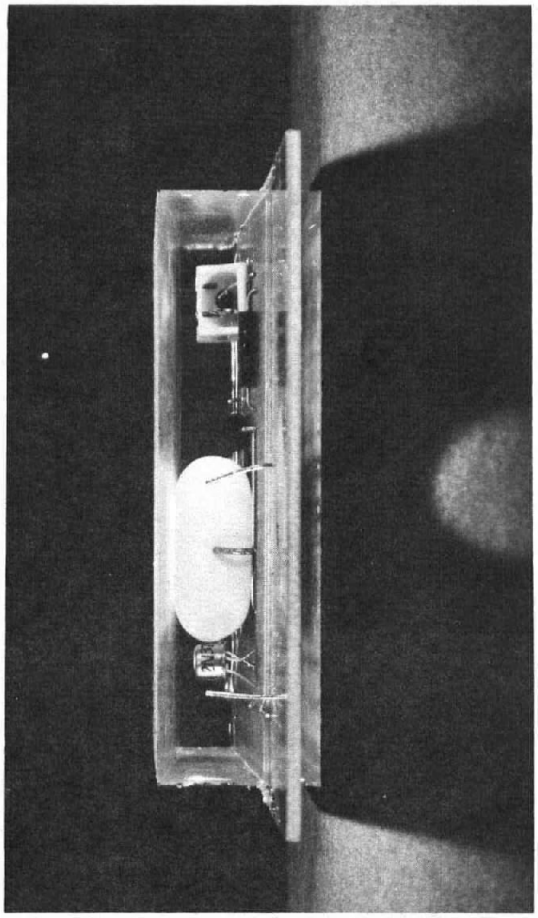

b. Front view of RC network

Photo P801-D-79053

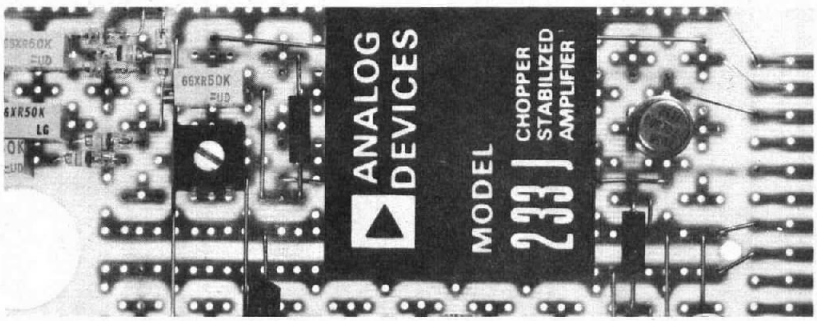

c. Top view of operation amplifier network

Photo P801-D-73158

Figure 8.— Electronic filter printed circuit boards.

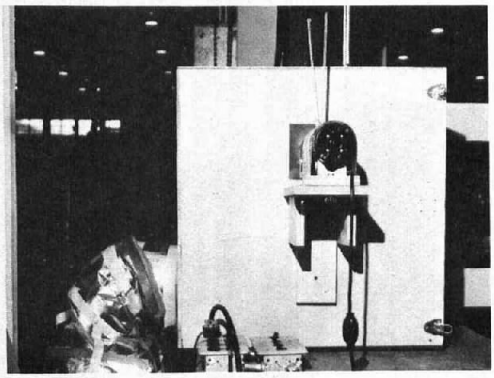

a. Sideview of environmental test chamber
Photo P801-D-79055

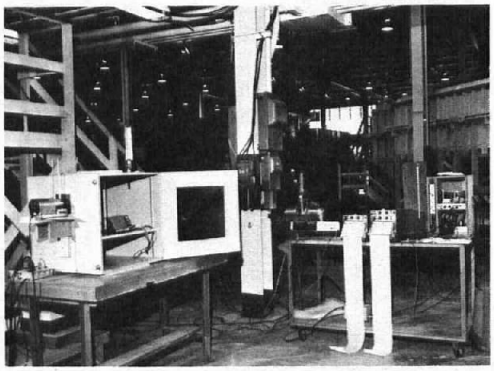

b. Overall view of electronic filter laboratory test facilities Photo P801-D-79058

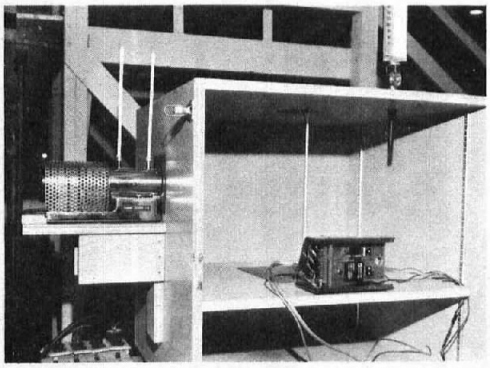

c. Frontview of the electronic filter inside the environmental test chamber
Photo P801-D-79057

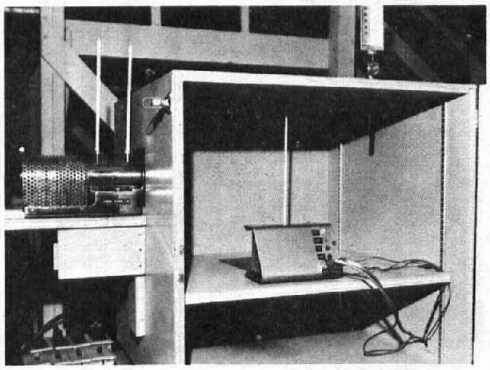

d. Rear view of electronic filter inside environmental test chamber Photo P801-D-79056

Figure 9.— Laboratory environmental test chamber used to simulate canal bank conditions.

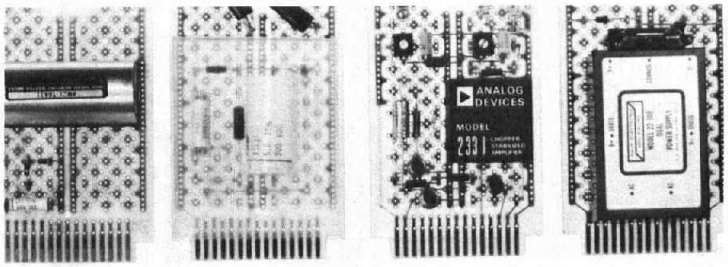

a. Printed circuit boards located in the downstream control chassis

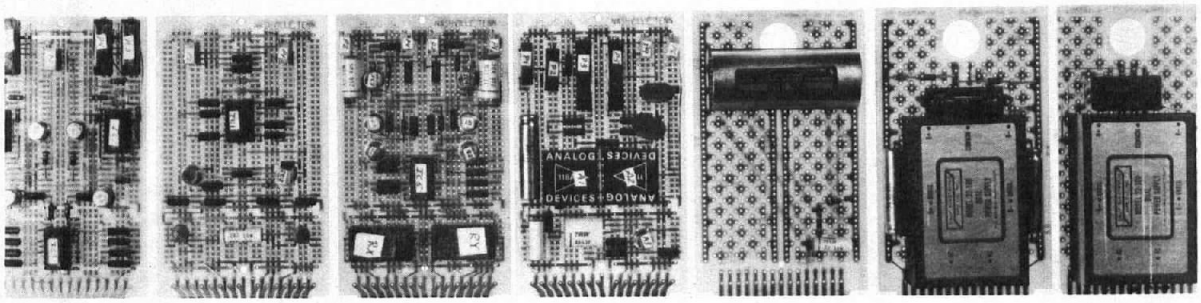

b. Printed circuit boards located in the upstream control chassis

Figure 10.— Electronic components of the prototype EL-FLO plus RESET analog computer controller mounted on printed circuit boards. Photo P801-D-79059

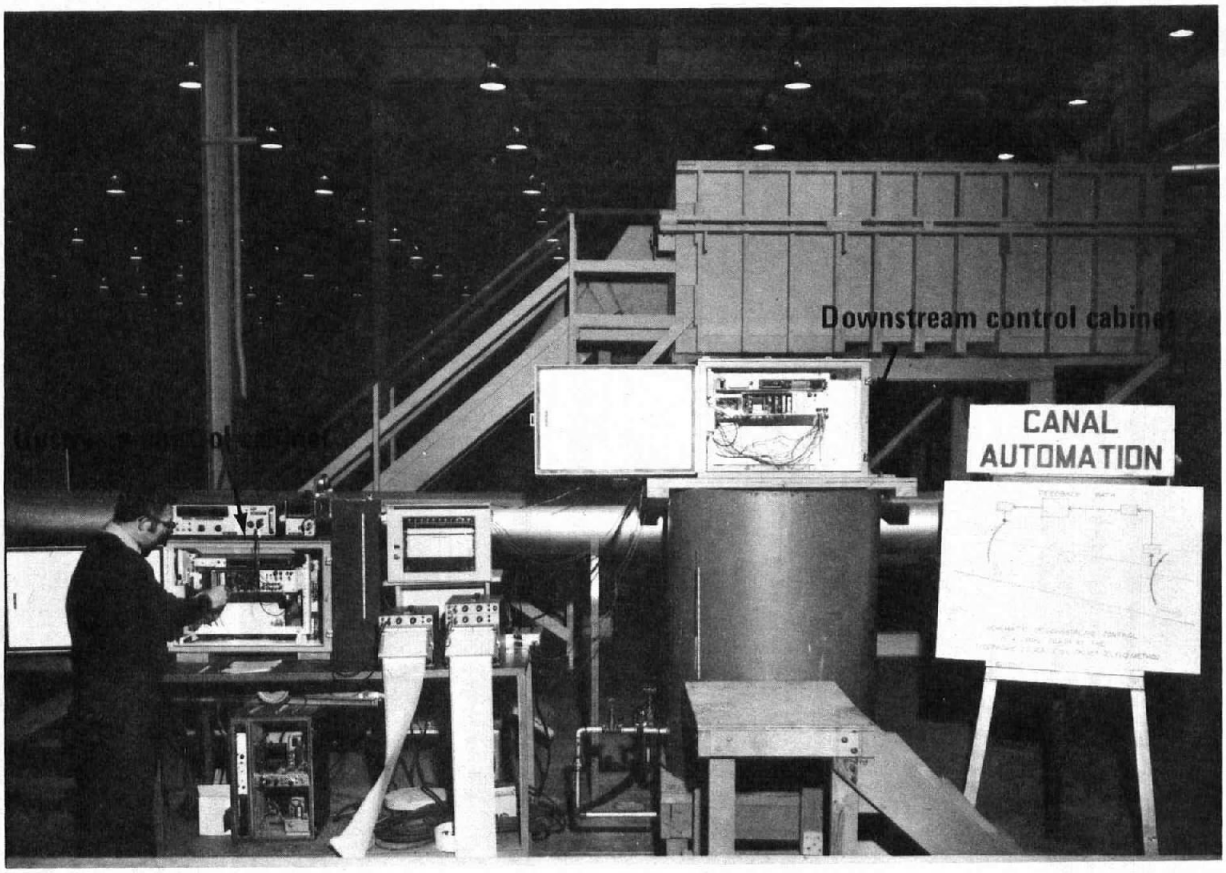

Figure 11.— Laboratory test facilities used for the EL-FLO plus RESET controller laboratory test program. Photo P801-D-79060

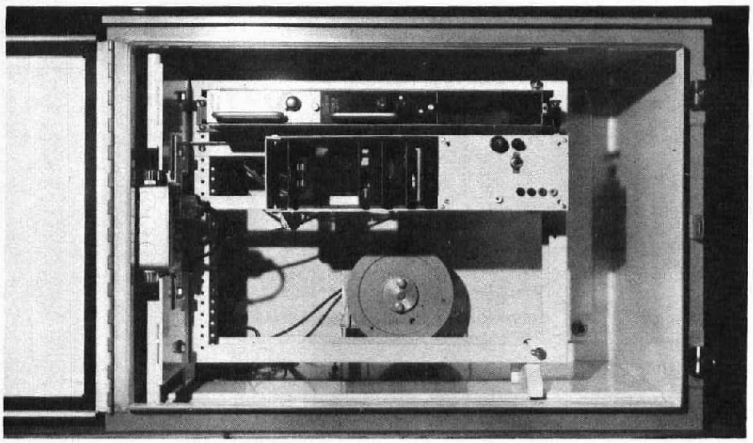

a. Downstream EL-FLO plus RESET control chassis mounted on swingout rack

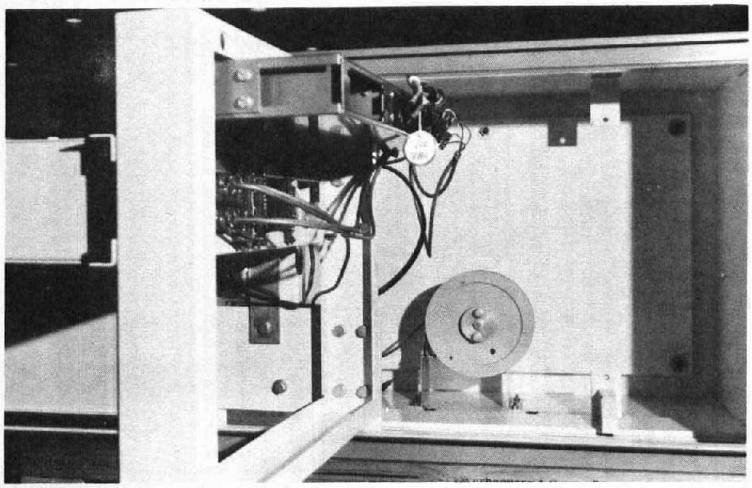

b. Downstream EL-FLO plus RESET control chassis with swingout rack in open position. Note water level sensor pulley arrangement

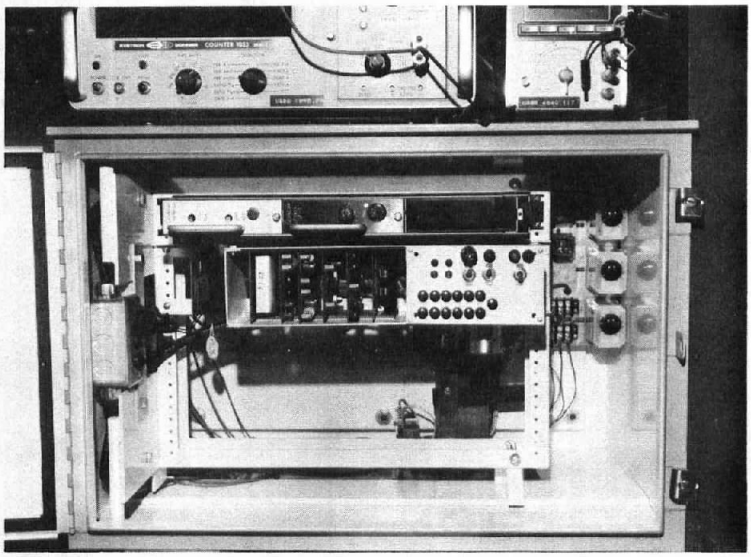

c. Upstream EL-FLO plus RESET control chassis mounted on swingout rack inside wall mount cabinet. Note the Colvin controller installed in the back of the cabinet

Figure 12.— Prototype EL-FLO plus RESET control chassis mounted inside a wall mount weatherproof cabinet.
Photo P801-D-79061

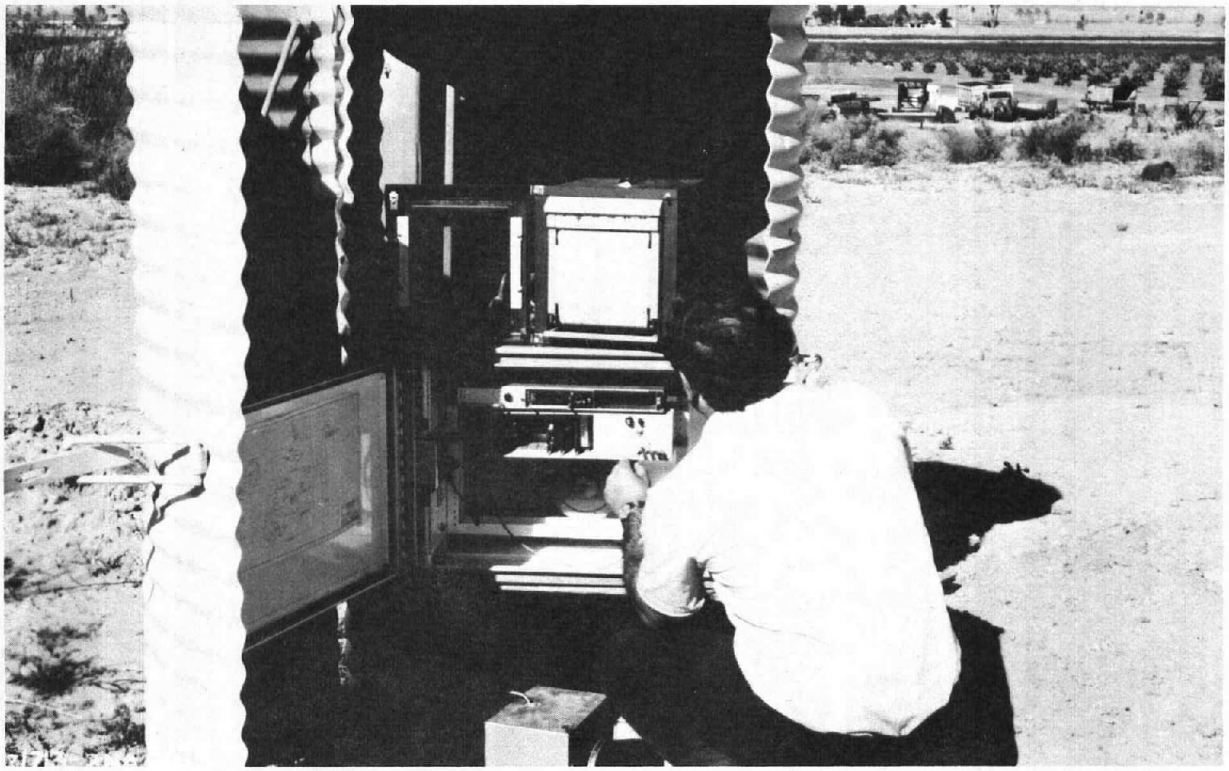

Figure 13.— Prototype EL-FLO plus RESET control cabinet installed inside one of the South Gila Canal stilling well instrument shelters. Data recorders are on top of the EL-FLO cabinet. Photo P801-D-79066

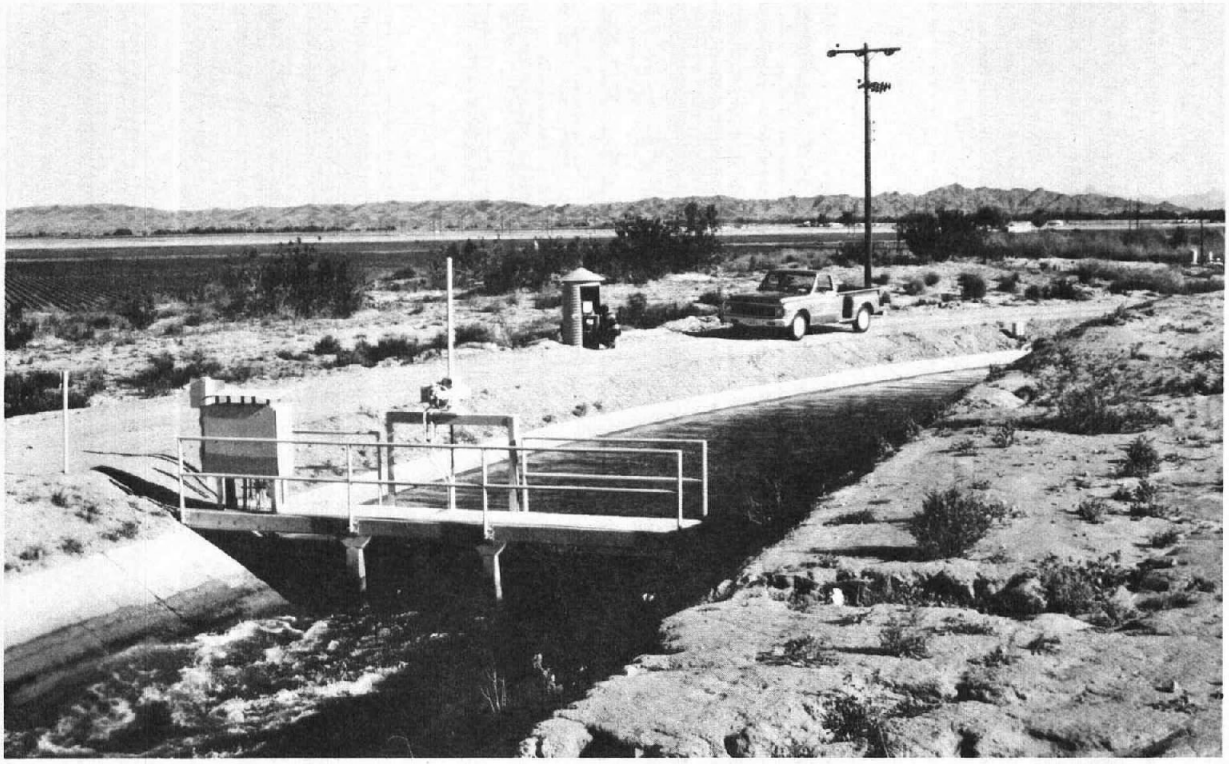

Figure 14.— Prototype installation of the EL-FLO plus RESET and the Colvin controllers housed inside the stilling well above the South Gila Canal check gate No. 1. Photo P801-D-79067

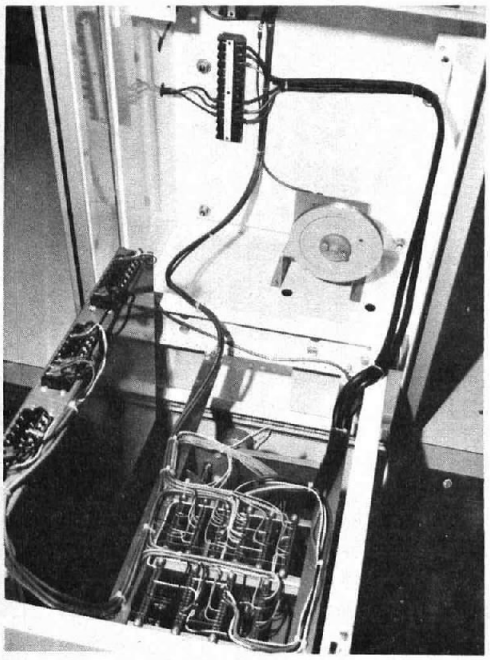

a. Inside view of weatherproof cabinet with the swingout rack in the open position. Note the water level sensor arrangement

b. Front view of the weatherproof cabinet with the swingout rack in the closed position and the front panel for the Printed Circuit board racks removed

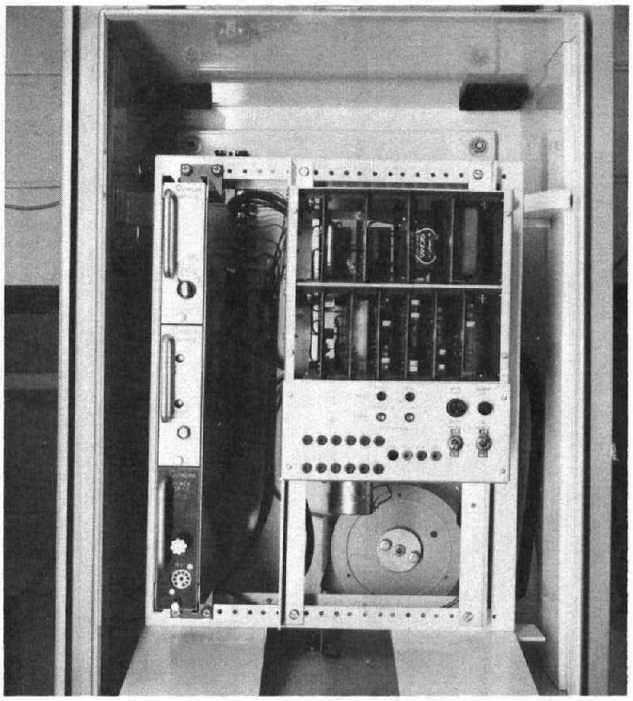

Figure 15.— Final prototype EL-FLO plus RESET controller and installation on the Corning Canal. Photo P801-D-79064

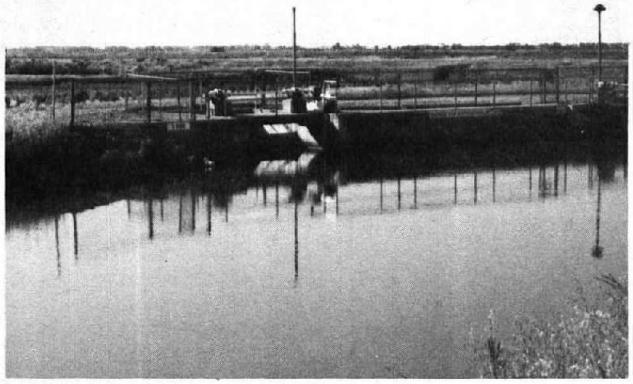

c. Overall view of Check No. 3, a typical radial gate check structure on the Corning Canal (M. P. 8.08) looking downstream Photo P801-D-79068

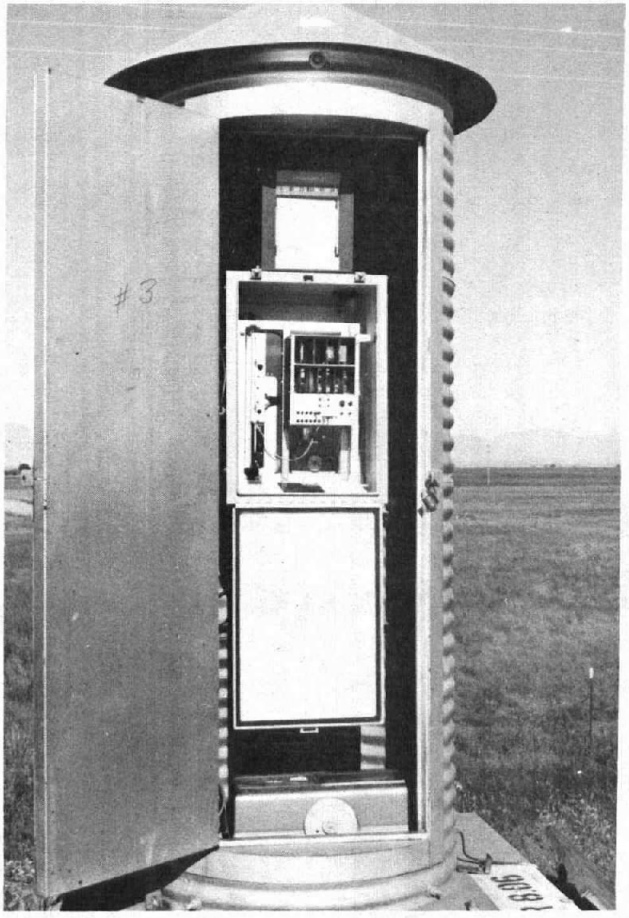

d. Typical installation of the final prototype EL-FLO plus RESET Controller in the stilling well shelters located approximately 30 m (100 ft) upstream of check No. 3 (M. P. 8.06) on the Corning Canal
Photo P801-D-79069

Figure 15.—Final prototype EL-FLO plus RESET controller and installation on the Corning Canal.—Continued

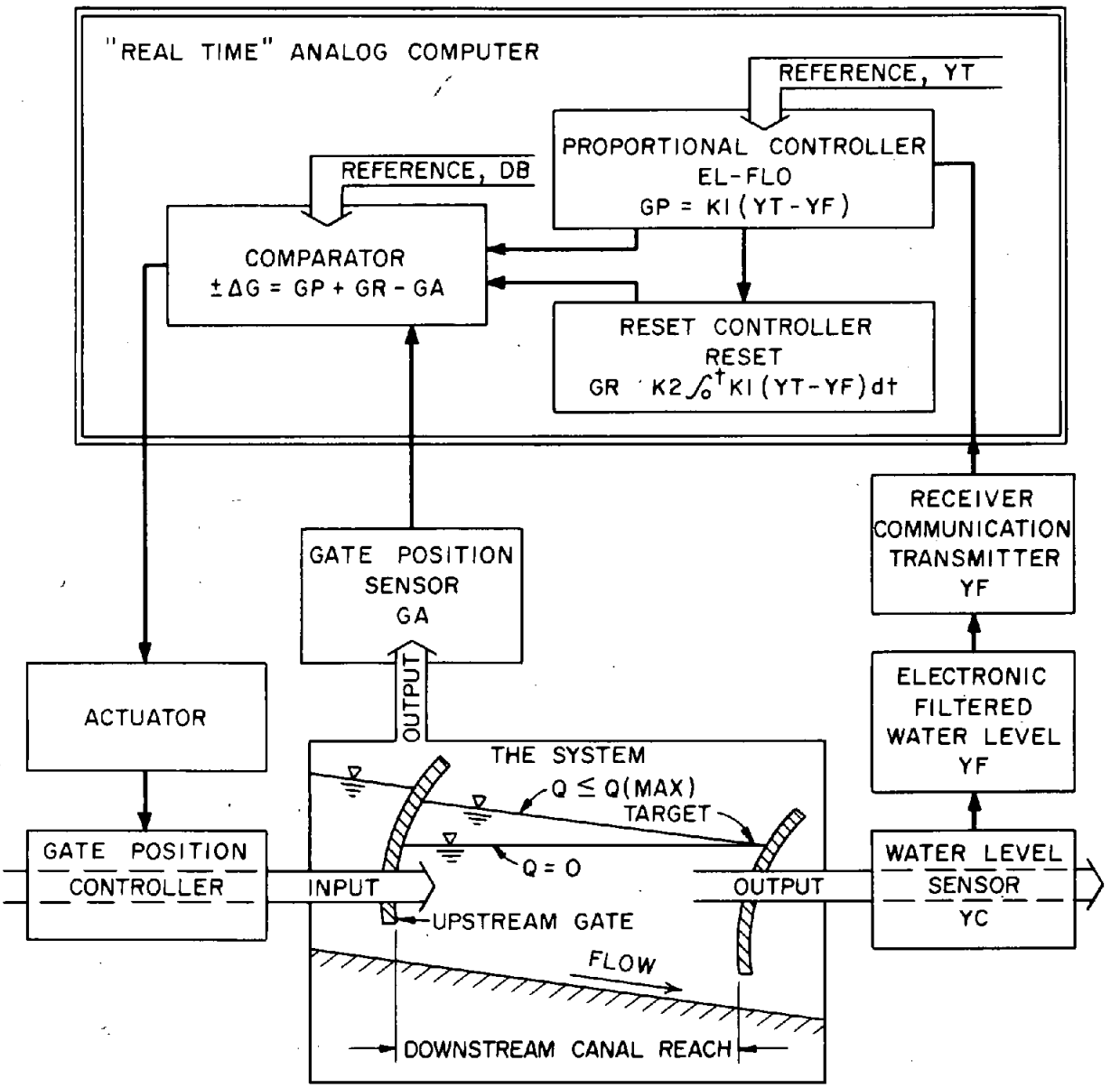

Figure 16.– EL-FLO plus RESET feedback control system.

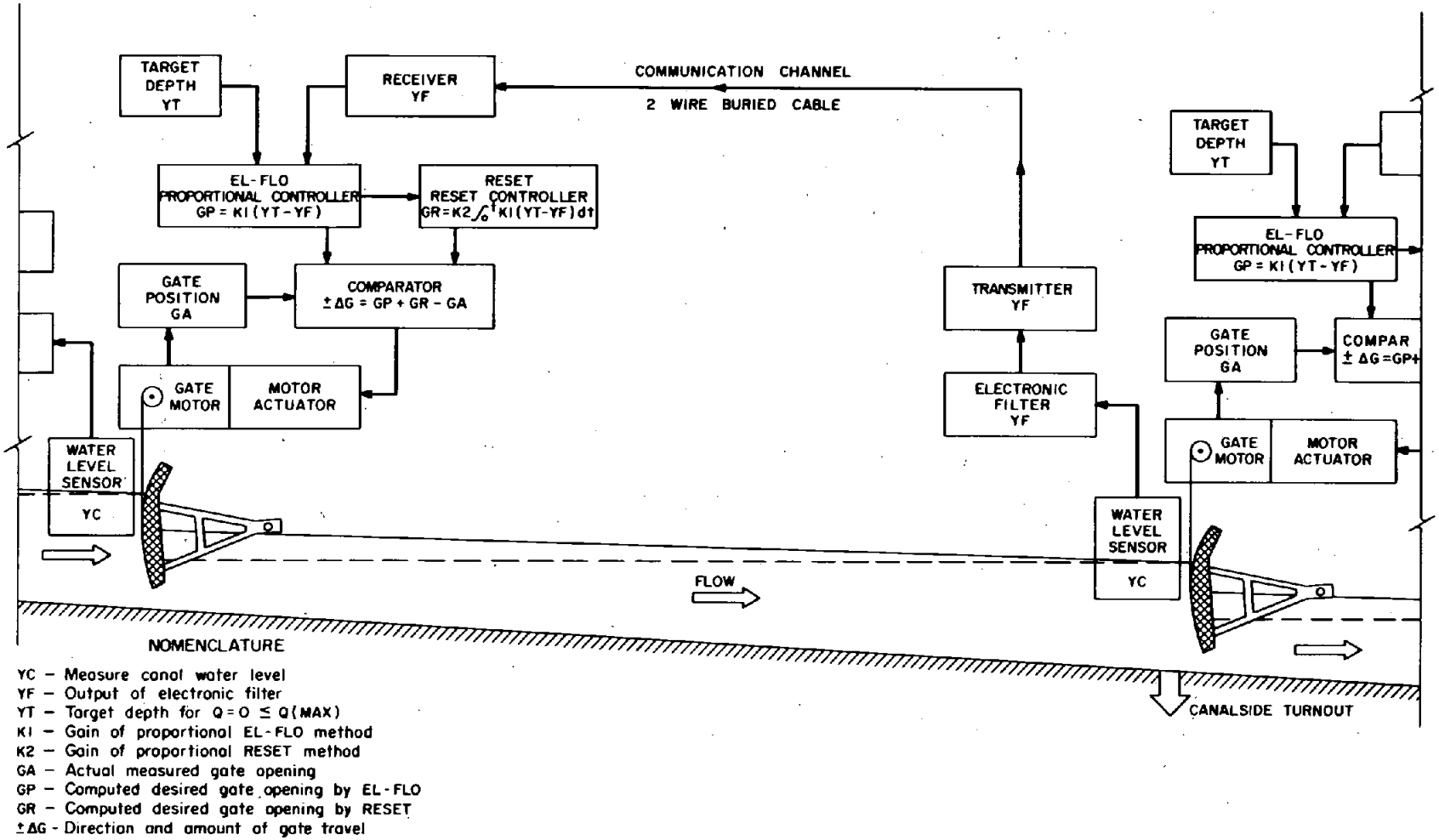

Figure 17.— Block diagram of automatic downstream control by the EL-FLO plus RESET prototype equipment.

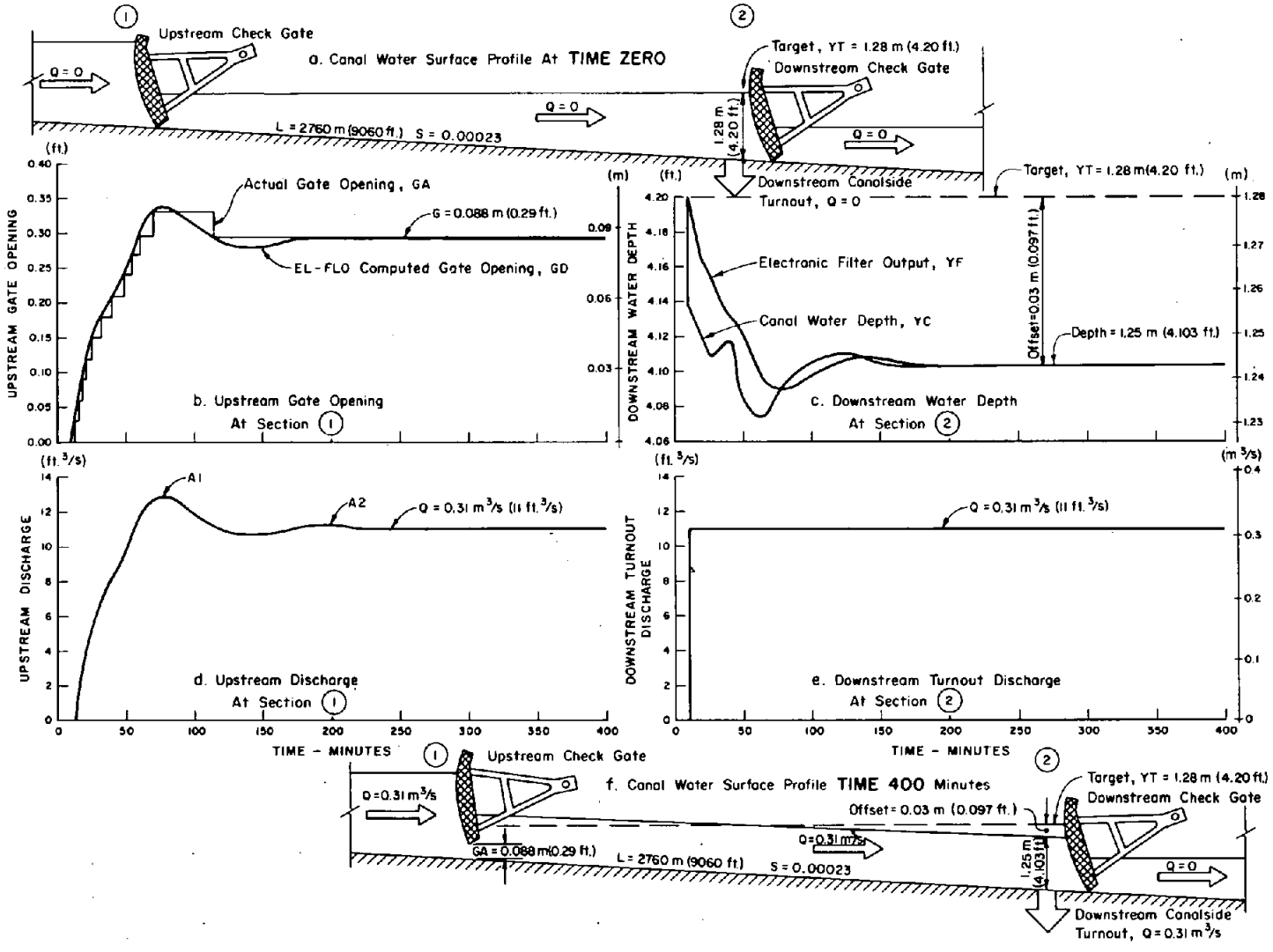

Figure 18.— Canal reach characteristic response by the EL-FLO method of automatic downstream control. (Proportional mode of control.)

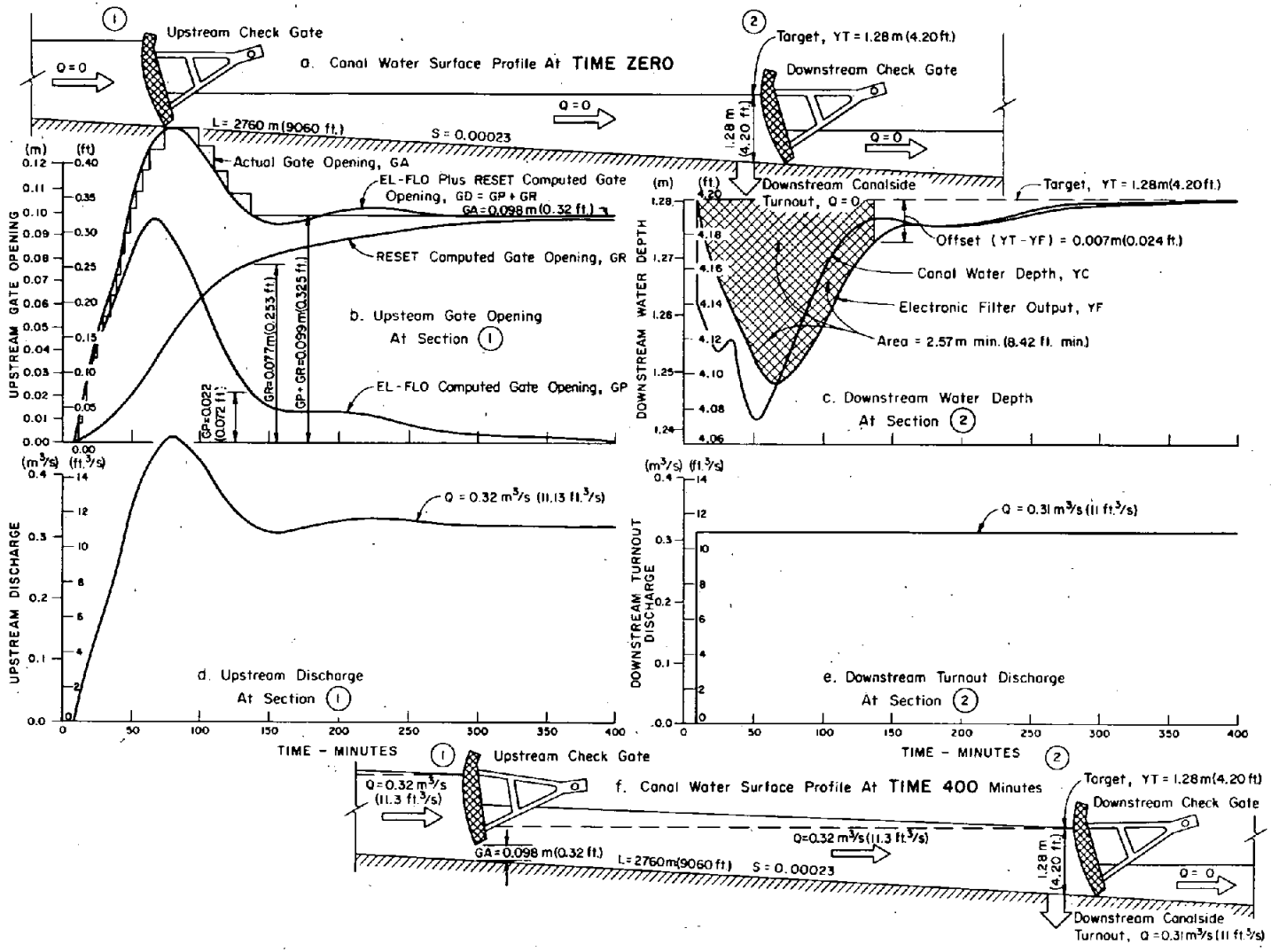

Figure 19.— Canal reach characteristic response by the EL-FLO plus RESET method of automatic downstream control. (Proportional mode plus proportional RESET mode of control.)

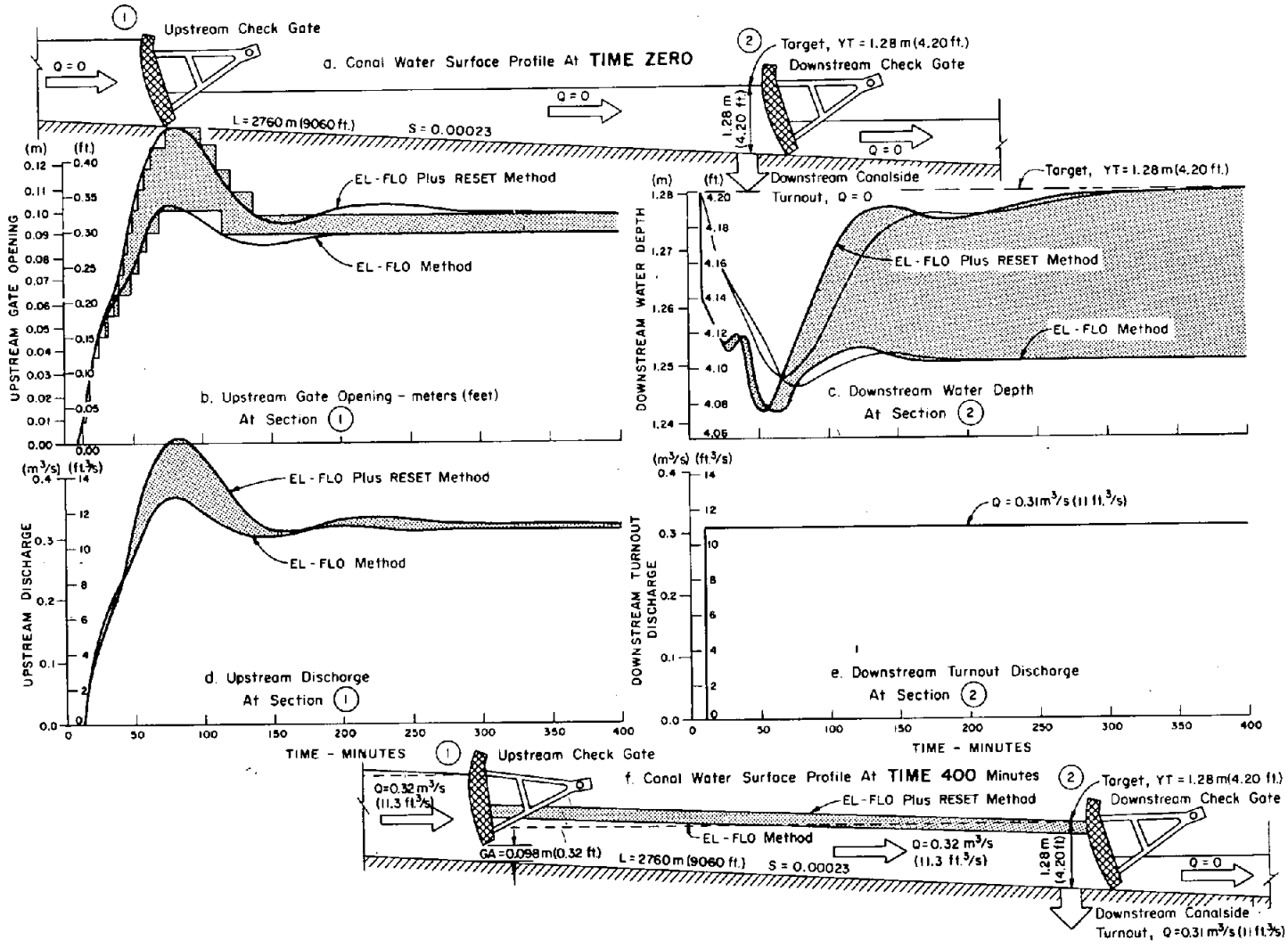

Figure 20.— Canal reach characteristic response by the EL-FLO plus RESET versus the EL-FLO method of automatic downstream control. (Proportional mode plus proportional RESET versus proportional mode of control.)

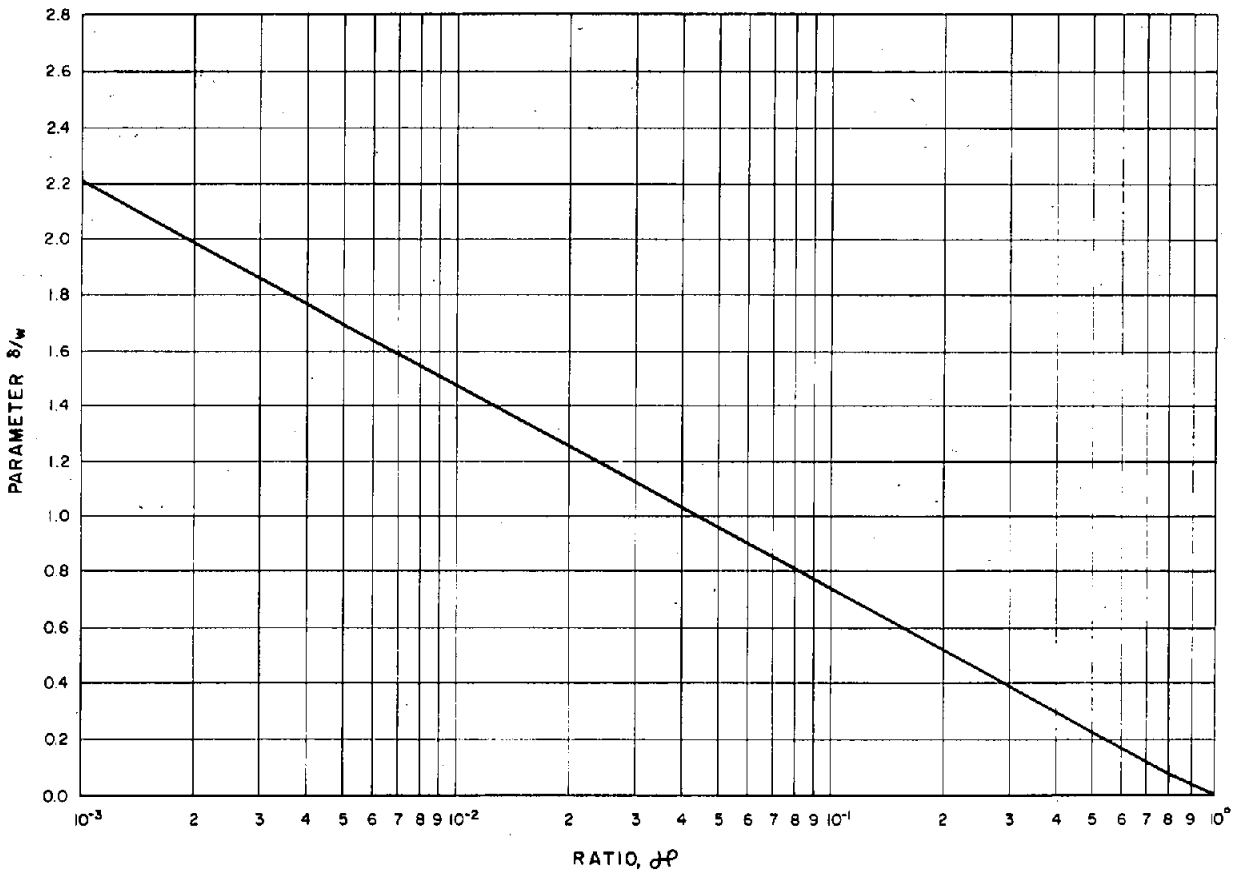

Figure 21.– Parameter δ/ω of a component response versus the ratio ρ of two successive amplitudes.

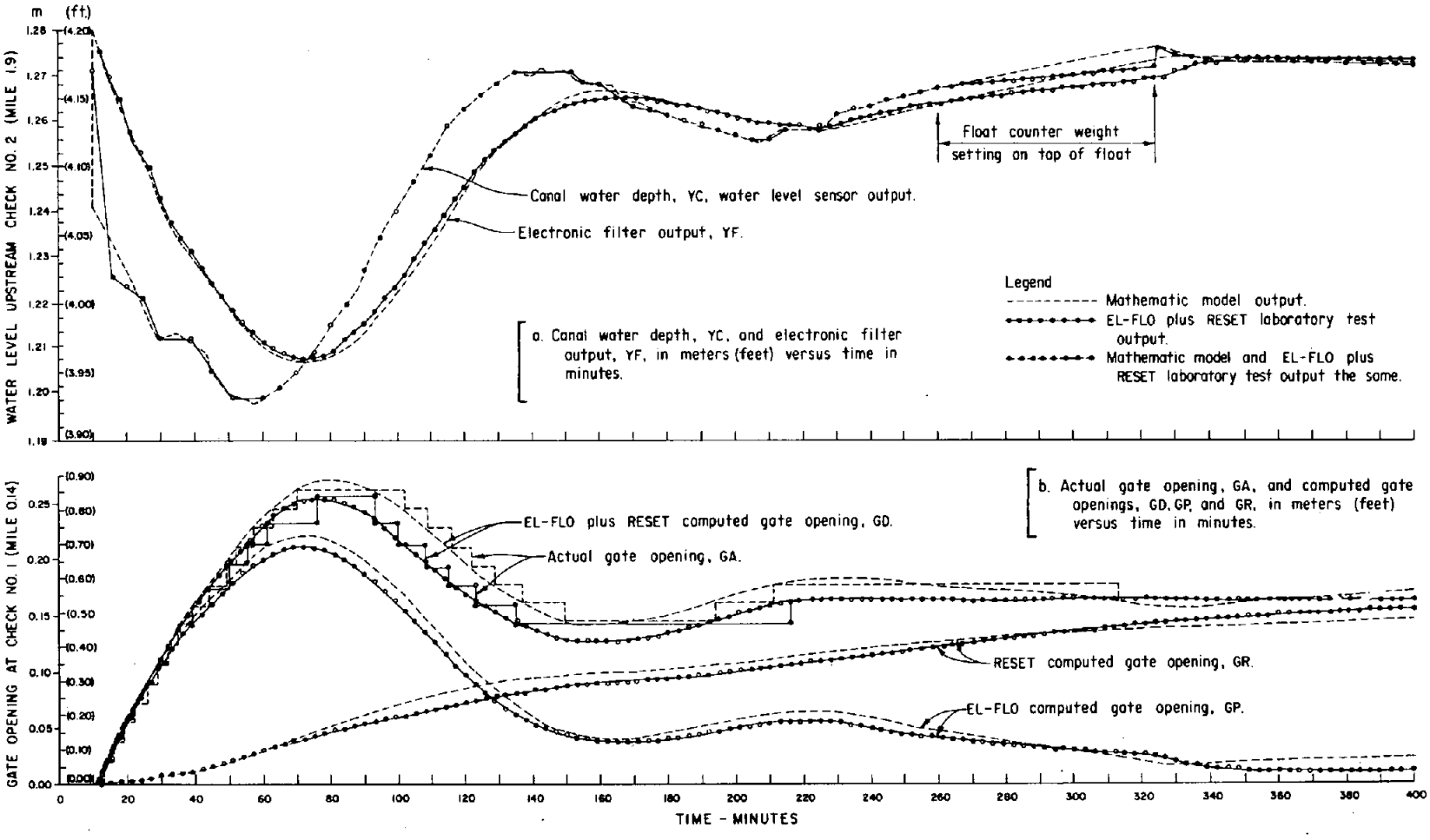

Figure 22.– Laboratory verification test mathematical model versus prototype EL-FLO plus RESET control equipment.

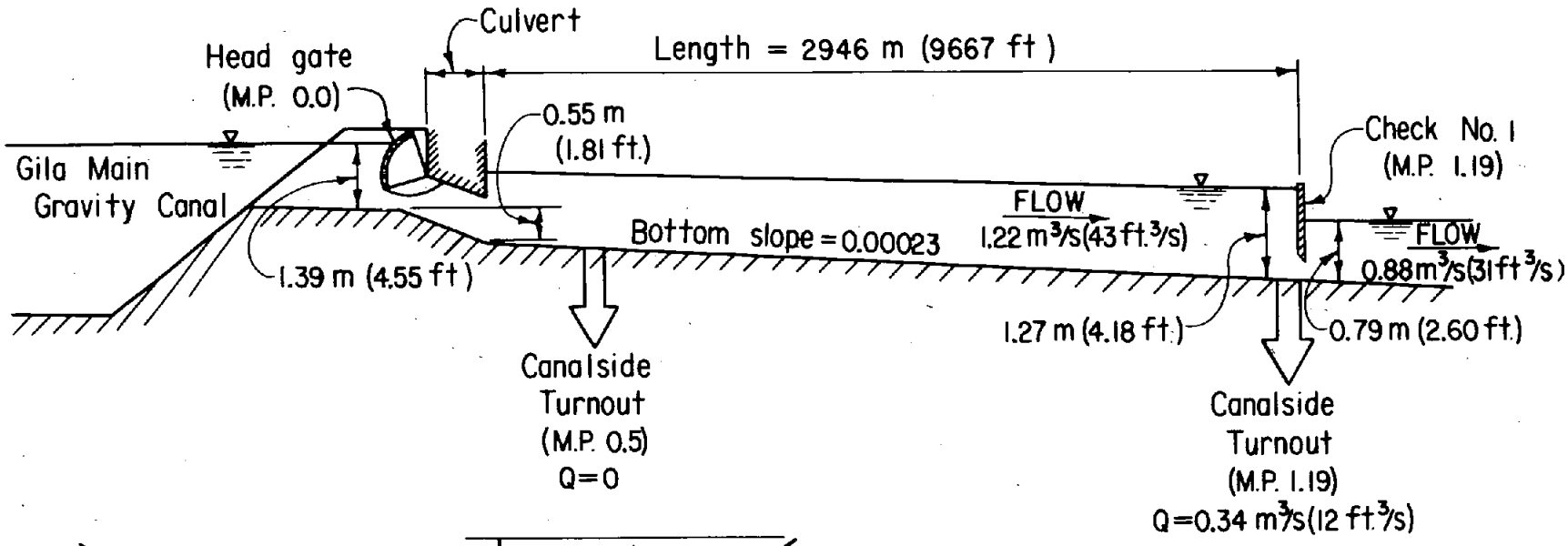

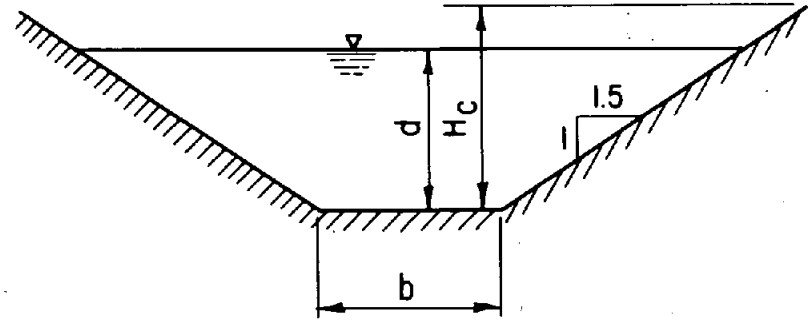

Canal cross section configuration

Design Properties

Q max. = 3.1 m^3/s (110 ft^3/s)
Area = 4.38 m^2 (47.1 ft^2)
Velocity = 0.71 m/s (2.34 ft/s)
b = 1.52 m (5.0 ft.)
d = 1.27 m (4.18 ft)
Hydraulic radius = 0.72 m (2.35 ft)
Mannings "n" = 0.017
Bottom slope = 0.00023
H_C = 1.58 m (5.2 ft)

Figure 23.— Schematic of South Gila Canal configuration at steady-state flow conditions at time zero.

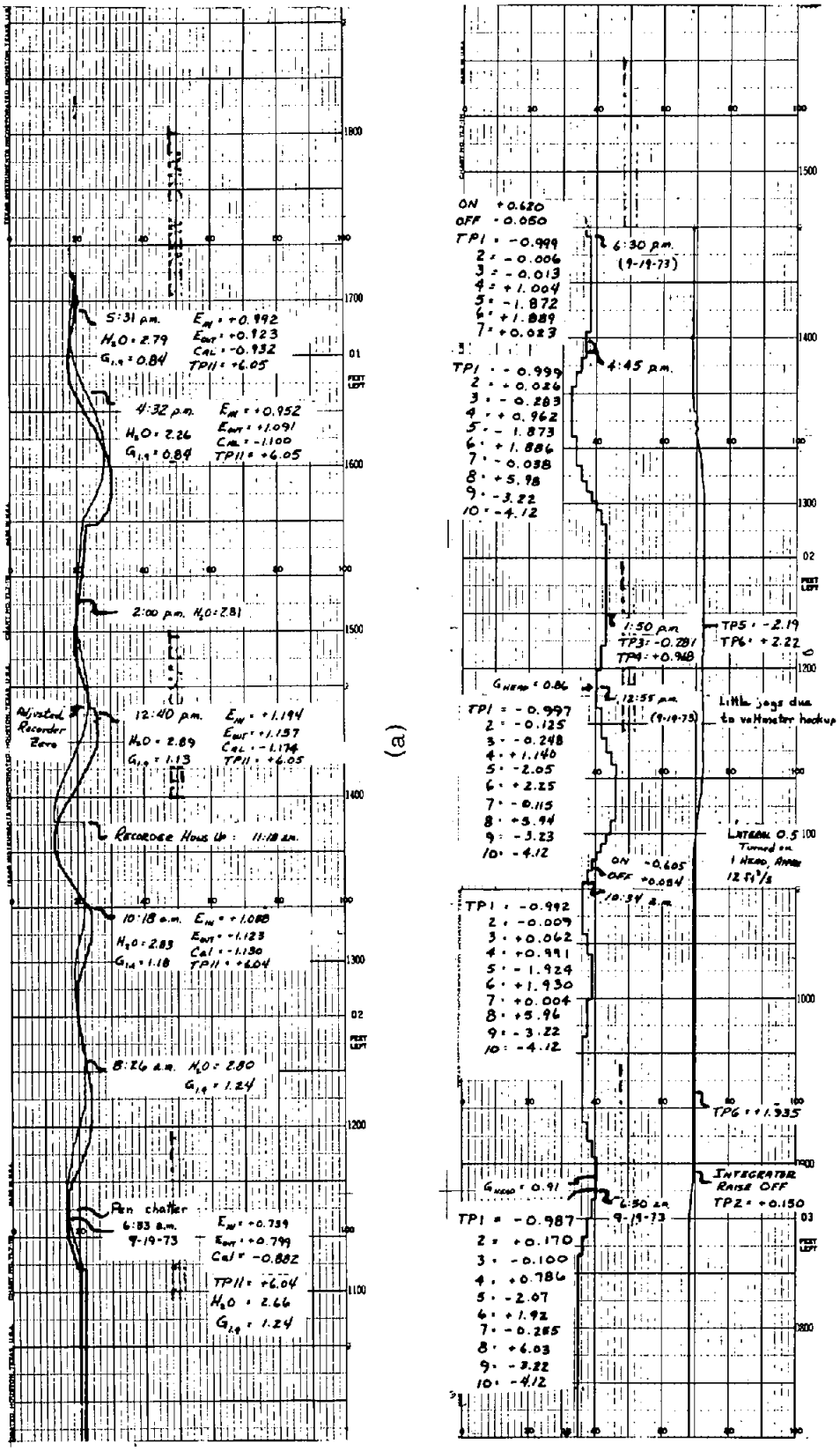

Figure 24.— Electronic chart recordings of the South Gila Canal prototype field test. Conducted September 19, 1973.

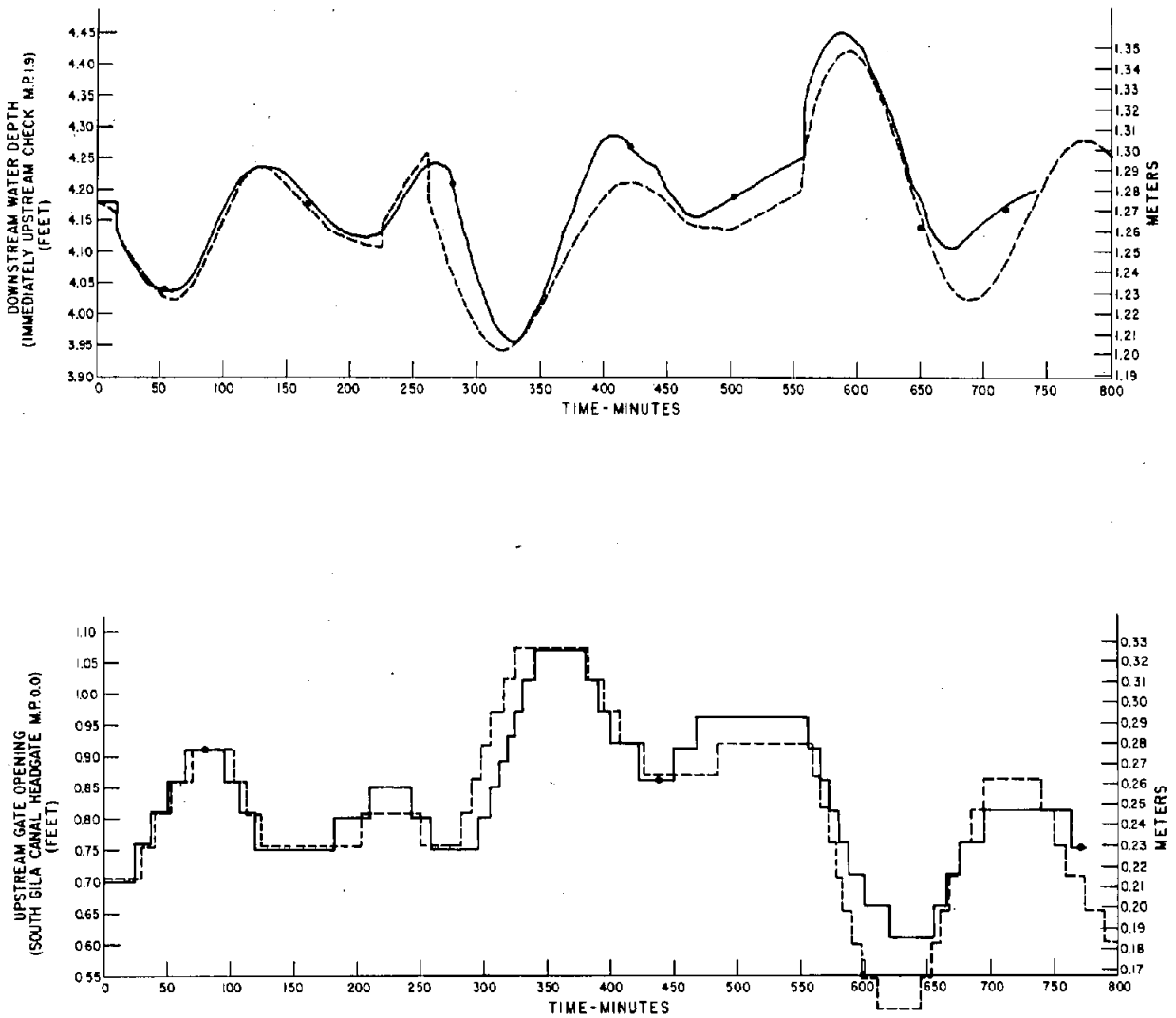

Figure 25.— South Gila Canal field verification test mathematical model versus prototype EL-FLO plus RESET control equipment.

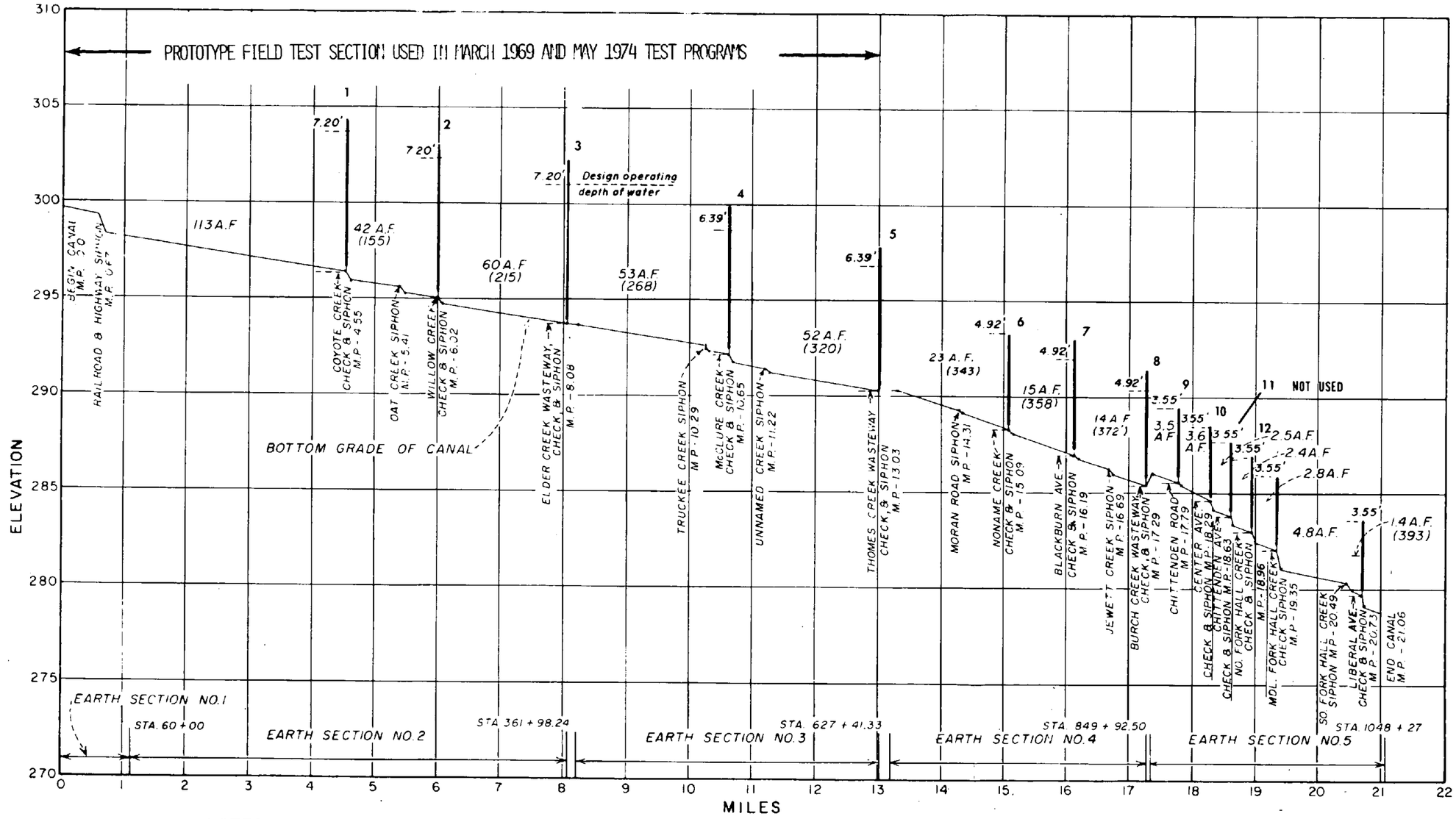

NOTES

FIGURES IN ACRE-FEET INDICATE CHECKED STORAGE AT DESIGNED LEVEL.

FIGURES IN PARENTHESIS ARE CUMULATIVE STORAGE (ACRE-FEET).

SEPTEMBER 1964; REV. 12-21-70

Figure 26.—Bottom grade profile of Corning Canal.

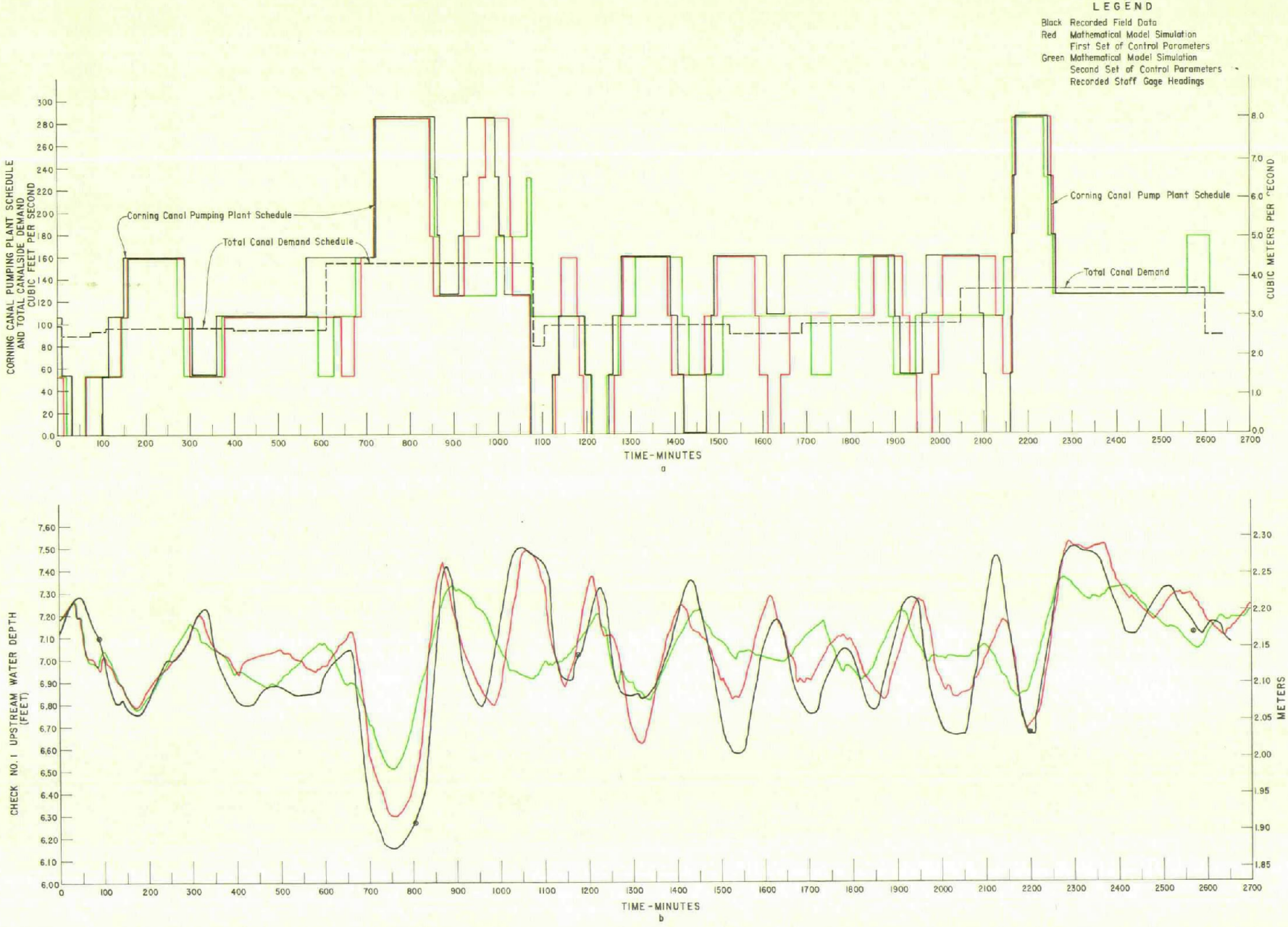

Figure 27.—Corning Canal prototype test - EL-FLO control field verification.

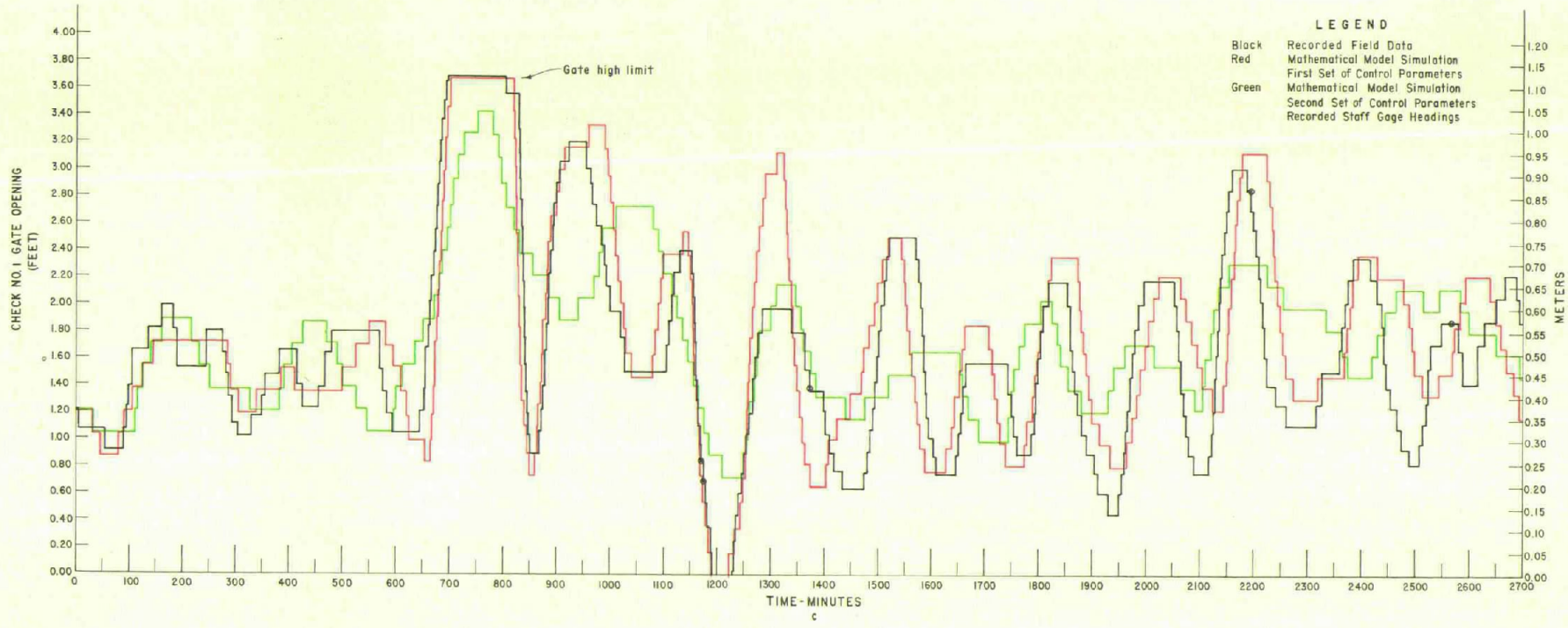

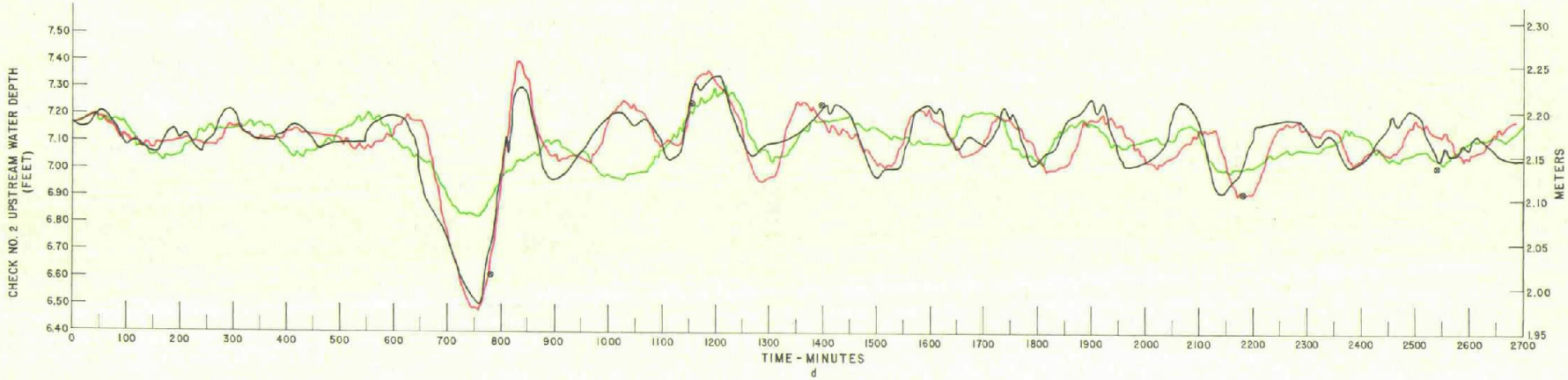

Figure 27.—Corning Canal prototype test - EL-FLO control field verification.—Continued

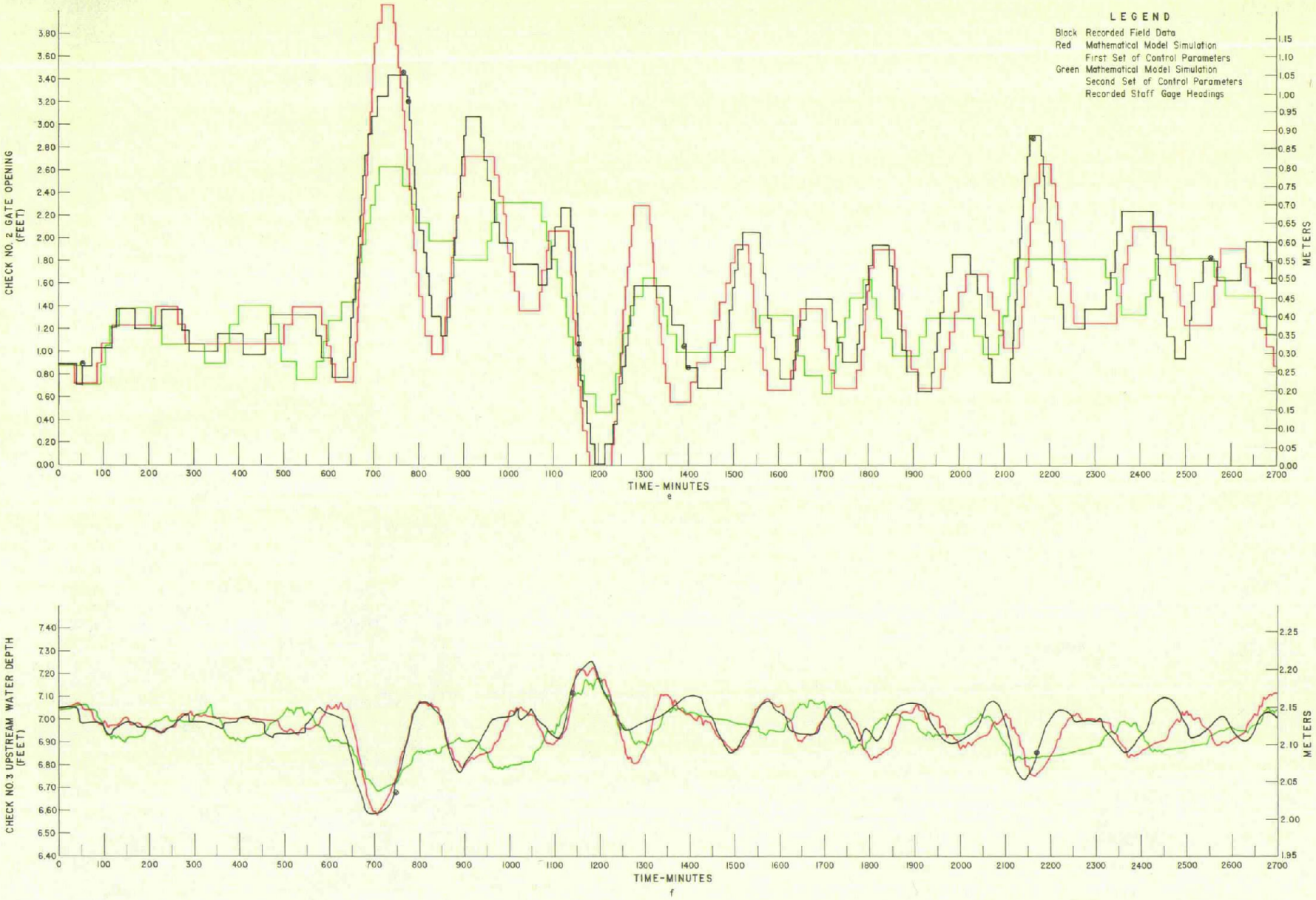

Figure 27.—Corning Canal prototype test - EL-FLO control field verification.—Continued

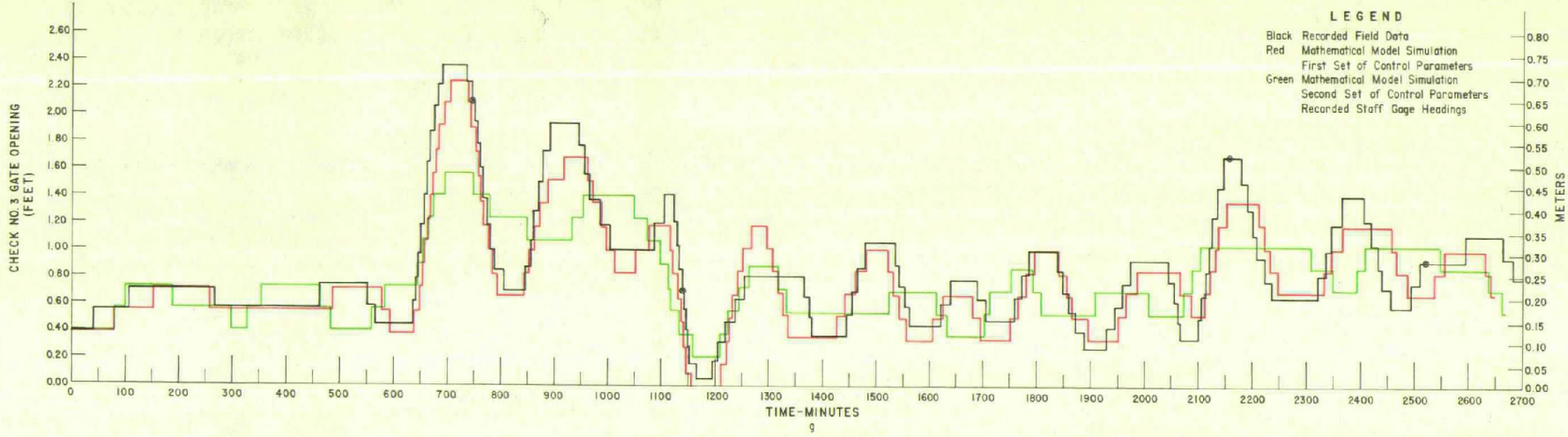

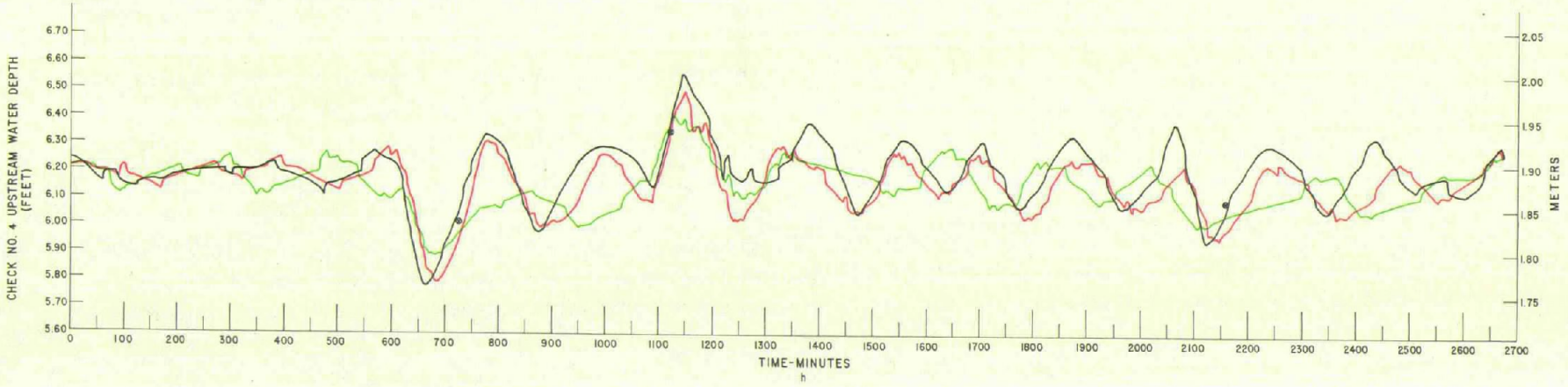

Figure 27.—Corning Canal prototype test - EL-FLO control field verification.—Continued

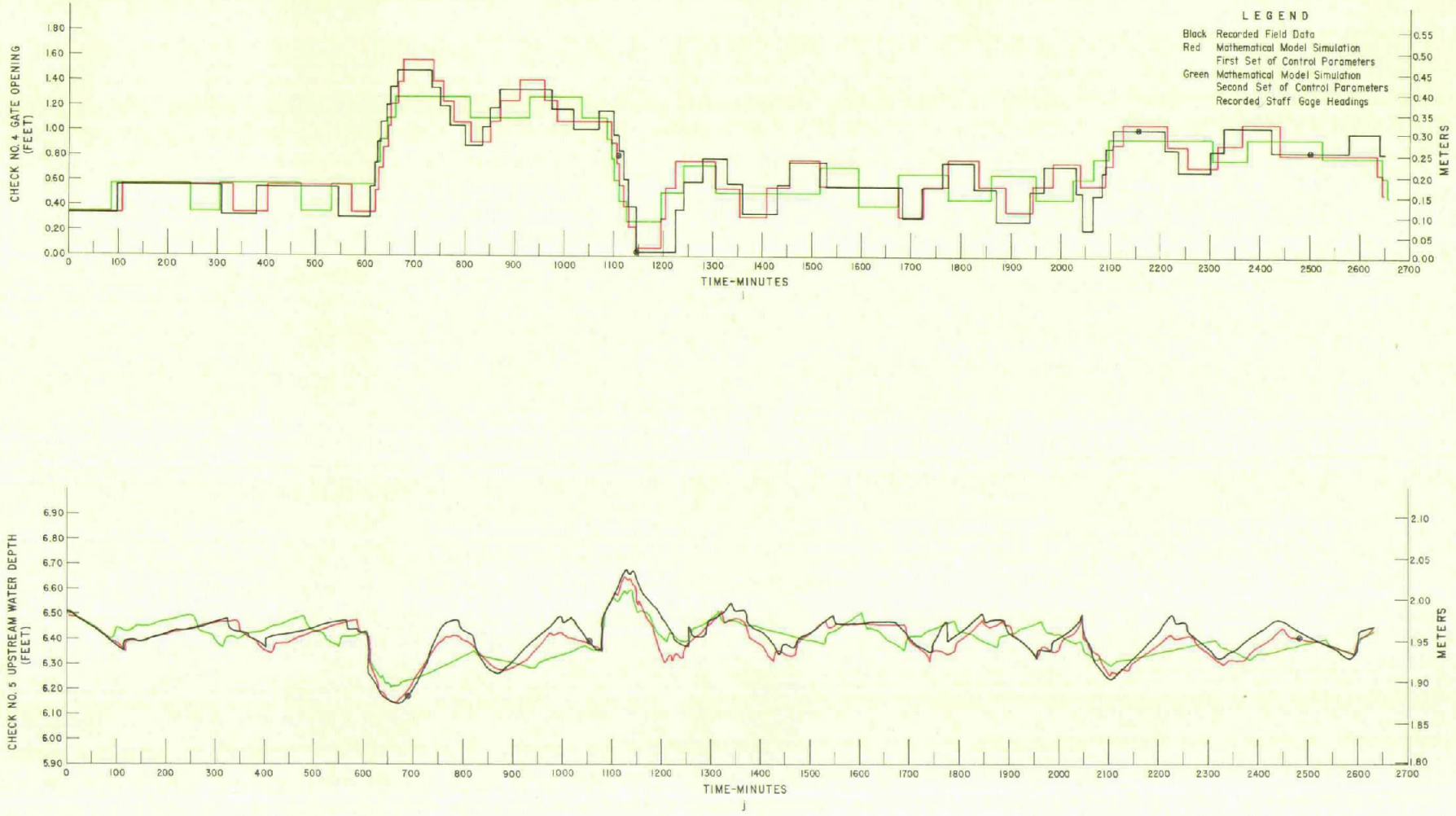

Figure 27.—Corning Canal prototype test - EL-FLO control field verification.—Continued

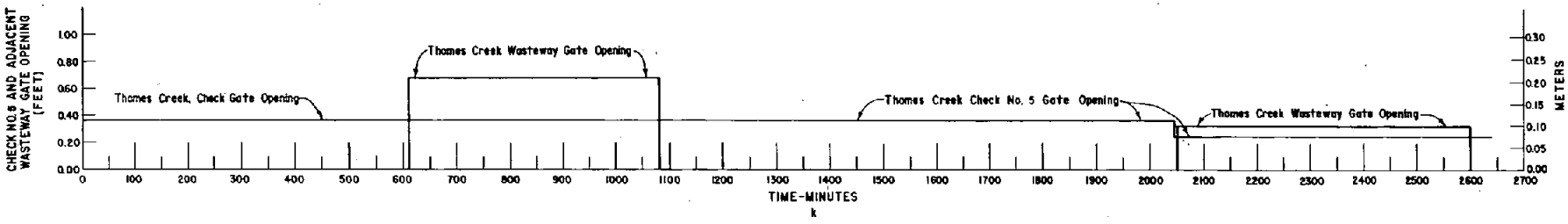

Figure 27.—Corning Canal prototype test - EL-FLO control field verification.—Continued

APPENDIXES

I. Electronic Filter and EL-FLO Plus RESET Control Chassis Environmental Tests

II. Electronic Filter Time Constant Calibration

III. Technical Description of Each EL-FLO Plus RESET Feedback Control System Element

IV. Report on the Condition of the EL-FLO Controller Receiver Unit - South Gila Canal Automation

V. Conversion of Selected Control Parameters to Electronic Equivalences

VI. Detailed Analysis of Laboratory Verification Test

Appendix I

ELECTRONIC FILTER AND EL-FLO PLUS RESET CONTROL CHASSIS ENVIRONMENTAL TESTS

Summary

Four electronic filters were constructed in accordance with figure III-4. Each filter was operated at least 200 hours in the laboratory. Over 1000 hours of operation were accumulated on all the units constructed. The extensive testing program eliminated possible "burn-in" failures of the electronic components. The laboratory environmental test program disclosed that all components must have good high temperature characteristics and the entire high impedance circuit must be perfectly sealed against moisture. Each unit was tested at temperatures of 65 °C (150 °F) and three units were tested at 100 percent humidity at about 18 °C (65 °F). The filter output will drift a small amount for temperature variations from 21 to 65 °C (70 to 150 °F). The magnitude of the filter temperature drift (about ±80 mV, or 4 percent full scale, at 65 °C (150 °F)) will not cause system instability. The filter output drift at high humidity was very minor. The small drift experienced (about ±4 mV at 100 percent humidity and 18 ° C) demonstrated that the final humidity protection technique used (Sylgard[1] 184 encapsulating resin) was successful.

The final design of the electronic filters and the control chassis uses solid-state components that have a high reliability. The filter was designed to operate continuously for very long periods of time in the "canalbank environment" without maintenance.

High Humidity Tests

It was anticipated that the high impedance circuit of the electronic filter (within the dashed area of fig. 6 and the components on the *RC* network card No. 2 of fig. III-4) must be packaged in a hermetically sealed enclosure. Humidity tests began with the Model A electronic filter, figure 7, using a SILASTIC[1] sealer coating on the high impedance circuit. The Model A was placed inside the environmental chamber (fig. 9). A fog nozzle that emitted a very fine mist was placed below the intake hood and a small fan was used to blow the mist into the chamber creating an environment of 100 percent humidity in a short period of time.

[1] Trademark Dow Corning.

Figure I-1a shows an example of one of the first humidity test runs made on the Model A filter. The filter *EF INPUT* was held constant. However, a runaway-filter *EF OUTPUT* occurred immediately as the result of not completely coating the entire high impedance *RC* network, arranged into one area on the card for a convenient humidity protection enclosure.

The final electronic filter arranged the necessary high impedance *RC* network electrical components onto one printed circuit card. The entire card was then encapsulated with Sylgard 184 encapsulating resin as shown in figure 8 (a and b). The entire filter unit (fig. 9c and d) was then tested for high humidity as shown in figure I-1b which is chart recordings of humidity test No. 2H. The drift of the filter *EF OUTPUT* was −5 millivolts at 100 percent humidity. The drift of −5 millivolts was attributed to a decrease in temperature from 23 °C (74 °F) at the beginning to 17 °C (63 °F) at the end of the test. Therefore, it was concluded the arrangement of high impedance components on one card and the use of the Sylgard 184 encapsulating resin provided an excellent hermetically sealed enclosure for use in high humidity.

Humidity test runs were conducted on the first three electronic filter units and are summarized in table I-1. The drift, which is considered to be minor, of the filter *EF OUTPUT* ranged from a +13 to −5 millivolts for an average of +4 millivolts and was contributed to the decrease in temperature as the humidity increased to 100 percent. Humidity testing of the fourth unit, constructed at a later time, was not considered necessary because of the successful test results on the first three units.

The entire EL-FLO plus RESET control chassis, figure 12c, without the electronic filter and the transmitting-receiving equipment was also tested at 100 percent humidity for 2 hours inside the environmental chamber. The results showed a very minor drift of the output at test point TP3, also attributed to a decrease in temperature. There were no erratic voltage changes noted at TP3 although condensate formed to a point of water dripping off the printed circuit cards after 2 hours of 100 percent humidity. All the printed circuit glass epoxy cards, figure 10, were cleaned and sprayed with a corrosion and humidity protective coating before conducting the humidity test on the chassis.

The results of the humidity test program were successful and demonstrated that the final prototype EL-FLO plus RESET controller should perform satisfactorily in a high humidity environment on the canalbank.

Table I-1.—*Electronic filter humidity tests data summary*

Test No.	Date Mo /Day/Year	Electronic filter unit	Test start conditions					Test end conditions					Test run time, hours	Net *EF OUTPUT* drift, mV
			Time	*EF INPUT*, volts	*EF OUTPUT*, volts	Temp, °C (°F)	Humidity, percent	Time	*EF INPUT*, volts	*EF OUTPUT*, volts	Temp, °C (°F)	Humidity, percent		
1H	5-9-72	2	8:15 a.m.	1.003	0.998	23 (74.0)	57	10:30 a.m.	0.985	1.003	17 (62.5)	100	2.25	+13
2H*	5-10-72	1	8:25 a.m.	1.000	1.000	23 (74.0)	N/R	10:30 a.m.	0.996	0.991	17 (62.5)	100	2.00	−5
3H	5-16-72	3	8:00 a.m.	0.995	0.991	23 (77.0)	24	10:15 a.m.	0.995	0.995	17 (62.5)	100	2.25	+4
												Average Net *EF OUTPUT* Drift, +4mV		

*Chart recordings for humidity test No. 2H is shown in figure I-1b.

High Heat Tests

High heat tests using the same environmental chamber as used in the humidity test program began with the Model A electronic filter. Early tests showed that there would be a drift in the filter *EF OUTPUT* at high temperatures. An extensive high heat test program on the four constructed prototype electronic filters began soon after the Model A filter heat tests were completed.

Initial heat tests revealed a significant drift in the filter *EF OUTPUT* and was traced to the circuit of the reed relay (*RC* network card No. 2 on fig. III-4 and fig. 8a and b) used to initialize the high impedance circuit. The first circuit design switched the reed relay coil to ground in order to energize the coil and close the relay contact. Under this arrangement, the 15-volt d-c power supply was continuously available on the other side of the coil. At high temperatures (65 °C), the 15-volt potential was leaking through the reed relay nylon mounting bracket onto the high impedance side of the reed relay contact causing a runaway drift of the filter *EF OUTPUT*. To prove this occurrence, the nylon bracket was cut away around the +15-volt terminal and further heat tests did not have the runaway drift previously experienced. However, rather than remove the nylon mounting bracket from around the terminal, the initializing circuit was redesigned to switch the 15-volt d-c power supply to the coil instead of the ground side in order to initialize the filter. Under this arrangement, there would not be a high potential present that could leak onto the high impedance circuit.

The next step in the high temperature test program was to determine if the electronic filter MOSFET (metal oxide semiconductor field effect transistor) could be made to operate with zero drift as the temperature increased by adjusting the drain current, I_{DSS}, at the trim potentiometer P3 on the electronic filter card No. 1. Figure I-2 illustrates the temperature drift characteristics of the constructed electronic filter units 1 through 4 for various temperatures up to 65°C with various MOSFET drain currents. Filter unit 2 shows that the ideal drain current (I_{DSS}) for zero temperature drift would be 1.3 mA. However, for units 1, 3, and 4, the zero temperature drift and the ideal drain current of the MOSFET was considerably different and, in all cases, exceeded the limits of drain current capabilities of the circuit. The tests showed that each MOSFET would have a different ideal drain current for zero drift characteristics; each would have to be calibrated to find this value which would be time consuming and difficult for field calibration. However, the tests showed that a drain current set at the value for a gate to source voltage drop of zero volts; that is, the drain current adjusted to the I_{DSS} value would have temperature drift characteristics that would be acceptable.

The drain current, I_{DSS}, for each filter unit is shown on figure I-2 as a horizontal line. The maximum filter *EF OUTPUT* drift at 65 °C (150 °F) ranged from +77 to −4 millivolts. The magnitude of temperature drift within ±80 millivolts (4 percent full scale) at 65 °C (150 °F) is considered to be insignificant and will not cause system instability.

Figure I-3 is the final temperature drift characteristics of the four electronic filter units at the I_{DSS} drain current for temperatures up to 65 °C. Filter units 1 and 2 *EF OUTPUT* drifted in the negative direction which is an indication that each MOSFET has its own temperature drift characteristics that would be difficult to predict. Figure I-4 is the chart recordings of a typical heat test run, No. 30T, an example of 35 heat test runs that were conducted to develop the data for figures I-2 and I-3.

Table I-2 summarizes eight heat test runs made on the four filter units to determine the temperature drift characteristics with the MOSFET drain current set at the I_{DSS} value. There is an interesting average drift to the four filter units *EF OUTPUT*; at 38 °C (100 °F), the average drift was zero; at 52 °C (125 °F), the average drift was +3 millivolts; and at 65 °C (150 °F), the average was only +1 millivolt for the four filter units. Based on this limited sample, it could be assumed the temperature drift would cancel out for multiple electronic filter installations on a series of canal reaches and would be a negligible factor in the total system performance.

The EL-FLO plus RESET control chassis was subjected to high temperatures. It was discovered in these tests that the slider on wire-wound trim potentiometers would shift position at high temperatures because of thermo expansion causing a sudden change in the controller output at TP3 (fig. III-3). Figure I-5 illustrates a high temperature drift of a wire-wound trim potentiometer experienced in the laboratory heat tests on the control chassis. The wire-wound trim potentiometers were replaced with a cermet metal-film type that provides infinite resolution. The cermet-type trim potentiometers eliminated the chassis output drift experienced with the wire-wound type under heat tests.

An example of a heat test run (No. 35T) conducted on the final prototype EL-FLO plus RESET control chassis is shown in figure I-6. The temperature was increased from 20.8 to 60 °C (69.5 to 140 °F) over an

Table I-2.—*Summary of temperature drift characteristics of electronic filter units 1 through 4 with MOSFET drain current set at I_{DSS}*

Electronic filter unit	Heat test No.	MOSFET drain current I_{DSS}, mA	Temperature/drift 38 °C (100 °F) mV	52 °C (125 °F) mV	65 °C (150 °F) mV
1	23T	1.50	−2	+2	+20
1	14T*	1.50	+1	+5	+19
2	24T	0.63	+2	+11	+66
2	1T*	0.63	+11	+34	+77
3	25T	0.64	0	−1	−39
3	16T*	0.64	−4	−13	−44
4	31T	0.64	−3	−11	−53
4	30T*	0.64	−2	−11	−38
	Average drift =		0	+3	+1

*Denotes heat test run data plotted on figure I-2. All other heat test run data plotted on figure I-3.

8-hour period. The input to the chassis, the filter *EF OUTPUT*, changed from 1.039 volts at the beginning to 1.035 volts at the end of the test run for a change of −4 millivolts. The chassis system gain, *A1A2*, for the test run was 10. Therefore, the change of −4 millivolts in the chassis input would produce a change of −40 millivolts in the chassis output TP3. The lower chart recording of figure I-6 is the chassis output TP3. The chassis output TP3 changed from −7 millivolts at the beginning to −162 millivolts at the end of the test run for a change of −155 millivolts. The net change of TP3 was −115 millivolts after accounting for the change in the input during the test run.

The temperature drift of the control chassis of −115 millivolts, with the temperature changing from 20.8 to 60 °C, is considered to be minor. Typically, a 1-volt change at TP3 will move the check gate 0.03 m (0.10 ft). Therefore, the temperature drift would cause a check gate change of about 0.003 m (0.01 ft). For the South Gila Canal, the maximum gate opening is 1.28 m (4.2 ft) and the temperature drift equivalent of 0.003 m (0.01 ft) would be 0.3 percent full scale. On the Corning Canal, the maximum gate opening is 2.2 m (7.2 ft) and the temperature drift equivalent would be about 0.2 percent full scale.

The high temperature test program results demonstrated that all components have good temperature characteristics and the magnitude of temperature drift is minor and will not cause system instability.

Each electronic filter unit was put into continuous operation including the final prototype control chassis to eliminate infant mortality failures of the electronic solid-state components. Solid-state components have a high failure rate during the first 100 hours of operation. Unit 1 had 200 hours, unit 2 had 244 hours, unit 3 had 377 hours, and unit 4 and the control chassis had an estimated 250 hours for a total of about 1071 hours of operation before being shipped to the Corning and South Gila Canals for the prototype field testing programs to verify laboratory studies.

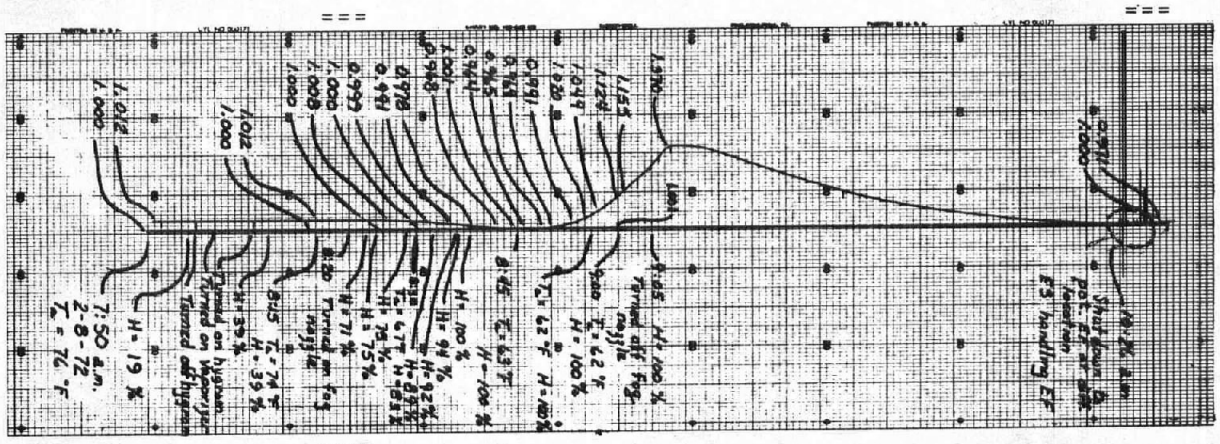

(a) Example of model "A" electronic filter runaway output at 100 percent humidity when the high impedance circuit is not completely encapsulated.

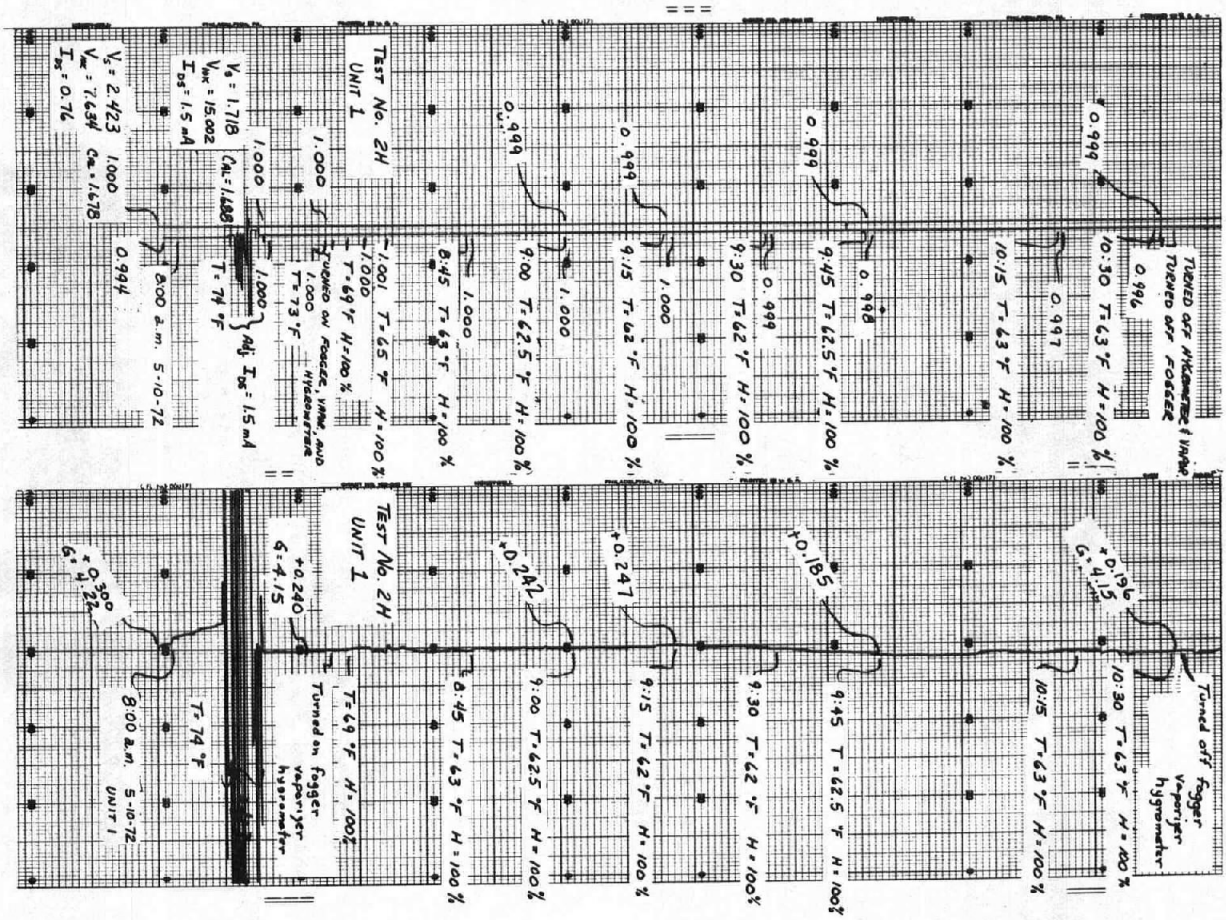

(b) Humidity test No. 2H - Chart recording shows excellent protection of the high impedance circuit.

Figure I-1.— Chart recordings for humidity tests of model "A" electronic filter and final prototype electronic filter unit 1.

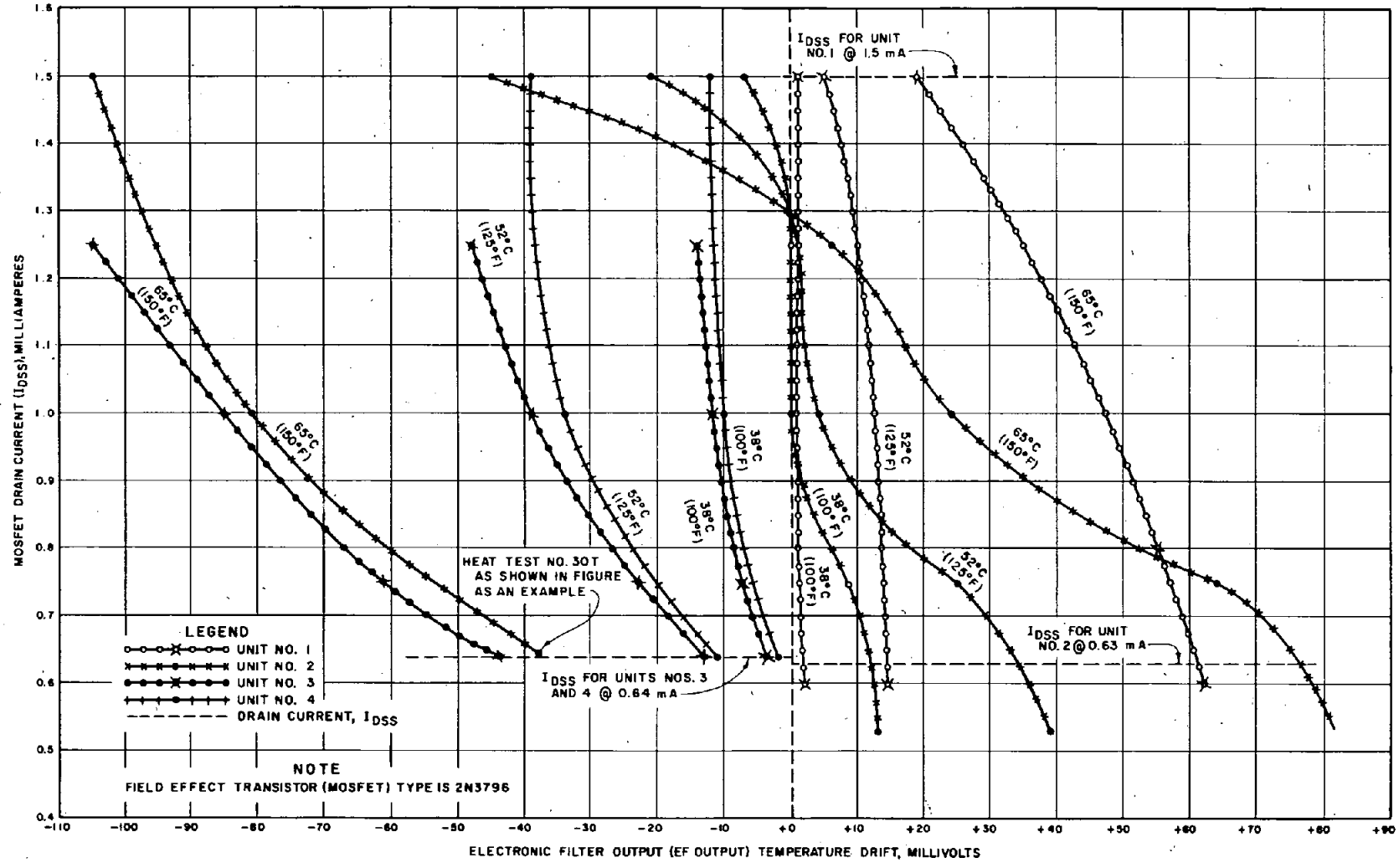

Figure I-2.— Temperature drift characteristics of the electronic filter units 1 through 4 for various temperatures and at various field effect transistor drain currents.

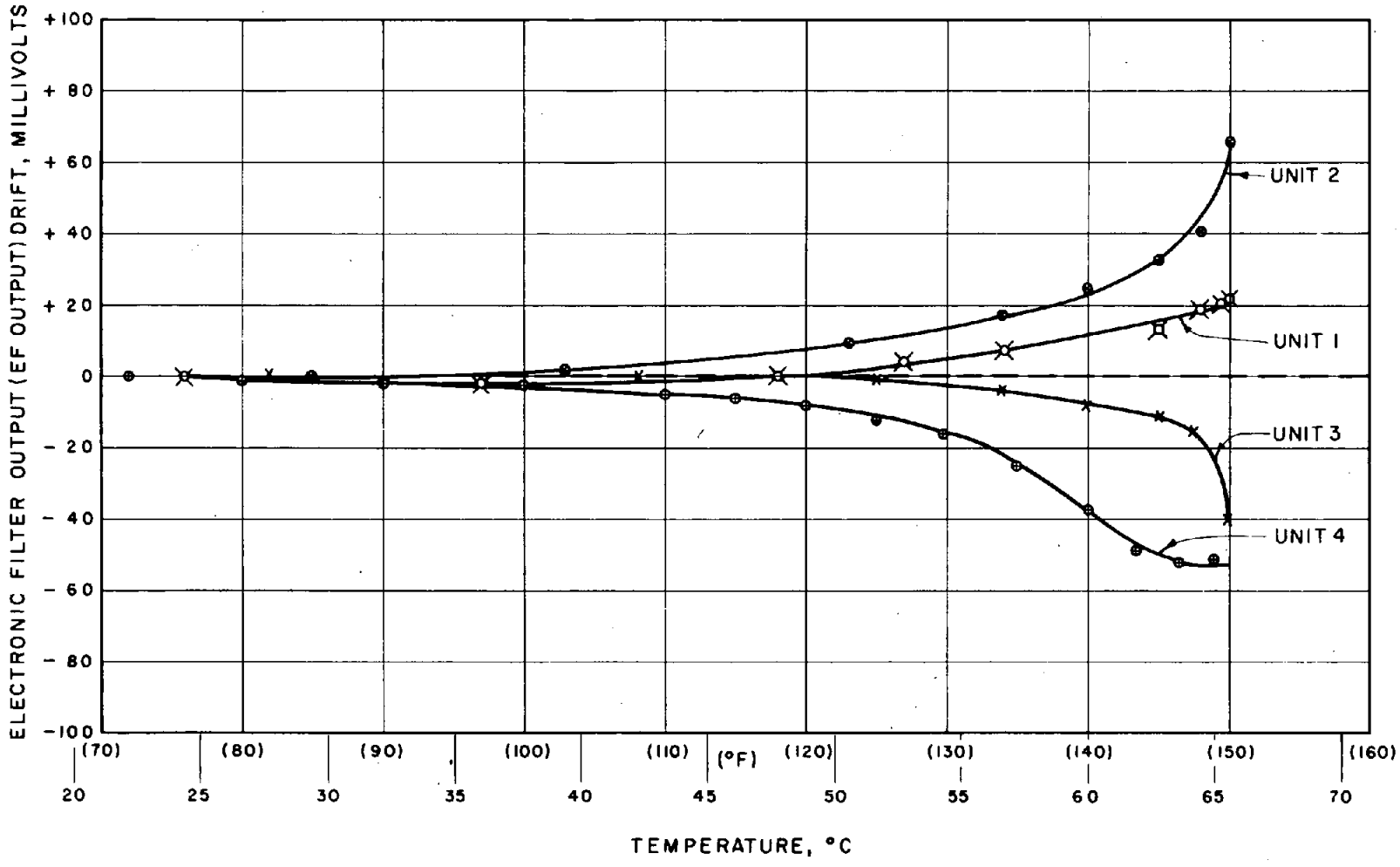

Figure I-3.— Final temperature drift characteristics of the electronic filter output (EF OUTPUT) for units No.1 through No.4 at I_{DSS} drain current versus temperature.

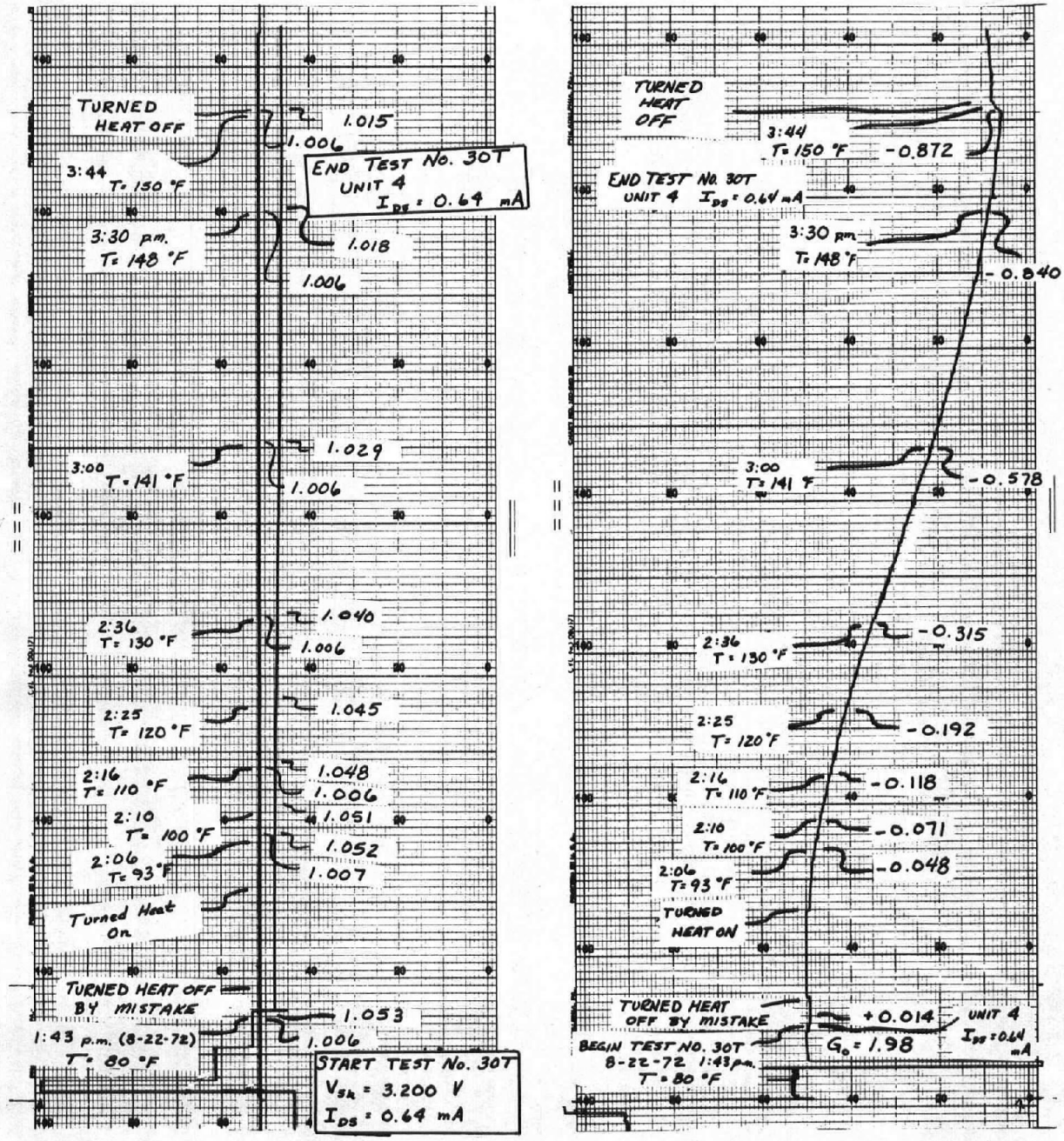

Figure I-4.— An example of a high-temperature test run conducted on electronic filter unit 4.

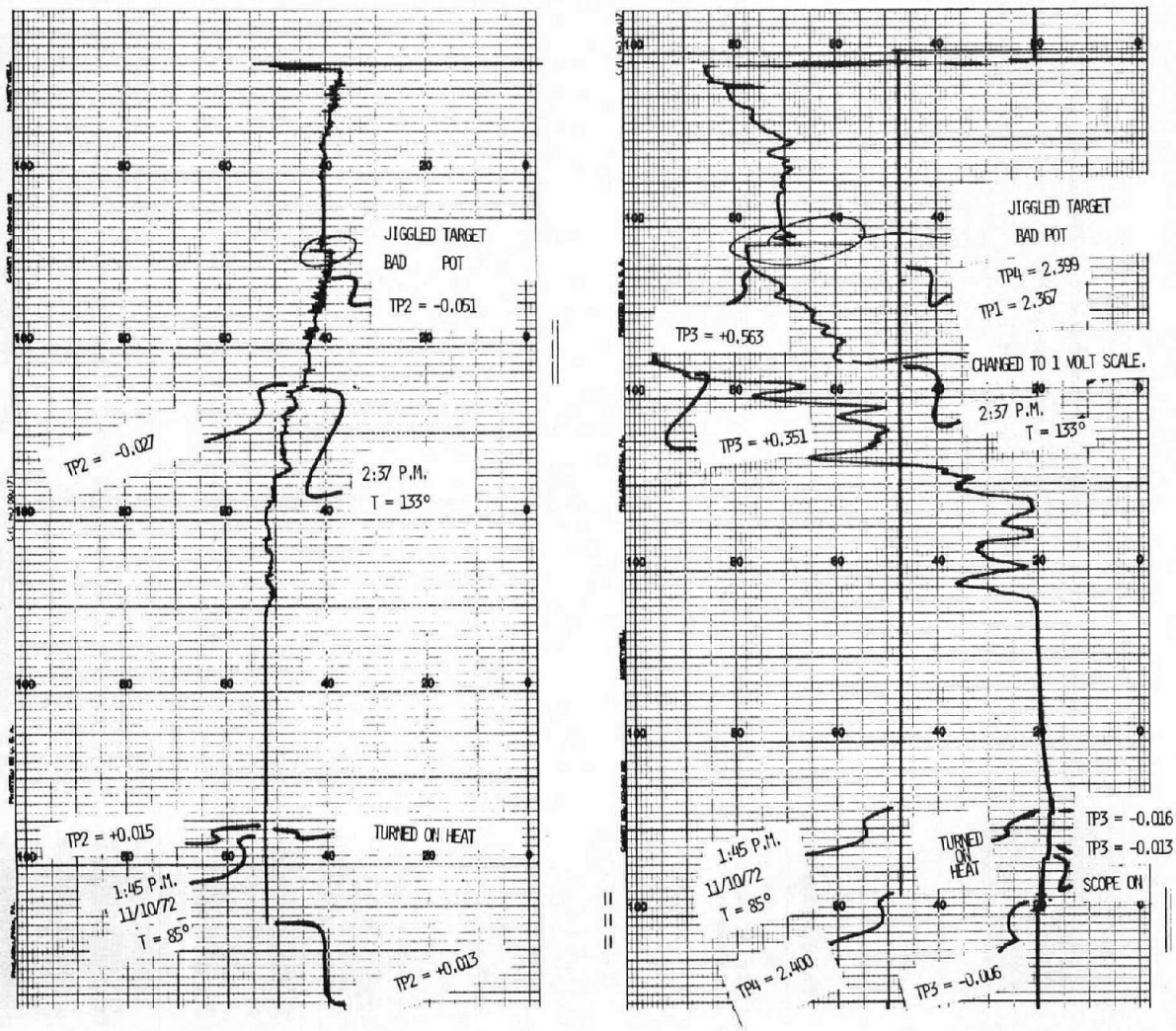

Figure I-5.— Temperature drift of the EL-FLO plus RESET control chassis.

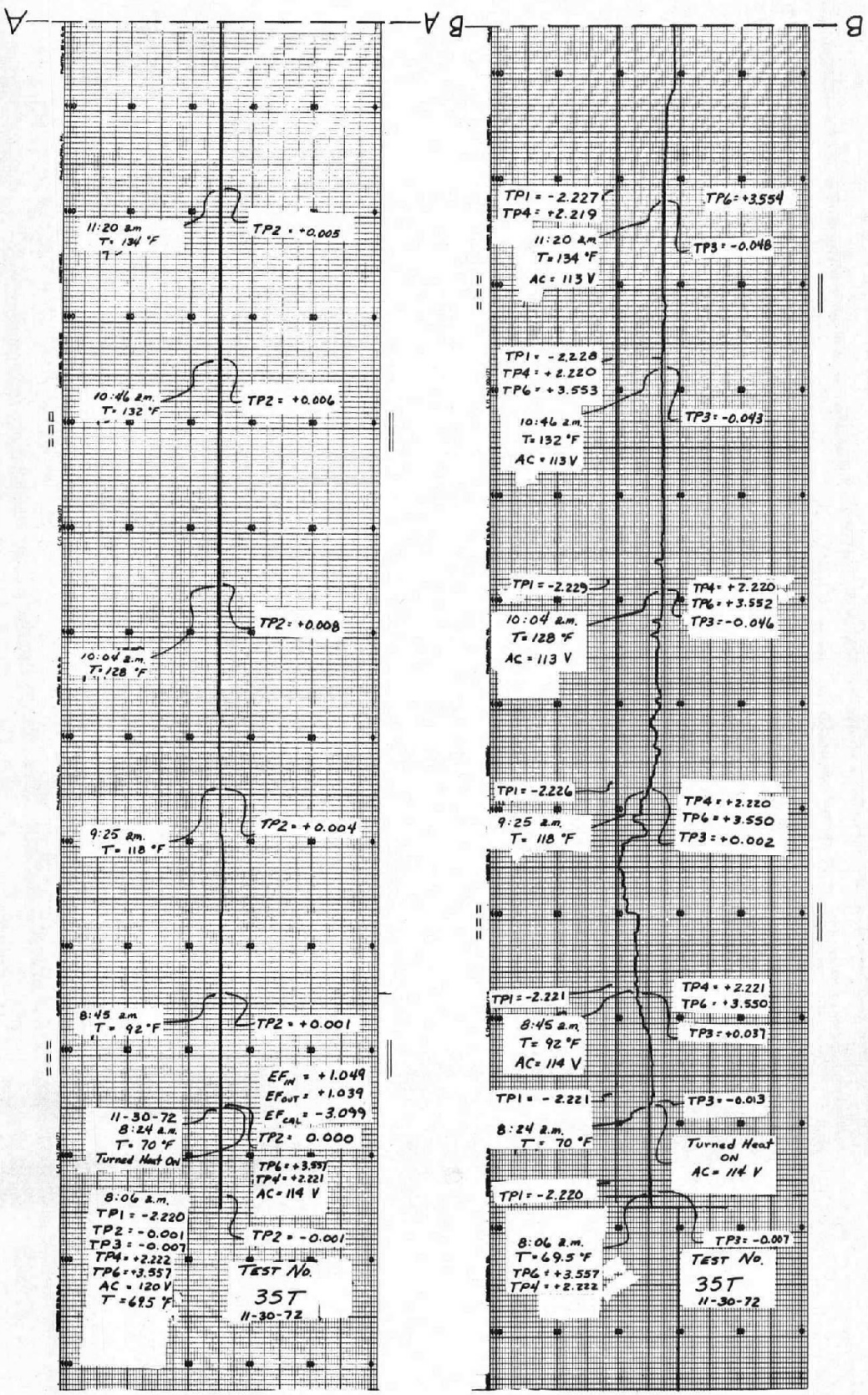

Figure I-6.– Example heat test run No. 35T for temperature drift characteristics on the final prototype EL-FLO plus RESET control (Sheet 1 of 2).

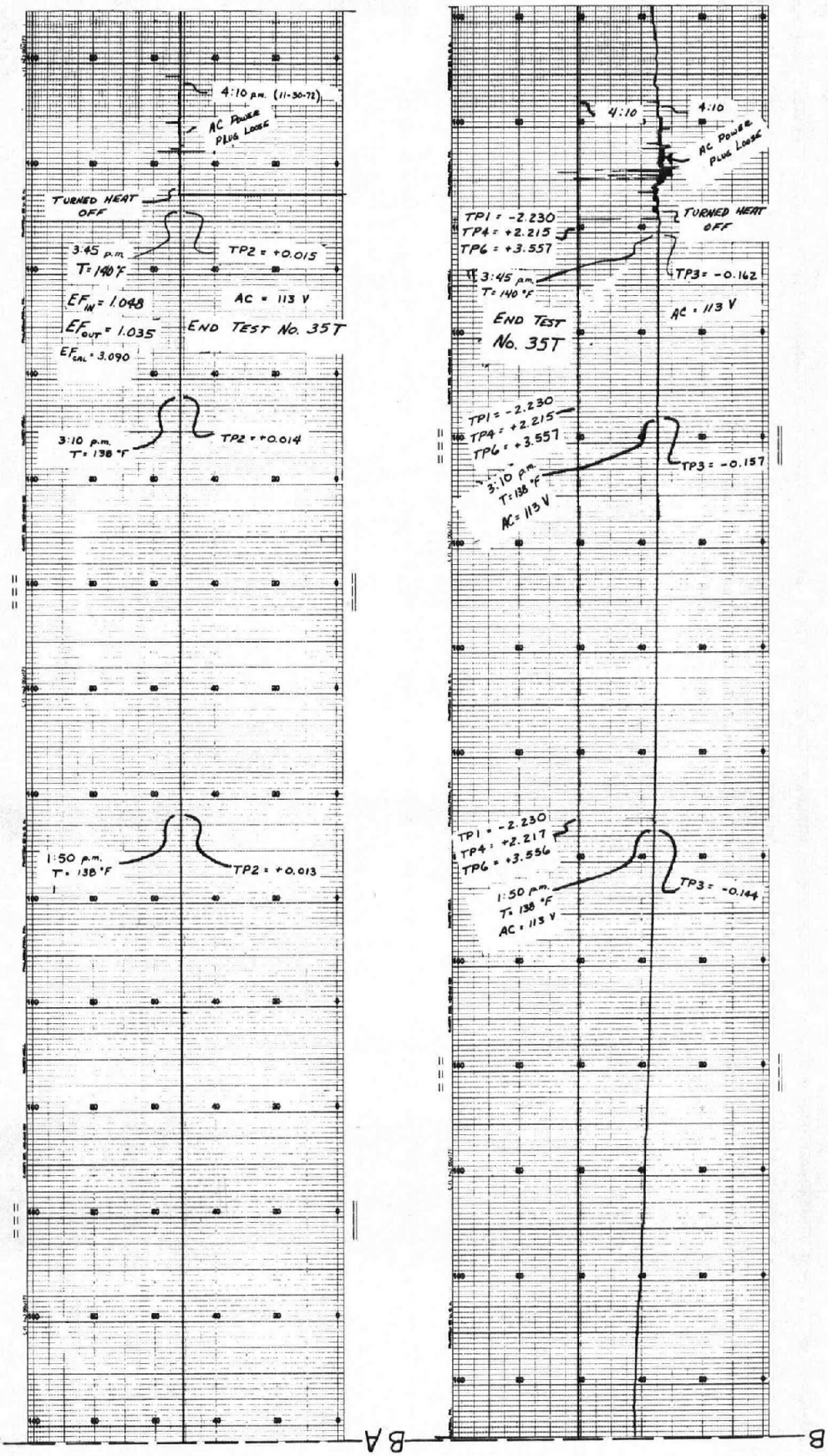

Figure I-6.— Example heat test run No. 35T for temperature drift characteristics on the final prototype EL-FLO plus RESET control (Sheet 2 of 2).

Appendix II

ELECTRONIC FILTER TIME CONSTANT CALIBRATION

General

The electronic filter is an element of the feedback path, figure 16, and provides one of the primary control parameters, the filter time constant. The primary function of the electronic filter is to govern the stability of the control system by filtering out critical frequencies of disturbances that tend to be amplified by the controller. The selection of the filter time constant is based on consideration of the hydraulic transient behavior of the open channel under study, the desired rate of control action of the system, or the amount of damping within a period of potential oscillation, as well as the desired magnitude of the offset from the target value [1, 2].

The primary factor that influences the time constant selection is the length of canal reach being controlled. For canal reaches longer than 3.2 km (2 mi), the time constant required in the filter element may be as high as 4000 seconds. For short canal reaches of about 0.8 km (0.5 mi), the time constant may be about only 100 seconds. Therefore, the filter time constant is different for each canal reach and the electronic equipment is designed to provide an adjustable time constant. The procedure for adjusting the time constant to the selected value (determined from mathematical model studies) is explained in appendix V. The range of filter time constant settings is limited to the selection of the *RC* network. Usually, the resistor *R* of the *RC* network is changed to obtain time constant values within a desired range using equation II-1.

The filter time constant for a particular canal reach can also vary as a function of canal flow. For very low canal flows, the time constant is the maximum. For maximum canal flows, the time constant required of the filter is usually zero. However, the electronic equipment is not designed to vary the filter time constant as a function of the canal flow or water level offset from target. Usually, a mean value is selected and then checked by mathematical model studies for disturbances at the low flows and then at the higher flows to ensure that the desired canal response characteristics are achieved.

A detailed procedure for selecting the filter time constant for the proportional mode of control can be found in reference 4. However, the addition of the proportional reset mode will change the control parameters derived for the proportional mode of control. At the present time, the control parameter selections for proportional plus proportional reset mode of control is largely done by trial and error using the mathematical model output to measure the desired results. The procedure for selecting control parameters including the filter time constant is presently being improved and will probably be the subject of another report in the future.

Electronic Filter Calibration

The equation for the electronic filter is as follows:

$$TF = RC\,(1 + A) \qquad \text{(II-1)}$$

where TF is the filter time constant in seconds,

RC is the resistance and capacitance of

the RC network, and

A is the gain of the operational amplifier

The value of the *RC* network will vary as much as ±10 percent for each component depending on the manufacturer's tolerances.

A series of calibration test runs were made on the four constructed electronic filters to determine the linearity and the magnitude of error that would result if equation II-1 is used instead of a calibration curve to determine the filter gain A required for a desired time constant.

Table II-1 are the data collected for two typical electronic filter calibration test runs on unit 4 (tests No. 64 and 65). At time zero, the filter *EF INPUT* was adjusted +0.600 volt for test No. 64 and −0.600 volt for test No. 65. The filter gain was set at 1.0 for both test runs. Figure II-1 is the chart recording of the filter *EF INPUT* and *EF OUTPUT* (upper chart) and the output of the EL-FLO plus RESET controller at TP3 (lower chart). The upper chart demonstrates how the filter responds with a step change in the *EF INPUT* or water level as measured by the water level sensor. The lower chart shows how the comparator unit moves the gate measured at TP3, ΔG ±0.03m (±0.10 ft) (equation 5) or the electronic equivalence at TP3 of ±1.0 volt.

The data of table II-2 is plotted in figure II-2. The time constant by definition is the time for the *EF OUTPUT* to reach 63.2 percent of the *EF INPUT*. The step change in the *EF INPUT* for both test runs was 0.600

Table II-1.—*Electronic filter unit 4 time constant calibration, tests No. 64 and 65*

Test No.	Time: Seconds	Time: Minutes	Electronic filter *EF OUTPUT*,[2] volts	Δv, volts	$\frac{\Delta v}{\Delta V}$	$1 - \frac{\Delta v}{\Delta V}$	Initial conditions at time zero
64	0	0	[1] 1.011	0.000	0.000	1.000	[1] *EF INPUT* = 1.000 volt
	300	5	1.153	+0.142	0.237	0.763	[1] Δ*EF INPUT* = 1.600 volts
	600	10	1.261	+0.250	0.417	0.583	ΔV = +0.600 volt
	900	15	1.342	+0.331	0.552	0.448	*OA OUTPUT* = 1.011 volts
	1200	20	1.402	+0.391	0.652	0.348	*GAIN A* = $\frac{OA\ OUTPUT}{OA\ INPUT}$
	1500	25	1.446	+0.435	0.726	0.274	= $\frac{1.011}{1.011}$
							= 1.000
	At a value of $1 - \frac{\Delta v}{\Delta V}$ = 0.632 (ΔV) = 0.632 (0.600 V) = 0.379 V from figure II-2, the electronic filter time constant is 1100 seconds.						
65	0	0	[1] 1.005	0.000	0.000	1.000	[1] *EF INPUT* = 0.990 volt
	300	5	0.860	−0.145	0.242	0.758	[1] Δ*EF INPUT* = 0.390 volts
	600	10	0.753	−0.252	0.420	0.580	ΔV = −0.600 volt
	900	15	0.670	−0.335	0.558	0.442	*OA OUTPUT* = 1.002 volt
	1200	20	0.611	−0.394	0.657	0.343	*GAIN A* = $\frac{OA\ OUTPUT}{OA\ INPUT}$
	1500	25	0.566	−0.439	0.733	0.267	= $\frac{1.002}{1.005}$
							= 0.997
	At a value of $1 - \frac{\Delta v}{\Delta V}$ = 0.632 (ΔV) = 0.632 (0.600 V) = 0.379 V and from figure II-2, the electronic filter time constant is 1080 seconds.						

[1] For initial *EF INPUT* and *EF OUTPUT* voltage values at time zero, refer to figure II-1.
[2] *EF OUTPUT* equals *OA INPUT*.

volt and, therefore, the change of *EF OUTPUT* at the time constant, *TF*, interval of time is:

$$EF\ OUTPUT \text{ at } TF = 63.2\% \times \Delta V \quad \text{(II-2)}$$
$$= 0.632\ (0.600\ V) \quad \text{(II-3)}$$
$$= 0.379\ V \quad \text{(II-4)}$$

The time constant *TF* can be determined from figure II-2 at the intersection of:

$$1 - \frac{\Delta v}{\Delta V} = 0.379 \text{ volt} \quad \text{(II-5)}$$

For test No. 64, the time constant was 1100 seconds and for test No. 65, the time constant was 1080 seconds. There is a small error that occurs between the *EF INPUT* positive step change and the negative step change of about 2 percent. The error is caused by the slight nonlinearity of the MOSFET offset between the gate and source terminals as the *EF INPUT* changes from 0 to 2 volts, shown in columns 2 and 3 of table II-2. This nonlinearity is considered to be negligible in the total system performance.

The time constant calculated from equation II-1 with gain *A* equal to 1.0 gave a value of:

$$TF = 500\ (1 + A) = 1000 \text{ seconds} \quad \text{(II-6)}$$
where R = 100 megohms and C = 5 microfarads
or RC = 500 seconds (II-7)

The average *TF* of tests No. 64 and 65 is 1090 seconds. The error between the calibration test runs and equation II-1 would be 90 seconds (9 percent) which is within the ±10 percent tolerance. However, with one test-run calibration, an *RC* network value can be calibrated:

$$RC = \frac{TE}{1 + A} = \frac{1090}{1 + 1.0} = 545 \text{ seconds} \quad \text{(II-8)}$$

Table II-2—*Final calibration data for the prototype electronic filter units 1 through 4*

Unit	*EF INPUT,* volts	*EF OUTPUT,* volts	*OA OUTPUT,* volts	V_5 (pin No. 11) volts	V_{5k} or 10k volts	Power supply +15 volts	Power supply −15 volts	Filter *GAIN A1*	Filter I_{DS}, mA
					V_{5k}				
2	2.000	1.940	7.307	1.944	3.378	14.974	14.893	3.77	0.674
2	1.500	1.467	5.529	1.472	3.282	14.974	14.893	3.78	0.656
2	1.001	0.994	3.746	0.998	3.187	14.974	14.893	3.78	0.637
2	0.504	0.527	1.987	0.530	3.094	14.974	14.893	3.77	0.619
2	0.001	0.047	0.183	0.051	2.998	14.974	14.893	3.90	0.599
	at pin No. 15 = 6.03 volts, *TF* = 2300 seconds								
					V_{10k}				
1	2.004	1.879	3.177	2.641	15.834	14.974	14.893	1.69	1.583
1	1.497	1.435	2.427	2.174	15.411	14.973	14.893	1.69	1.541
1	1.001	1.000	1.694	1.718	15.000	14.974	14.893	1.69	1.500
1	0.501	0.562	0.953	1.259	14.585	14.973	14.893	1.69	1.458
1	0.001	0.126	0.213	0.801	14.171	14.975	14.893	1.69	1.417
	at pin No. 15 = 5.995 volts, *TF* = 1500 seconds								
					V_{5k}				
3	2.005	1.950	11.048	1.951	3.376	14.977	14.894	5.67	0.673
3	1.501	1.472	8.343	1.474	3.280	14.978	14.894	5.67	0.656
3	1.002	0.997	5.657	0.999	3.185	14.977	14.894	5.67	0.637
3	0.499	0.520	2.951	0.522	3.090	14.977	14.894	5.67	0.618
3	0.000	0.048	0.272	0.048	2.995	14.978	14.893	5.67	0.599
	at pin No. 15 = 6.002 volts, *TF* = 3550 seconds								
					V_{5k}				
2	1.999	1.938	11.153	1.942	3.387	14.976	14.908	5.75	0.677
2	1.499	1.464	8.432	1.467	3.293	14.976	14.907	5.75	0.659
2	0.998	0.991	5.716	0.997	3.197	14.976	14.907	5.76	0.639
2	0.497	0.517	2.986	0.521	3.101	14.976	14.906	5.78	0.620
2	0.000	0.047	0.285	0.052	3.006	14.976	14.906	6.06	0.601
	at pin No. 15 = 5.998 volts, *TF* = 3240 seconds (recalibrated)								
					V_{5k}				
4	2.000	1.930	1.934	2.120	−3.45	14.96	15.04	1.003	0.690
4	1.500	1.461	−1.465	1.650	−3.35	14.97	15.04	1.003	0.670
4	1.001	0.993	0.995	1.176	−3.26	14.98	15.03	1.003	0.652
4	0.500	0.526	0.527	0.703	−3.16	14.98	15.02	1.003	0.632
4	0.000	0.057	−0.057	0.228	−3.06	14.98	15.02	1.000	0.601
	at pin No. 15 = 6.06 volts, *TF* = 1120 seconds								

If the filter gain A was set to a value of 3.8 instead of 1.0, the filter time constant by equation II-1 with a calibrated RC value of 545 seconds would be 2606 seconds. Calibration test No. 57 (not included in this report) on unit 4, with a gain of 3.8, produced a time constant of 2680 seconds for an error of about 3 percent which is an improvement from equation II-1. Equation II-1 gives a time constant value of 2400 seconds, about 10 percent from the calibrated value of test No. 57.

Figure II-3 is a summary of the electronic filter units 1 through 4 time constant calibration tests No. 25 through 65. Test runs No. 64, 65, and 57 are noted and the dashed line is equation II-1. Unit 2 is about 3 percent less than equation II-1, unit 3 is about 6 percent more, unit 4 is about 10 percent more, and unit 1 is about 11 percent more for an average error of 6 percent for the four units.

It was concluded that errors of ±10 percent in the time constant derived from equation II-1 would not affect system stability. It could, however, have a small effect on the characteristic response of the canal reach such as the $\mathcal{H}$ value for equation 6 and the percent overshoot derived for equation 11.

Better accuracy of the filter time constant calculation could be obtained by accurate measurement of the resistor and capacitor values of each RC network for use with equation II-1. This procedure was considered to be difficult to implement on a total system basis because each R and C for each filter would have to be measured and each filter then would have a different equation II-1. The significantly increased documentation does not appear to be warranted to improve the accuracy of the time constant to achieve a slightly improved accuracy on the total system characteristic response.

Table II-2 summarizes the final calibration data for the final prototype electronic filters, units 1 through 4, made prior to the shipment of the equipment to the Corning and South Gila Canals for field prototype tests. The data in table II-2 became very useful in the field to check the performance of the electronic components to determine if the equipment changed as a result of continuous operation in the canal bank environment for long periods of time. Field tests on the South Gila Canal established that the solid-state equipment showed excellent stability after 4 months of continuous field operation (table V-2).

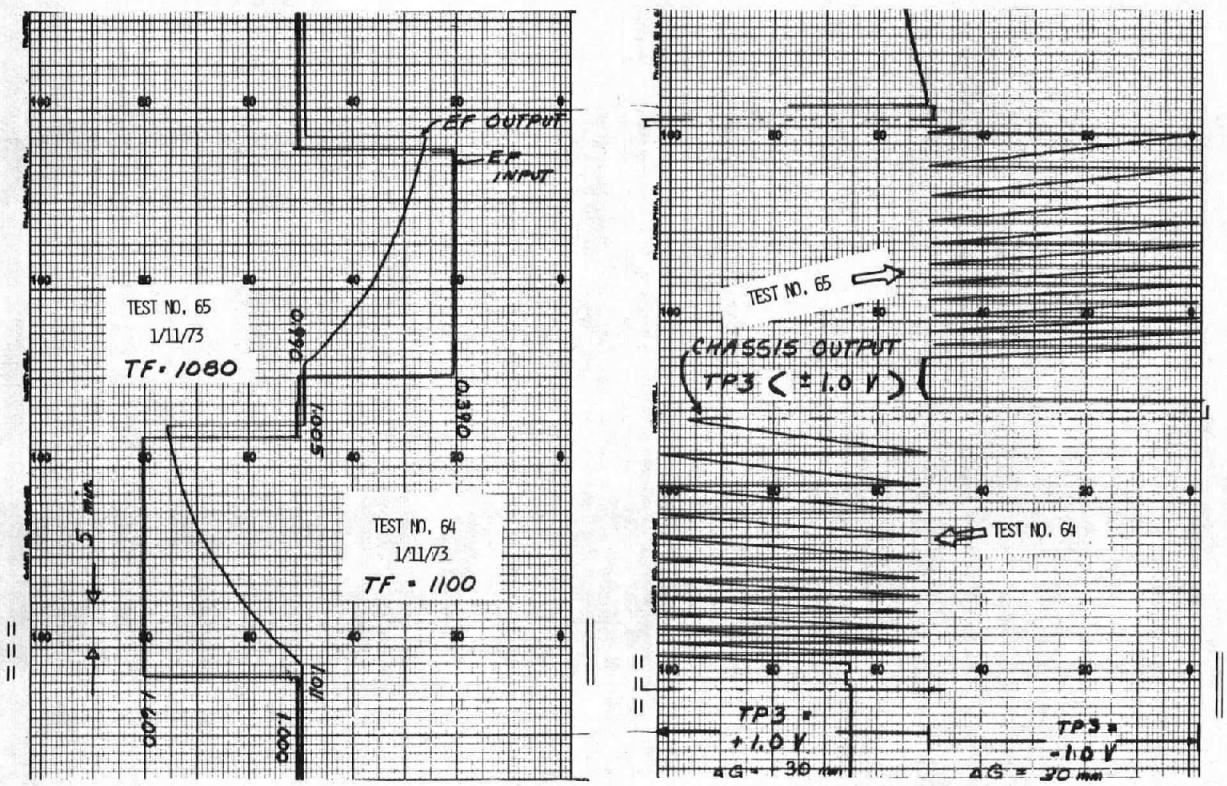

Figure II-1.— Recorder charts of electronic filter unit 4 time constant calibration, tests No. 64 and 65.

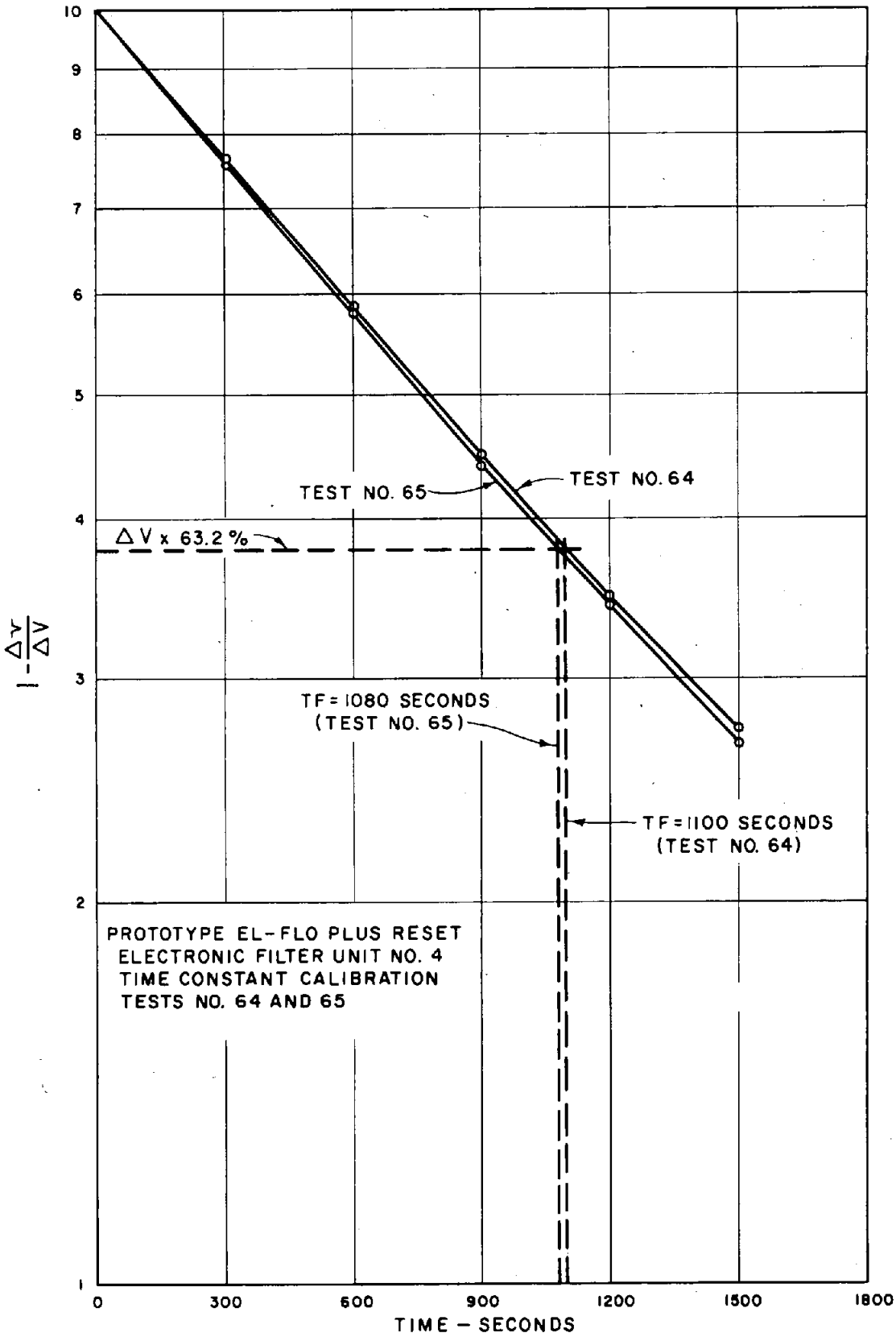

Figure II-2.— Example of electronic filter time constant calibration using test Nos. 64 and 65 on unit 4.

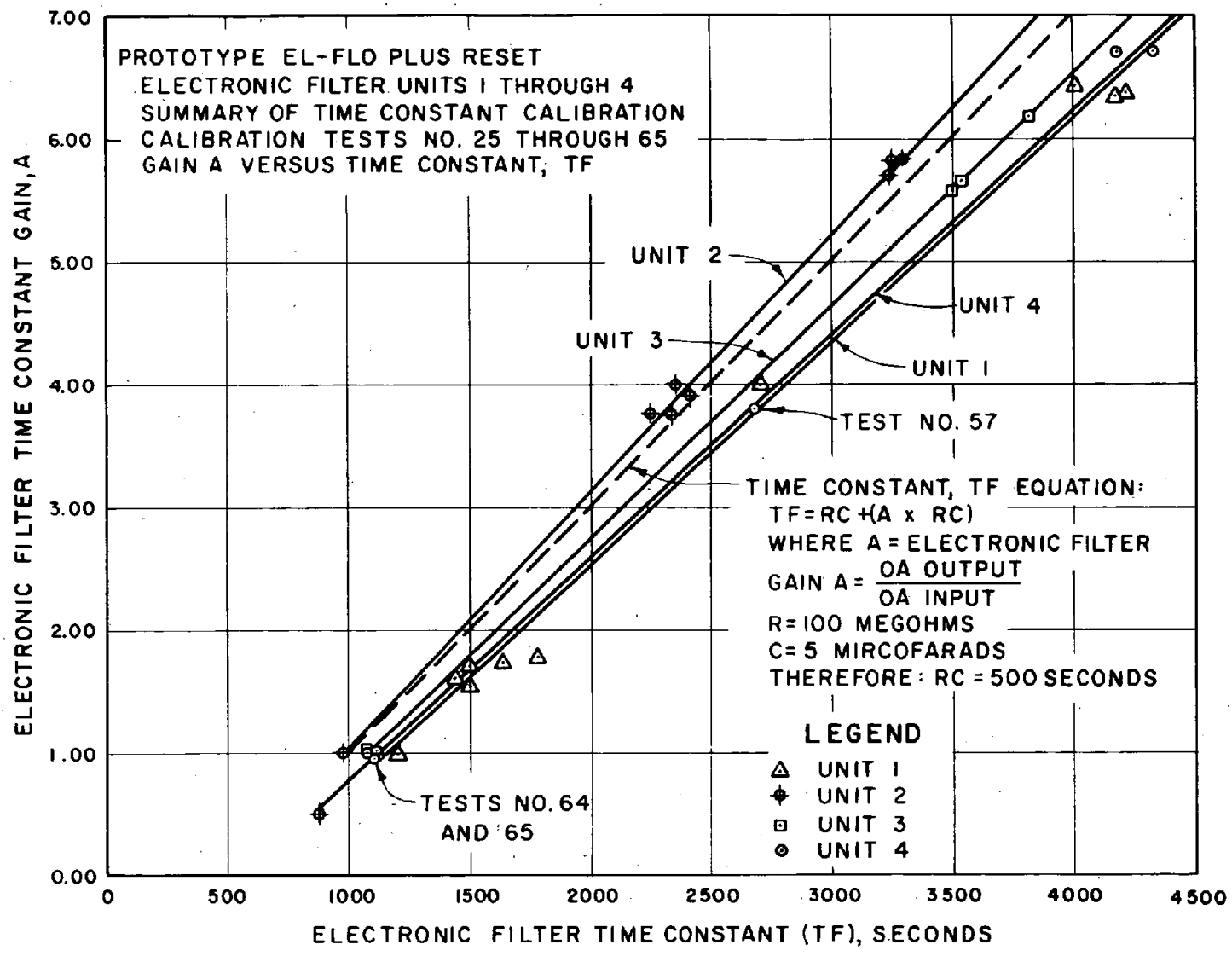

Figure II-3.— Summary of electronic filter units 1 through 4 time constant calibration of calibration test Nos. 25 through 65.

Appendix III

TECHNICAL DESCRIPTION OF EACH EL-FLO PLUS RESET FEEDBACK CONTROL SYSTEM ELEMENT

General

The electronic circuit design strategy for the EL-FLO controller was based on the following criteria:

1. All solid-state components
2. High reliability
3. Packaging for ease in maintenance
4. Operable in changing environmental conditions
5. Capable of being used on canals with widely different hydraulic characteristics
6. Capable of operation over direct-wire, unconditioned-type communication channels
7. Simple to operate and adjust
8. Simple to troubleshoot and repair

These criteria led to the selection of silicon integrated circuits throughout the EL-FLO controller design and use of solid-state and mercury-wetted contact input-output relays.

The circuit design was approached on the basis of isolating each functional requirement of the EL-FLO method and designing the complete circuit necessary to perform each of the required functions. Selection of the packaging method resulted from using this same strategy.

The electronics for the EL-FLO controller can be shown as a series of functional blocks represented in figure III-1. From figure III-1, the major functional blocks of the EL-FLO controller are:

Downstream Check Structure

1. Transmitter
2. Water surface elevation sensor
3. Electronic filter

Upstream Check Structure

1. Receiver
2. Proportional controller and comparator
3. Reset controller
4. Output control
5. Output relays
6. Gate position sensor

The EL-FLO controller provides proportional plus reset type of control action on the controlled device (gate) based on information contained in the input signal (conditioned water level). Closed-loop control of the controlled device (gate) is obtained by providing the controlled device position information to the controller and this position is compared to the desired position computed by the controller. The equipment at the upstream and downstream checks is operating open loop with respect to one another while the hydraulic system (canal) is operating closed loop.

The EL-FLO controller required the design of electronic-type circuitry of a novel type because of the extremely poor operating environment and the extremely slow time response of the hydraulic systems to be controlled. The design strategy used for each functional block of the EL-FLO controller is discussed in detail for each specific electronic circuit.

System Description

The EL-FLO plus RESET feedback control system functional block diagram is shown in figure III-1. The functions of the control system are separated for the downstream equipment and the upstream equipment. The system can be described on the basis of the operation for a single check structure since operation of the electronic equipment for multiple check structures is identical.

The downstream equipment provides water surface elevation information to the upstream equipment via a communication circuit. The communication path between the upstream and downstream equipment locations can be a direct wire circuit or microwave/radio communication circuits. A direct wire, twisted pair, buried cable was used as the communication media for the development of the EL-FLO plus RESET prototype system described in this report.

Downstream Equipment.—The electronic equipment assembly for the downstream location of the EL-FLO system provides for water surface elevation measurement, water surface elevation filtering, and signal conditioning for transmission over the communication circuit.

a. Water surface elevation sensor.—The water surface elevation is measured in an appropriate canal side stilling well and the surface elevation is mechanically converted to an appropriate electrical signal.

The water surface elevation sensor output signal is connected to the EL-FLO equipment using a direct-wire cable. The sensor signal output is relatively low voltage and a shielded cable is required to prevent unwanted noise signals in the EL-FLO

electronics. The sensor is located within the EL-FLO equipment enclosure and, therefore, cable length consideration is not a significant factor.

b. Electronic filter.—The electronic filter acts as an extremely long-time constant low-pass *RC* filter. Typical *RC* time constants for the low-pass filter are from 500 to 3500 seconds. The electronic filter provides the necessary signal delay between the upstream and downstream check structures to maintain stable control during changes in the hydraulic system operation.

c. Analog transmitter.—The analog transmitter conditions the output signal of the electronic filter to provide a suitable signal that can be transmitted over considerable direct-wire distances. The method of signal conversion used does not affect the operation of the control system. One popular method to transmit analog information over a direct wire is the use of variable frequency signaling. The variable frequency signaling method provides long distance signal transmission by converting the analog signal input (usually a voltage quantity) to a low frequency (5— to 25—Hz) signal output that is directly applied to the direct-wire line. The variable frequency output is directly proportional to the analog signal voltage input. The use of a variable frequency for the telemetering signal permits communications between the transmitter and receiver over relatively long distances (15 km) or operation over audio tone channels via radio or microwave. The latter application permits transmission over any distance since the modulated tones can be carried over any voice-grade facility such as radio, microwave, or leased commercial circuits. Up to 27 analog frequency telemetry channels can be multiplexed on a single 300— to 3000—Hz bandwidth circuit.

The distances between check structures on most USBR canal systems are between 2 and 8 km (1 and 5 mi) which led to the selection of the variable frequency telemetry system and a direct-wire communication channel.

d. Transmitter communication circuit interface.—The direct-wire communication circuits are usually exposed to electromagnetic and electrostatic fields of sufficient magnitude to damage solid-state electronic circuitry and are subject to low values of signal-to-noise ratio. In order to isolate these field energies from the solid-state components in the transmitter and provide tremendous improvement in the signal-to-noise ratio, relay isolation is used between the transmitter output and the direct-wire line. High-speed relays with a significant operational life are required since the relay must operate at the 5— to 25—Hz signal rate of the transmitter output. The 25 operations per second speed requirement plus the considerable number of operations that are required suggest the use of high-speed, mercury-wetted contact-type relays. A typical speed at which mercury-wetted contact relays operate is 200 times per second and the typical contact life is 1000 million operations. In addition to the high speeds and long contact life, mercury-wetted contact relays typically have extremely sensitive operating coils that allow relay operation over direct wire for considerable distances (up to 15 km). This characteristic is consistent with the distance that frequency telemetry signaling can be used.

Upstream Equipment.—The electronic equipment assembly for the upstream location of the EL-FLO system provides for reception of the signal over the direct-wire communication path, measurement of the gate position, performing analog computations, and operating the canal check gate motor control circuitry.

a. Receiver communication circuit interface.—The purpose of the receive interface is identical to that of the transmitter interface and provides the required isolation between the direct-wire communication circuit and the solid-state variable frequency signaling analog receiver input.

b. Analog receiver.—The analog receiver converts the 5— to 25—Hz variable frequency signal from the transmitter to an electrical current. The current output of the receiver has a range of 0 to 5 mA. This current output is converted to a voltage value that is proportional to the transmitted water surface elevation.

c. Proportional controller.—The proportional controller is part of the analog computation electronics that sums the water surface elevation signal to a set-point "target" water surface elevation signal and performs multiplication of the results by a fixed constant. The constant is referred to as the "gain" of the proportional controller.

d. Reset controller.—The reset controller is also part of the analog computation electronics that provides intergration, with respect to time, of the water surface elevation. The output signal of the reset controller provides for the elimination of the canal water surface "offset" produced by the proportional controller. The extremely slow response of the hydraulic system required the use of a unique design of the reset controller so that the time integration of the canal water surface elevation would

not cause integrator "windup" for all values of flow changes in the canal. Integrator "windup" results in the integrator output signal reaching a maximum value before the input signal has reached a constant value.

e. Comparator and output drivers.—The output signals of the proportional controller and reset controller are compared to the position of the canal gate through a comparator circuit. The comparison is made by selecting proper voltage polarities for the inputs to a summing circuit. The output signal of the summing or comparator circuit is used to operate the output driver circuitry.

The output driver circuits consist of dual Schmitt triggers. The Schmitt trigger output driver design was chosen to operate the gate motor raise and lower control circuits because of the requirements for an adjustable gate operation dead band to prevent excessive gate operation and adjustable but precise gate movement steps. To eliminate the interaction between dead band adjustments and gate movement step adjustments, operational amplifiers were used for the Schmitt trigger design. Two Schmitt triggers are required, one for operating the raise gate control relay and one for operating the lower gate control relay. Raise or lower operation is determined by the polarity of the summing or comparator circuit output. The outputs of the raise and lower Schmitt triggers operate the solid-state raise and lower gate interposing relays.

f. Gate raise/lower interposing relays.—The EL-FLO controller interfaces with the gate motor electrical controls through solid-state interposing relays. These interposing relays provide isolation between the alternating-current gate motor power source and the low-voltage, direct-current-powered solid-state electronic circuits, and provide sufficient current and voltage to operate the canal gate hoist motors.

The interposing relays of the EL-FLO controller are connected to the gate electrical control equipment using buried cables.

Cable runs can be as long as required provided the conductors are sized such that the voltage drop in the conductors is not sufficient to prevent operation of the motor contactors. The solid-state interposing relays in the EL-FLO controller are rated for 400-volt peak resistive, 10-ampere operation; this rating is sufficient for operation of most gate motor contactors without additional interface equipment.

g. Gate position sensor.—The gate position sensor is mechanically connected to the canal gate operating mechanism so that the electrical output of the sensor is proportional to the gate position. The sensor output signal is scaled to interface directly with the summing/comparator circuitry. The gate position sensors signal is connected to the EL-FLO equipment by a buried cable. The sensor signal is of relative low voltage and shielded cable is required for this connection to prevent unwanted noise signals from entering the EL-FLO controller electronics. The sensor can be located a considerable distance from the EL-FLO control equipment since current requirements for operating the summing/comparator circuitry are extremely small. The sensor cable used in the prototype EL-FLO controller design was a four-conductor, shielded No. 22 AWG instrument cable. A metal foil cable shield with drain wire for grounding provides the best protection against noise signals and electromagnetic radiated fields being coupled to the signal conductors of the sensor.

Circuit Descriptions

The operational description of each electronic circuit that comprises the EL-FLO control system are described in this section. The circuit description is divided into the categories of upstream equipment and downstream equipment as shown on figure III-1. The circuit description will be confined to those that comprise the EL-FLO control system. Descriptions of specific circuits that comprise the analog transmitter and receiver can be found in documentation furnished by the manufacturer of this type of equipment.

Downstream Equipment — Transmit Section.—The EL-FLO controller equipment located at the downstream check structure location is schematically shown on figure III-4. The equipment shown consists of four circuit cards designated Cards No. 1, 4, 5, and 6; analog transmitter module, analog transmitter power supply module and water surface elevation sensor and condition modules, respectively. The following circuit descriptions are associated with the function of the EL-FLO controller according to each circuit card number and major equipment function.

a. Power supply — Electronics — Card No. 1.—The power supply for the electronic circuits is a modular type and furnishes 100 milliamperes at plus and minus 15 volts direct current from a 115-volt alternating-current source. The source side of the modular power supply is protected with a metal oxide varistor (MOV) to prevent alternating-current line noise and over voltages from damaging the

power supply. The MOV was selected because of its high energy dissipation characteristics and small size. The MOV is a solid-state device and requires no maintenance or voltage settings for its operation. The output of the power supply is overvoltage protected with two 20-volt direct-current Zener diodes and overcurrent protected with a 250-milliampere fuse. A single fuse is used in the common lead of the power supply to protect both plus and minus 15-volt direct-current voltage outputs. Zener diodes were selected as overvoltage protective devices because of the low voltage requiring protection, fast operating characteristic, small size, and ability to provide continuous protection with negligible power drain from the power supply.

The power supply voltage of plus and minus 15-volts direct current was selected because most hybrid and integrated circuit operational amplifiers perform most efficiently at 15 volts direct current. Also, this value of direct current voltage offers some protection against false operation from induced noise and transients.

b. Transmitter relay — Card No. 4.—The transmitter relay is a mercury-wetted contact, low operating current coil, high-speed type. This type of relay was used because of the need for high-speed operation (25 times per second), over a long distance (15 km), long contact life (over 1000 million operations), and small size.

The 2.7-kilohm resistor that is in series with the coil allows operation of the transmit relay for a distance of up to 15 km.

The *RC* circuit across the relay coil reduces the oscillation caused by the relay coil being operated at the rate of 25 times per second from the analog receiver switching transistor output and thereby eliminates cross talk that could exist in multiconductor, direct-wire communications circuits.

c. Electronic filter - *RC* network — Card No. 6.—The electronic filter *RC* network card was specially designed so that all components on this card could be encapsulated with a extremely low conductivity, humidity proof encapsulant. The components located on this card that are extremely sensitive to relative humidity are the 100-megohm resistor and the insulated gate metal oxide semiconductor (IG-MOS) field effect transistor (FET) designated Q1. Laboratory tests revealed that epoxy- and silicone-type encapsulants did not provide sufficiently high insulation for satisfactory operation. The encapsulant used was a silastic RTV encapsulating compound labeled Sylgard 184[a] manufactured by Dow Chemical Company and has an insulating quality better than 1×10^{12} ohms. This high insulating property prevents the encapsulant from effecting operation of the electronic filter *RC* network card.

The *RC* network card also contains a glass enclosed contact reed relay. The reed relay must not be enclosed in either plastic or epoxy. Nonencapsulated reed relays with a glass enclosed contact and nylon terminal brackets were used in the prototype design.

The input of the water level sensor (float-driven, 5-kilohm potentiometer) is applied directly to the 100-megohm resistor. Changes in the sensor voltage are integrated by the *RC* network preceding the gate of the MOSFET. The MOSFET is connected as a source follower and therefore the signal on the gate lead is transferred to the source lead with no amplification or inversion. The source signal is different from the gate signal by the amount of gate to source voltage, (*Vgs*). In order to have the gate voltage and source voltage equal in value, the MOSFET must be operated on its characteristic curve where the gate to source voltage is equal to zero. This operating characteristic of *Vgs* equaling zero is also required so that the capacitor in the gate *RC* network cannot discharge through the MOSFET. The required adjustment potentiometer for setting the operating characteristic of the MOSFET at *Vgs* = 0 is located on card No. 5 because no adjustment can be made on card No. 6 after encapsulation.

The operating characteristics of the MOSFET are effected by the ambient temperature and the drift associated with *Vgs* is computed as follows:

$$\text{Drift} = D = 2.2\,(1-(ID/ID(z))^{0.5})$$

in millivolts per degree Celsius

Where *ID* = drain current at operation point
ID(z) = Zero temperature coefficient drain current.

The MOSFET used in the electronic filter circuit design is a Motorola 2N3796 and has a zero temperature coefficient drain current of approximately 0.065 milliamperes. This value of *ID(z)* was confirmed by laboratory measurement. (Refer to table I-2). In addition, the operating current required for the gate-to-source voltage *(Vgs)* to be equal to zero is approximately 0.7 mA. Substituting these values into the drift equation, the voltage is minus 5.3 mV/ °C. Therefore, the actual operating point of the MOSFET will change for temperature variation and

[a] Trademark Dow Corning

this change in operating point would be interpreted by the EL-FLO control system as an actual change in the downstream water surface elevation.

In order to meet both criteria of minimum change in the MOSFET operating point with temperature change and the gate to source voltage (*Vgs*) equal to 0 volt, an offset adjustment potentiometer is provided in the MOSFET source lead. This potentiometer allows operation of the MOSFET at an operating point near the zero temperature coefficient drain current (*ID(z)*) by providing an output voltage adjustment that cancels the effect of *Vgs* not being equal to 0 volt. Therefore, by proper setting of the drain current and adjusting the offset potentiometer so that the gate voltage and potentiometer slider voltage are equal, the effects of temperature drift on the electronic filter MOSFET become negligible.

Laboratory tests were used to confirm that the leakage current of the MOSFET would not affect the filter circuit operation in the temperature range from 25 to 65 °C. For the 2N3796 MOSFET, the leakage current at 25 °C doubles for each 15 °C temperature rise. The maximum voltage change for the 40 °C temperature change, from 25 to 65 °C, was calculated to be 1.56 millivolts.

The reed relay is used to provide a fast charge path for the capacitor during initial power-up and calibration of the electronic filter. The contact from the reed relay is used to insert a 5-kilohm resistor across the 100-megohm resistor so that the *RC* time constant of the filter is reduced by a factor of 20 000.

d. Electronic filter - Operational amplifiers — Card No. 5.—The electronic filter operational amplifier card contains all the electronic components that do not require encapsulation but are essential for proper operation of the electronic filter circuit. This card contains the MOSFET drain current and offset voltage adjustment potentiometers, the reed relay driver and operational logic, the water level sensor calibration potentiometer, and two operational amplifiers.

The purpose of the MOSFET operating point adjustment potentiometers has been discussed in preceding subsection c. Since adjustment potentiometers are required to be operated only to match the operating characteristics of the particular MOSFET selected, the adjustment potentiometers are only accessible when the circuit card is plugged into an extender board. Potentiometer *P1* and *P2* are not accessible from the front of the card since the operating characteristics of the MOSFET should not change throughout its useful life.

The automatic initialize logic is provided on this card to operate the reed relay that is mounted on encapsulated card No. 6. Transistor *Q1* acts as an electronic switch that permits operation of PNP transistor *Q2*. Also, the manually operated push button switch (*SW1*) will operate PNP transistor *Q2*. Operation of transistor *Q2* causes positive 15 volts direct current to be applied to the coil of the reed relay thus causing the form "a" (normally open) contact of the reed relay to operate (close). Operation of transistor *Q2*, and thus the reed relay, is provided in two ways. One, operation of the manual pushbutton switch will operate the reed relay. This mode of operation is used during testing and calibration checks of the EL-FLO controller. Since operation of the switch causes the voltage output of the electronic filter to be equal to the input voltage in 25 milliseconds or less, the switch was mounted directly on card No. 6 to prevent access to the switch and greatly reduce the possibility of accidental operation of the initialize switch during normal operation of the EL-FLO control system. Two, operation of the reed relay will occur when power is initially applied to the EL-FLO controller, and when significant duration power outages occur. Capacitor *C1* and resistor *R1* combine to provide about 2 seconds of base current to *Q1* when power is initially applied to card No. 5. This time is sufficient for the reed relay to operate and to charge capacitor *C1* on card No. 6 to the value of the water level sensor signal. In order for *Q1* to have sufficient base current to operate *Q2*, capacitor *C1* on card No. 5 must be approximately 80 percent discharged. To ensure that *C1* discharges to this 80 percent value, steering diode *D7* provides a discharge path to ground for capacitor *C1*. Diode *D7* does not effect the charging time of *C1*. This quick discharge design of the automatic initialize logic allows the electronic filter to follow the water surface elevation for all types of momentary or long duration power outages of the primary supply power to the EL-FLO controller.

Operational amplifier *A2* is used as an impedance matching amplifier. The connection of the operational amplifier is called a "voltage follower" because signals applied to the input will be transferred to the output without changing the value or sign of the signal. The primary purpose of using this amplifier is to provide impedance isolation between the MOSFET source follower and the analog transmitter input. Since the output impedance of the source

follower is approximately 12 kilohms, the input circuitry associated with the analog transmitter will effectively change the operation of the MOSFET source follower. Operational amplifier $A2$ provides an extremely high impedance load to the source follower and an extremely low impedance input to the analog transmitter, while it does not effect the water level information signal required to be transmitted to the upstream EL-FLO equipment. A general purpose operational amplifier equipped with internal frequency compensation is sufficient for use in this connection and application.

Operational amplifier $A1$ is connected as an inverting gain amplifier. Signals at the amplifier input are transferred to the output with selected amplification and sign change. Amplifier $A1$ is used to allow capacitor $C1$ on card No. 5 to appear like a much larger capacitor than its rated value. Also, the amplifier gain is simpler to adjust than would be the value of capacitance particularly since the capacitor must be encapsulated and the amplifier does not. The time constant of the electronic filter is directly proportional to the value of R_2 and $C1$ on card No. 6 such that the time in seconds for the output signal to change to 63 percent of the input signal is R_2C_1 seconds. The operational amplifier provides longer times with the values of R_2 and C_1 selected as follows:

$$\text{Time constant} = R_2C_1\ (1 + A)$$

where A = amplification factor (gain) of operational amplifier $A1$

Operational amplifier $A1$ is designed to provide variable amplification of the input signal based on the magnitude of the input signal.

The printed circuit card has been etched to allow the addition of jumper wires to insert the necessary input circuitry for implementing the variable amplification operation. Operation of the amplifier in this mode is described in succeeding sections. First, assume that the input circuitry consists only of resistor $R6$ that has a value of 4.99 kilohms. The amplification factor of the inverting operational amplifier can be shown to equal the ratio of the feedback impedance ($P2$) to the input impedance ($R6$). Therefore:

$$A = P2/R6 = Rf/Rin = \frac{\text{feedback impedance}}{\text{input impedance}}$$

This relationship is most accurate for operational amplifiers with open-loop gains of 100 000 or greater. Referring back to the time constant equation, the electronic filter time constant can be rewritten using the expression for the amplification factor shown:

$$\text{Time constant} = R_2C_1\ (1 + P2/R6)$$

where, $A = P2/R6$

The circuit values shown on figure III-4 can be substituted into this expression and the time constant with these circuit values can be shown to range from a minimum of 1000 seconds to a maximum of 5500 seconds. The calculated maximum time constant assumes that the operational amplifier can amplify all values of input voltage without regard to the input voltage value or power supply requirements. The practical values of gain for which amplifier $A1$ can be adjusted is a $P2$:$R6$ ratio of approximately six due to the values of the maximum input voltage (2 volts) and power supply limitations (±15 volts). Therefore, the practical time constant variation obtainable from the electronic filter is from 1000 seconds to approximately 3500 seconds.

The variable gain input circuitry shown on figure III-4 can be used to provide automatic time constant adjustment of the electronic filter based on the amount of change of water surface elevation. The value of $R6$ must be changed from 4.99 kilohms to 49.9 kilohms and the jumpers must be inserted for the variable gain amplifier operation. The diodes and potentiometers provide the various gains that can be obtained. The diodes provide the voltage breakpoint to select which input circuit is inserted, and the potentiometers provide the slope adjustment for gains between breakpoints. The need for this type of operation was not substantiated in canal model studies, therefore, this particular feature of the electronic filter was not used during testing of the EL-FLO controller prototype design.

Since operational amplifier $A1$ determines the time constant value for the electronic filter, an extremely stable, low-drift operational amplifier is required. The prototype design employed a hybrid-type, chopper-stabilized operational amplifier to satisfy the long-stability, low drift requirements. The time constant of the electronic filter must remain constant in order for canal system stability requirements to be obtained; therefore, the chopper-stabilized operational amplifier eliminated errors in the time constant calculation due to electronic circuit stability and drift characteristics.

The water surface elevation sensor calibration circuits are also located on card No. 5. The maximum value of voltage that can be obtained on the water surface sensor is limited to approximately 8 volts. This value is sufficient to allow a precise adjustment of the water surface elevation sensor. Adjustment of potentiometer *P4* sets the maximum voltage range to the water surface elevation sensor from 5 to 8 volts. Full range adjustment from 0 to 100 percent was not provided to conserve power supply current; furthermore, investigation of practical gear ratios for float-type operating mechanisms indicated that full range adjustment was unnecessary.

e. Water surface elevation sensor.—The water surface elevation sensor is a 10-turn, precision, wirewound potentiometer. The value of the potentiometer was selected to be 5 kilohms to allow sufficient current to flow in the potentiometer to eliminate low signal noise pickup from affecting the measurement and is of sufficiently high value to minimize loading of the electronics power supply. The potentiometer is connected to a float-driven pulley and gear assembly through a flexible shaft formed from TYGON tubing. It was found through field testing that a short length of TYGON tubing, 25 to 40 mm (1 to 1.5 inches), provided the best method of flexible coupling for the potentiometer. The tubing offers sufficient coupling to prevent the potentiometer shaft from slipping while it protects the potentiometer when unexpected overtravel of the float occurs.

f. Analog transmitter equipment.— The analog transmitter design and operation is described in manufacturer's instructions for this equipment. The particular type of equipment used for the EL-FLO prototype design was Quindar Inc. model No. QATT-20-525-0024-U-R-G-A. The required power supply equipment necessary to operate the analog transmitter is a Quindar Inc. model No. QP-3 with a 12-volt, 300-milliampere direct-current output.

The Quindar QP-3 power supply also is used to provide the necessary 12 volts direct current to operate the analog receiver relay coil located at the upstream check structure.

Upstream Equipment - Receive Section.—The EL-FLO controller equipment located at the upstream check structure is shown schematically in figure III-3. The equipment shown on the drawing consists of eight circuit cards (designated cards No. 1, 2, 3, 4, 7, 8, 9 and 10), analog receiver module, analog receiver power supply module, and gate position sensor. The following circuit descriptions are associated with the function of the EL-FLO controller according to each circuit card number and major equipment function.

a. Power supply - Electronics - Card No. 1 - Figure III-3.—The power supply for the electronic circuits operates and is designed as described in the Downstream Equipment-Transmit section. The electronics power supply in both the upstream and downstream locations are identical and interchangeable.

b. Power supply - Relays - Card No. 2.—The power supply for relay operation is a modular type and furnishes plus and minus 15 volts direct current at 100 milliamperes from a 115-volt alternating-current source. The modular power supply is identical to that located on card No. 1. A separate power supply was used for operation of relays because operation of the relays create an unbalance in current flow on the plus and minus 15-volt outputs. This current unbalance causes the regulation of the power supply to compensate by lowering the output potential of the power supply. If the electronics power supply were to be used to operate the unbalanced relay loads, the electronic circuitry would not operate correctly because the power supply output of 15 volts would change each time a relay load was energized.

The primary relays that are operated from this power supply are the gate motor raise and lower interposing relays and the integrator motor rotation direction selection relays. A miniature dual form C contact, reed relay is mounted on the power supply card and inhibits gate motor operation and integrator motor operation during failures of the communication line, or failures of the analog transmitter or receiver between the upstream and downstream check structures. Operation of the gate motor and integrator motor is prevented by operating the coil of the reed relay from the loss-of-signal output of the analog receiver and connecting the plus and minus 15-volt power leads from the modular power supply through the reed relay normally open contacts and then to the gate and integrator motor control relays. The loss-of-signal output from the analog receiver will keep the coil of the reed relay energized as long as a valid signal is being received by the analog receiver. Therefore, power to the gate motor control relays and integrator motor control relays will also be available as long as a valid signal is being received by the analog receiver.

c. Receiver relay - Card No. 4.—The receiver relay type and circuit operation is identical to that described for the transmitter relay circuit.

The relays used for both the transmitter and receiver were assembled on one circuit card because of space and interchangeability considerations.

d. EL-FLO controller - Proportional and comparator circuit - Card No. 7.—The EL-FLO controller circuit card provides for the analog computation of the desired gate position (GP) and computes the amount of actual gate travel required (ΔG) to obtain the desired gate position.

The circuit card contains three operational amplifiers. Two of the operational amplifiers are of the hybrid construction type and one is of the medium-scale integrated (MSI) circuit type. The amplifiers designated $A1$ and $A2$ are the hybrid-type amplifiers. Hybrid-type operational amplifiers contain both MSI circuits and discrete component semiconductors within a single modular encapsulated enclosure. High quality, stable operation, temperature and frequency compensated types of amplifiers were used for $A1$ and $A2$ because of the critical analog computation performed by the circuits in which they operate. Hybrid-type operational amplifiers were superior in all operating characteristics to the MSI circuit type operational amplifiers at the time of the EL-FLO controller design.

Amplifier $A1$ is connected and operated as a summing amplifier. The amplifier adds two signals that electrically represent the target canal depth ($Y(T)$) when the flow (Q) is equal to zero, and the actual water surface elevation ($Y(F)$), at the downstream check structure. In addition to the summing operation, amplifier $A1$ also provides multiplication of the two summed inputs by a constant, designated as $K1$. The summing amplifier is also connected such that the output voltage value will be opposite in polarity to the sum of the input voltage values. Therefore, the resultant output signal of amplifier $A1$ represents the proportional control element of the EL-FLO control system and is represented by the following equation:

$$E_{01} = K1[Y(T) - Y(F)]$$

E_{01} = output voltage of $A1$
$K1$ = gain or amplification of $A1$
$Y(T)$ = target set point value
$Y(F)$ = conditioned water surface elevation (downstream) value

The output voltage of $A1$ represents the computed or desired gate position. Therefore, when E_{01} is replaced with GP, the previous equation is identical to that shown in figure 16.

The signal designated $Y(F)$ is the output signal of the analog receiver. The receiver output is a 0- to 5-milliampere current source signal that is directly proportional to the output of the electronic filter. The receiver output is terminated with a 2-kilohm potentiometer in parallel with a 100-microfarad capacitor. The potentiometer provides for adjustable signal inputs to amplifier $A1$ of 0 to 10 volts. The capacitor prevents spurious signals that may be contained in the desired receiver output signal from affecting the operation of amplifier $A1$.

The signal designated $Y(T)$ is the target voltage and its value is obtained from potentiometer $P1$. A 5-kilohm resistor is connected in series with potentiometer $P1$ to provide a more precise voltage adjustment for the target value. The target voltage is a negative polarity signal.

Signal inputs $Y(F)$ and $Y(T)$ are connected to the inverting input of amplifier $A1$ through 50-kilohm resistors. The 50-kilohm resistor value was selected to reduce loading on each input signal potentiometer to less than 1 percent.

The gain or amplification factor of amplifier $A1$ is controlled by the 1-megohm potentiometer connected from the amplifier output to the inverting input. The 1-megohm feedback potentiometer and the 50-kilohm input resistors provide a theoretical value of $K1$ that is adjustable from 0 to 20. Since operational amplifiers do not operate as specified when operated at gains of less than unity, the practical adjustment for $K1$ is from 1 to 20. Since amplifier $A1$ is operating as an inverting amplifier, the output signal will be opposite in polarity to the input signal.

Hybrid operational amplifiers are not factory adjusted so that the output voltage is exactly zero for 0 volt at the input. A 50-kilohm potentiometer designated as the "trim" adjustment has been provided in each of amplifier $A1$ and $A2$ circuits for making the necessary trim adjustment. This setting need be made only once during the calibration of the amplifiers. The trim potentiometers are only accessible when the circuit card is plugged into an extender board.

Amplifier $A2$ is also connected and operated as a summing amplifier. This amplifier adds the signals that electrically represent the desired gate position (GP) as computed by the proportional circuit, and the actual measured gate position (GA) and the desired gate position (GR) as computed by the reset or integration circuit. In addition to the summing operation, amplifier $A2$ also provides multiplication

of the three summed inputs by a constant, designated as $A2$. Amplifier $A2$ is also connected as an inverting amplifier similar to amplifier $A1$. Therefore, the output signal of amplifier $A2$ represents the amount of gate position change that is necessary to make the actual gate position equal to the desired gate position and is represented by the following equation:

$$E_{02} = A2(GP + GR - GA)$$

E_{02} = output voltage of $A2$
$A2$ = gain or amplification of $A2$
GP = desired gate position - proportional circuit computation
GR = desired gate position - reset circuit computation
GA = actual measured gate position

The output voltage of $A2$ is equal to the amount of gate movement required to obtain the calculated desired gate position. Therefore, if E_{02} is replaced with $\pm\Delta G$ and $A2$ is assumed equal to unity gain, the above equation is identical to that shown in figure 16.

Signal inputs GP, GR, and GA are connected to the inverting input of amplifier $A2$ through 50-kilohm resistors for the same reasons as described for amplifier $A1$.

The gain of amplifier $A2$ is controlled by the 500-kilohm potentiometer connected from the amplifier output to the inverting input. The 500-kilohm feedback potentiometer and the 50-kilohm input resistors provide a practical value of $A2$ that is adjustable from 1 to 10. In addition to the 500-kilohm potentiometer, a 0.1-microfarad capacitor is also connected in parallel with the feedback potentiometer. This capacitor was necessary to reduce amplification of alternating-current noise. Since amplifiers $A1$ and $A2$ are connected in series, the total amplification from card input to card output is the product of the amplifier gains. Thus, $K1A2$ could be as high as 200, creating a large gain factor for low signal alternating-current noise. The value of this capacitor was determined experimentally.

The third operational amplifier on this card, designated $A3$, is a MSI integrated circuit type of operational amplifier and is used to change the sign of the measured gate position input signal. The amplifier is connected as an inverting amplifier with unity gain. The output of the amplifier is used on card No. 10 as the signal to operate the electronic limit switches. Operating characteristics of this amplifier are not critical to the analog computations of the EL-FLO control system.

The 200-kilohm input resistor was selected to minimize the loading effect on the 50-kilohm input resistors of amplifier $A2$.

The 0.47-microfarad capacitor shown connected between the integration input signal (GR) and common was used to eliminate unwanted alternating-current noise that was introduced by cross-talk within the chassis wiring. The value for this capacitor was determined experimentally.

e. RESET controller - Cards No. 8 and 9.—The RESET controller is designed to perform extremely long time integration of its input signal with respect to time. The RESET controller performs analog computation on the following equation:

$$GR = K2 \int_0^t GP\,dt$$

where GR = Desired gate position
$K2$ = Gain or amplification of the RESET controller
GP = Desired gate position computed by proportional controller (amplifier $A1$ on card No. 7)
t = Intergration time period

The computation performed to determine GP has previously been described and the parameters that are part of the computation are repeated:

$$GP = K1[Y(T) - Y(F)]$$

Therefore, the RESET controller equation can be rewritten including the parameters used for computation of GP as follows:

$$GR = K2 \int_0^t K1\,[Y_{(T)} - Y_{(F)}]\,dt$$

The value for GP is the output signal of operational amplifier $A1$ on card No. 7. Therefore, this output is used as the input to the RESET controller. The signal is integrated and multiplied by a constant and the RESET controller output GR is used as an input to operational amplifier $A2$ on card No. 7 as previously described.

The integration period (t) for the RESET controller is extremely long. The changes in the actual water surface elevation are time filtered by the electronic filter and may have a time constant of 3500 seconds, or approximately 1 hour. In addition, as discussed in the General Theory section of this report,

the practical recovery of the canal system must be limited to about 90 percent within 4 hours from the time of the initial disturbance. Therefore, the integrator time period could be as long as 8 hours and the RESET controller output signal must not be limited by integrator windup for at least this period of time. In order to accomplish such a long integration time, a variable-speed, low-speed d-c motor was used to perform the required integration. The output signal from the integrator or RESET controller is derived from a 10-turn precision potentiometer driven by the shaft of the integrator motor. The relationship between the d-c motor integrator and the equation for the analog computation of the RESET controller is as follows:

$$GR = K2 \int_{o}^{t} GP\,dt$$

where $GP = K1(Y(T) - Y(F))$

$K2$ = RESET controller gain

t = Integration time period

The value of GP is used to control the speed (r/min) of the d-c motor and is proportional to the speed of the d-c motor, thus:

$$GP \propto K(\text{r/min})$$

Therefore:

$$GR = K2 \int_{o}^{t} K(\text{r/min})\,dt$$

The expression relating the desired gate position as calculated by the proportional controller is directly proportional to the speed of the d-c motor because the motor speed varies linearly with applied voltage. The constant (K) shown in the expression is the slope of the line relating motor speed to applied voltage (see fig. V-7). The value of $K2$ is determined from mathematical modeling studies, and the procedure for determining the constant K is described in appendix V.

The RESET controller consists of two circuit cards. Card No. 8 provides direction control and travel limit setting for the d-c motor, and card No. 9 provides for controlling the speed of the d-c motor. The description of operation of each circuit card is presented in the following paragraphs.

(1) Motor direction control - Card 8.—The integrator motor direction control circuit card contains the motor control reed relay driver circuits, the high-low travel limit switches and the voltage adjusting network for the integrator potentiometer.

Operational amplifiers *IC*3 and *IC*4 are connected as "hard limit" comparators and use an extremely low drift integrated circuit (MSI) type of operational amplifier. Operational amplifier *IC*4 provides motor rotation direction control for a negative signal input and operational amplifier *IC*3 provides motor rotation direction control for a positive signal input. The input (*GP*) to the comparators is the signal output from amplifier *A*1 on card No. 7. Each comparator is provided with a dead band adjustment potentiometer designated *P*3 and *P*4 with a value of 50 kilohms and connected between common and the plus 15- and minus 15-volt power supply outputs, respectively. These "potentiometers" provide a turn-on adjustment for the comparators so that the signal input (*GP*) is required to be a specific positive or negative value before the motor direction control reed relays operate. The input resistors to the operational amplifier are considerably different. The large value of input resistance (220 kΩ) was used from the adjustment potentiometer input so that small values of voltage dead band (0.01 V) could be obtained while the voltage output of the potentiometer is approximately 20 times greater (0.20 V). The 220-kilohm value is large enough to provide reasonable voltage adjustment of the 50-kilohm potentiometer and is not so large that unwanted noise is introduced into the circuit.

The feedback network for the hard limit comparators consists of an 8-volt Zener diode and a 0.47-microfarad capacitor. The Zener diode is used to "hard limit" the operational amplifier output to 8 volts when the input signal exceeds the "dead-band" voltage value. The capacitor provides for extremely fast switching from the "off" or 0-volt output mode to the "on" or 8-volt output mode. Since the Zener diode does not provide a fixed feedback impedance, the operational amplifiers in the comparator circuits are operating in the "open-loop" gain mode. The "open-loop" gain of the 1319 integrated circuit operational amplifier is greater than 100 000. Therefore, the comparators change state from "on" to "off" for an extremely small deviation between the input voltage value and the dead-band set point value.

The output of operational amplifier *IC*4 operates an NPN transistor switch and operational amplifier *IC*3 operates a PNP transistor switch. The output transistors are used to operate the direction control reed relays and to operate a LED (light emitting diode) visual display lamp. The

amber lamp provides visual indication that the negative comparator has operated and the red lamp provides visual indication that the positive comparator has operated. Neither lamp illuminated indicates that both positive and negative comparators are within the dead-band adjustment limits.

The directional control reed relays are designated as relay X and relay Y. Each relay has two form C contacts. The normally-open contacts of each relay are used to connect the positive 15-volt supply to the motor terminals. The X relay contacts cause the d-c motor shaft to turn in the clockwise direction and the Y relay contacts cause the d-c motor to operate in the counter-clockwise direction. Reed relays were chosen for the directional control relays because of their small size and glass-enclosed sealed contacts. The diodes across each relay coil protect the driver transistors from high-voltage transients that occur after the relay coil is deenergized. The diode limits the maximum voltage transient to approximately 0.7 volt.

The "high" and "low" limit operational amplifiers (*IC5A* and *IC5B*) are also connected as hard limit comparators. The limit comparators were designed using a dual amplifier integrated circuit (MSI) type. The amplifiers are frequency compensated but do not have extremely good temperature stability and drift characteristics. These comparators operate identically to comparators *IC3* and *IC4*. The capacitor is omitted from the feedback circuit since output switching for limit comparisons is not critical. The low limit comparator has two inputs. One input is from a fixed voltage divider that provides the low limit set point. The second input is the actual signal from the integrator potentiometer output. The fixed low limit voltage divider provides for a low limit of approximately 0.03 volt. The high limit comparator has one input from the integrator potentiometer output and a second input from an adjustable potentiometer. The high limit adjustment varies for each canal reach because the constant *K2* is different for each canal reach and, therefore, a potentiometer is required to make the proper limit setting. The low limit comparator output operates an NPN transistor which shunts the base current from the negative comparator reed relay driver transistor. Shunting of the base current to common causes the relay driver transistor to turn off and results in deenergization of the Y reed relay which stops the motor shaft rotation. The high limit comparator operates in a similar manner to deenergize the X relay and stop the motor shaft rotation. The limit comparators prevent damage to the integrator potentiometer due to motor shaft rotation that could occur beyond the stops of the 10-turn integrator potentiometer.

The voltage adjustment network provides setting of the correct voltage on the integrator potentiometer. The adjustment potentiometer is connected so that voltages from plus 15 volts to plus 1.4 volts can be obtained.

(2) Motor speed control - Card No.9.—The integrator motor speed control circuit card contains an absolute value computation circuit, a voltage-controlled oscillator, and motor driver transistor.

The input signal to the integrator motor speed control card is obtained from amplifier *A1* on card 7 as described in (1) for the directional control card. The input voltage is a bipolar signal and this signal must be made unipolar for proper operation of the voltage-controlled oscillator. This signal conversion is accomplished through (MSI) integrated circuit *IC1*. Integrated circuit *IC1* contains two operational amplifiers and these amplifiers are connected to perform an absolute value computation on the input signal. The absolute value circuit provides a negative signal output for a bipolar signal input and performs multiplication by a constant to the input signal. Amplifier *A* in the absolute value circuit is designed so that for positive input signals its output is approximately 0 volt, and for negative input signals it operates as a unity gain inverting amplifier so its output signal is equal to the value of the input voltage but has a positive value.

The diodes in the feedback path provide for insertion or shunting of the 10-kilohm feedback resistor depending upon the polarity of the output signal. Amplifier *B* adds the signal from the output of amplifier *A* to the input signal and provides an inverted output of this sum multiplied by a constant. It should be noted that the input resistor for the signal from amplifier *A* is one-half the value of the resistor for the signal input. The output signal of amplifier *A* must be divided by two since the signal input is negative and the output signal from amplifier *A* is positive and therefore the difference of these two signals must always equal the value of the input signal.

The output signal of amplifier *B* is a negative polarity signal that is equal to the value of *GP*

multiplied by a constant. The constant is designated as K in previous discussions.

The voltage control oscillator uses a low-drift (MSI) integrated circuit operational amplifier identical to that used for the positive and negative direction comparators. The operational amplifier is connected as a phase-shift oscillator. Each RC network provides approximately 60° of phase shift to the output signal. Since the output signal is phase shifted by three 60° phase-shift networks, the resultant output is shifted by 180° and returned to the input of the amplifier through a 10-kilohm feedback resistor. Therefore, the amplifier will sustain oscillation and the output signal from the amplifier will oscillate between approximately plus and minus 10 volts. The output signal is a square wave with a duty cycle of 1 with 0 signal input and an amplitude of approximately plus and minus 10 volts. The frequency of operation of the oscillator was matched to the integrator motor and was determined experimentally to be approximately 25 kilohertz. This frequency of operation provides the best speed control range for the d-c motor. The duty cycle (ratio of positive half-cycle duration to negative half cycle duration) of the oscillator can be changed by application of a d-c signal input at the amplifier inverting input. Therefore, the signal output of the absolute value circuit (KGP) is used to control the duty cycle of the oscillator. The oscillator output drives an NPN transistor that is connected in series with the d-c motor winding. By controlling the duty cycle with the input voltage, the duration of the on-time and off-time of the NPN transistor can be controlled and thus the speed of the motor can be changed. The switching type of control was used rather than simply varying the voltage to the motor winding because the switching control maintains the motor torque approximately constant and at the maximum operating motor voltage value for all motor speeds. Therefore, extremely slow speed operation of the motor can be maintained without the loss of sufficient motor torque to operate the integrator potentiometer. The diode that is in series with the NPN transistor base lead removes the negative portion of the square wave signal to prevent damage to the base-emitter junction of the transistor.

Potentiometer $P1$ is used to set the proper duty cycle of the oscillator output for the desired input signal range. It should be noted that when the signal input to the oscillator is 0 volt, the duty cycle is approximately equal to unity. Positive signal input reduces the duty cycle and negative signals increase the duty cycle. Therefore, potentiometer $P1$ supplies a positive input to the amplifier that reduces the duty cycle of the square wave output and provides the minimum speed motor operation. The value of K from the absolute value circuit must be sufficient to provide an input signal to the oscillator amplifier that will ensure full range motor speed control.

The motor calibration curves and illustration of computing the constant (K) are shown in appendix V.

(3) Integrator motor.—The d-c motor selected for use as the integrator motor is a slow-speed, high accuracy timing motor. The speed of the motor selected for the prototype EL-FLO control system was 1/72 revolution per minute at 12 volts direct current. The motor has built-in noise suppressing circuitry to minimize commutation spikes from entering the winding potential source. As previously discussed, some additional capacitor filtering was required on the EL-FLO controller proportional circuit to further reduce commutation noise on the d-c power supply. Power supply No. 2, used for operating the reed relays, was also used as the potential source for the d-c motor to further isolate the noise from effected critical circuit operation within the EL-FLO controller receive chassis.

f. Gate driver raise/lower - Dual Schmitt trigger - Card No. 10.—The check gate motor control circuitry and electronic gate high and low limit switches are located on card No. 10. The motor control circuits consist of MSI circuit operational amplifiers connected to operate as extremely accurate Schmitt triggers. The electronic limit switches consist of an MSI circuit and are connected to operate as hard-limit comparators.

The "raise" and "lower" Schmitt triggers are designed using one dual integrated circuit operational amplifier for each circuit. The $IC1$ comprises the lower Schmitt trigger circuit and $IC2$ comprises the raise Schmitt trigger circuit. Only the operation of the lower Schmitt trigger will be described because both circuits operate identically except for signal input and output polarities.

The basic Schmitt trigger type of circuit is a bistable multivibrator that produces an output for adjustable values of input signals and returns to its normal

state (usually off) for a different value of input signal than that required to produce an output signal (turn on).

The input level adjustment for turn-on is called the "trip-point" and the turn-off point adjustment is called hysteresis. Conventional Schmitt trigger designs have an inherent deficiency in that adjustment of the hysteresis causes interaction with the trip-point adjustment so that specific values of trip-point and hysteresis are difficult to achieve.

The circuit design used for the EL-FLO control system avoids this interactive adjustment drawback and allows the trip-point and hysteresis to be adjusted independently without interaction. Amplifier *A* operates as an inverting summing amplifier. The output voltage is negative and is limited to the value obtained from the feedback components comprised of diode *D*1, and the 6.8- and 2.2-kilohm resistors. Diode *D*2 limits the positive output excursions to approximately 0.6 volt. Amplifier *B* operates as an inverting amplifier and provides precision rectification of the output of amplifier *A*. The output of amplifier *B* is fedback to amplifier *A* through potentiometer *P*4 (positive type feedback) and provides for the hysteresis adjustment of the circuit.

The hysteresis adjustment is a function of the ratio of potentiometer value *P*4 and the 10-kilohm input resistor. The trip-point adjustment is determined by the setting of potentiometer *P*3. On figure III-4, the hysteresis adjustment has been labeled dead band adjustment to indicate that the state of the Schmitt trigger output does not change between the trip-point and hysteresis set point.

The output of amplifier *B* operates an NPN transistor. The transistor is used to operate the solid-state gate motor interposing relay and a LED visual display lamp. The amber lamp provides visual indication that the lower gate relays are operating and the red lamp indicates that the raise gate relay is operating. Neither lamp illuminated indicates that both Schmitt trigger circuits are in the off state.

The input to the "raise" and "lower" Schmitt triggers is the output of comparator amplifier *A*2 on card No. 7. The input signal is bipolar so both raise and lower Schmitt triggers are connected to operate from this bipolar signal. When the signal is positive, the lower Schmitt trigger operates and when the signal is negative, the raise Schmitt trigger operates.

The high and low limit operational amplifiers *IC3A* and *IC3B* are connected as hard-limit comparators. The operation of these comparators is identical to that previously described. The input to the comparators is from amplifier *A*3 on card No. 7. The output of amplifier *A*3 on card No. 7 is the inverted signal from the gate position sensor. The electronic high and low limit comparators are set so that they operate prior to the mechanical limit switches associated with the canal gate operating mechanism.

A detailed analysis of the operational amplifier Schmitt trigger circuit is included in the Detailed Circuit Analysis section of this appendix.

g. Output relays - Card No. 3.—The interposing relays that interface the solid-state electronic hardware from the alternating-current gate motor control circuitry are located on this card. One interposing relay for gate raise operation and one interposing relay for gate lower operation are mounted on this card. The interposing relays are of the solid-state type. The output contact of the relays is a solid-state Triac switch. The output load rating of the relay is 400 volts rms at 10 amperes.

The solid-state interposing relay is operated through a built-in reed relay. Therefore, complete isolation between the load alternating-current output and low-voltage, direct-current input is obtained through the reed relay contact.

Solid-state relays were used in the design because they require no periodic maintenance. They are extremely reliable and their relatively small size permitted printed circuit board mounting.

h. Gate position sensor.—The gate position sensor is a 10-turn, precision, wire-wound potentiometer. The value of the potentiometer was selected to be 5 kilohms to allow sufficient current to flow in the potentiometer; this eliminates low signal noise pickup from affecting the gate position measurement and the value is sufficiently high to minimize loading of the electronics power supply. The potentiometer is connected to the limit switch shaft of the gate motor operating mechanism. The connection is made through a flexible shaft formed from TYGON tubing as described previously for the water surface elevation sensor. The gate potentiometer signal leads are connected from the gate location to the EL-FLO controller chassis location using shielded, twisted pair instrumentation cable. During field testing at some gate locations, it was found that alternating-current noise pickup was introduced onto the gate position sensor leads. This noise is eliminated by installing a 0.02-microfarad capacitor on the terminal strip in the EL-FLO controller chassis across the potentiometer slider and common leads. Since the

capacitor is not usually required, it was not incorporated into the printed circuit card designs.

i. Analog receiver equipment.—The analog receiver design and operation are described in manufacturer's instructions for this type of equipment. The particular type of receiver used for the EL-FLO prototype design was Quindar, Inc., model No. QATR-20-525-U-I. The power supply required to operate the analog receiver is a Quindar, Inc., model No. QP-3 with a 12-volt, 300-millampere direct-current output.

The analog receiver is designed to convert the 5- to 25-hertz input from the downstream equipment to a current source output that has a range from 0 to 5 mA. The maximum load that the receiver can drive is 2.5 kilohms.

j. Gate power switch.—A double-pole, single-throw (DPST) switch is used to isolate the gate raise and lower relay outputs from the gate motor control circuitry. This switch allows operation of the EL-FLO control system in a test mode, without actually operating the canal check gates. The switch electrical rating is matched to the particular motor control circuitry to which it interfaces.

Packaging Design

The EL-FLO control system electronic equipment, analog telemetry equipment, gate sensor, and surface elevation sensor are required to be packaged so that installation of the control system equipment is convenient and relatively simple. Most USBR canal systems do not have permanent shelters for equipment at each check structure location. The packaging design for the EL-FLO control system equipment was based on these criteria. The prototype EL-FLO control system packaging design was modified in the final design because the prototype packaging design was somewhat restrictive to be suitable for most USBR canal check structure locations.

EL-FLO Equipment Location.—The best suited location for the EL-FLO equipment was determined to be within the stilling well shelter located at each check structure site. This location was selected because on most USBR canal systems, a shelter or house is provided to protect existing recording equipment used to monitor the upstream water surface elevation at each canal check gate location. The stilling well shelter provides protection of the EL-FLO equipment from vandals and inclement weather conditions. In addition, the EL-FLO control system requires monitoring of the upstream water surface elevation and this location allows the water surface elevation sensor to be packaged with the EL-FLO control system equipment. Typical installation of the prototype EL-FLO control equipment is shown on figures 13 and 14.

Equipment Cabinet.—The equipment cabinet requirements for the installation of the EL-FLO control system components had the following constraints associated with its design based on the decision to locate the EL-FLO control equipment within the stilling well shelter:

(1) The size of the cabinet was restricted to the amount of space within the shelter.
(2) The equipment cabinet had to accommodate all of the necessary electronic equipment plus the water surface elevation sensor.
(3) The cabinet had to be suitable for mounting within the shelter.
(4) Electronic equipment within the cabinet had to be accessible from the front of the cabinet.
(5) The cabinet had to protect the electronic equipment from high humidity conditions that exist within the stilling well shelter.
(6) The equipment cabinet had to be ventilated to prevent excessive internal temperature rise while preventing the entrance of foreign substances and insects.
(7) The EL-FLO equipment had to be readily accessible for testing, calibration operation, and maintenance.
(8) The cost of the cabinet had to be reasonable with respect to the overall EL-FLO control system costs.

Based on these criteria, a standard commercially available No. 14 gage, wall-mounted, swing rack, NEMA-12 cabinet was selected for the EL-FLO control system equipment enclosure. A cabinet size was selected that was sufficient to accommodate all of the required control system equipment.

The cabinet arrangement for the prototype EL-FLO control system design used the swing rack cabinet so that the door of the cabinet opened from right to left and also, the swing rack rotated from right to left. This arrangement was consistent with the design of the purchased cabinet. However, during prototype testing, it was discovered that the width of the cabinet was such that some restriction could occur in stilling well shelters that were designed in prior years. This restriction necessitated a change in the equipment arrangement from that used in the prototype EL-FLO design. A cabinet arrangement that could be used universally in USBR check structure stilling well shelters was designed and the EL-FLO equipment that was purchased to operate the Corning Canal used the new cabinet

equipment arrangement. The general equipment arrangement for the final design EL-FLO control system is shown on figure III-7. The assembly drawing showing the equipment arrangement for the swing rack panel is shown on figure III-8. Figure 15 shows views of the final equipment assembly.

In both the original prototype and final designs, the cabinet ventilation was provided by making a 50-mm (2-in) square opening at the top of the cabinet and covering the opening with a dust filter pad glued securely in place. Also, dust filter pads were placed over the float tape holes located on the bottom of the cabinet to prevent insect entrance within the cabinet. The dust filter pads had to be slotted to allow the float tape to operate without excessive friction. All electrical conduit entrances to the cabinet were sealed through the use of waterproof conduit connectors. The cabinet was also supplied with a gasketed front door.

The final equipment arrangement design used for the EL-FLO control system provided for mounting the cabinet on one end so that the cabinet door would open from top to bottom. Also, the swing rack rotation would be from top to bottom. To prevent the cabinet from becoming unbalanced with the swing rack rotated to its maximum position, the cabinet is required to be securely fastened to the mounting shelf within the stilling well shelter.

Installation of the cabinet within the shelter must be such that the door of the cabinet can be opened to its maximum vertical position and the EL-FLO equipment is easily accessible for operation and adjustment.

Electronic Equipment Mounting.—The electronic equipment that comprises the EL-FLO control system is mounted in a specially designed card cage, so those cards could be mounted adjacent to the analog telemetry equipment. The card cage design used in the to accommodate this standard mounting. The printed circuit cards that comprise the EL-FLO controller were mounted in a specially designed card cage, so that those cards could be mounted adjacent to the analog telemetry equipment. The card cage design used in the final cabinet arrangement consists of an upper card file and lower card file. The upper card file contains circuit cards No. 1 through 4 and the lower card file contains circuit cards No. 5 through 10. The power supplies and relays are mounted in the upper card file and the control cards are mounted in the lower card file.

In the final cabinet arrangement, the calibration, test, and maintenance control panel is mounted adjacent to and below the card cage. The integration motor and associated integrator potentiometer is located behind the control panel.

Sufficient space between the analog telemetry equipment and the card cage was maintained in the final design so additional telemetry equipment, as required, could be mounted in the cabinet.

The equipment cabinet is designed to house both the downstream and upstream EL-FLO control system equipment at one location. Therefore, each cabinet contains the transmit equipment for the upstream check and the receive equipment from the downstream check. This installation was used to eliminate the need for two separate cabinets at one check structure location.

The electronic equipment mounting on the swing rack is shown on figure III-8.

Water Surface Elevation Sensor Mounting.—The water surface elevation sensor is mounted in the cabinet directly behind the swing-rack assembly. Sufficient space was available behind the card cage for mounting the sensor. All components that comprise the water surface elevation sensor, except the float itself, are mounted within the cabinet. Access to the sensor equipment requires that the swing rack be in its maximum rotation position. The maximum rotation of the swing rack is 90° from vertical; therefore, access to the sensor equipment is somewhat limited. Since the sensor equipment does not require periodic adjustment or maintenance, its location within the cabinet was not considered to be too restrictive for adequate equipment maintenance and operation.

The location of the water surface elevation sensor is shown in figures III-7 and 15a.

Calibration, Testing, and Maintenance

The EL-FLO controller prototype design was intended to be adaptable to most USBR canal systems. In order to design a controller that is adaptable to numerous canal systems, the parameters that effect overall stable canal operation are required to be tailored to fit particular canal reach operating characteristics. Therefore, numerous adjustments to the EL-FLO control circuits are required to adapt the control system to a particular canal reach. Once the EL-FLO controller is tailored for a particular canal reach, the equipment is designed to operate for the period of a complete irrigation season without further major calibration adjustments.

Each printed circuit card that requires adjustment to adapt it to a particular canal reach has been designed so

the adjustments can be made from the front of the cabinet without removing the printed circuit card from its position. The adjustments required to tailor particular electronic components to the overall circuit operation are located on the printed circuit card so they are **not** adjustable without removing the card from the card cage. This design prevents inadvertent adjustments that would effect the proper operation of the electronic circuits.

All adjustments for canal reach parameter setting are made with 20-turn precision, infinite resolution, metal film potentiometers. This type of potentiometer was used because wire-wound precision potentiometers have finite resolution and did not perform well during simulation of elevated temperature and humidity environments during laboratory testing of the prototype equipment. All canal parameter adjustments are made by converting the parameter value to a voltage value that can be measured on an easily accessible test point. The adjustment potentiometers are located on the printed circuit cards so they are easily identifiable and are arranged in a logical sequence along the front edge of the printed circuit card.

A control panel was provided adjacent to the card cage in the prototype design and provided below the card cage in the final design. The control panel contains all the required test points that are connected to monitor electronic circuit voltage values. These test points are used for testing, calibration, and maintenance of the EL-FLO electronic circuits. The control panel also contains the primary input power switch for the EL-FLO controller, the gate raise and lower power switch, the main input source fuse, and the visual display lamps for determining the integrator and gate motor operation states. The control panel is also used to access test point voltage values during maintenance and electronic circuit calibration. A specially designed circuit card extender was manufactured for this purpose. The extender allows the circuit card to be operated as part of the control system outside the confines of the card-cage. The extender not only provides for electronic circuit calibration, but also allows more extensive testing of the circuit cards than is possible with the test points that are wired to the control panel. The control panel layout in the final design is shown on figures III-2 and 15. The control panel layout in the prototype design is shown on figures III-3 and III-4.

The analog telemetry equipment used for the prototype design was furnished with integral mounted test facilities. Testing of the telemetry equipment is performed by using the integral test features furnished with the equipment. A module extender board for the analog telemetry equipment is required so that more extensive testing and maintenance of the telemetry equipment modules can be performed.

The cabinet wiring for the upstream and downstream prototype EL-FLO equipment is shown on figures III-5 and III-6.

The complete wiring diagram for the equipment cabinet used in the final design is shown on figure III-9.

Maintenance Strategy

The EL-FLO control system electronic equipment was designed using highly reliable solid-state components so that periodic maintenance would not be required. The electronic analog computing circuits have been designed with precision low-drift operational amplifiers so that periodic calibration would not be required. The mechanical components in the system were selected for long-life and trouble-free operation, but periodic maintenance is required on these components.

The printed circuit card design was based on each circuit card representing a major functional element associated with the EL-FLO control system. A circuit card design based on the functional element approach enables the control system to be tailored to meet many control applications for the least cost by using only those functional elements required for the particular application. For example, the EL-FLO controller can be configured as a proportional controller without reset action by eliminating the use of the reset controller cards, timing motor, and integrator potentiometer. In addition to versatile control system configuration, the functional element approach to the printed circuit card design allows maintenance of the equipment by personnel without in-depth knowledge of the total system operation or explicit details of the circuit design.

Diagnostics of control system trouble can be localized to a specific card by monitoring the test points on the control panel. When a particular functional block of the system appears to be defective from the test point measurements, the defective circuit card can be removed and a nondefective circuit card can be used in its place. Substituting circuit cards to correct control system operation allows maintenance of the equipment at the site location without the need to return the equipment to a central maintenance and repair center. All control system malfunctions can be diagnosed to the circuit card level from the test points provided on the control panel. Thus, the only diagnostic instrumentation required by maintenance personnel is a four-digit, portable digital volt-ohmmeter.

Maintenance testing of the EL-FLO control system requires that the sequence of testing begin at the downstream transmitter location and continue to the equipment at the upstream receiver location. Testing in this sequence established the operational condition of the communication circuit between the two locations.

The electronic filter, card No. 6, is the single card in the EL-FLO control system equipment that requires special precaution when handling, inserting, or removing from the chassis, and when repairing. The components on this card are encapsulated in an encapsulant that is pliable so the encapsulant can be removed and circuit component parts replaced. Due to the insulated gate metal oxide field effect transistor (MOSFET) located on this card, it is easily damaged by static electric charges. When the card is not located in the chassis, the MOSFET device should be protected with a jumper wire placed between the input gate circuit and the source of the MOSFET. The prototype circuit card design provided two binding posts on the card for this purpose. Therefore, whenever the card is required to be removed from the chassis, a jumper wire would be placed between the binding posts before removing the card from service. Also, to further protect the card from damage, the card should be wrapped in **conductive** plastic or metal foil whenever it is required to be stored or transported. Since encapsulating the card requires controlled environmental conditions, repair of this card must be performed by personnel who are familiar with the installation of MOSFET-type components and encapsulating techniques. The card was successfully repaired several times during prototype testing by using the proper encapsulating techniques and proper handling procedures of the MOSFET.

In addition to the plug-in printed circuit card design, maintenance of printed circuit cards is also simplified through the use of plug-in socket mountings for the integrated circuit dual-in-line packaged integrated circuits. Use of sockets permits simple replacement of defective integrated circuits without unsoldering and resoldering.

The swing rack design for mounting the electronic hardware enables accessability to the rear connectors of the equipment for testing and repair without removing electronic printed circuit cards or the analog telemetry modules. Also, the swing rack can be rotated so access to the water surface elevation sensor, for periodic maintenance of the mechanical assembly, is possible without removing the electronic equipment card or module cages.

Summary

The EL-FLO prototype equipment design was extensively tested in laboratory conditions before actual testing in the field environment. A special environmental chamber was built so the entire chassis could be operated at temperatures from 0 to 65 °C and humidity levels from 0 to 100 percent. In addition, the equipment was thoroughly life tested in the laboratory in order to eliminate infant mortality failures of the solid-state components.

During the tests in the environmental chamber, major component evaluations were made and component substitutions were made to the prototype control equipment as required. During these tests, wire-wound precision potentiometers used to make calibration adjustments did not perform as well as metal film precision potentiometers. Therefore, all precision potentiometers used to determine critical control constants are the metal film type. Also, all fixed resistors used on the circuit cards are metal film type.

The suitability of various encapsulating compounds was also determined in the environmental test chamber. The tests that were performed and results of these tests are described in detail in appendix I.

Laboratory simulation of electromagnetic and electrostatic field noise was used to determine the suitability of the EL-FLO control system equipment internal and external wiring methods. These tests provided data for determining the best location for insertion of noise suppression capacitors within the electronic circuits. Also, these tests provided data for determining exact cable shielding and grounding requirements for the control system equipment.

The laboratory tests also provided valuable information on the maintainability of the equipment and proved that the packaging and printed circuit card design was sufficient and met or exceeded the design criteria requirements for accessibility, periodic maintenance, and ease of operation and maintenance repair.

Operation of the prototype equipment during field testing and actual operation of the final design equipment provided data on the overall reliability of the control system equipment during actual operating conditions. The following major areas related to the field operation led to equipment design modifications or additions that were necessary to improve the overall operation of the equipment and to make the equipment more adaptable to field operating conditions.

Lightning Protection.—The communication circuits between the upstream and downstream equipment and the primary alternating-current feeder circuits to the equipment are susceptible to lightning strikes during thunderstorm conditions. The communication circuits were equipped with gas-tube-type lightning arrestors in the original field installations.

Lightning strikes during thunderstorms was probably the most significant contributor to failures of the EL-FLO control equipment. The lightning surge voltages that caused damage to the equipment was found to be affecting the electronic equipment through the communication circuits. The communication circuit was isolated from the electronic equipment using the transmit-receive reed relays, and it was difficult to determine how the lightning strikes were causing damage to the EL-FLO electronic equipment since isolation was purposely provided to protect against such damage. It was determined that the method of operating the transmit and receive relays, using the QP-3 12-V, d-c analog telemetry equipment power supplies, produced a ground-loop between the communication circuit ground and the EL-FLO chassis ground; this caused components within the EL-FLO controller to be damaged due to overvoltage when lightning struck the communication circuit. The lightning protection scheme was redesigned using an additional separate power supply for operating the communication line relays and newly developed solid-state protectors were inserted on the communication lines in place of the older gas-tube protectors. This design modification appears to have reduced the susceptibility to failure of the EL-FLO equipment from lightning strikes on the communication circuits.

Lightning strikes on the primary feeder circuits must be suppressed at the feeder source. It was discovered that the source feeder alternating-current circuits that supplied power to the EL-FLO control equipment had not had lightning protection installed. As a minimum, high-voltage lightning arrestors and fuses are required to reduce the surges generated by lightning strikes on the feeder circuits. The EL-FLO equipment is protected for nominal alternating-current source fluctuations but direct lightning strikes on the feeder are coupled to the EL-FLO equipment and the protective equipment is not designed or intended to suppress such large voltage surges. Therefore, the alternating-current feeder circuits that supply power to the EL-FLO equipment should have lightning protection in order to prevent damage to the control equipment.

Electronic Filter.—As previously discussed, the electronic filter card No. 6 is extremely sensitive to damage when the card is outside the card cage. Removal, repair, and replacement of the card requires extreme caution and results in card replacement and repair being not totally successful by field operations personnel. The reliability of card No. 6 is very good and repair or replacement was seldom necessary, but during diagnostic maintenance the card was removed and replaced frequently and this action sometimes created failures to the card due to handling and not to a component malfunction.

To eliminate the special handling requirements of the electronic filter circuit card, a digital filter prototype was designed and laboratory tested. The digital filter, while considerably more expensive to implement, does not alter the analog operation of the EL-FLO control system. This solution, to the delicate handling requirements of the original designed electronic filter card, has not been field tested to date. Once the techniques for handling card No. 6 are mastered, the inadvertent failure rate will decline considerably; therefore, for the prototype and final system design field tests, the card failure rate was not sufficiently high to warrant the considerable expense of replacing the electronic filter cards with the digital-type design.

Card Cage Connectors.—The connectors used for the prototype and final design EL-FLO equipment card cage assembly became fatigued after about 2 years of operating in the field and created some problems due to poor electrical contact with the card fingers. This problem is attributed to the many card insertions and removals that were made during the test period. The numerous card insertions into the connectors caused the spring tension of the connector pins to become fatigued. The life of the connectors would be greatly extended in a nontest operational mode of the control system. The connector itself could be changed to a different type to improve the life with expected numerous card insertions. This problem is not considered a major design deficiency of the EL-FLO equipment; however, an improved connector would be used for future installations to eliminate the possibility of connector failures.

Multiturn Potentiometer Sensors.—The precision 10-turn, wire-wound potentiometers that were used for gate position, water surface elevation, and integrator output sensors failed on a few occasions. The failures were related to the slider output of the potentiometer periodically being open circuited. No hard failures of the potentiometer slider operating in this manner occurred, so consequently, all the data analysis related to this failure was based on an intermittent-type failure that could not be duplicated in the laboratory. The suspected failed potentiometer was returned to the manufacturer for evaluation and analysis. No specific reason

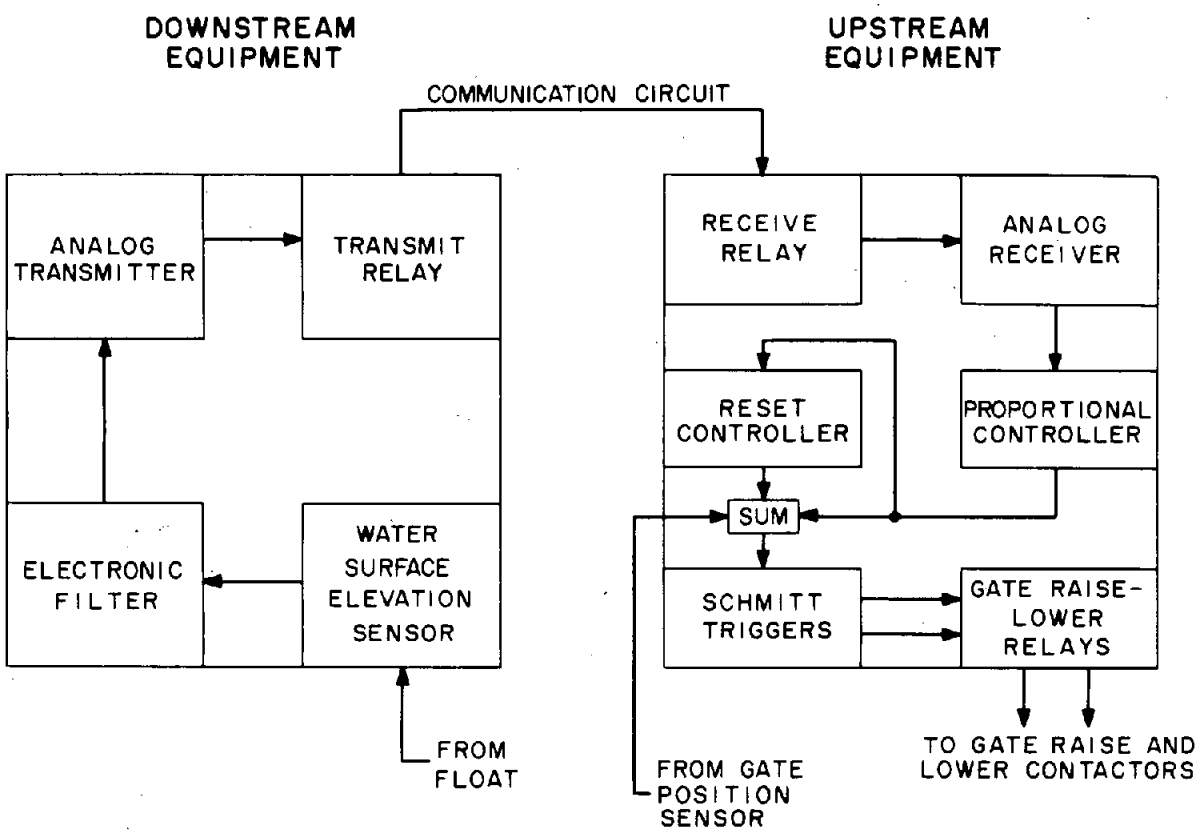

Figure III-1.— EL-FLO controller system functional block diagram.

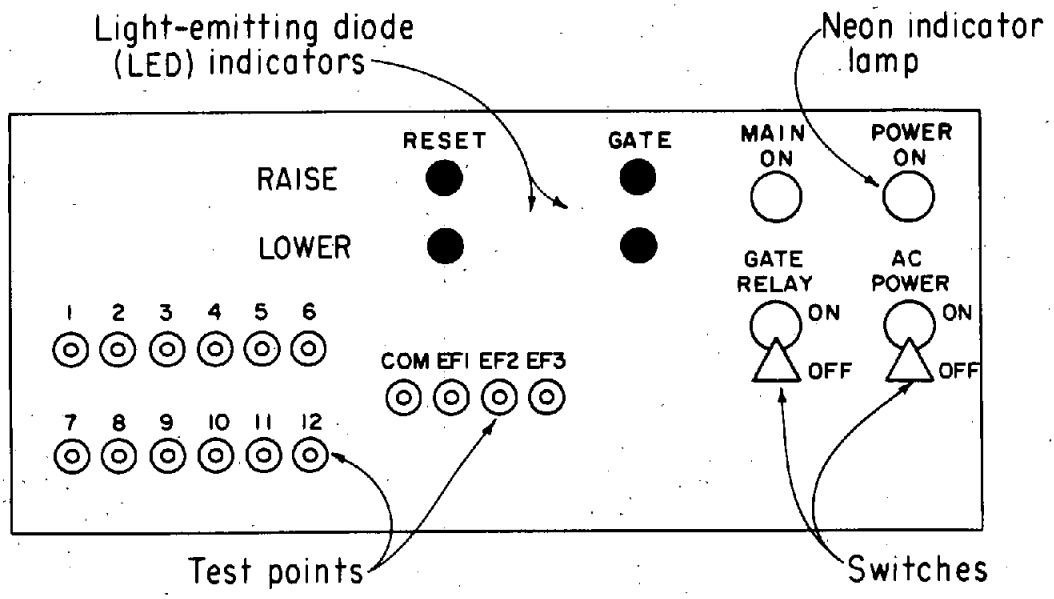

Figure III-2.— EL-FLO controller system control panel.

was identified for the intermittent failures but the manufacturer did discover an improper seal of the potentiometer case. No known reason for the failure exists other than an improper seal; however, it was not substantiated that the improper seal would cause the type of failure that was being experienced.

Because of the lack of conclusive data on the reasons for the potentiometer intermittent failures, the design using these types of potentiometers was not changed. The failures that occurred were not of significant magnitude to warrant a major change in the sensor design.

Alarm System.—During the field test period of the prototype equipment, a system component failure occurred that caused the EL-FLO control system to malfunction and resulted in considerable damage to the canal system. See appendix IV for additional details.

This failure indicated the need for an alarm monitoring system to be installed at each check structure, so equipment malfunctions could be detected at the site and the incidence of an occurring malfunction could be transmitted to a central-manned location for appropriate action. The need for an alarm monitoring system is a definite necessity on canal systems that have EL-FLO system equipment installed at many check structure locations. A central facility can then be immediately alerted when malfunctions occur and operations personnel can then dispatch appropriate maintenance personnel to the specific site where the malfuntcion has occurred. Immediate notification of system trouble will prevent serious damage from occurring to the canal system and associated facilities due to automatic control system malfunctions.

The overall basic design of the EL-FLO control system hardware proved to be sound and the equipment performed well within expectations. The thorough laboratory testing of the equipment is the primary reason for the success that was realized in its implementation. The problems that developed during field testing and long-term use were not substantially significant to warrant major design changes. The basic control system is a reliable, cost effective approach to canal system control and operation.

Detailed Circuit Analysis

The following detailed circuit analyses are included for the electronic filter circuit and the Schmitt trigger circuit because the operation of these circuits is not particularly straightforward. The remaining circuits that are described in the Circuit Description section operate in a conventional manner and a detailed analysis of these circuits is unnecessary.

ELECTRONIC FILTER

I. Simplified Circuit Diagram

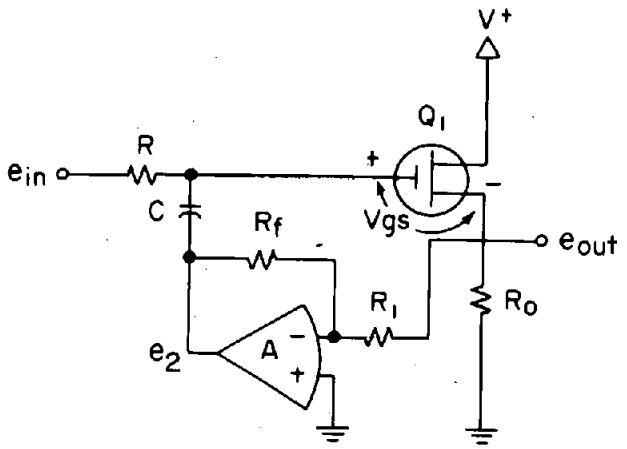

II. Equivalent Circuit Diagram (Input Only)

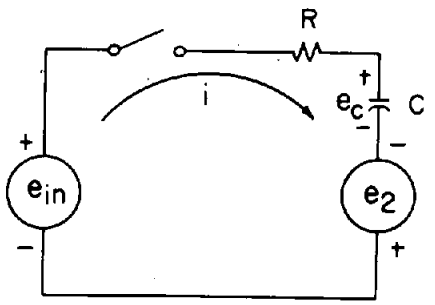

where :

$$e_2 = Ae_{out},\ A = \frac{R_f}{R_1}$$

$$e_{out} = e_{in} - iR - Vgs$$

$$\therefore e_2 = \frac{R_f}{R_1}(e_{in} - iR - Vgs) = A(e_{in} - iR - Vgs)$$

III. Capacitor Voltage Calculation (e_c)

equivalent circuit loop equation :

$$e_{in} - iR - e_c + e_2 = 0$$
$$e_{in} - iR - e_c + A(e_{in} - iR - V_{gs}) = 0$$
$$e_{in}(1+A) - iR(1+A) - V_{gs}A - e_c = 0$$

substitute : $i = C\frac{de_c}{dt}$

$$e_{in}(1+A) - RC(1+A)\frac{de_c}{dt} - V_{gs}A - e_c = 0$$
$$RC(1+A)\frac{de_c}{dt} + e_c = e_{in}(1+A) + V_{gs}A$$
$$\frac{de_c}{dt} + \frac{1}{RC(1+A)}e_c = \frac{e_{in}}{RC} + \frac{V_{gs}A}{RC(1+A)}$$

let : $a = \frac{1}{RC(1+A)}$, $b = \frac{e_{in}}{RC} + \frac{V_{gs}A}{RC(1+A)}$

then : $\frac{de_c}{dt} + ae_c = b$

now let : $L\{e_c\} = f(s)$, $L\{e'_c\} = sf(s)$

then : $sf(s) + af(s) = \frac{b}{s}$

$$\therefore f(s) = \frac{b}{s(s+a)} = b\left[\frac{1/a}{s} - \frac{1/a}{s+a}\right] = \frac{b}{a}\left[\frac{1}{s} - \frac{1}{s+a}\right]$$

and : $L^{-1}\{f(s)\} = e_c = \frac{b}{a}\left[1 - e^{-at}\right]$

$$\text{or : } e_c = \frac{\left[\frac{e_{in}}{RC} + \frac{V_{gs}A}{RC(1+A)}\right]\left[1 - e^{-\frac{t}{RC(1+A)}}\right]}{\frac{1}{RC(1+A)}}$$

so : $e_c = \left[e_{in}(1+A) + V_{gs}A\right]\left[1 - e^{-\frac{t}{RC(1+A)}}\right]$

IV. Output Voltage Calculation (e_{out})

circuit loop equation (from part I)

$$e_{out} = e_{in} - iR - Vgs = e_{in} - RC\frac{de_c}{dt} - Vgs$$

but: $$\frac{de_c}{dt} = \left[e_{in}(1+A) + VgsA\right]\left[\frac{1}{RC(1+A)}\right] e^{\frac{-t}{RC(1+A)}}$$

$$\frac{de_c}{dt} = \left[\frac{e_{in}}{RC} + \frac{VgsA}{RC(1+A)}\right] e^{\frac{-t}{RC(1+A)}}$$

$$\therefore e_{out} = e_{in} - RC\left[\frac{e_{in}}{RC} + \frac{VgsA}{RC(1+A)}\right] e^{\frac{-t}{RC(1+A)}} - Vgs$$

$$e_{out} = e_{in} - e_{in}\, e^{\frac{-t}{RC(1+A)}} - \frac{VgsA}{(1+A)}\, e^{\frac{-t}{RC(1+A)}} - Vgs$$

$$e_{out} = e_{in}\left(1 - e^{\frac{-t}{RC(1+A)}}\right) - Vgs\left(1 - \frac{A}{(1+A)}\, e^{\frac{-t}{RC(1+A)}}\right)$$

let: $Vgs = 0$

so: $$e_{out} = e_{in}\left(1 - e^{\frac{-t}{RC(1+A)}}\right)$$

and the circuit time constant is: $T = RC(1+A)$

V. Conclusions

The above analysis indicates that the effective capacitance of capacitor C in the circuit shown in part I is modified by the factor $(1+A)$ so that its equivalent value is $C(1+A)$.

SCHMITT TRIGGER

I. Circuit Diagram

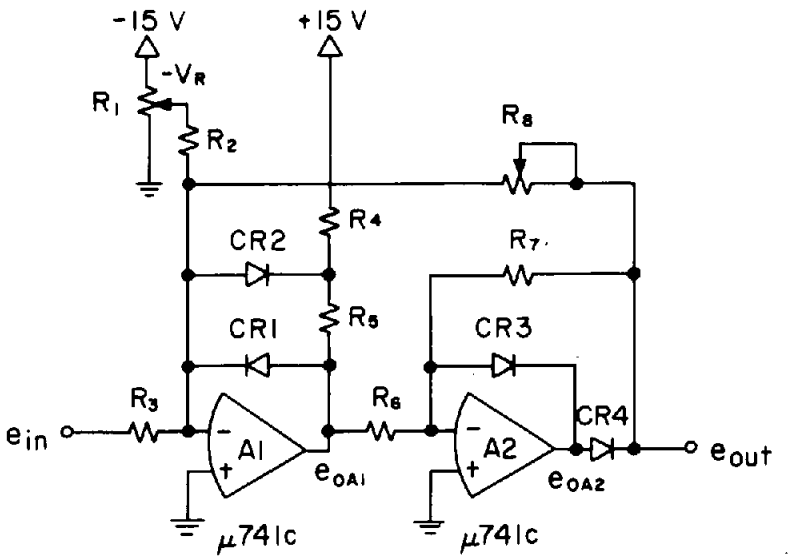

II. Output Calculations

with: $e_{in} = 0$

then: $e_{OA1} \approx +0.6$ volts (due to the limiting action of CR1)

and: $e_{OA2} \approx -0.6$ volts

$e_{out} \approx 0.0$ volts

with: $e_{in} = 1$ volt $+ \Delta V$ (CR2 is forward biased for small negative ΔV)

and: $V_R = 1$ volt

then: $\frac{e_{in} - e_g}{R_3} + \frac{(-V_R - e_g)}{R_2} + \frac{e_{OA1} - V_{CR2} - e_g}{R_5} + \frac{15 - V_{CR2} - e_g}{R_4} = 0$ for the A1 stage; e_g is the value of the voltage on the minus input terminal of A1 and V_{CR2} is the voltage drop across the diode CR2.

but for high open loop gain: $e_g \approx 0$

SO: $\frac{e_{in}}{R_3} - \frac{V_R}{R_2} + \frac{e_{OA1} - V_{CR2}}{R_5} + \frac{15 - V_{CR2}}{R_4} = 0$

or: $\frac{e_{OA1}}{R_5} = \frac{V_{CR2}}{R_5} + \frac{V_R}{R_2} - \frac{e_{in}}{R_3} - \frac{15}{R_4} + \frac{V_{CR2}}{R_4}$

with: $e_{in} = V_R$ and $R_3 = R_2$

then: $e_{OA1} = R_5 \left[\frac{V_{CR2}}{R_5} + \frac{V_{CR2} - 15}{R_4}\right] = \underline{\underline{V_{CR2} + \frac{R_5}{R_4}(V_{CR2} - 15)}}$

also: $e_{OA2} = -\frac{R_7}{R_6} e_{OA1} = -\frac{R_7}{R_6}\left[V_{CR2} + \frac{R_5}{R_4}(V_{CR2} - 15)\right]$

or: $\underline{\underline{e_{OA2} = \frac{R_7}{R_6}\left[\left(\frac{R_5}{R_4}\right)(15) - V_{CR2}\left(1 + \frac{R_5}{R_4}\right)\right]}}$

III. Hysteresis Calculations

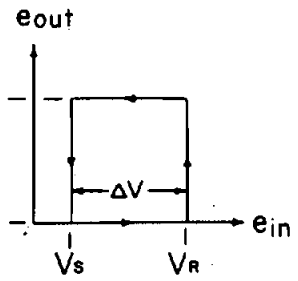

from the figure: $\Delta V = V_R - V_s$

from the circuit layout of part I and as calculated above:

$$e_{OA1} = V_{CR2} + \frac{R_5}{R_4}\left(V_{CR2} - 15\right) = \left(-\frac{R_5}{R_4}\right)\left[15 - V_{CR2}\left(1 + \frac{R_4}{R_5}\right)\right]$$

$$e_{OA2} = \left(\frac{R_7}{R_6}\right)\left[\left(\frac{R_5}{R_4}\right)15 - V_{CR2}\left(1 + \frac{R_5}{R_4}\right)\right] \text{ when } e_{in} = V_R \text{ and } R_3 = R_2$$

also from the circuit layout of part I:

$e_{out} = e_{OA2} - V_{CR4}$ where V_{CR4} = diode voltage drop across CR4

Utilizing the above expressions, the sum of currents into operational amplifier A1, assuming $e_g \approx o$ again as in part II is:

$$\frac{e_{in}}{R_3} - \frac{V_R}{R_2} + \frac{e_{out}}{R_8} + \frac{e_{OA1} - V_{CR2}}{R_5} + \frac{15 - V_{CR2}}{R_4} = 0$$

by allowing $e_{in} = V_s$ and $R_2 = R_3$ we have:

$$\frac{V_S}{R_3} - \frac{V_R}{R_3} + \frac{e_{out}}{R_8} + \frac{e_{OA1} - V_{CR2}}{R_5} + \frac{15 - V_{CR2}}{R_4} = 0$$

then substituting for e_{OA1} we get:

$$\frac{V_S}{R_3} - \frac{V_R}{R_3} + \frac{e_{out}}{R_8} + \frac{1}{R_5}\left[\left(V_{CR2} + \frac{R_5}{R_4}\left(V_{CR2} - 15\right)\right) - V_{CR2}\right] + \frac{15 - V_{CR2}}{R_4} = 0$$

expanding we have:

$$\frac{V_S}{R_3} - \frac{V_R}{R_3} + \frac{e_{out}}{R_8} + \frac{V_{CR2}}{R_5} + \frac{V_{CR2}}{R_4} - \frac{15}{R_4} - \frac{V_{CR2}}{R_5} + \frac{15}{R_4} - \frac{V_{CR2}}{R_4} = 0$$

simplifying:

$$\frac{V_S}{R_3} - \frac{V_R}{R_3} + \frac{e_{out}}{R_8} = 0$$

since hysteresis is defined as $\Delta V = V_R - V_S$ we have:

$$V_R - V_S = \Delta V = \frac{R_3}{R_8} e_{out}$$

substituting for e_{out}:

$$\Delta V = \frac{R_3}{R_8}\left(e_{OA2} - V_{CR4}\right)$$

now substituting for e_{OA2} we have:

$$\Delta V = \frac{R_3}{R_8}\left\{\left(\frac{R_7}{R_6}\right)\left[\left(\frac{R_5}{R_4}\right)(15) - V_{CR2}\left(1 + \frac{R_5}{R_4}\right)\right] - V_{CR4}\right\}$$

or:

$$\Delta V = 15\left[\left(\frac{R_3}{R_8}\right)\left(\frac{R_7}{R_6}\right)\left(\frac{R_5}{R_4}\right)\right] - V_{CR2}\left[\left(\frac{R_3}{R_8}\right)\left(\frac{R_7}{R_6}\right)\left(1 + \frac{R_5}{R_4}\right)\right] - V_{CR4}\left[\left(\frac{R_3}{R_8}\right)\right]$$

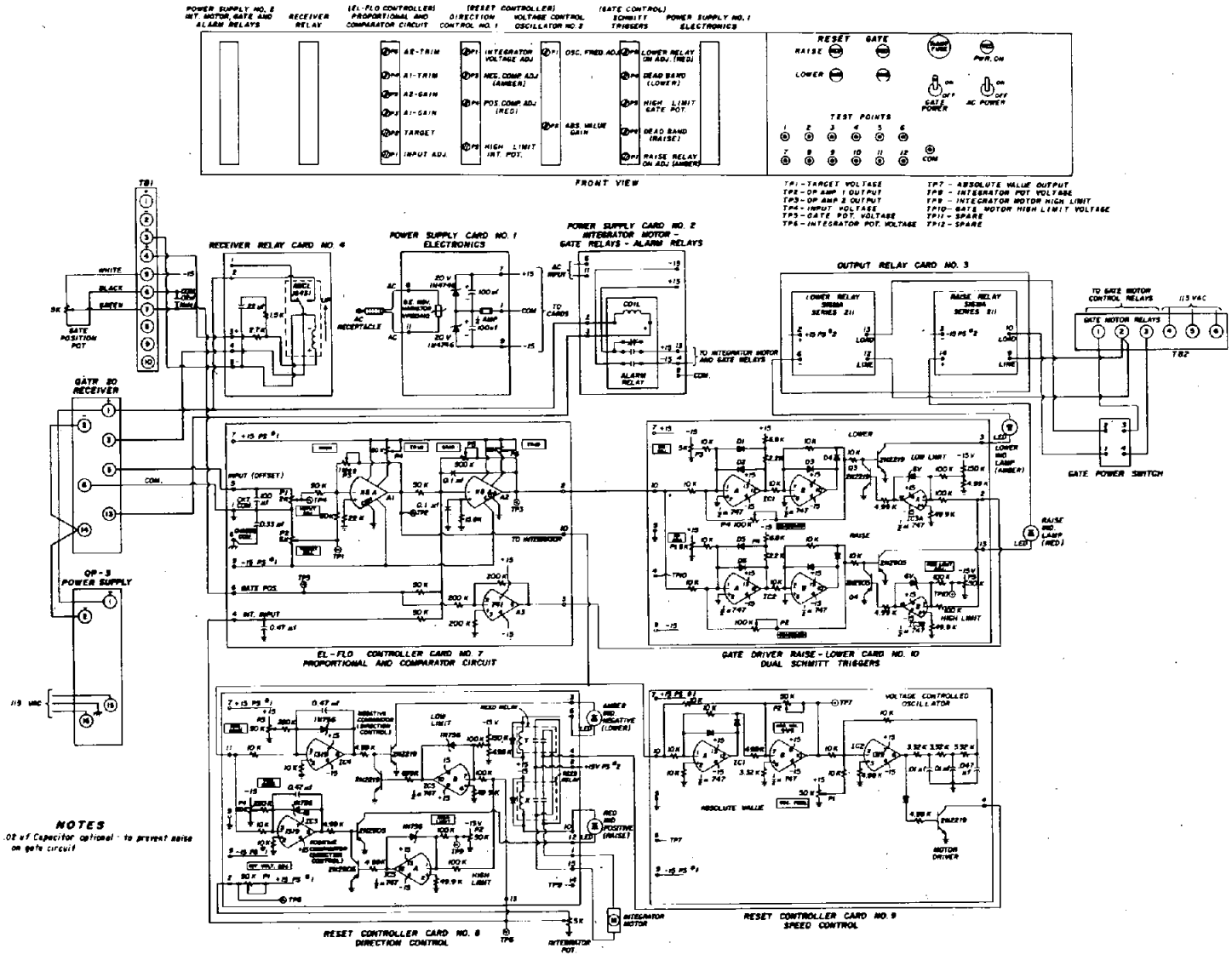

Figure III-3.– EL-FLO controller prototype upstream chassis equipment layout and schematic diagram (801-D-149).

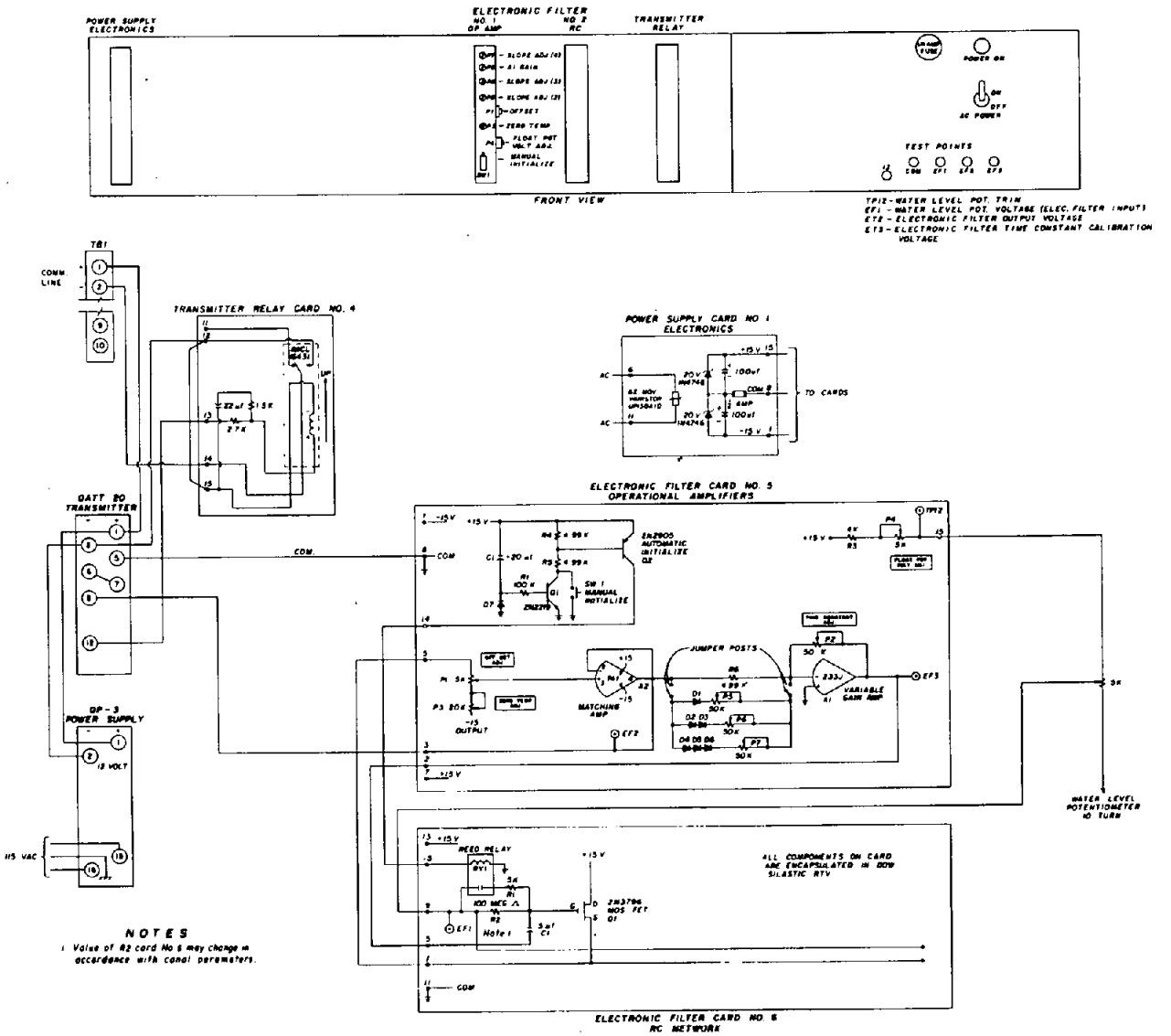

Figure III-4.— EL-FLO controller prototype downstream chassis equipment lay-out and schematic diagram (801-D-150).

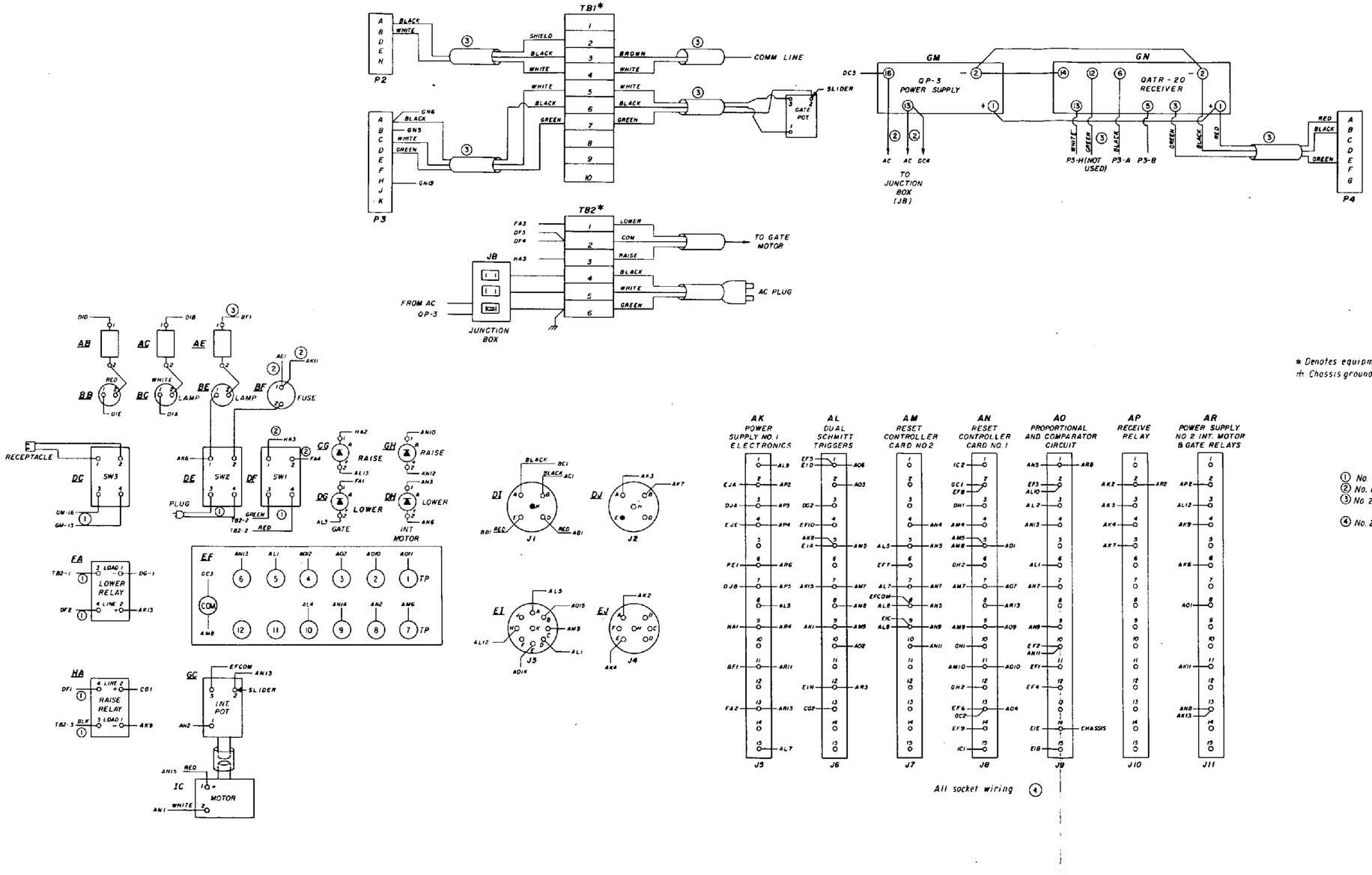

NOTES

* Denotes equipment mounted on cabinet.
th Chassis ground or cabinet ground.

WIRE KEY

① No. 14 AWG - 3 Conductor power cord.
② No. 14 AWG - Stranded wire.
③ No 22 AWG - 4 Conductor twisted pair with shield instrument cable.
④ No. 20 AWG - Single conductor - solid copper wire.

Figure III-5.— EL-FLO controller prototype upstream cabinet wiring diagram (801-D-151).

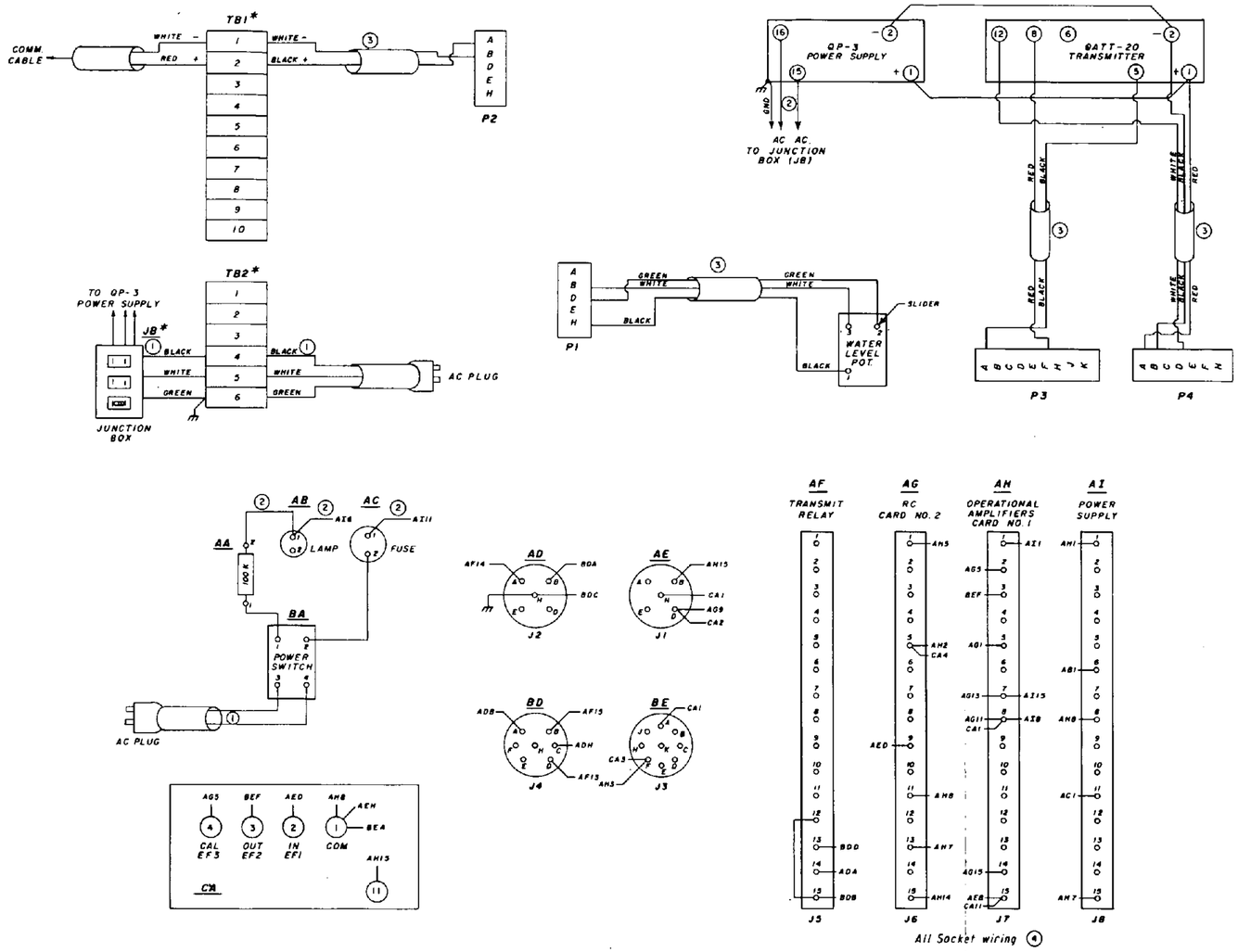

NOTES

*—Denotes equipment mounted on cabinet
⫽—Chassis or cabinet ground.

WIRE KEY

① No. 14 AWG-3-conductor power cord
② No. 14 AWG- Stranded wire
③ No. 22 AWG- 4-conductor twisted pair with shield instrument cable.
④ No. 20 AWG Single conductor solid copper wire.

Figure III-6.— EL-FLO controller prototype downstream cabinet wiring diagram (801-D-152).

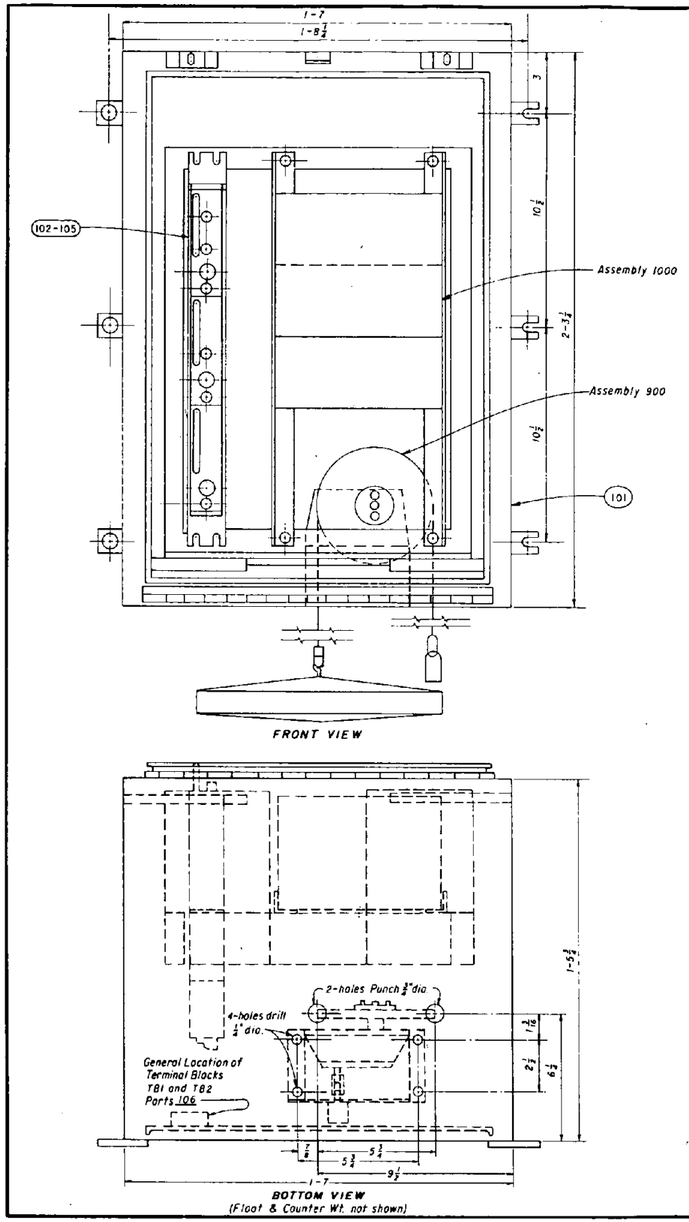

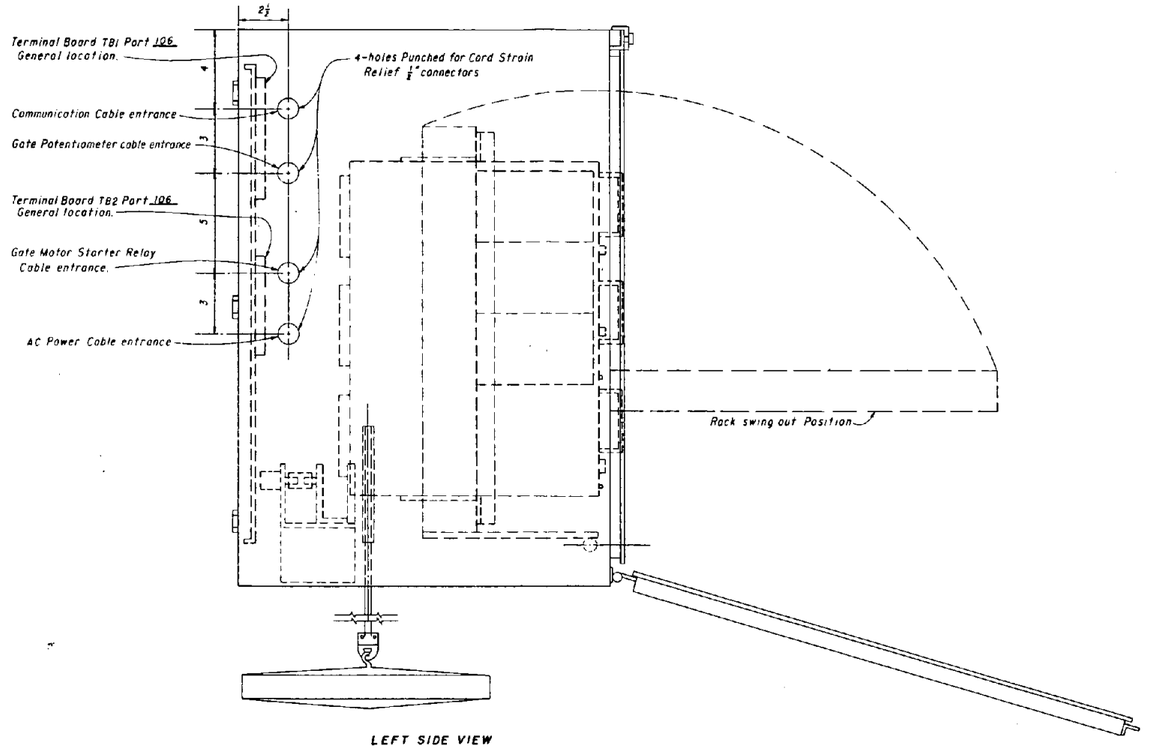

NOTES

1. Terminal Boards TB1 (Part 106) and TB2 (Part 106) shall be located in upper left hand corner on wall cabinet back panel Detail for mounting not shown.
2. A hole or holes having a 2 inch square area shall be punched in the top of the wall cabinet and a filter pad shall be glued over the area from the inside to provide air circulation.
3. The same filter pad material as used in note 2 above shall be placed over the float tape holes on the inside bottom of the wall cabinet and slits cut for the float tape.

Figure III-7.— EL-FLO controller wall mount cabinet general layout (801-D-166).

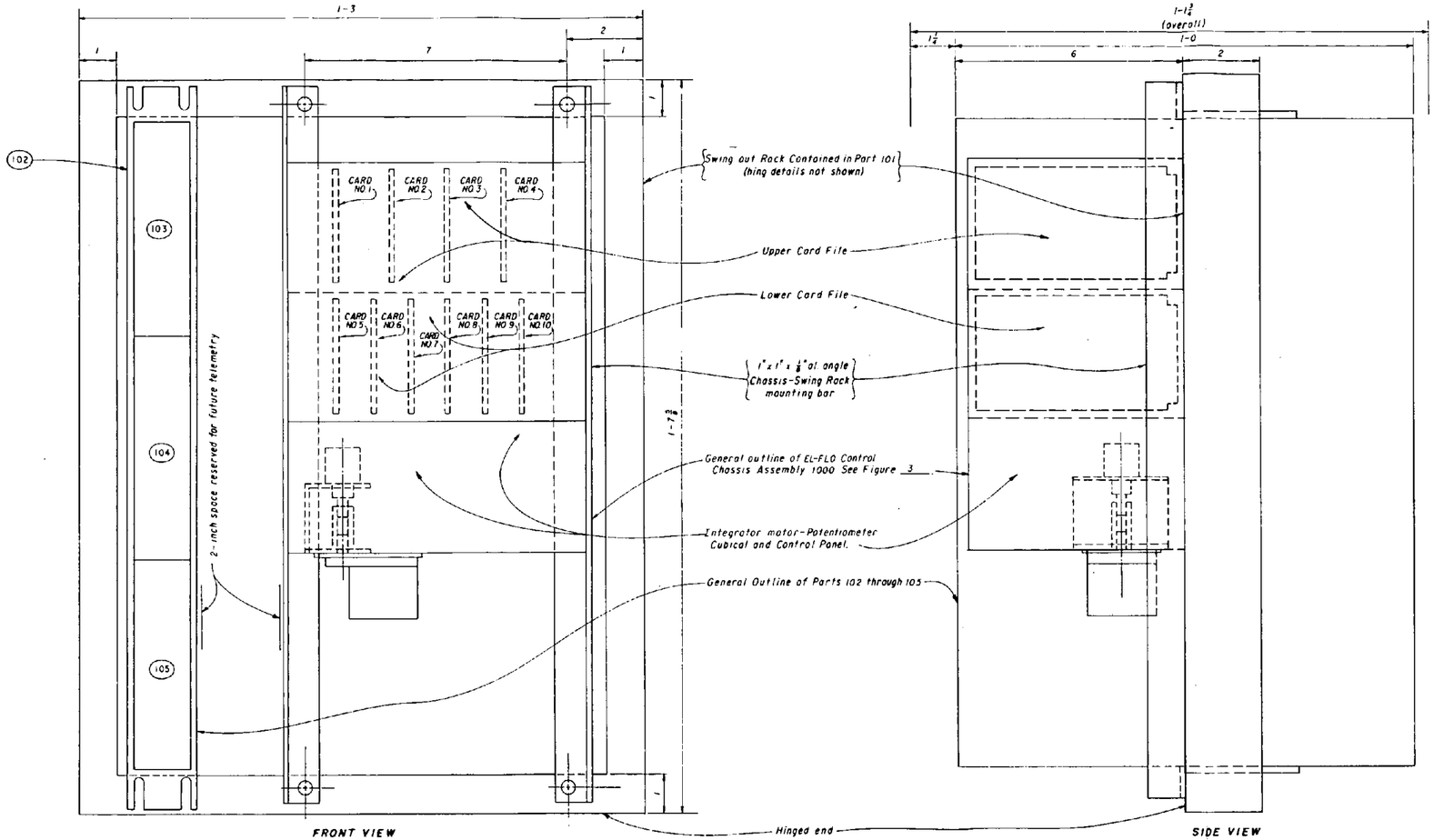

Figure III-8.— EL-FLO controller wall mount cabinet swing rack assembly drawing (801-D-167).

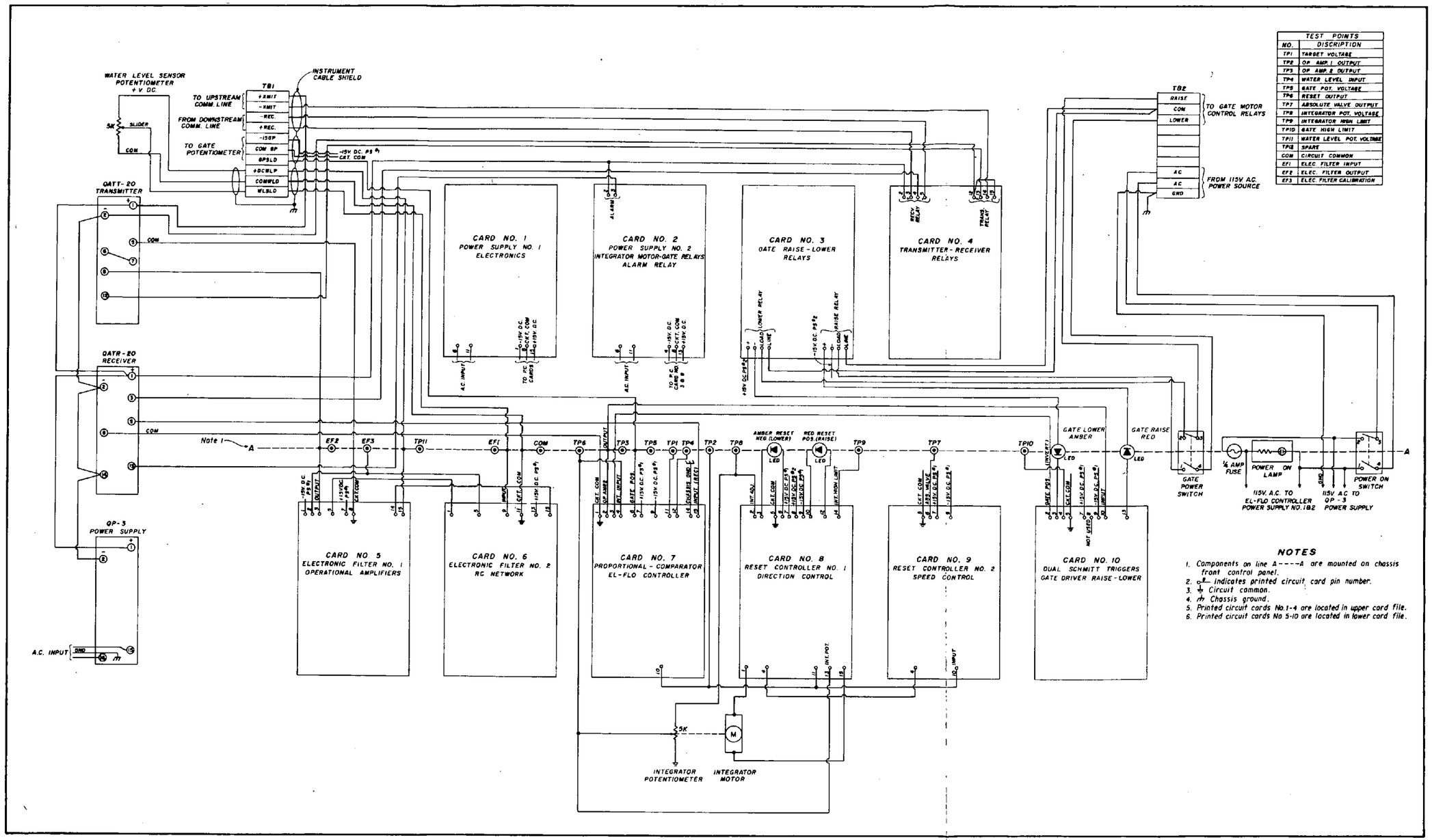

TEST POINTS	
NO.	DISCRIPTION
TP1	TARGET VOLTAGE
TP2	OP AMP. 1 OUTPUT
TP3	OP AMP. 2 OUTPUT
TP4	WATER LEVEL INPUT
TP5	GATE POT. VOLTAGE
TP6	RESET OUTPUT
TP7	ABSOLUTE VALVE OUTPUT
TP8	INTEGRATOR POT. VOLTAGE
TP9	INTEGRATOR HIGH LIMIT
TP10	GATE HIGH LIMIT
TP11	WATER LEVEL POT. VOLTAGE
TP12	SPARE
COM	CIRCUIT COMMON
EF1	ELEC. FILTER INPUT
EF2	ELEC. FILTER OUTPUT
EF3	ELEC. FILTER CALIBRATION

NOTES

1. Components on line A----A are mounted on chassis front control panel.
2. ○ Indicates printed circuit card pin number.
3. ⏚ Circuit common.
4. ⏚ Chassis ground.
5. Printed circuit cards No.1-4 are located in upper card file.
6. Printed circuit cards No 5-10 are located in lower card file.

Figure III-9.— EL-FLO controller schematic wiring diagram (801-D-175).

Appendix IV

REPORT ON THE CONDITION OF THE EL-FLO CONTROLLER RECEIVER UNIT – SOUTH GILA CANAL AUTOMATION

United States Department of the Interior

BUREAU OF RECLAMATION
ENGINEERING AND RESEARCH CENTER
P.O. BOX 25007
BUILDING 67, DENVER FEDERAL CENTER
DENVER, COLORADO 80225

DEC 1973

IN REPLY
REFER TO: D-1530
567.

To: Project Manager, Yuma, Arizona

From: Chief, Division of General Research

Subject: EL-FLO Controller Receiver Unit Malfunction of September 23, 1973 - South Gila Canal - Gila Project

We have completed our laboratory analysis of the EL-FLO controller receiver unit which malfunctioned during real time automatic operation of the South Gila Canal headgate on September 23, 1973.

Enclosed is a copy of our report entitled "Report on the Condition of the EL-FLO Controller Receiver Unit" dated November 12, 1973, for your information.

The results of the laboratory analysis isolated the cause of the receiver unit malfunction to the internal failure of the signal output reed relay contacts. Laboratory tests demonstrated that the signal output relay would fail to its open position when either (1) the power supply was mometarily interrupted (power outage), (2) the signal input was momentarily interrupted (loss of communication channel signal), (3) the relay was vibrated, and (4) when operating during normal power and signal conditions. Any one of the above conditions could have occurred and initiated the signal output relay to fail to its open position. The open contacts caused the loss of signal output of the receiver unit producing a zero input signal to the EL-FLO control equipment. The input to the EL-FLO controller, therefore, suddenly changed from a normal value representing 4.2 feet of water depth upstream of the 1.9 check to a zero depth. The EL-FLO controller which was functioning normally proceeded to open the headgate to supply additional water based on the false input signal. As a result, the EL-FLO controller opened the headgate to its maximum position increasing the flow into the South Gila Canal from about 40 ft^3/s to about 110 ft^3/s. The increased flow continued long enough to cause flooding and damage to the lower end of the canal before the ditchrider could manually close the headgate.

Parallel to the signal output reed relay contacts are two other identical reed relay contacts (one for the receiver "ON" lamp and one for the alarm output) all of which are operated by the same relay coil. These two lamp and alarm relays did not fail during laboratory tests nor did they fail on September 23. Since only one of the three similar type reed relay contacts failed, we consider the receiver unit malfunction to be the result of a component failure not associated with field operation or by environmental conditions on the canal bank. The component failure could possibly be the result of poor quality control during production or of marginal design. We believe that reed relays of this type may be subject to this kind of failure. We, therefore, plan to take steps to correct this deficiency.

We had planned to purchase and install EL-FLO controllers and an alarm system at all the check structures on the South Gila Canal next year. The Yuma Irrigation District understands clearly, as the result of our prototype testing, the benefits they would receive from the proposed installation. However, we believe the short duration of prototype testing on the South Gila, together with experienced interruptions and required modifications, the September 23, 1973 malfunction, fails to demonstrate to the District sufficient equipment reliability. They foresee the possibility of having considerable maintenance cost associated with the installation which could easily negate any associated benefits (refer to Travel Report by Mr. Clark P. Buyalski, dated October 25, 1973, copy sent to you).

We recommend and understand the District concurs, that the proposed installation of EL-FLO controllers and additional experimentation on the South Gila Canal be deferred until the control system reliability is further established. This coming spring we will be installing EL-FLO controllers and an alarm system (of the same design proposed for the South Gila) on the Corning Canal, Central Valley Project, near Red Bluff, California, at 14 check structures. The Corning Canal EL-FLO control installation will provide a good facility to demonstrate performance. The first year's operation should provide a sufficient period of time to obtain data regarding equipment reliability. We plan to keep your office and the District informed of the Corning Canal progress through periodic correspondence and/or by direct telephone contact. After the Corning Canal EL-FLO system has been in continuous operation for at least a period of 6 months, we suggest representatives of your office and the Yuma Irrigation District (and perhaps from other Districts in the area who may be interested) travel to the Red Bluff O&M Office and observe first hand the EL-FLO installation and learn from the O&M personnel their operational experience.

We express our gratitude and appreciation to your office and to the Yuma Irrigation District for the continued patience and tolerance towards our prototype testing on the South Gila Canal. The test program has provided us with valuable information on equipment performance and has verified theoretical studies. The September 23 malfunction necessitated a considerable amount of repair work be performed by the District. Their positive attitude towards the development of canal automation remains unchanged and is greatly appreciated by the Bureau of Reclamation.

If you have any questions regarding the above or the enclosed report, please advise.

This letter has the concurrence of the Director of Design and Construction and the Chief, Division of Water O&M.

Howard J. Cohan

Enclosure

Copy to: Commissioner, Attention: 105
Regional Director, Boulder City, Nevada, Attention: 430
Regional Director, Sacramento, California, Attention: 430
Project Construction Engineer, Willows, California
(each with copy of enclosure)
E&R Center, Codes D-200, D-400

Blind to: 1500
1550
243

CPBuyalski:pmn-V2

REPORT ON THE CONDITION
OF THE
EL-FLO CONTROLLER RECEIVER UNIT
SOUTH GILA CANAL AUTOMATION
NOVEMBER 12, 1973

Laboratory tests were made on November 11, 1973, to isolate the exact cause of the South Gila Canal prototype EL-FLO controller receiver unit which failed during real time automatic operation of the canal headgate on September 23, 1973. The receiver unit is manufactured by the Quindar Electronics, Inc., Model QATR-20 having the number EE 0541 stamped on the chassis. Attached is the manufacturer's electrical drawing titled "SCHEMATIC QATR-20," No. 12572D, for reference to component numbers used in this report.

Paragraph 4.5.6 of the manufacturer's instruction manual states, "Transistor Q7 amplifies receiver input signals, energizing alarm relay K1. Relay contacts complete the output circuit (underlining supplied), a front-panel lamp (L1) circuit, and an external alarm circuit. If the input signal is interrupted, relay K1 deenergizes, opening the output circuit and the alarm circuit and deenergizing the front-panel lamp."

Using the information in the above paragraph as a guide for normal operation, d-c power and an input signal were applied according to Paragraph 5.2.3.2 of the instruction manual. A 2000-ohm resistor was connected as an output load for the purpose of monitoring the output signal.

The receiver unit was then subjected to the following test conditions:

1. Variable temperature (both above and below room temperature)

2. Variable d-c power supply voltage (slow variations between 10 and 12 voltes and also full on-off cycles of the d-c power)

3. Alternate on-off cycles of the input signal (with on-off period long enough to operate relay K1)

4. Vibration by light tapping on the receiver unit, particularly on relay K1

It was found that the signal output reed relay contacts (circled in red on the attached schematic) of relay K1 were intermittent. The reed relay was found to be abnormally sensitive to small amounts of vibration, although vibration was not necessary for failure. The reed relay could be caused to fail by a short interruption of either d-c power or input signal. There were instances where the relay operated properly for a period of time and then failed for no apparent reason.

Each time the receiver unit malfunctioned, the malfunction involved only the failure of the signal output reed relay contacts. Identical relay contacts for the alarm circuit and for the lamp L1 which are operated by the same relay coil K1 did not fail during these tests.

Attachments

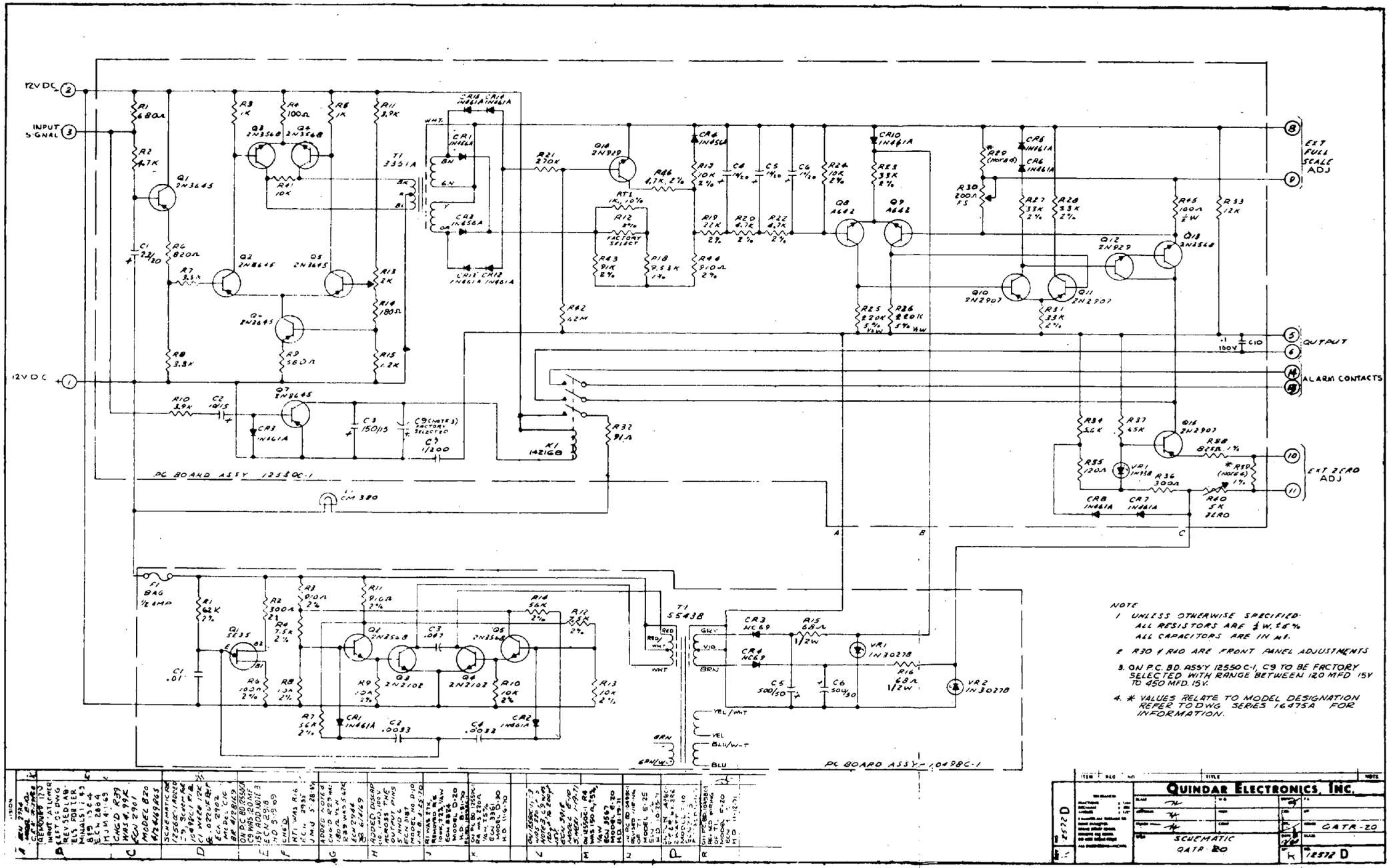
12V DC
INPUT SIGNAL
12V DC
PC BOARD ASSY 12558C-1
K1 1421GB
CM 380
F1 8AG 1/2 AMP
T1 3351A
T1 5543B
PC BOARD ASSY-10498C-1
EXT FULL SCALE ADJ
OUTPUT
ALARM CONTACTS
EXT ZERO ADJ
ZERO
NOTE
1 UNLESS OTHERWISE SPECIFIED:
ALL RESISTORS ARE ½W, ±5%
ALL CAPACITORS ARE IN MF.
2. R30 & R40 ARE FRONT PANEL ADJUSTMENTS
3. ON P.C. BD. ASS'Y 12550C-1, C9 TO BE FACTORY SELECTED WITH RANGE BETWEEN 120 MFD 15V TO 450 MFD. 15V.
4. * VALUES RELATE TO MODEL DESIGNATION REFER TO DWG SERIES 16475A FOR INFORMATION.
QUINDAR ELECTRONICS, INC.
SCHEMATIC
QATR-20
QATR-20
12572 D

Appendix V

CONVERSION OF SELECTED CONTROL PARAMETERS TO ELECTRONIC EQUIVALENCES

General

The information included in this appendix is a detailed procedure for converting selected control parameters to electronic equivalences used in the prototype EL-FLO plus RESET controller during the 1973 prototype field testing program conducted on the first reach of the South Gila Canal near Yuma, Ariz. Computations for the electronic control parameters used in the EL-FLO plus RESET controller at the first four check structures on the Corning Canal near Red Bluff, Calif., for the 1974 field prototype test program, are briefly summarized. The parameters derived for the two prototype test programs described earlier in this report represent the EL-FLO plus RESET controller configurations used in verifying the mathematical model simulation for field operation.

South Gila Canal

The EL-FLO plus RESET controller operates around a target water depth, *YT*, defined as the depth to be maintained for all steady-state flows from zero to maximum discharge. A decrease in the water level below the selected depth signifies an increase of flow, while an increase in the water level above the selected target depth signifies a decrease of flow. The change of flow per linear depth change in water level or "offset" below the target is an important factor.

The South Gila Canal was designed for a maximum flow of 3.1 m^3/s (110 ft^3/s) at a uniform depth of 1.28 m (4.20 ft), selected as the target depth (*YT*). Thus, the discharge per offset for the first reach of the South Gila Canal was approximately 10.3 $(m^3/s)/m$ (113.5 $(ft^3/s)/ft$), equation 9. Because water deliveries could not be made satisfactory from the South Gila Canal at depths below 1.28 m (4.20 ft), the RESET controller was added to the EL-FLO controller to eliminate the residual "offset" of the EL-FLO proportional controller (fig. 19).

Step No. 1. - The first step, in establishing parameters for control, required the selection of a convenient electronic voltage scale for the water level, *YC*, (fig. 19c) sensor potentiometer. Since the equipment used to transmit the output of the electronic filter to the upstream check gate, (fig. 17) was limited to 2.4 volts maximum without a voltage divider, a scale of 6.6 V/m (2 V/ft) of water level change appeared satisfactory.

The water level sensor output was set to 1.0 volt at the target water depth, *YT*, of 1.28 m (4.20 ft). With a selected water level sensor voltage scale of 6.6 V/m (2 V/ft), the water level change from a target value of 1.0 volt would be ±1.0 volt, or ±0.15 m (±0.50 ft). The change in canal discharge based on the factor of 10.3 $(m^3/s)/m$ (113.5 $(ft^3/s)/m$) for a ±0.15-m (±0.50-ft) change in water level would be approximately ±1.5 m^3/s (±55 ft^3/s). A rapid change of flow of 50 percent of the maximum design discharge of the canal reach occurs rarely and was not considered a normal change of downstream demands.

The typical flow changes range from 0 to 20 percent of the maximum flow capacity of the canal which would be within a ±0.15-m (±0.50-ft) change of water level. With the RESET controller, the water level change is temporary and will return to the target value after a period of 2 to 4 hours. Figure V-1 illustrates the water level sensor voltage scale selection.

Step No. 2. - The next step is to calibrate the water level sensor potentiometer to obtain the selected voltage scale (refer to fig. V-1). The water level sensor includes a float-tape-pulley standard A35 recorder gear assembly with a 450-mm (18-inch) pulley circumference and a gear ratio of 1:5. A 0.3-m (1-ft) change in water level will rotate the pulley 0.667 revolution and the potentiometer 3.33 revolutions. To obtain the selected voltage scale at 3.33 revolutions, the potentiometer must be calibrated at 0.6 volt per revolution. For a 10-turn potentiometer, the maximum voltage on the high side of the potentiometer would be 6 volts. The 6 volts are supplied from the 15-volt d-c power supply at trimpot *P4*, measured at test point 12 on electronic filter card No. 1, refer to figure III-4.

Step No. 3. - The next step is to insert the selected time constant parameter into the electronic filter. The selected time constant for the South Gila Canal controller was 1000 seconds, determined from mathematical model simulation studies. The equation for the electronic filter is:

$$TF = RC + ARC \qquad \text{(V-1)}$$

where *TF* is the selected time constant of 1000 seconds, *R* is the resistance and *C* is the capacitance of the electronic *RC* network and *A* is the amplifier gain. Solving for *A*, the equation is:

$$A = \frac{TF - RC}{RC} \qquad \text{(V-2)}$$

The resistance was 100 megohms and the capacitance was 5 microfarads for the electronic filter card No. 2 ($R1$ and $C1$) shown on figure III-4. Therefore, the amplifier gain was:

$$A = \frac{1000 \text{ seconds} - (100 \text{ megohms})(5 \text{ microfarads})}{(100 \text{ megohms})(5 \text{ microfarads})} \quad \text{(V-3)}$$

$$= \frac{1000 - 500}{500} = 1.0 \quad \text{(V-4)}$$

This is the minimum time constant, TF, that can be obtained with these $R1$ and $C1$ values.

The time constant adjustment in the controller is achieved by adjusting trimpot $P2$ for an amplifier $A1$ gain of 1.0, or test point *EF3 CAL* voltage divided by test point *EF2 OUT* equals 1.0 (refer to electronic filter card No. 1 on fig. III-4).

A measurement of the electronic filter time constant was made in the field and the data are tabulated in table V-1 and plotted in figure V-2. Table V-2 is a listing of test point voltages measured in the laboratory before the prototype equipment was shipped to the South Gila Canal and measured in the field on May 8, 1973. Gain A of amplifier $A1$ is the ratio of *EF3 CAL* to *EF OUT* listed in table V-2 and was very close to 1.0. The time constant measured for the electronic filter was 1120 seconds which was within the manufacturer's tolerances of the $R1$ and $C1$ components.

Step No. 4. - The next step is to determine the voltage scale per distance of gate opening, GA. Table V-3 and figure V-3 are a conversion of the South Gila Canal radial headgate arc distance to vertical distance of travel. Figure V-4 shows the relationship of arc distance to vertical distance was not linear, requiring the use of a best straight line fit. A value of 0.3 m (1 ft) of vertical distance relating to 0.4 m (1.3 ft) of arc distance was selected to set the voltage scale of the gate position potentiometer driven by the gate hoist shaft.

One revolution of the gate hoist drum was computed to be:

$$d = 3.14\ (216 \text{ mm}) = 678 \text{ mm} \quad \text{(V-5)}$$

$$\text{or } 3.14\left(\frac{8.5 \text{ in}}{12.0 \text{ in/ft}}\right) = 2.225 \text{ ft}$$

Thus, 0.3 m (1 ft) vertical distance of gate travel would be:

$$\frac{\text{arc distance}}{\text{vertical distance per drum revolution}} = \frac{0.4 \text{ m}}{0.678 \text{ m}} \quad \text{(V-6)}$$

$$\text{or } \frac{1.3 \text{ ft}}{2.225 \text{ ft}} = 0.584 \text{ revolution of the hoist drum}$$

A five-turn potentiometer with a −15-volt d-c input on the high potential gave 3.0 volts per revolution for gate position sensor. The gate position potentiometer was thus scaled for 0.3 m (1 ft) vertical distance of gate travel (1.92 drum revolutions per meter, or 0.584 r/ft, times 3.0 volts per revolution of the potentiometer) to be equal to 5.75 volts per vertical meter of gate opening (1.752 V/ft).

Step No. 5. - With voltage scales of the water level and gate position sensors determined, the electronic proportional gain, $A1$, can be calculated as follows:

$$EL\text{-}FLO\ GAIN\ A1 = K1\left(\frac{\text{volts per gate movement distance}}{\text{volts per depth of water}}\right) \quad \text{(V-7)}$$

where $K1$ is the selected control parameter for the proportional gain of 1.3. The desired electronic equivalent gain $A1$ is calculated to be:

$$EL\text{-}FLO\ GAIN\ A1 = 1.3\left(\frac{5.75 \text{ V/m}}{6.56 \text{ V/m}}\right) \text{or } 1.3\left(\frac{1.752 \text{ V/ft}}{2 \text{ V/ft}}\right) \quad \text{(V-8)}$$

$$= 1.14 \quad \text{(V-9)}$$

During the field tests on the South Gila Canal conducted during the week of September 18, 1973, the EL-FLO control gain was decreased. An examination of the field data listed in table V-2 for September 18, 1973, shows that the *EL-FLO GAIN A1* inserted into the controller was 0.86 and can be verified as follows:

$$EL\text{-}FLO\ GAIN\ A1 = TP2/(TP1 - TP4) = \frac{0.170 \text{ volt}}{0.994 \text{ volt} - 0.796 \text{ volt}} \quad \text{(V-10)}$$

$$= \frac{0.170}{0.198} = 0.86 \quad \text{(V-11)}$$

An examination of field data on September 19, 1973, figure 24, Field Verification Tests section, shows that the voltage scale of the headgate potentiometer was 4.05 V/m (1.238 V/ft) determined as follows:

At time 70 minutes, headgate potentiometer
= 2.070 volts at 0.277 m (0.91 ft)

At time 764 minutes, headgate potentiometer
= 1.872 volts at 0.229 m (0.75 ft)

$\Delta V = 0.198$ volt $\Delta G = 0.049$ m (0.16 ft) (V-12)

Table V-1.—*South Gila Canal EL-FLO controller prototype field data - electronic filter unit 4 calibration*

Time seconds	*EF OUT* volts	Δv	$\frac{\Delta v}{\Delta V}$	$1-\frac{\Delta v}{\Delta V}$	Remarks
0	1.000				
300	1.140	0.140	0.240	0.760	Initial V = 1.016
600	1.245	0.245	0.420	0.580	Reset V = 1.600
900	1.324	0.324	0.555	0.445	$+\Delta V$ = +0.584
1100	1.345	0.345	0.409	0.409	63.2% (ΔV) = 0.370 V
1000	1.365	0.365	0.375	0.375	*EF* No. 4 set at min. gain = 1.00
					OA = 1.005
1200	1.383	0.383	0.657	0.343	Temp. = 31 °C
1500	1.426	0.426	0.730	0.270	*TF* = 1120 s

Table V-2.—*Electrical measurements, EL-FLO plus RESET controller — South Gila Canal*

Test point	Laboratory[a] measurement volts	Field measurement[a] volts May 8, 1973	Field measurement[b] volts Sept. 18, 1973
Check M.P. 0.14			
Power supply No. 1	14.97	14.96	
Power supply No. 1	−15.01	−14.98	
Power supply No. 2	14.94	15.00	
Power supply No. 2	−14.94	−14.99	
Test point No. 1	−0.900	−0.914	−0.994
Test point No. 2	−0.675	−0.681	0.170
Test point No. 3	12.40 (sat.)	12.39 (sat.)	1.330
Test point No. 4	1.35	1.35	0.796
Test point No. 5	−6.90	−6.77	−1.649
Test point No. 6	0.480	0.461	1.338
Test point No. 7	−1.056	−0.997	−0.253
Test point No. 8	9.00	9.00	6.08
Test point No. 9	−8.65	−8.64	−3.21
Test point No. 10	−8.65	−8.64	−4.11
Check M.P. 1.9			
Test point No. 11	6.06	6.06	6.03
EF IN	1.315	1.314	0.777
EF OUT	1.290	1.293	0.783
EF CAL	1.295	−1.292	−0.785
Power supply	14.97	15.01	
Power supply	−15.04	−15.02	
5−kΩ resistor	−3.29	−3.32	
Integrator motor speed	0.007 25 r/min	0.007 55 r/min	

[a] Laboratory and field measurements of May 8, 1973, were for the EL-FLO plus RESET control of check gate M.P. 0.14.

[b] Field measurements of Sept. 18, 1973, were for the EL-FLO plus RESET control of the headgate. Measurements listed for check M.P. 1.9 were taken at 8:18 a.m. and check M.P. 0.14 at 9:02 a.m.

Table V-3.—*Calculation of arc distance versus vertical distance of gate travel for the South Gila Canal headgate*

Gate vert. opening GA		$PH - GA$		$\text{Sin}\alpha = (PH - GA)/R$	Angle α, degrees	$\Delta\alpha$, degrees	Arc distance $\frac{\Delta\alpha}{360}(2\pi R)$	
m	(ft)	m	(ft)				m	(ft)
0	0	1.829	6.00	0.686	43.4	0.0	0	0.000
0.076	0.25	1.753	5.75	0.657	41.1	2.3	0.107	0.352
0.152	0.50	1.676	5.50	0.629	39.0	4.4	0.205	0.673
0.229	0.75	1.600	5.25	0.600	36.9	6.5	0.303	0.994
0.305	1.00	1.524	5.00	0.571	34.8	8.6	0.400	1.312
0.457	1.50	1.372	4.50	0.514	30.9	12.5	0.582	1.910
0.610	2.00	1.219	4.00	0.457	27.2	16.2	0.756	2.48
0.762	2.50	1.067	3.50	0.400	23.6	19.8	0.924	3.03
0.914	3.00	0.914	3.00	0.343	20.1	23.3	1.085	3.56

$$\frac{\Delta V}{\Delta G} = \frac{0.198\ \text{V}}{0.049\ \text{m}} = 4.05\ \text{V/m or } \frac{0.198\ \text{V}}{0.16\ \text{ft}} = 1.238\ \text{V/ft}$$

The EL-FLO proportional gain as used in the field prototype test installation was calculated to be 1.39 instead of 1.3 as follows:

$$\text{EL-FLO gain, } K1$$

$$= 0.86\left[\frac{6.56\ \text{V/m (water level)}}{4.06\ \text{V/m (gate)}}\right] = 1.39 \qquad \text{(V-13)}$$

$$= 0.86\left[\frac{2.0\ \text{V/ft}}{1.238\ \text{V/ft}}\right] = 1.39$$

The gain of 1.39 was used in the mathematical verification studies. The electronic equivalent gain, $A1$, was adjusted into the EL-FLO controller on trimpot $P3$ of the EL-FLO controller card, figure III-3, so that the output of the amplifier at $TP2$ was 0.86 of the electronic sum of target value at $TP1$ and the filter output at $TP4$. The electronic target value was −1.0 volt and was adjusted at the trimpot $P2$.

Step No. 6. - This step determines the comparator unit gain, $A2$, by selecting a desirable dead band of gate opening, ΔG, of 10.7 mm (0.035 ft), referenced input equation 5 and figure 16, and a Schmitt Trigger "on" level of 0.60 volt. The comparator unit gain, $A2$, was calculated as follows:

$$\textit{COMPARATOR GAIN, } A2$$

$$= \frac{\pm 0.6\ \text{V}}{(0.0107\ \text{m})\ (5.748\ \text{V/m})} = 9.8$$

$$= \frac{\pm 0.6\ \text{V}}{\pm 0.035\ \text{ft}\ (1.752\ \text{V/ft})} = 9.8 \qquad \text{(V-14)}$$

Since the head gate potentiometer voltage scale measured during the field test was different from the calculated value, the actual dead band of the gate opening would be:

$$\frac{\pm 0.60\ \text{V}}{(9.8)\ (4.13\ \text{V/m})} = \pm 0.015\ \text{m}$$

$$\text{or } \frac{\pm 0.60\ \text{V}}{(9.8)\ (1.238\ \text{V/ft})} = \pm 0.05\ \text{ft} \qquad \text{(V-15)}$$

The value was used in the mathematical model verification.

Step No. 7. - The next step was to adjust the RESET controller to the selected proportional reset mode gain, $K2$, of 0.006 per minute as determined from mathematical model studies. The simplest procedure is as follows:

A. Assume the electrical equivalent, YF, of a 0.15-m (0.5-ft) water level occurred for a 10-minute period.

B. The integrated area of the EL-FLO controller proportional gate opening, GR, would then be:

$$GR = K2\ K1\ (YF)\ \Delta t = \qquad \text{(V-16)}$$
$$0.006\ \text{min}^{-1}\ (1.39)\ (0.15\ \text{m})\ (10\ \text{min}) = 0.0125\ \text{m}$$

or

$$= 0.006\ \text{min}^{-1}\ (1.39)\ (0.5\ \text{ft})\ (10\ \text{min}) = 0.0417\ \text{ft}$$

or

$$(0.0125\ \text{m})\ (4.13\ \text{V/m}) = 0.0516\ \text{volt} \qquad \text{(V-17)}$$
$$(0.0417\ \text{ft})\ (1.238\ \text{V/ft}) = 0.0516\ \text{volt}$$

C. At an offset, ($YT - YF$), of 0.15 m (0.5 ft), the EL-FLO proportional gate opening, GP, would be:

$$GP = K1\,(YT - YF)$$
$$= 1.39\,(0.15\text{ m} - 0.21\text{ m}) = -0.083\text{ m}$$
$$= 1.39\,(0.5\text{ ft} - 0.695\text{ ft}) = -0.271\text{ ft}$$

or the voltage equivalent of

$$GP = 0.21\,(6.67\text{ V/m}) = 1.390\text{ volts}$$
$$= 0.695\text{ ft}\,(2\text{ V/ft}) = 1.390\text{ volts,} \qquad \text{(V-18)}$$

the input signal to the RESET controller.

D. The RESET controller integrator d-c motor speed output can be determined from the calibration curve, figure V-5, which would be 1.125×10^{-2} revolution per minute with an input of 1.39 volts.

E. Using the integrator motor speed of 1.125×10^{-2} revolution per minute, the required integrator potentiometer volts per revolution can be determined as follows:

$$\text{RESET integrator potentiometer volts per revolution} = \frac{0.0516\text{ volt}}{0.011\,25\text{ r/min (10 min)}} = 0.458\text{ volt per revolution} \qquad \text{(V-19)}$$

The RESET integrator 10-turn potentiometer high level voltage would then be (0.458 V/r) x (10 r), or 4.58 volts, and can be adjusted by trimpot $P1$ on the RESET controller card No. 1 (fig. III-3).

The RESET integrator potentiometer high level potential was set at 6.08 volts (refer to table V-2, September 18, 1973 field measurements at $TP8$ = 6.08 volts). The larger field measurement of 6.08 volts as compared to the 4.58 volts (eq. V-19, 0.458 V/r at 10 turns) was the result of using a larger voltage scale for the headgate potentiometer and a larger EL-FLO *GAIN A*1, for the September 1973 field calibration. Therefore, the actual RESET proportional reset gain, $K2$, of the South Gila Canal 1973 prototype test program, including the actual measured headgate potentiometer voltage scale of 4.13 V/m (1.238 V/ft) of gate, can be calculated as follows:

$$\textit{RESET proportional reset gain, } K2,$$
$$= \frac{0.608\text{ V/r}}{0.458\text{ V/r}}\,[0.006\text{ min}^{-1}] \qquad \text{(V-20)}$$
$$= 0.008\text{ min}^{-1}$$

This was used in the mathematical model verification studies.

Step No. 8. - This step includes the calculations for determining the electronic limits of gate opening, RESET maximum limit, and the dead band for the RESET controller on-off values.

A. Maximum gate opening of the South Gila Canal headgate was estimated to be 0.9 m (3.0 ft). The voltage required is 4.13 V/m times 0.9 m (1.238 V/ft x 3 ft) equals 3.72 volts. A voltage offset of 0.7 volt is used when the gate is at zero position to prevent the gate potentiometer from breaking if the gate hoist lowers past zero position (usually a small amount to slacken the hoist cables when the gate is closed). Adding 0.7 volt of gate potentiometer offset when the headgate is at zero position will give 4.42 total volts required for a maximum gate opening of 0.9 meter (3.0 ft).

However, the high limits for the gate potentiometer and RESET integrator potentiometer were set at 6.0 volts (because of using the larger headgate potentiometer voltage scale), using trimpots $P5$ measured at $TP10$ on gate driver raise-lower card and $P2$ measured at $TP9$ on RESET controller card No. 1, respectively (fig. III-3). The low limits are set by fixed resistors and each was 0.5 volt.

B. The on-off values of the integrator are selected as ±0.15 m (±0.05 ft) of water level from the target level. The voltage level for the on-off point would be (±0.15 m)(6.67 V/m)(0.86), or (±0.05 ft)(2 V/m)(0.86), equals ±0.086 volt. This voltage was adjusted on trimpots $P3$ and $P4$ on the RESET controller card No. 1 (fig. III-3) using a ±0.086-V change at $TP2$ and LED lamp indication.

This step concludes a detailed description of the procedure used to convert selected control parameters to electronic equivalences and to determine the actual control parameters used during the September 19, 1973 prototype field tests of the South Gila Canal headgate EL-FLO plus RESET prototype controller. One procedure not discussed was the procedure for calculating the *ABSOLUTE GAIN* for the speed of the RESET integrator motor to a desired speed. The process was improved for the Corning Canal and will be discussed in detail in subsequent paragraphs, refer to equation V-36.

Corning Canal

The Corning Canal calculations for converting selected control parameters to electronic equivalences are briefly summarized for check No. 1 and data for checks No. 1 through 4 are tabulated in tables V-4 and V-5. The procedure for setting the RESET con-

Table V-4.—*Corning Canal EL-FLO plus RESET control parameters, first set, units of meters (feet)*

Check No. and M.P.	Target elevation m	(ft)	Elec. filter[1] time const. (s)	EL-FLO[1] gain $K1$	RESET[1] gain $K2$ (water/gate) $K2$/min	Check gate data: Arc distance per vert. distance	One revolution of hoist drum m	(ft)	Hoist revolutions per 1 unit of vert. lift m	(ft)	Gate dead band m	(ft)	RESET dead band m	(ft)	High limit m	(ft)
1 4.55	92.1	(302.2)	800	9.1	0.03/0.0033	1.19	0.7178	(2.355)	1.66	(0.505)	0.457	(0.15)	0.0091	(0.03)	2.19	(7.2)
2 6.02	91.7	(300.8)	1000	7.7	0.02/0.0024	1.26	0.7178	(2.355)	1.76	(0.536)	0.457	(0.15)	0.0091	(0.03)	2.19	(7.2)
3 8.08	91.0	(298.5)	1300	4.5	0.02/0.0042	1.23	0.7178	(2.355)	1.71	(0.522)	0.457	(0.15)	0.0091	(0.03)	2.19	(7.2)
4 10.65	90.4	(296.6)	1700	4.3	0.02/0.0047	1.23	0.7178	(2.355)	1.71	(0.522)	0.457	(0.15)	0.0091	(0.03)	1.95	(7.4)

[1] Selected parameters from mathematical model studies.

Table V-5.—*Corning Canal EL-FLO plus RESET control parameters, first set, electronic equivalences*

Check No. and M.P.	Target	Water level scale V/m	V/ft	Water level pot. volts	Electronic filter gain A	EL-FLO gain $A1$	Absolute gain	RESET potentiometer V/r	10-turn pot. volt	Gate volt scale (10-turn pot.) V/m	V/ft	Schmitt trigger ±volts	Comparator gain $A2$	RESET integrator dead band ±volts	High limit and RESET volts
1 4.55	1.0	6.56	2.0	6.0	[1] 2.2	3.45	1.31	1.44	14.4	2.49	0.758	1.0	8.80	0.21	5.5
2 6.02	1.0	6.56	2.0	6.0	[2] 1.0	3.10	1.46	0.95	9.5	2.64	0.805	1.0	8.28	0.19	5.8
3 8.08	1.0	6.56	2.0	6.0	[2] 1.6	1.76	2.58	0.93	9.3	2.57	0.784	1.0	8.50	0.11	5.6
4 10.65	1.0	6.56	2.0	6.0	[2] 2.4	1.70	2.66	1.00	10.0	2.57	0.784	1.0	8.50	0.10	5.0

[1] Refer to figure 6, 50-MΩ card.
[2] Refer to figure 6, 100-MΩ card.

troller integrator motor speed is described in detail in following sections.

Check No. 1 (Coyote)

Arc distance per vertical offset (V-21)

$$= \frac{0.762\text{ m}}{0.64\text{ m}} = \frac{2.50\text{ ft}}{2.10\text{ ft}} = 1.19$$

One revolution of hoist drum (V-22)

$= \pi d = 3.14\ (0.23\text{ m}) = 0.718\text{ m}$

$= 3.14\ (0.75\text{ ft}) = 2.355\text{ ft}$

1 meter vertical lift (V-23)

$$\equiv \frac{1.190\text{ (arc)}}{0.718\text{ m (arc/r)}} \equiv 1.66\text{ revolutions}$$

$$1\text{ foot vertical lift} \equiv \frac{1.190\text{ (arc)}}{2.355\text{ ft (arc/r)}} \equiv 0.505\text{ revolution}$$

Gate 10-turn potentiometer = 1.5 V/r (V-24)

Volts per 1 vertical meter (V-25)

$= (1.5\text{ V/r})\ (1.66\text{ r}) = 2.49\text{ V}$

Volts per 1 vertical foot

$= 1.5\text{ V/r}\ (0.505\text{ r}) = 0.758\text{ V}$

$$\textit{EL-FLO GAIN } A1 = \frac{9.1}{6.6\text{ V/m}}\ (2.49\text{ V/m}) = 3.45$$

$$= \frac{9.1}{2.0\text{ V/ft}}\ (0.758\text{ V/ft}) = 3.45 \quad \text{(V-26)}$$

$$\textit{ABSOLUTE GAIN } A1 = \frac{4.53}{3.45} = 1.31 \quad \text{(V-27)}$$

Schmitt Trigger operates at ±1.0 V for a gate opening change of ±0.0457 m (±0.15 ft).

Voltage for ±0.046 m of gate opening is 2.49 V/m x ±0.0457 m = ±0.1137 V (0.758 V/ft x 0.15 ft = ±0.1137 V) (V-28)

$$\textit{COMPARATOR GAIN } A2 = \frac{\pm 1.0\text{ V}}{\pm 0.1137\text{ V}} = 8.8 \quad \text{(V-29)}$$

Set RESET integrator motor speed at 0.008 r/min at water level offset of 0.15 m (0.5 ft), or 1.0 V. Required integration for 10 minutes is:

$$GR = (0.033\text{ min}^{-1})\ (3.45)\ (1\text{ V})\ (10\text{ min}) = 0.115\text{ V} \quad \text{(V-30)}$$

where 0.033 min^{-1} is the selected *RESET GAIN K2* and 3.45 is the *EL-FLO GAIN A1*.

Integrator potentiometer volts per revolution

$$= \frac{0.115\text{ V}}{0.008\text{ r/min (10 min)}} = 1.44\text{ V} \quad \text{(V-31)}$$

Integrator 10-turn potentiometer = 1.44 V/r x 10 = 14.4 V.

Integrator dead band set at (V-33)

±0.0091 m (6.56 V/m) (3.45) = ±0.21 V

or

(±0.03 ft) (2 V/ft) (3.45) = ±0.21 V

Integrator and gate high limit set of

2.19 m (2.49 V/m) = 5.5 V (V-34)

(7.2 ft) (0.758 V/ft) = 5.5 V

ELECTRONIC FILTER GAIN A (V-35)

$$= \frac{800\text{ seconds} - 50\text{ megohms (5 }\mu\text{F)}}{50\text{ megohms (5 }\mu\text{F)}} = 2.2$$

To determine the *ABSOLUTE GAIN* for the RESET integrator motor speed, the first step is to select 0.15 m (0.5 ft) of "offset," (*YT* − *YF*), at which point the integrator motor is to operate at half speed or 0.008 revolution per minute. Using figure V-7, the voltage requirement across the integrator motor terminals is 7.6 volts at a speed of 0.008 revolution per minute. Using figure V-8 and 7.6 volts for voltage across the motor terminals, the voltage requirement at test point 7 (*TP7*) is 4.53 volts. Therefore, the *ABSOLUTE GAIN* requirement for check No. 1 is:

ABSOLUTE GAIN

$$= \frac{TP7}{A1\ (YT - YF)} = \frac{4.53\text{ volts}}{3.45\ (1\text{ volt})} = 1.31 \quad \text{(V-36)}$$

where *A1* (*YT* − *YF*) is the EL-FLO analog computer output, *GP*, in volts, and the water level offset of 0.15 m (0.5 ft) equals 1.0 volt.

The *ABSOLUTE GAIN* adjustment is made on the trimpot *P2* of the RESET controller card No. 2 (fig. III-3). With an input measured at *TP2* of 3.45 volts, trimpot *P2* is adjusted until the voltage measured at *TP7* is 4.53 volts.

The control parameters for checks No. 1 through 4 were reduced after mathematical studies indicated excessive amplification of downstream canalside demand changes would occur in the upper canal reaches when the EL-FLO plus RESET controllers were added to the remaining Corning Canal reaches checks No. 5 through 12. The final control parameters selected and used on all of the EL-FLO plus RESET control units

Table V-6.—*Corning Canal EL-FLO plus RESET control parameters, second set, units of meters (feet)*

Check No. and M.P.	Target elevation m	(ft)	Elec. filter time const. (s)	EL-FLO gain *K1*	RESET gain *K2* Water *K2*/min	Gate *K2*/min	Check gate data: Arc distance per vert. rise	One rev. hoist drum m	(ft)	Hoist revolutions per 1 unit of vertical rise 1 m	(ft)	Gate dead band ±m	(±ft)	RESET dead band ±m	(±ft)	High limit m	(ft)
1 4.55	92.0	(302.0)	480	6.5	0.01	0.001 54	1.19	0.7178	(2.355)	1.66	(0.505)	0.0457	(0.15)	0.0152	(0.05)	1.95	(6.4)
2 6.02	91.6	(300.6)	730	5.4	0.01	0.001 85	1.26	0.7178	(2.355)	1.76	(0.536)	0.0457	(0.15)	0.0152	(0.05)	1.71	(5.6)
3 8.08	90.9	(298.3)	1030	3.5	0.01	0.002 86	1.23	0.7178	(2.355)	1.71	(0.522)	0.0457	(0.15)	0.0152	(0.05)	1.40	(4.6)
4 10.65	90.4	(296.6)	1000	4.0	0.01	0.002 50	1.23	0.7178	(2.355)	1.71	(0.522)	0.0457	(0.15)	0.0152	(0.05)	1.40	(4.6)
5 13.03	89.4	(293.2)	900	3.5	0.0076	0.002 18	1.23	0.7178	(2.355)	1.71	(0.522)	0.0213	(0.07)	0.0152	(0.05)	1.25	(4.1)
6 15.09	88.8	(291.4)	550	2.0	0.0050	0.002 50	1.23	0.7178	(2.355)	1.71	(0.522)	0.0213	(0.07)	0.0152	(0.05)	1.49	(4.9)
7 16.19	88.4	(290.2)	550	2.0	0.0054	0.002 70	1.23	0.7178	(2.355)	1.71	(0.522)	0.0213	(0.07)	0.0152	(0.05)	1.49	(4.9)
8 17.29	88.1	(289.0)	200	1.0	0.0050	0.005 0	1.19	0.4785	(1.57)	2.49	(0.758)	0.0213	(0.07)	0.0152	(0.05)	1.22	(4.0)
9 17.79	87.8	(288.1)	250	1.1	0.0050	0.004 54	1.0		N/A	[2] 0.34	(0.1034)	0.0152	(0.05)	0.0152	(0.05)	1.04	(3.4)
10 18.29	87.3	(286.4)	350	1.5	0.0050	0.003 34	1.0		N/A	[2] 0.34	(0.1034)	0.0152	(0.05)	0.0152	(0.05)	1.04	(3.4)
11 18.96	87.0	(285.5)	250	1.0	0.0050	0.005 00	1.0		N/A	[2] 0.34	(0.1034)	0.0152	(0.05)	0.0152	(0.05)	1.04	(3.4)
12 19.35	86.5	(283.8)	750	2.3	0.0050	0.002 18	1.0		N/A	[2] 0.34	(0.1034)	0.0152	(0.05)	0.0152	(0.05)	1.04	(3.4)

[1] Checks No. 9 through 12 are vertical lift gates.
[2] Gate indicator.

Table V-7.—*Corning Canal EL-FLO plus RESET control parameters, second set, electronic equivalences*

Check No. and M.P.	Target	Water level scale V/m	(V/ft)	Water level pot. volts	Electronic filter gain *A*	EL-FLO gain *A1*	Absolute gain	RESET potentiometer V/r	10-turn pot. volt	Gate volt scale (5 or 10 turn) V/m	(V/ft)	Schmitt trigger ±volts	Comparator gain *A2*	RESET integrator dead band ±volts	[c]High limit and RESET volts
1 4.55	2.0	6.56	(2.0)	6.0	[a] 1.00	[b] 2.46	1.38	0.65	6.5	2.49	(0.758)	1.0	8.8	0.25	5.6
2 6.02	2.0	6.56	(2.0)	6.0	[d] 1.92	[b] 2.18	1.57	0.68	6.8	2.64	(0.805)	1.0	8.3	0.22	5.2
3 8.08	1.0	6.56	(2.0)	6.0	[d] 1.06	1.37	2.52	0.66	6.6	2.57	(0.784)	1.0	8.5	0.14	4.4
4 10.65	1.0	6.56	(2.0)	6.0	[d] 1.00	1.57	2.56	0.60	6.0	2.57	(0.784)	1.0	8.5	0.16	4.4
5 13.03	1.0	6.56	(2.0)	6.0	[a] 2.6	2.7	1.0	0.99	9.9	5.15	(1.57)	1.0	9.1	0.27	7.4
6 15.09	1.0	6.56	(2.0)	6.0	[e] 4.5	1.6	1.7	0.85	3.5	5.15	(1.57)	1.0	9.1	0.16	8.4
7 16.19	1.0	6.56	(2.0)	6.0	[e] 3.5	1.6	1.7	0.85	8.5	5.15	(1.57)	1.0	9.1	0.16	8.4
8 17.29	[f] 2.0	6.56	(2.0)	6.0	[e] 1.0	1.1	2.4	1.14	11.4	7.48	(2.28)	1.0	6.3	0.11	10.1
9 17.79	[g] 0.85	6.56	(2.0)	6.0	[e] 1.5	1.0	4.1	0.65	6.5	5.09	(1.55)	0.7	9.0	0.09	6.3
10 18.29	1.0	6.56	(2.0)	6.0	[e] 2.5	1.16	3.0	0.65	6.5	5.09	(1.55)	0.7	9.0	0.12	6.3
11 18.96	[h] 0.78	6.56	(2.0)	6.0	[e] 1.5	1.0	4.5	0.65	6.5	5.09	(1.55)	0.7	9.0	0.18	6.3

[a] 50-megohm resistor.
[b] Includes gain of 2.0 set into *TP4*.
[c] Includes 0.5-turn gate potentiometer volts for zero position.
[d] 100-megohm resistor.
[e] 20-megohm resistor.
[f] Voltage divider on transmitter.
[g] Includes gain of 0.85 set into *TP4*.
[h] Includes gain of 0.78 set into *TP4*.

for the entire Corning Canal system are tabulated in tables V-6 and V-7 for units of meters (feet) and electronic equivalences, respectively. This information is included in this report to bring the Corning Canal EL-FLO control system up to date and for record purposes. Future studies on canal response characteristics may also find this information useful. Table V-8 is a tabulation of pertinent information regarding the Corning Canal Alarm Probe elevations.

Table V-8.—*Corning Canal alarm probe elevations*

Check No.	M.P.	Elevation bypass crest m	(ft)	Elevation high alarm m	(ft)	Elevation low alarm m	(ft)	Spread m	(ft)
1	4.55	92.66	(304.0)	92.69	(304.10)	92.32	(302.90)	0.37	(1.20)
2	6.02	92.14	(302.30)	92.20	(302.50)	91.90	(301.50)	0.30	(1.00)
3	8.08	91.71	(300.88)	91.71	(300.90)	91.41	(299.90)	0.30	(1.00)
4	10.65	91.01	(298.60)	91.07	(298.80)	90.80	(297.90)	0.27	(0.90)
5	13.03	90.45	(296.77)	90.50	(296.90)	90.25	(296.10)	0.25	(0.80)
6	15.09	89.41	(293.34)	89.44	(293.44)	89.18	(292.60)	0.26	(0.84)
7	16.19	88.96	(291.87)	88.94	(291.80)	88.67	(290.90)	0.27	(0.90)
8	17.29	88.50	(280.34)	88.53	(290.44)	88.00	(288.70)	0.53	(0.74)
9	17.79	88.21	(289.39)	88.25	(289.55)	87.90	(288.40)	0.35	(1.15)
10	18.29	87.91	(288.42)	87.93	(288.50)	87.60	(287.40)	0.33	(1.10)
11	18.96	87.41	(286.79)	87.45	(286.90)	87.11	(285.80)	0.34	(1.10)
12	19.35	87.13	(285.87)	87.17	(286.00)	86.84	(284.90)	0.33	(1.10)
End	20.73	86.56	(284.00)	86.56	(284.00)	86.35	(283.30)	0.21	(0.70)

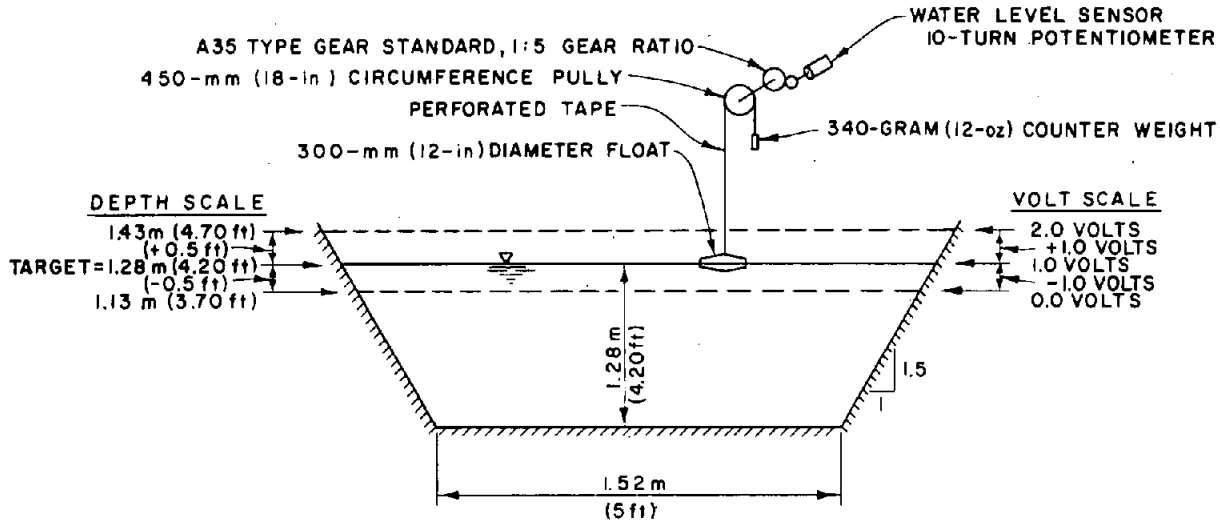

Figure V-1.— Sketch of water level sensor-potentiometer operating depth and voltage scale.

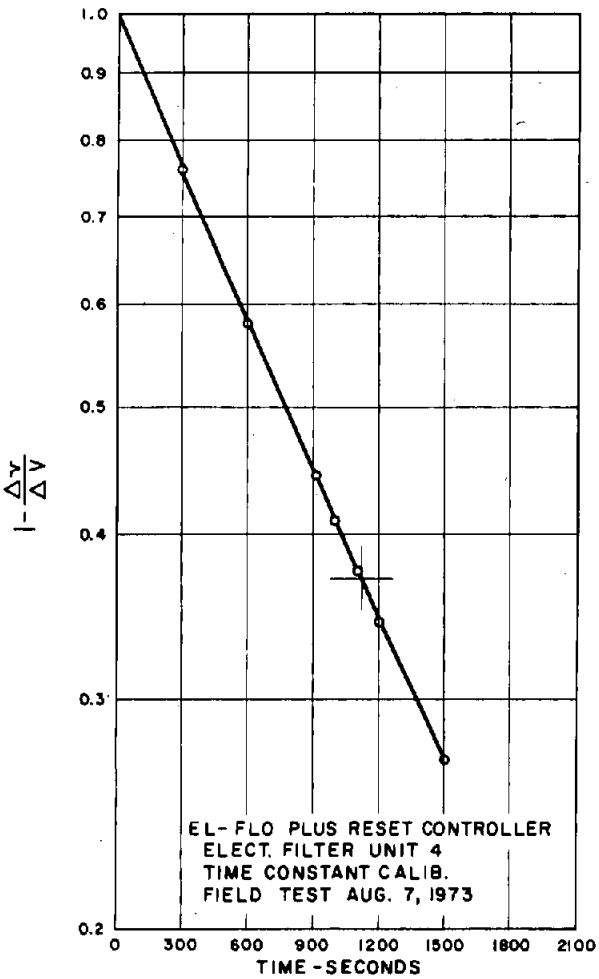

Figure V-2.— South Gila Canal EL-FLO plus RESET controller electronic filter unit 4 time constant calibration.

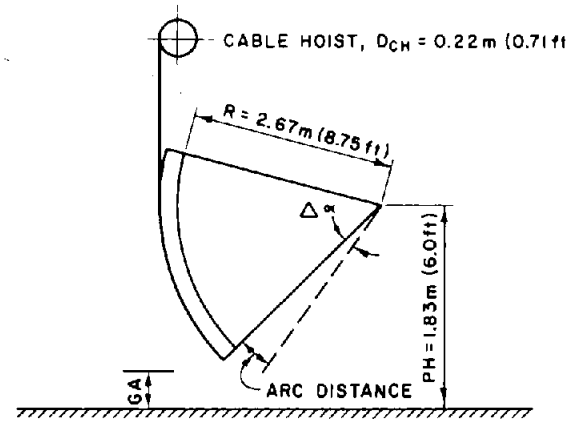

Figure V-3.— Schematic of radial gate properties.

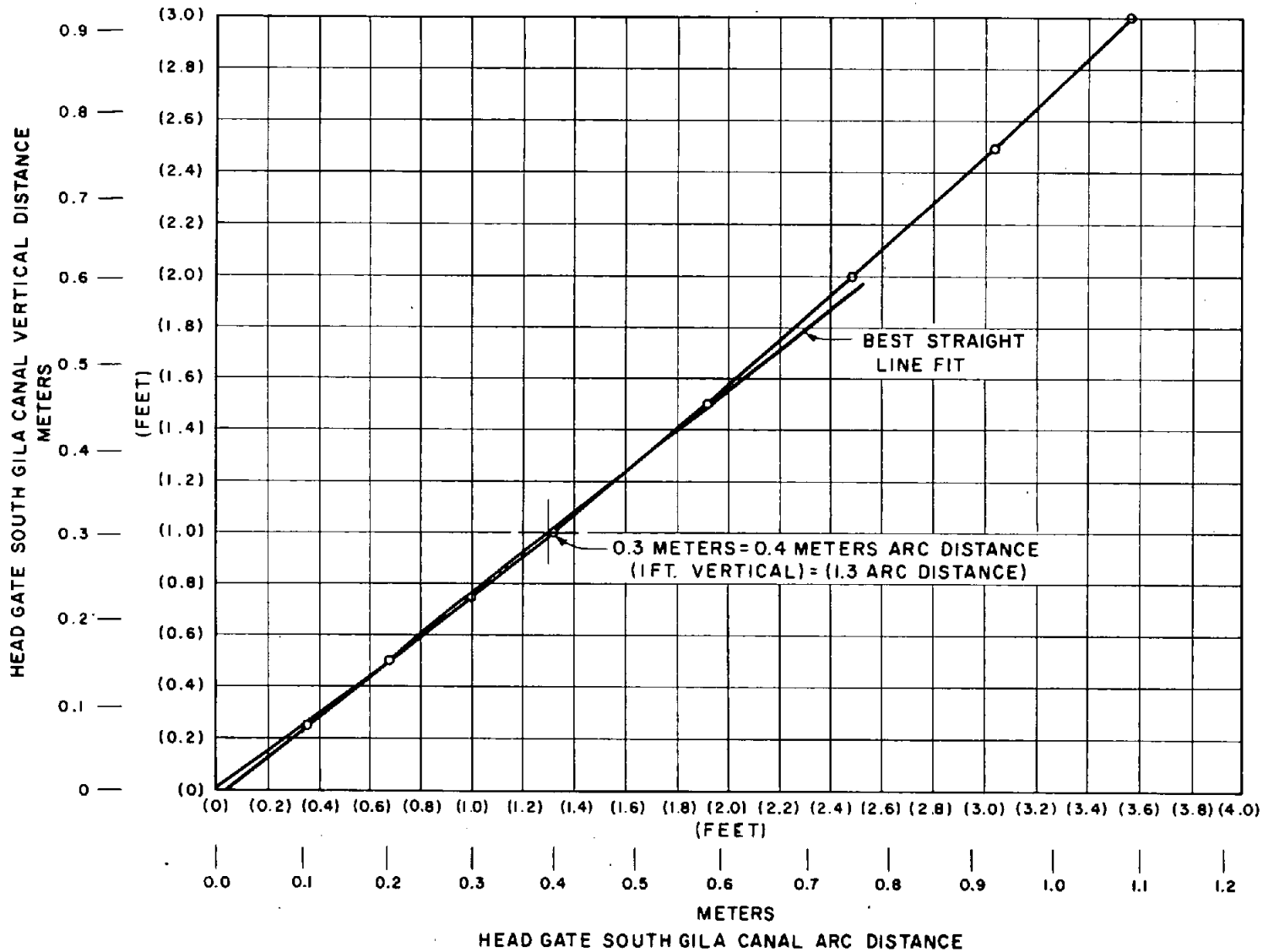

Figure V-4.— South Gila Canal radial headgate calibration.

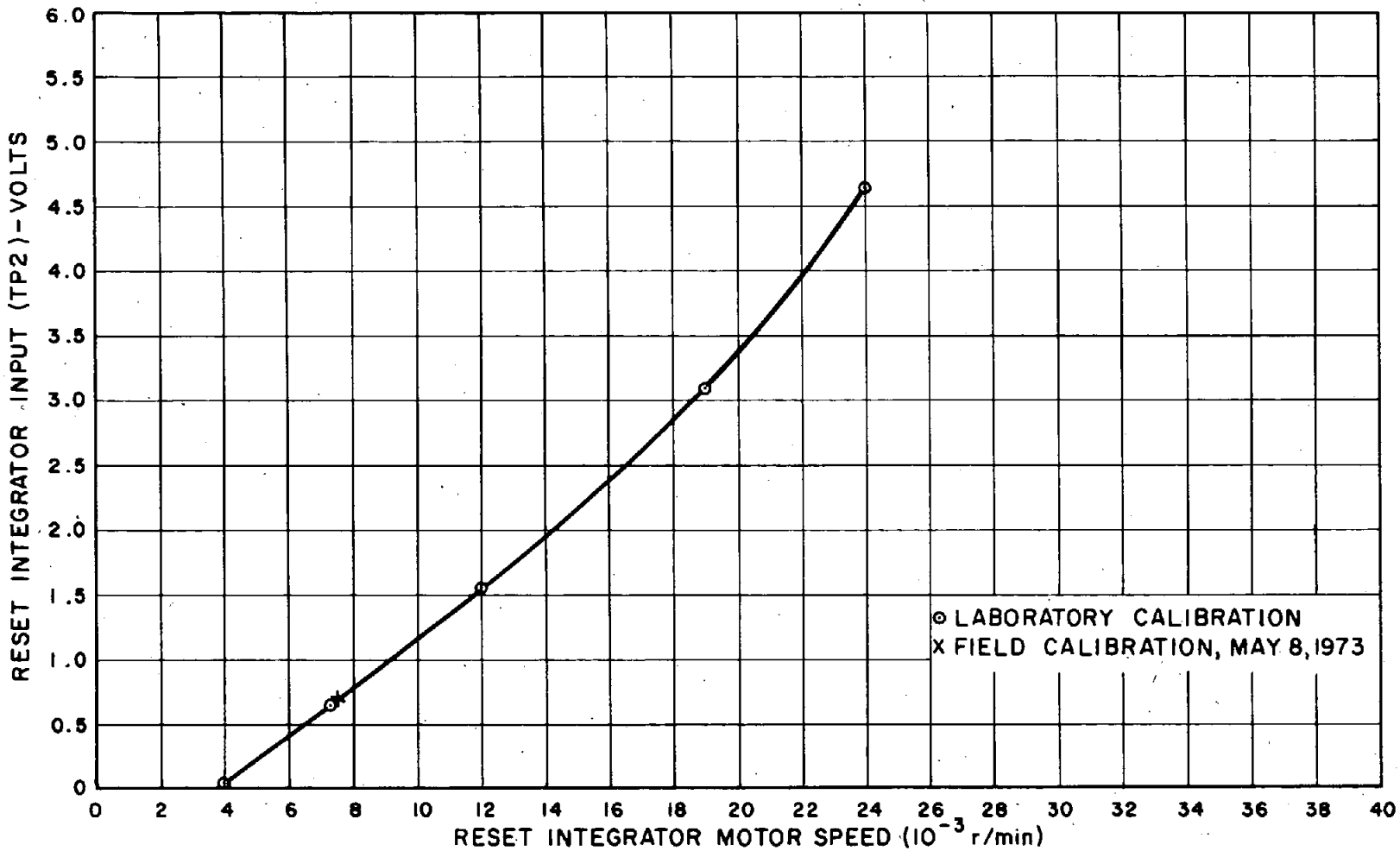

Figure V-5.— South Gila Canal EL-FLO plus RESET controller RESET integrator calibration.

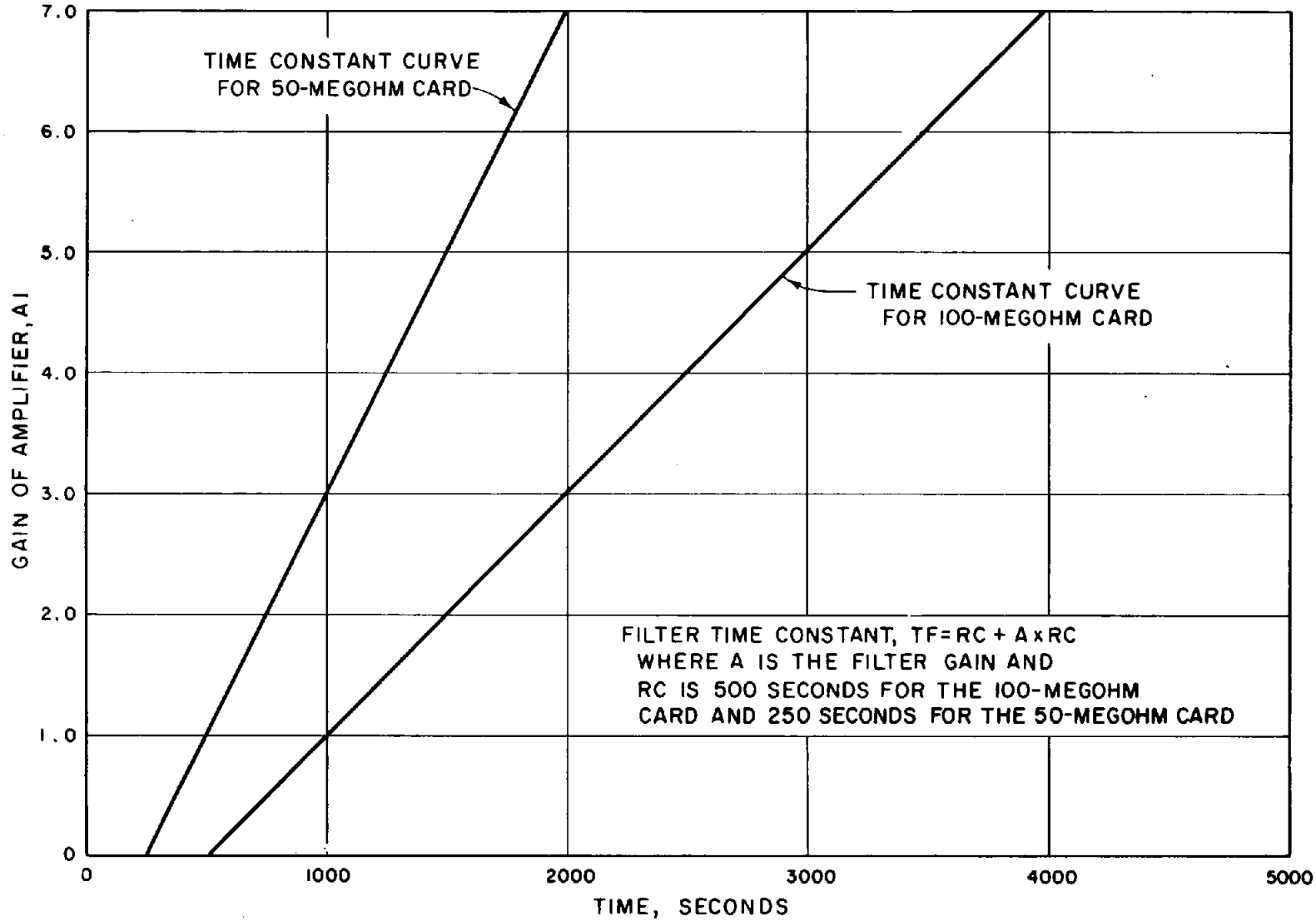

Figure V-6.— Time constant of electronic filter in seconds with 50- and 100-megohm resistance.

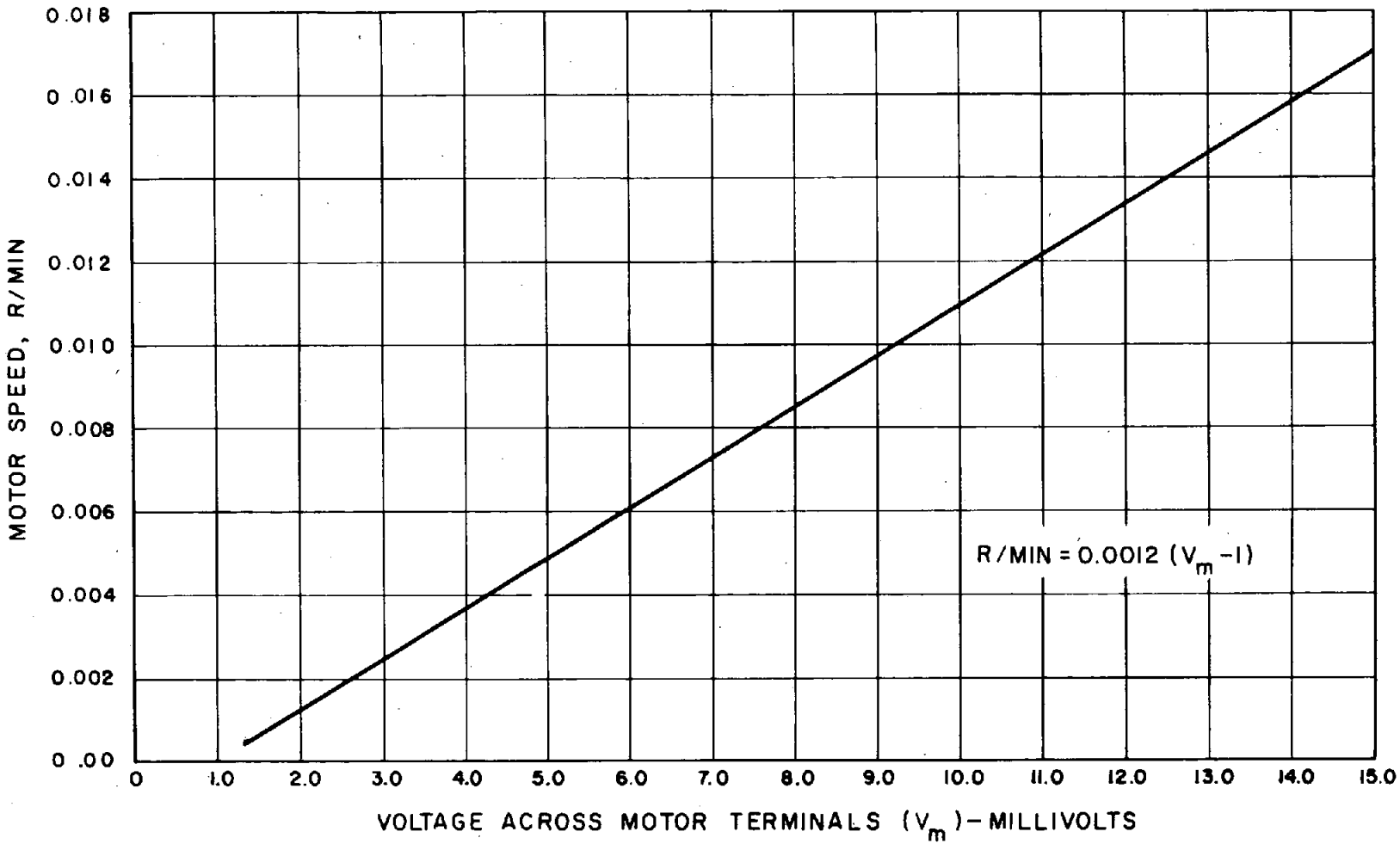

Figure V-7.– RESET integrator motor speed calibration curve No. 1.

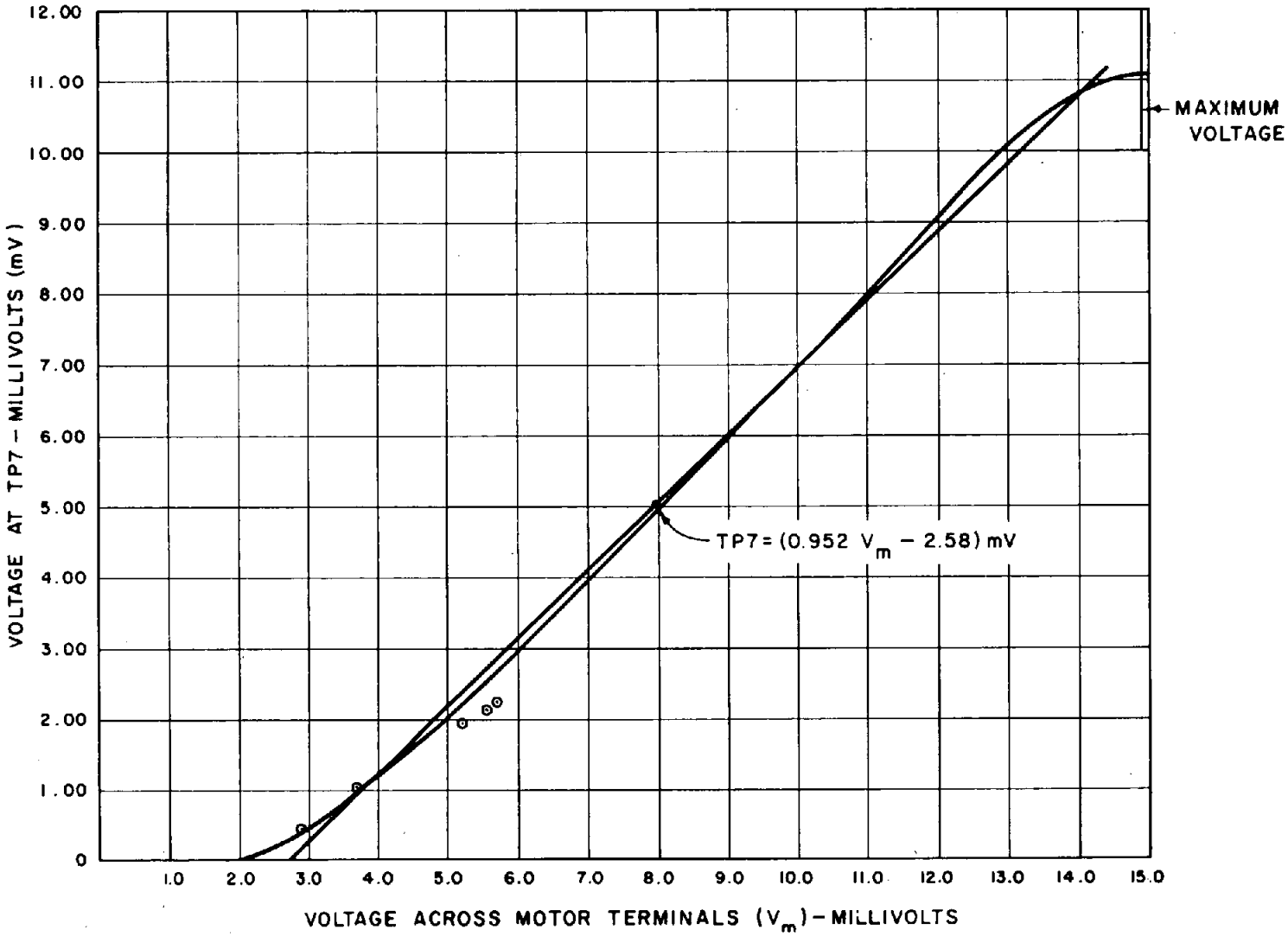

Figure V-8.– RESET integrator motor speed calibration curve No. 2.

Appendix VI

DETAILED ANALYSIS OF LABORATORY VERIFICATION TEST

A detailed analysis of the prototype equipment output conditions was made at time 120 minutes of the test run to define the differences and possible cause of error as compared to the mathematical model output at the same period of time. Reference is made to figure 22 in the Laboratory Verification Test section of this report.

At time 120 minutes, the canal water depth of the mathematical model was 1.2628 m (4.143 ft); the actual water level in the water tank of 1.2625 m (4.142 ft), as measured by a water level manometer gage. The water level sensor output was 1.2625 m. There was an error of −0.0003 m (−0.001 ft) between the mathematical model and the water level in the tank caused by the manual control of the water level in the tank. There was no measurable difference between the water level in the tank and the water level indicated by the sensor; thus, showing the sensor assembly is an accurate water level measuring device.

The depth indicated by the mathematical model simulated electronic filter at time 120 minutes was 1.2436 m (4.080 ft). The prototype electronic filter equipment was 1.2454 m (4.086 ft) for a difference of +0.0018 m (+0.006 ft). The error of +0.0018 m plus the −0.0003-m error in the water level gives a total error of +0.0021 m (+0.007 ft). This difference is attributed to the nonlinearity characteristic of the field effect transistor (MOSFET) between its gate and source terminals as discussed in Electronic Filter Calibration, appendix II.

In reference to figure 22b, at 120 minutes, the EL-FLO computed gate opening from the mathematical model output was 0.1091 m (0.358 ft) and the prototype equipment output was 0.0969 m (0.318 ft) for a difference of −0.0122 m (−0.040 ft). An examination of the data measured at the controllers test points (*TP*'s) during the test gives an electronic equivalence gain, $A1$, of the proportional mode of:

$$A1 = \frac{TP}{(TP1 - TP4)/2} \qquad \text{(VI-1)}$$

$$= \frac{0.657 \text{ volt}}{(1.993 \text{ volts} - 1.555 \text{ volts})/2} = 3.0$$

Converting the gain, $A1$, to the equivalent gain, $K1$, will give a value of:

$$K1 = \frac{\text{(volts per depth of water level)}}{\text{(volts per level of gate opening)}} \times (A1) \qquad \text{(VI-2)}$$

$$= \frac{6.56 \text{ V/m}}{6.76 \text{ V/m}}(3.0) = 2.9$$

$$= \frac{2.00 \text{ V/ft}}{2.06 \text{ V/ft}}(3.0) = 2.9$$

Therefore, an error was made in the calibration of the EL-FLO controller gain, $K1$, prior to the test run. The smaller gain, $K1$, accounts for −0.0034 m (−0.011 ft) of the difference of −0.0122 m (−0.040 ft) between the mathematical model and the prototype EL-FLO analog computer output. The error of the water level and the electronic filter output of 0.0021 m (0.007 ft) when multiplied by the gain, $K1$, accounts for another −0.0061 m (−0.020 ft) for a total of −0.0094 m (−0.031 ft) leaving a remainder of −0.0027 m (−0.009 ft) of the difference to be examined. The remaining error of −0.0027 m (−0.009 ft) is attributed to electronic voltage drift caused primarily by a change of loading of the electronic circuits as the input changes. The target potentiometer voltage level which is the EL-FLO analog computer referenced input, *YT*, that is supposed to be constant, changed from 2.000 volts at time zero to 1.993 volts at time 18 minutes and remained at this level throughout the remainder of the test run. The change of −0.007 volt, or −0.0011 m (−0.0035 ft), in the reference input, *YT*, when multiplied by the gain, $K1$, is −0.0030 m (−0.010 ft) which accounts for the −0.0027-m (−0.009-ft) error that cannot be explained by errors in calibration and the filter output. The −0.0027-m difference in the EL-FLO controller equipment output represents an error of about −2.8 percent that can be present in analog control equipment. The accumulated error caused by electronic drift and nonlinearity of the equipment components is −0.0088 m (−0.029 ft), or −9.1 percent of the output of the EL-FLO controller.

The RESET computed gate opening, *GR*, from the mathematical model was 0.0872 m (0.286 ft) and the prototype RESET analog computer output was 0.0728 m (0.239 ft) at time 120 minutes for a difference of −0.0143 m (−0.047 ft). The accuracy of the RESET controller proportional reset gain, $K2$, equations 2 and 3, can be examined in three ways, (1) using the controller output conditions (fig. 22) at time 120 minutes, (2) the average output of the prototype equipment test point output data measured between time 117 and 123 minutes, and (3) computing the average gain, $K2$, between time 10 and 120 minutes using both figure 22 test point outputs.

The first method requires a measurement of the area under the prototype EL-FLO controller output, *GP*,

from time 10 to 120 minutes. The area measured by planimeter was 16.18 meter minutes (53.1 ft·min). The dead band area of 0.0061 m times 110 minutes, equal to 0.67 meter minutes (2.2 ft·min), is subtracted from the total area to get a net area of 15.51 meter minutes (50.9 ft·min) actually integrated by the RESET controller.

$$GP\ net\ area = \int_{t_1}^{t_2} K1(YT - YF)dt \qquad \text{(VI-3)}$$

$$-\int_{t_1}^{t_2} (dead\ band)\,dt = 15.51\ \text{m·min} \quad \text{or} \quad (50.9\ \text{ft·min})$$

The gain, $K2$, can be calculated using the GP net area measured from figure 22 and the RESET controller output, GR, 0.0728 m (0.239 ft) at time 120 minutes.

$$K2 = \frac{GR}{GP\ net\ area} = \frac{0.0728\ \text{m}}{15.51\ \text{m·min}} = \frac{(0.239\ \text{ft})}{(50.9\ \text{ft·min})} = 0.004\,69\ \text{min}^{-1} \qquad \text{(VI-4)}$$

The second method determines the gain, $K2$, of the RESET controller at time 120 minutes by averaging the prototype equipment test point outputs (electronic voltages) measured data between time 117 to 123 minutes. For the 6-minute period, the average gain, $K2$, is:

$$K2 = \frac{\text{Ave. motor speed (r/min) x avg. integrator ref. input (V/r)}}{\text{Ave. EL-FLO controller output, } GP \text{ (volts)}} \qquad \text{(VI-5)}$$

$$= \frac{0.0669\ \text{r/min} \times 0.483\ \text{V/r}}{0.678\ \text{V}} = 0.004\,77\ \text{min}^{-1} \qquad \text{(VI-6)}$$

A comparison of the gain, $K2$, as measured by the first two methods gives an indication that only a minor nonlinearity of motor speed existed during the first 120 minutes of the test run. The small difference in gain (0.000 08 min^{-1}) between the two methods accounts for −0.0012 m (−0.004 ft), (15.27 m·min x 0.000 08 min^{-1}).

The first two methods for measuring the gain determines the condition of the RESET controller calibration at time 120 minutes. The third method determines the average RESET controller calibration during the period from 10 to 120 minutes and is calculated as follows:

$$K2 = \frac{\text{Integrator x avg. integrator ref. input}}{\text{Gate voltage scale x total } GP \text{ area for the 110 min}} \qquad \text{(VI-7)}$$

$$= \frac{1.045\ \text{r} \times 0.486\ \text{V/r}}{110\ \text{min} \times 6.76\ \text{V/m} \times 16.18\ \text{m·min}} \qquad \text{(VI-8)}$$

$$= \frac{(1.045\ \text{r})\ (0.486\ \text{V/r})}{(110\ \text{min})\ (2.06\ \text{V/ft})\ (53.1\ \text{ft·min})} = 0.004\,64\ \text{min}^{-1}$$

The average gain, $K2$, derived from equation VI-8, is another indication of the RESET controller nonlinearity that was experienced during the first 120 minutes. However, since the analysis of errors is being made at time 120 minutes, the RESET controller gain derived in the third method will only be used for an indication of the calibration of the RESET controller. The mathematical model simulated RESET controller used a gain of 0.005 min^{-1}. Therefore, the error in the calibration of the prototype equipment (−0.000 36 min^{-1}) would account for 0.0055 m (−0.018 ft) [−0.00 36 min^{-1} x (15.27 m·min)] of the total difference of −0.0143 m (−0.047 ft) between the prototype equipment and the mathematical model.

The prototype RESET controller has a dead band of ±0.0061 m (±0.02 ft) (GP output) that was not included in the mathematical model. The prototype integration does not start until the EL-FLO controller output, GP, is −0.0061 m (−0.020 ft) accounting for −0.0030 m (−0.010 ft) [0.0061 m x 110 min x 0.00464 min^{-1}] of the difference.

The error in the output of the EL-FLO controller of −0.0122 m (−0.040 ft) would account for a −0.0030-m (−0.010-ft) error in the RESET controller. The −0.0030-m (−0.010-ft) error was derived by averaging the EL-FLO controller output giving a −0.0061-m (−0.020-ft) average error for the 110-minute period, multiplying by the 110-minute period, and by the average gain, $K2$, of 0.00464 min^{-1} (−0.0061 m x 110 min 0.00464 min^{-1}).

An error was caused by a drift in the voltage reference input to the RESET integrator potentiometer. The integrator potentiometer volts per revolution drifted downwards from 0.489 V/r at the beginning of the test run to 0.483 V/r at time 120 minutes for a difference of −0.006 V/r. During this time period, the potentiometer turned 1.045 revolutions which would change the RESET controller output by −0.0063 volt (1.045 x 0.006 V/r). Converting the -0.0063 volt to distance, the error is −0.0009 m (−0.003 ft).

The RESET controller output errors that have been identified are the nonlinearity of the motor speed, −0.0012 m (−0.004 ft), the calibration error of the gain, $K2$, −0.0055 m (−0.018 ft), the dead band of the prototype equipment, −0.0030 m (−0.010 ft), the error in the EL-FLO controller output, −0.0030 m (−0.010 ft), and the drift in the integrator reference

voltage, −0.0009 m (−0.003 ft), for a total of −0.0137 m (−0.045 ft). Only −0.0006 m (−0.002 ft) of the difference of −0.0143 m (−0.047 ft) between the prototype RESET controller output and the mathematical model was not identified, and was attributed to errors in measurement by test voltmeters of the various equipment test point outputs.

The errors attributed to equipment nonlinearity of the motor speed and voltage drift of the integrator reference are −0.0021 m (−0.007 ft) for the prototype RESET controller which is about −2.9 percent error. The RESET controller accumulated error, caused by electronic drift and nonlinearity of the filter and EL-FLO controller equipment components, is −0.0021 m (−0.007 ft), or −2.9 percent of the output of the RESET controller.

The EL-FLO plus RESET computed gate opening, *GD*, [equations 3 and 4 of the General Theory section] from the mathematical model was 0.1963 m (0.644 ft) and the prototype EL-FLO plus RESET controller output was 0.1698 m (0.557 ft) for a difference of −0.0265 m (−0.087 ft) at time 120 minutes. The accumulated errors of the EL-FLO controller output [−0.0122 m (−0.040 ft)] and the RESET controller output [(−0.0143 m (−0.047 ft)] were −0.0265 m (−0.087 ft). Therefore, no additional errors occurred when the outputs of the prototype EL-FLO and RESET controllers were added together. The accumulated error caused by electronic drift and nonlinearity of the filter and EL-FLO plus RESET equipment components is −0.0104 m (−0.034 ft), or −6.1 percent of the output of the filter and EL-FLO plus RESET controllers.